

Institute of Plant Genetics  
Polish Academy of Sciences

19

Dissertations and Monographs

# Methodology of system approach to study drought tolerance in barley

edited by

**Maria Surma and Paweł Krajewski**



Poznań 2014

# **Methodology of system approach to study drought tolerance in barley**

edited by

**Maria Surma and Paweł Krajewski**



**Institute of Plant Genetics PAS**

**Poznań 2014**

**Institute of Plant Genetics, Polish Academy of Sciences  
Dissertations and Monographs Vol. 19**

**Series Editorial Committee**

Tadeusz Adamski, Paweł Krajewski, Bolesław Salmanowicz, Maria Surma,  
Zbigniew Zwierzykowski

---

**Reviewers**

Zofia Banaszak, DANKO Plant Breeders LTD  
Jerzy Nawracała, Poznań University of Life Sciences  
Arkadiusz Kosmala, Institute of Plant Genetics PAS

**Editors**

Maria Surma, Institute of Plant Genetics PAS  
Paweł Krajewski, Institute of Plant Genetics PAS

Publication supported by the European Regional Development Fund through the Innovative Economy Program for Poland 2007-2013, project WND-POIG.01.03.01-00-101/08 POLAPGEN-BD „Biotechnological tools for breeding cereals with increased resistance to drought”



© Institute of Plant Genetics Polish Academy of Sciences  
Poznań 2014

ISBN 978-83-64246-24-1  
ISSN 1230-0721

Wydawnictwo-Drukarnia ProDRUK  
61-699 Poznań, Błażeja 3  
tel. (+48 61) 822 90 46

Motto

*Every day, it becomes more evident that successful breeding for stable high yield under drought conditions will only be possible when a true integration of traditional breeding with physiology and genomics is achieved.*

*(Cattivelli et al. 2008)*



## Contents

Foreword .....	7
ANDRZEJ KĘDZIORA, JANUSZ JANKOWIAK, DAMIAN JÓZEFczyk, GRZEGORZ KARG, JOANNA ANDRUSIAK Methodology for assessing of water conditions in Poland in terms of cultivation of spring barley .....	9
PIOTR OGRODOWICZ, KRZYSZTOF MIKOŁAJCZAK, ANETTA KUCZYŃSKA, KAROLINA KRYSKOWIAK, MARIA SURMA, TADEUSZ ADAMSKI Plant materials and analysed traits in the greenhouse and field experiments .....	19
ALICJA PECIO, DAMIAN WACH, ANNA KOCOŃ, GRZEGORZ JÓZEFACIUK A method for precision irrigation control in greenhouse experiment and its use to study drought stress effect on spring barley .....	29
JUSTYNA GUZY-WROBELSKA, KORNELIA GUDYS Construction of high quality 'function' maps for the identification of quantitative trait loci related to drought tolerance in barley .....	47
TOMASZ P. WYKA, AGNIESZKA BAGNIEWSKA-ZADWORNA Measuring anatomical variation in leaves of barley genotypes differing in drought tolerance .....	63
MALGORZATA ŁUKOWSKA, HENRYK CZACHOR Contact angle and surface free energy of plant leaves and their changes under drought conditions .....	79
MARIA FILEK, JOLANTA BIESAGA-KOŚCIELNIAK, MICHAŁ DZIURKA Determination of proline, carbohydrates and ethylene content and their role in drought stress in plant .....	95
JOLANTA BIESAGA-KOŚCIELNIAK, MARIA FILEK, MICHAŁ DZIURKA, AGNIESZKA OSTROWSKA, ANNA MAKSYMOWICZ, APOLONIA SIEPRAWKA Analysis of antioxi- dant system under abiotic stress .....	105

RENATA BĄCZEK-KWINTA The assay of oxygen free radicals and the enzyme decomposing them in barley leaves subjected to drought .....	115
KATARZYNA HURA, BARBARA JURCZYK, AGNIESZKA OSTROWSKA, MARCIN RAPACZ, KATARZYNA ŚNIEGOWSKA-ŚWIERK, MAGDALENA WÓJCIK-JAGŁA, KATARZYNA ŻMUDA, JOLANTA BIESAGA-KOŚCIELNIAK, JANUSZ KOŚCIELNIAK Physiological indicators of drought tolerance in barley .....	125
KATARZYNA ŚNIEGOWSKA-ŚWIERK, BARBARA JURCZYK, MARCIN RAPACZ Methods for the measurement of drought-induced changes in the expression of selected barley genes .....	133
TADEUSZ RORAT, ANNA TURSKA-TARASKA, AGNIESZKA KIELBOWICZ-MATUK, MATEUSZ DE MEZER The application of functional genomics to identify genes associated with adaptation of barley plants to water deficit .....	141
ALEKSANDRA ŚWIDA-BARTECZKA, KATARZYNA KRUSZKA, ANDRZEJ PACAK, WOJCIECH KARŁOWSKI, ARTUR JARMOŁOWSKI, ZOFIA SZWEYKOWSKA-KULIŃSKA Tools for defining barley microtranscriptome expression at the level of primary microRNAs and mature microRNAs .....	151
WOJCIECH FROHMBERG, ANETA SAWIKOWSKA, HANNA ĆWIEK, ZYGMUNT KACZMAREK, PAWEŁ KRAJEWSKI POLAPGEN-BD data collection, retrieval and processing infrastructure: a solution for systems biology research in plants .....	167
Technological deliverables of POLAPGEN-BD project .....	181

## Foreword

In past decades periods with reduced water availability occur in Central and West Europe resulting in severe economic impacts in agricultural sector. Moreover, predictions of climate changes indicate increased likelihood for drought in Europe. In the response to climatic changes breeding programmes should be aimed at creation of new cultivars with improved resistance to water shortage, particularly in spring cereals that are most vulnerable to drought. So far breeders have not had effective tools for selection of genotypes resistant to drought. Development of such tools could accelerate biological progress in agriculture and increase competitiveness of Polish breeding companies.

POLAPGEN-BD project is focused on drought tolerance in cereal crops, especially in barley. The idea of the project is the result of many discussions of scientists with breeders and growers on increasing desiccation of the environment, observed mainly in the Polish Lowland, which reflects the water deficit in the soil. The project consists of 23 research tasks carried out under POLAPGEN Consortium whose partners represent 2 breeding companies and 10 research units\*. All tasks are realized on the same plant material, which enables integration of all research teams around the same problem. Comprehensive approach to the problem of cereal resistance to water shortage enables to evaluate interdependence between various parameters associated with drought tolerance. System approach has been achieved by adopting a model of tolerance of plants to drought stress containing ecophysiological, morphological, anatomical, metabolic, proteomic, and molecular levels considered in the context of genetics.

To achieve expected results, a considerable effort had to be invested in development of methodologies and infrastructure appropriate for all tasks. The main challenges to meet were the requirements of the large experimental material used in the project and of the various experimental protocols. All research teams had been involved in similar studies before, however, many specific problems were solved specially for POLAPGEN-BD project. In this volume we collected papers describing those methodological advances. We start with the description of the methodology of studies needed to assess the environmental conditions of barley growth. Then the methods of phenotypic and genotypic plant evaluations follow. Next there are descriptions of the protocols used in anatomical and physiological studies, and in gene expression analysis. The volume is concluded with a chapter describing how the informatic infrastructure necessary for data processing and analysis was constructed.

On behalf of the project partners, we address this monograph to all scientists and practitioners interested in studying the stress reactions in plants. We hope that the described methodologies will be used not just in basic, but also in applied research. All results of the POLAPGEN-BD project will be presented in a number of publications that have already been published or are in preparation. From the formal point of view, the chapters included in this monograph are reports on technological solutions that were listed among the deliverables in the project's contract (for details see table at the end).

M. Surma and P. Krajewski

\* POLAPGEN-BD Consortium Members:

Danko Plant Breeders Ltd., Choryń  
Poznań Plant Breeders Ltd., Tulce  
Institute of Bioorganic Chemistry PAS, Poznań  
University of Agriculture, Kraków  
Institute of Plant Physiology PAS, Kraków  
Silesian University, Katowice  
Institute of Plant Genetics PAS, Poznań  
Adam Mickiewicz University, Poznań  
Poznań University of Life Sciences, Poznań  
Institute of Agricultural and Forest Environment PAS, Poznań  
Institute of Agrophysics PAS, Lublin  
Institute of Soil Science and Plant Cultivation – National Research  
Institute, Puławy

## **Methodology for assessing of water conditions in Poland in terms of cultivation of spring barley**

**Andrzej Kędziora, Janusz Jankowiak, Damian Józefczyk, Grzegorz Karg, Joanna Andrusiak**

*Institute for Agricultural and Forest Environment of Polish Academy of Sciences, Poznań, Poland*

### **Introduction**

The water requirements of plants are equal to the amount of water that is needed to produce high yield of crop in the optimal environmental conditions during the growing season. These requirements depend on the plant genetics, its development stage and the length of the growing season, as well as on climatic and soil conditions of habitat. In the period from sowing to harvesting, the water needs of spring crops in climatic and soil conditions in Poland are usually higher than precipitation (Dzieżyc 1989). It means that water shortages are a factor that limits yield of crops. Almost all plant cultivated species have critical periods of water needs, when water shortages result in strong decline of yields (Igras, Jankowiak 1998). In view of the changing climatic conditions causing, among others, intensification of extreme weather events, it will be very important to breed varieties of plants resistant to drought and also to periodic water excess. This will be one of the effective ways for adaptation to deteriorating environmental conditions for agricultural production (Arseniuk and Anioł 2009; Jankowiak and Bieńkowski 2011). Therefore, the full agrometeorological characterization of the country, especially water balance and its time changes during the growth period of spring crops, is the background for other studies investigated within the POLAPGEN project.

To get full climatic characterization, the study was performed in two ways:

1. Calculations were performed for a regular grid of squares (515 cells covering the entire country), for each 10-day period in the season from April to July (the growing season of spring barley). Two periods were taken into consideration: 1961-1990 as a reference period, and 2061-2090 as a projection period. Values

of meteorological elements for both periods have been generated by the model MPI-M-REMO developed at the Max Planck Institute für Meteorologie, which has the best compatibility with the actual data for the area of Poland, and were used as input data in all calculations. On the basis of meteorological data and the developmental phase of the plant, decade average values of heat balance components of spring cereals for each cell were calculated.

Heat balance was the basis to calculate the real evapotranspiration (ETR) and finally the water shortages as differences between precipitation and evapotranspiration (P-ETR).

2. During the period of 2010-2013, a special analysis of soil water conditions as well as of meteorological observations was done at five selected experimental stations belonging to the Research Centre for Cultivar Testing (COBORU), located in different regions of Poland (Fig. 1). The investigations were carried out at experimental plots with two varieties of spring barley, Suwren and Stratus.



Fig. 1. Location of 5 chosen experimental COBORU stations

### Methods used in calculation for country scale

To determine the values of water shortages, first the latent heat flux of ETR was calculated according to the formula (Olejnik and Kędziora 1991):

$$LE = -\frac{R_n + G}{1 + \beta}, \quad [1]$$

where  $R_n$  is the net radiation;  $G$  is the ground heat flux; and  $\beta$  is the Bowen ratio.

Based on equation [1], the real ETR in period (mm/period) was calculated as  $ETR = n \cdot LE / 28.34$ , where  $n$  is the number of days in the period. Computation of all values occurring in (1) is explained below.

Net radiation  $R_n$  was calculated according to the following formula:

$$R_n = (1-\alpha)R_o(0.22+0.54u)-5.68 \cdot 10^{-3} \cdot (t+273)^4 \cdot (0.56-0.08 \cdot e^{0.5}) \cdot (0.10+0.90u), \quad [2]$$

where  $\alpha$  is the albedo (dimensionless);  $R_o$  is the extra terrestrial solar radiation ( $W \cdot m^{-2}$ );  $u$  is the relative sunshine (dimensionless);  $t$  is the air temperature ( $^{\circ}C$ ); and  $e$  is the water vapor pressure (hPa).

Albedo for field crops and meadows ( $\alpha$ ) was calculated as follows:  $\alpha = 0.16 + 0.07f$ , where  $f$  is the plant developmental stage, changing from 0 (bare soil) to 1 (full development of plant cover). For water, the value of albedo was taken as 0.10, while for urban areas as 0.30. For forests, albedo was taken as 0.16 (averaged for coniferous and deciduous forests).

Soil sensible heat flux ( $G$ ) was calculated by the use of the following formula:

$$G = -0.2 \cdot R_n \cdot (1-0.75f) \cdot \sin\left[\frac{\pi}{6}(i-2)\right], \quad [3]$$

where  $i$  denotes the ordinal number of the respective month.

Bowen ratio  $\beta$  is derived from

$$\beta = 12.75/(W+3.9) - 0.02. \quad [4]$$

The factor  $W$  in equation [4] is calculated from the formula:

$$W = \frac{100 \cdot (d \cdot v^{0.5})^{art\left(\frac{\pi}{2}f\right)}}{t \cdot (u + 0.4)}, \quad [5]$$

where  $W$  is an agrometeorological empirical index, expressing the influence of the meteorological conditions and plant development stage on ETR. The higher the index value is, the greater the part of net radiation used for ETR,  $d$  is the saturation vapour pressure deficit (hPa),  $v$  is the wind speed ( $ms^{-1}$ ), and  $t$  is the air temperature ( $^{\circ}C$ ).

Water vapour pressure  $e$  and water vapour pressure deficit  $d$  were calculated as follows:

$$e = 5.5 \exp(0.05662t), \quad [6]$$

$$e_s = 6.123 \exp[17.25t/(t+237.2)], \quad [7]$$

$$d = e_s - e, \quad [8]$$

where  $e_s$  is the saturated water vapour pressure deficit.

The 30-year average values of water shortages for each 10-day period from April to July for each cell in reference and projection periods were calculated according to the formula:

$W = P - ETR$  (mm/10 days). Then three indices characterizing drought risk were calculated according to the following formulas:

$$WS1 = \frac{-LE \cdot N}{P \cdot 2448000}, \quad [9]$$

$$WS2 = \frac{R_n \cdot N}{P \cdot 2448000}, \quad [10]$$

$$KWSW = WS1 \times WS2, \quad [11]$$

where  $LE$  – a flux of energy used for evaporation [ $W \cdot m^{-2}$ ] (eq. 1),

$N$  – the number of seconds in the period,

$P$  – total rainfall during the period [mm],

$R_n$  – net radiation [ $W \times m^{-2}$ ] (eq. 2),

$\lambda$  – latent heat of vaporization [ $J \times kg^{-1}$ ], or [ $J \times mm^{-1} \times m^{-2}$ ].

The  $WS1$  (9) indicator is the ratio of actual evaporation to precipitation during the period, and  $WS2$  (10) is the ratio of the available energy (net radiation) to rainfall. So,  $WS1$  expresses the actual degree of dryness, while  $WS2$  is a measure of the potential degree of dryness.  $KWSW$  (comprehensive indicator of water stress) better differentiates spatial conditions of water stress than individual indicators  $WS1$  and  $WS2$  because in the cell where both are small (less than one), value of  $KWSW$  will be smaller than each of them and where they are higher, it will be greater than either of them.

The water shortages as well as all indices were mapped using Geographic Information System (GIS) procedure (Fig. 2).

Finally, the analysis of probability of occurrence of the given value of different parameters has been executed (Fig. 3). Two models of the probability distribution were used: logistic and Gompertz models described by the equations:

$$y = a/(1+b \exp(cx)) \quad \text{Logistic model} \quad [12]$$

$$y = a(\exp(-\exp(b-cx))) \quad \text{Gompertz model} \quad [13]$$

It is assumed that the coefficient  $a$  in both models must be equal to one, since the borders of curve of cumulative probability are values 0 and 1. Hence, the equations can be rearranged into

$$y = 1/(1+b \times \exp(cx)) \text{ and } y = \exp(-\exp(b-cx)),$$

and after linearization written as

$$Y = B + cx, \text{ where } Y = \ln((1-y)/y) \text{ and } B = \ln b, \quad [14]$$

$$Y = b - cx, \text{ where } Y = \ln(-\ln y). \quad [15]$$

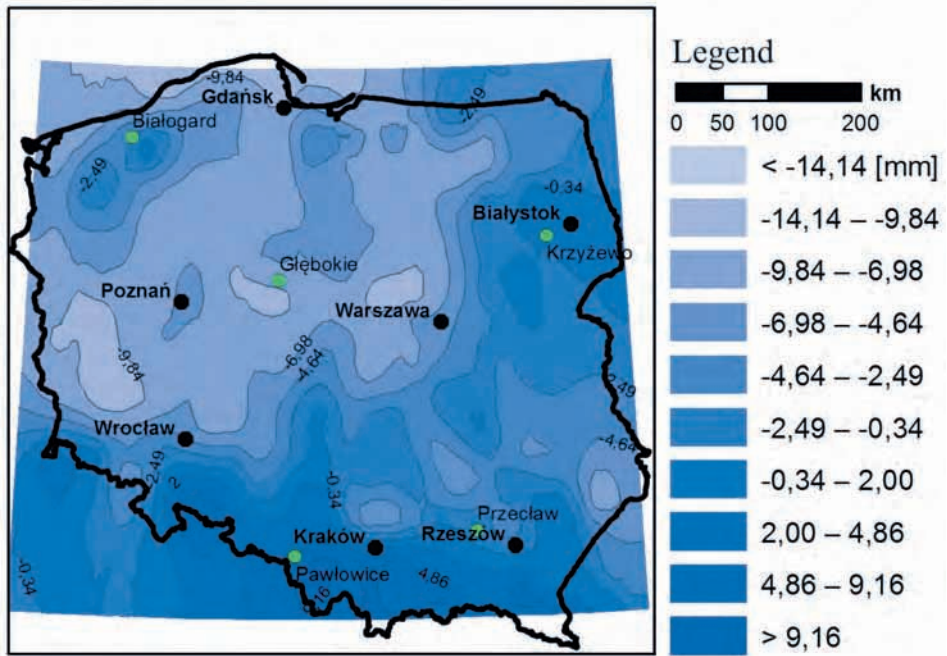


Fig. 2. Precipitation-evapotranspiration (P-ETR) [mm] in the second ten-day period of June

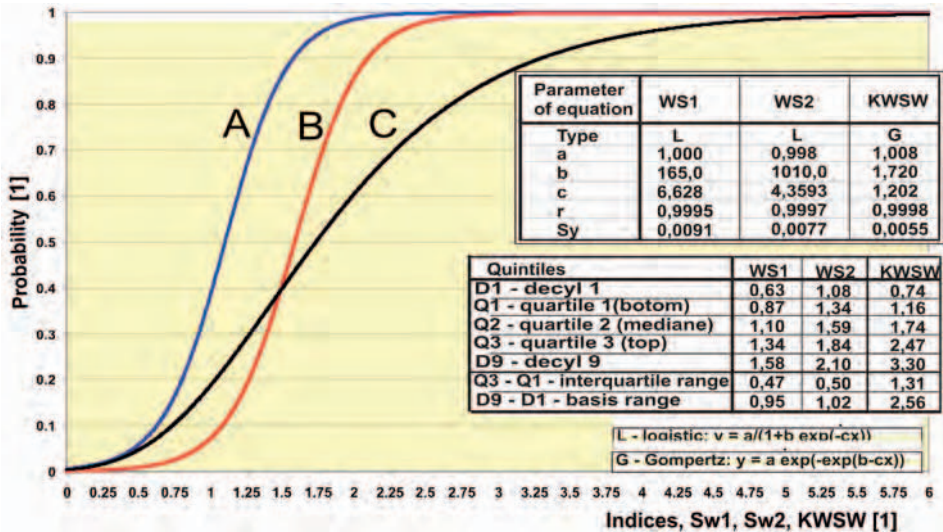


Fig. 3. Total cumulative probability (515 cells, 4 months, 3 ten-day, 2 period) of indices of water stress; blue line A – WS1, red line B – WS2, black line C – KWSW

Using this form, one can estimate the coefficients  $b$  and  $c$  using the least squares method.

Because the values of the coefficient  $a$  were assumed to be one instead of real values, the optimization of the coefficients  $b$  and  $c$  must be executed. The criterion of stopping the optimization process is reaching the minimum value of  $(y-y')$  and value of  $(y-y')^2$ . Example of such procedure result is shown in Figure 4. Very low value of the standard error of estimation  $S_y$  as well as very high value of the determination coefficient  $R^2$  show that the logistic model fits very well to the experimental data.

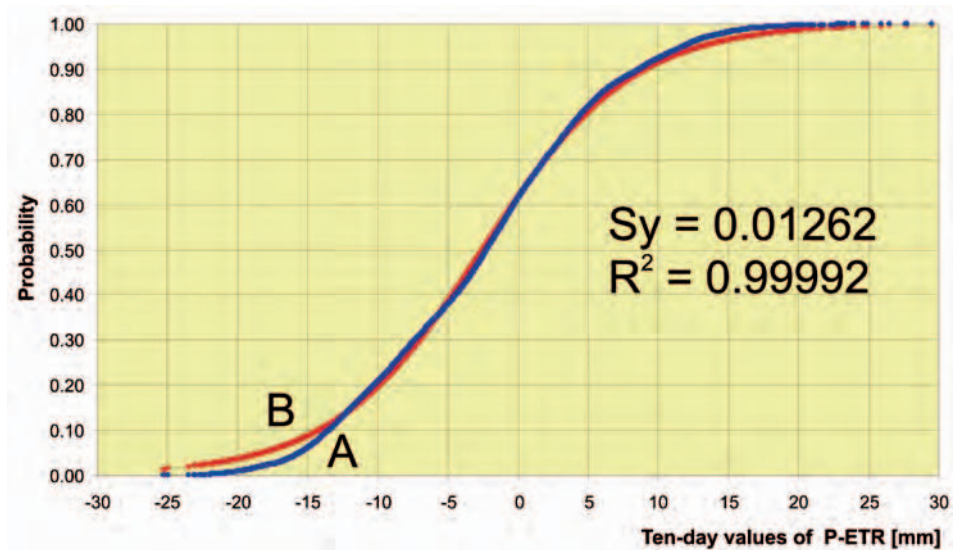


Fig. 4. Cumulative probability distribution for the two periods (reference and projection), season IV-VII, ten day values of P-ETR [mm],  $N = 515 \times 2 \times 4 \times 3 = 12360$ ; blue line A – experimental data, red line B – calculated by the use of logistic model  $y = 1/(1 + b \exp(cx))$

## Methods used in field experiments in regional scale

To get the picture of regional variation of soil water conditions important for spring barley cultivation, five stations belonging to COBORU, uniformly distributed across the country, have been selected (Fig. 1). These are the following stations: Głębokie (province Kuyavian-Pomeranian), Białogard (province Pomeranian), Krzyżewo (province Podlaskie), Przeclaw (province Subcarpathian) and Pawłowice (province Silesian). Tensiometers for soil water potential measurement at two depths, 30 and 60 cm, in two fields of two varieties of spring barley (*Suweren* and *Stratus*) and at two levels of agricultural technology

(A1 and A2) have been installed (Fig. 5). Persons who conducted observations have been trained, and they were given the following instructions.



Fig. 5. Tensiometers (A) for two depths, 30 and 60 cm, installed in the field of spring barley (B, C)

## Manual of tensiometer use

### *Principle of tensiometer working*

Tensiometer works on the following principle. If the soil is not fully saturated with water, the water penetrates the ceramic cup into the soil. The force with which the soil “sucks” water from a cup (called soil suction force) is read on the gauge. If the soil becomes wetter, the suction force decreases and the water flows from the soil into the cup. At any time, there is a balance between the strength of the soil suction and pressure in tensiometer. Soil suction force is equivalent to the soil water potential, which defines the work that must be done by the plant to get water from the soil. Indications of tensiometer between 0 and 10 centibars indicate excessive soil moisture. Indications above 80 centibars indicate the need for irrigation.

### *Operation of the instrument*

1. Tensiometer is a simple and convenient instrument for measuring of the potential of water in the soil.
2. Tensiometer consists of a ceramic cup (1), tensiometer tube (2), and a manometer (3), and the supplementary tank of water (4) (Fig. 6).

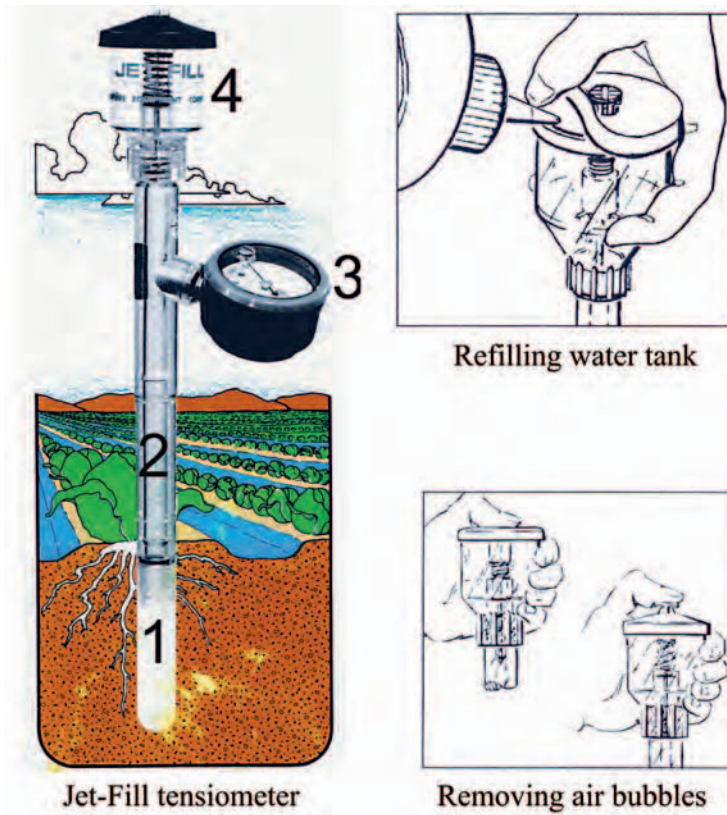


Fig. 6. Operation of tensiometer

3. Tensiometer must be placed in the soil in such a way that it ensures good contact between the cup and the soil. For this purpose, using the installation tool (proper steel tubular with a sharpened edge), the hole in the soil is made in the place where we put the tensiometer. In case of installation of the tensiometer in dry soil, pour into the bottom hole soil slightly dissolved in water coming from the hole made.
4. A properly installed tensiometer, usually after a few hours, achieves a balance of power, and readings are correct.
5. In a working tensiometer, the water level in the supplementary tank should not fall below  $\frac{3}{4}$  of the capacity.
6. Loss of water in a plastic reservoir can be made up by slightly lifting the rubber cover and adding water (Fig. 6).
7. In a working tensiometer, air bubbles coming out of the water and the ceramic cup are collected in the tensiometric tube. They should be removed by the use

of a “jet-fill” device placed in the supplementary tank by performing a dozen of quick pressures (Fig. 6). Air bubbles should disappear.

*Frequency of readings*

1. Readings on the gauge are made with accuracy of 1 centibar. Gauge covers the range from 0 to 100 centibars.
2. If difference between two successive readings is less than 1-2 centibars, the next measurement can be made after 2 days.
3. For larger changes, readings are taken on a daily basis.

The results are saved in the accompanying booklet, stating the date, time and value of the reading (Table 1).

**Table 1. Observation sheet for tensiometer measurement**

<b>OBSERVATION SHEET</b>											
<b>Observation sheet</b>											
Station.....	Name of observer .....							Year .....			
<b>Site:...</b> Suweren A1 .....	<b>Tensiometer number.....</b>							1	30 cm	2	60 cm
<b>Site:...</b> Suweren A2 .....	<b>Tensiometer number.....</b>							3	30 cm	4	60 cm
<b>Site:...</b> Stratus A1 .....	<b>Tensiometer number.....</b>							5	30 cm	6	60 cm
<b>Site:...</b> Stratus A2 .....	<b>Tensiometer number.....</b>							7	30 cm	8	60 cm

Date	Hour	Reading [cbar] at tensiometer number:							
		1	2	3	4	5	6	7	8

In each of the five stations, eight combinations of measurements have been obtained (2 varieties × 2 agrotechnical levels × 2 depths). All measurements were analysed graphically and statistically. Figure 7 shows the course of the water potential at two depths, the course of rainfall and saturation water vapour pressure deficit of air, for a given plant variety, and the level of agrotechnics.

The measurements concerning water conditions obtained according to the protocol described in this paper and barley yields for each year and each station were analysed, and regionalization of the country on the basis of usefulness for barley cultivation has been elaborated; these results will be a subject of a separate publication.

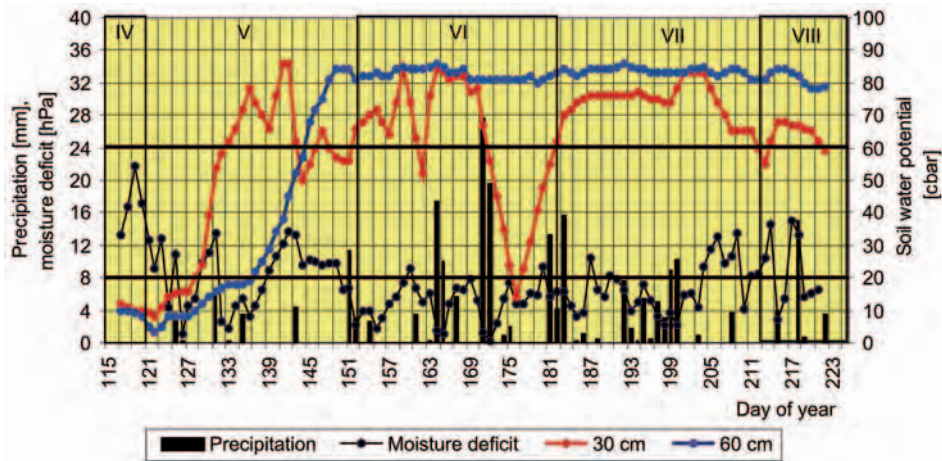


Fig. 7. Course of soil water potential at 30 cm and 60 cm depth against the background of agrometeorological conditions; location Głębokie, year 2012, variety Suveren, treatment A1

## References

- Arseniuk E., Anioł A. 2009. Biological progress and technologies of crop production in a changing climate. I Kongres Nauk Rolniczych Nauka – Praktyce 2009 [<http://www.cdr.gov.pl/kongres1/files/2.2.1.pdf>] [dostęp: 5.08.2013]. (In Polish).
- Doroszewski A., Demidowicz G., Górski T. 1997. The impact of rainfall deficiency for losses in the production of spring cereals in Poland. *Rocz. AR Pozn., CCXCI, Melior. Inż. Środ.* 17: 223-231. (In Polish).
- Dziężyc J. 1989. *Agriculture under irrigation*. PWRiL, Warszawa. (In Polish).
- Igras J., Jankowiak J. 1998. Effect of nitrogen fertilization on water use by plants growing field. *Fragm. Agronomica* 2/98: 72-86. (In Polish).
- Jankowiak J., Bieńkowski J. 2011. *Shaping and use of water resources in agriculture. Infrastructure and Ecology of Rural Areas*. PAN, Oddz. w Krakowie. Nr 5: 39-48. (In Polish).
- Szwed M., Karg G., Pińskwar I., Radziejewski M., Graczyk D., Kędziora A., Kundzewicz Z.W. 2010. Climate change and its effect on agriculture, water resources, and human health sectors in Poland. *Nat. Hazards Earth Syst. Sci.* 10: 1725-1737.
- Olejnik J., Kędziora A. 1991. A model of heat and water balance estimation and its application to land-use and climate variation. *Earth Surface Processes and Landforms* 16: 601-617.

## **Plant materials and analysed traits in the greenhouse and field experiments**

**Piotr Ogrodowicz, Krzysztof Mikołajczak, Anetta Kuczyńska,  
Karolina Krystkowiak, Maria Surma, Tadeusz Adamski**

*Institute of Plant Genetics, Polish Academy of Sciences, Poznań, Poland*

### **Introduction**

Recent climate changes have forced the breeding programmes to select new cultivars resistant to water deficiency, particularly of spring cereals that are most vulnerable to drought. For this purpose, barley genotypes originating from low-rainfall areas with genetically conditioned adaptability to drought seem to be promising (Zare et al. 2011).

Materials for the studies in POLAPGEN-BD project consisted of three populations of spring barley (*Hordeum vulgare* L.) recombinant inbred lines (RILs). Various plant materials have been applied in genetic and genomic studies, among them populations of homozygous lines derived by different methods are the most commonly used (e.g., Heun et al. 1991; Ramsay et al. 2000; Hori et al. 2003; Zare et al. 2011; Mansour et al. 2014). Homozygous lines can be attained by the use of doubled haploid (DH) system or single seed descent (SSD) technique. Both DH and SSD systems allow to obtain homozygous lines in a relatively short time, but DHs are completely homozygous, whereas SSD lines may contain the residual heterozygosity. However, the advantage of the SSD over DH technique is the higher probability of obtaining favourable recombinants in SSD populations due to the greater number of *crossing-over*.

Barley populations derived from crosses between local cultivars and adapted to dry environments, with conjunction to molecular approaches, may permit to select genotypes that combine desirable features from both parents and result in high, stable productivity in optimal as well as under periodic stress conditions in Europe. We researched the genetic background of Syrian germplasm to exploit its natural adaptive potential of growth in arid areas. For this reason, the European and Syrian parental varieties were used as a female and male, respectively.

## Plant materials

Three populations of RILs obtained from the crosses between European and Syrian cultivars: Maresi  $\times$  Cam/B1/CI08887//CI05761 (MCamB), Lubuski  $\times$  Cam/B1/CI08887//CI05761 (LCamB) and Georgie  $\times$  Harmal (GH) were used in the studies.

Lubuski is an old Polish cultivar derived from Heines-Haisa/Skrzeszowicki hybrid. Maresi is a German semi-dwarf cultivar with the pedigree Cebeco-6801/GB-1605//HA-46459-68. Georgie is a British cultivar with the pedigree Vada/Zephyr (Fig. 1). Cam/B1/CI08887//CI05761 and Harmal are a Syrian breeding line and cultivar, respectively, adapted to areas with shortage of water. The Syrian genotypes were supplied to Dr. A. Górny by Drs. S. Grando and S. Ceccarelli from ICARDA in Aleppo, while European cultivars originated from the collection of IPG PAS Poznań. Parents for crosses were chosen on the basis of earlier studies conducted by Górny and coworkers (Krzemińska and Górny 2003; Górny and Ratajczak 2008). Additionally, two modern European cultivars, Sebastian and Stratus, were included in the experiments as the standards. Sebastian is a Danish variety with short straw and moderate susceptibility to lodging and straw breakdown with the pedigree Viskosa/Lux. Stratus (registered in 1999, Poland) is a two-row malting barley with good lodging resistance.

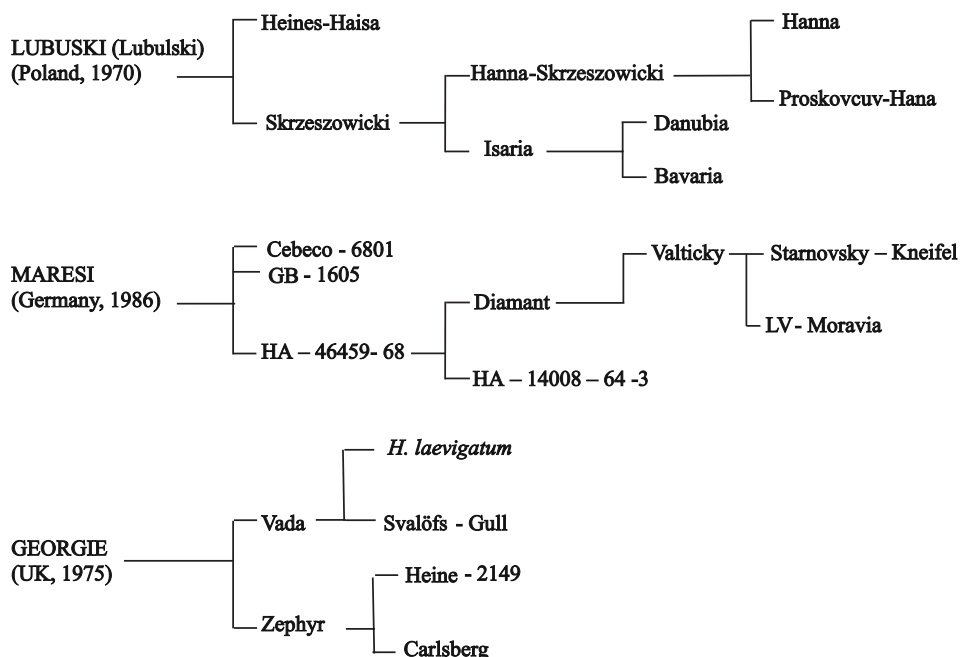


Fig. 1. Pedigree of parental cultivars

The SSD was proposed by Goulden (1939) and later modified by Grafius (1965). The use of RILs for construction of genetic maps is very powerful as each line is nearly homozygous and can be propagated as genetically identical individuals, allowing genotyping and phenotyping of many traits under various environmental conditions to be performed on the same material. SSD populations have been hypothesized to vary from DH populations because of more opportunities for genetic recombination (Snape 1976; Riggs and Snape 1977). One great advantage of this technique is the opportunity to grow three successive generations in 1 year (spring cereals) under greenhouse conditions. The plants can be grown in dense populations, and larger numbers can be kept under controlled conditions to accelerate the generation time, since no selection is made until homozygosity has been achieved (Surma et al. 2006; Kuczyńska et al. 2007).

With this procedure, one seed is collected from each individual plant starting from  $F_2$  hybrids and then  $F_3$  generation is grown. Similarly in  $F_3$  and subsequent generation, one random seed is selected from every plant (Table 1). In  $F_6$  or later generation, when plants become nearly homozygous, all seeds from each plant are harvested.

**Table 1. The SSD method**

Step	Description
Hybridization	Crossing of selected parents
$F_1$ generation	$F_1$ seeds grown and bulk collected
$F_2$ generation	One seed from each $F_2$ plant is selected randomly and mixed
$F_3$ generation	$F_3$ seeds are grown and collected as above
$F_4$ – $F_7$ generation	The similar procedure as above is carried out
$F_8$ generation	Seed multiplication for distribution

RILs were developed in the Institute of Plant Genetics Polish Academy of Sciences using SSD technique associated with *in vitro* culture as follows: the crosses between Maresi and Cam/B1/CI, Lubuski and Cam/B1/CI, Georgie and Harmal were performed to produce  $F_1$  seeds. Growing  $F_1$  plants and selfing to produce  $F_2$  generations were done. SSD lines were created starting from  $F_2$  individuals for six generations until  $F_8$ . In each cross combination, about 150 lines were developed, and out of them, 100 were randomly chosen for the experiments. Seeds from plants of  $F_2$  generation were collected about 16 days after flowering stage (milky ripe stage), and then the embryos were isolated. Immature embryos were cultured *in vitro* on B5 medium of Gamborg (1968) (Table 2).

**Table 2. Composition of the Gamborg's B5 basal medium**

Ingredients	Milligrams/litre
$(\text{NH}_4)_2\text{SO}_4$	134
$\text{KNO}_3$	2500
$\text{NaH}_2\text{PO}_4 \times \text{H}_2\text{O}$	150
$\text{CaCl}_2 \times 2\text{H}_2\text{O}$	150
$\text{MgSO}_4 \times 7\text{H}_2\text{O}$	250
$\text{FeSO}_4 \times 7\text{H}_2\text{O}$	28
KI	0.75
$\text{MnSO}_4 \times \text{H}_2\text{O}$	10
$\text{H}_3\text{BO}_3$	3
$\text{ZnSO}_4 \times 7\text{H}_2\text{O}$	2
$\text{Na}_2\text{MoO}_4 \times 2\text{H}_2\text{O}$	0.25
$\text{CuSO}_4$	0.025
$\text{CoCl}_2 \times 6\text{H}_2\text{O}$	0.025
Sucrose	20,000
Myo-inositol	100
Nicotinic acid	1
Pyridoxine-HCl	1
Thiamine-HCl	10
pH	5.6-5.8
Agar	8000

The embryos were incubated in the dark at 22-25°C for 1 week. Then the probes were incubated in light under a 16-h photoperiod at the same temperature for 4 days. Green plantlets were transplanted in pots containing 3 kg of the peaty soil with an admixture of sand (fraction 0-2 mm). All the plants were placed in the greenhouse and kept at 20°C/16°C day/night temperature regime with 16-h photoperiod to reach the maturity and produce seeds. The seeds were collected in the appropriate phase of plant development (Fig. 2).

This procedure was repeated until the  $F_8$  generation. All seeds were collected from each of the 100  $F_8$  plants. Seed multiplication for distribution was performed in Nagradowice Breeding Station of Cereals (Fig. 3).

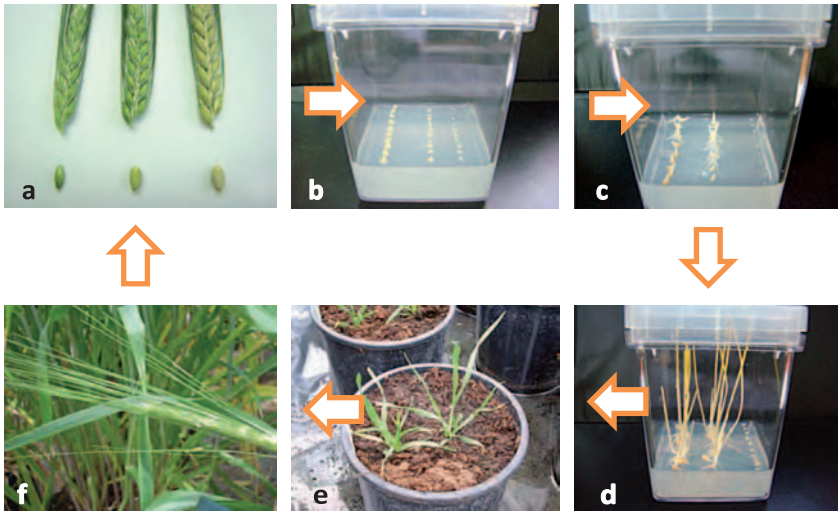


Fig. 2. Steps in the procedure of obtaining RIL combined with *in vitro* culture: (a) spikes and immature kernels from which the embryos were dissected; (b) embryos placed on B5 medium; (c) embryos developed after 4 days of culture; (d) plantlets after 8 days of *in vitro* culture; (e) plants transplanted in pots; and (f) spike plants after flowering stage



Fig. 3. Seed multiplication plots in Nagradowice Breeding Station of Cereals

## Greenhouse experiment

Yield and yield-forming traits were observed in lines and their parental genotypes as well as standard cultivars. Phenotyping was related to 22 characteristics associated, among others, with the spike morphology (Fig. 4), plant architecture, grain and straw yield, as well as dates of achieving selected development stages. Plants were harvested on maturity and wrapped up awaiting for biometric observations (Figs 5 and 6). The evaluated traits and measurements methods are



Fig. 4. Variation of the spike morphology within the studied barley populations



Fig. 5. Barley plants harvested on maturity and secured for biometric observations

listed in Table 3. Plants were observed under control and water-deficit conditions according to the procedure described by Pecio et al. (2014, this volume) with the exception of treatment I, which was applied in the three-leaf stage (13 in BBCH scale) for 10 days.

### **Field experiments**

Three populations of RIL (100 lines per each population), their parental genotypes as well as standard cultivars were evaluated at the Institute of Plant

**Table 3. Description of agronomic traits observed in the greenhouse experiments**

Trait (unit)	Trait description
Number of productive tillers per plant	Number of tillers with spikes containing grain in a plant, average for 10 mature plants in a pot
Number of tillers per plant	Number of tillers in a plant, average for 10 mature plants in a pot
Length of main stem (cm)	Length of main stem from ground level to the end of spike (without awns), average for 10 main stems in a pot
Length of main spike (cm)	Length of mature spike from main stem from the base to the top (without awns), average for 10 main spikes in a pot
Length of lateral stem (cm)	Length of lateral stem from ground level to the end of spike, average for 10 lateral stems in a pot
Length of lateral spike (cm)	Length of mature spike from lateral stem from base to the top (without awns), average for 10 lateral spikes in a pot
Number of spikelets per main spike	Number of spikelets in spike of main stem, average for 10 main spikes in a pot
Number of spikelets per lateral spike	Number of spikelets per one spike of lateral stem, average for 10 lateral spikes in a pot
Number of grains per main spike	Number of grains collected from one spike of main stem, average for 10 main spikes in a pot
Number of grains per lateral spike	Number of grains collected from one spike of lateral stem, average for 10 lateral spikes in a pot
Grain weight per plant (g)	Weight of grain collected from one plant, average for 10 plants
Straw weight per plant (g)	Weight of straw from a plant, average for 10 plants
Grain weight per lateral spike (g)	Weight of grain collected from one spike of lateral stem, average for 10 lateral spikes
Grain weight per main spike (g)	Weight of grain collected from one spike of the main stem, average for 10 main spikes
1000-grain weight (g)	Weight of 1000 grains, average ( $1000 \times$ average weight of one grain) for 20 spikes in a pot
Grain weight per pot (g)	Weight of grain collected from all plants in a pot
Straw weight per pot (g)	Weight of straw from all plants in a pot
Three leaves stage (days)	Number of days from sowing to emergence of third leaf (13 BBCH) observed for at least 50% of plants
Tillering stage (days)	Number of days from sowing to tillering (21 BBCH) observed for at least 50% of plants
Flag leaf stage (days)	Number of days from sowing to emergence of flag leaf (37 BBCH) observed for at least 50% of plants
Heading stage (days)	Number of days from sowing to emergence of inflorescence (spike) from the flag leaf (51 BBCH) observed for at least 50% of plants
Protein content in grain (%)	Average content (%) of protein in grains, calculated as ratio of mass of protein to whole grain mass for a sample of at least 10 g of grains from a pot

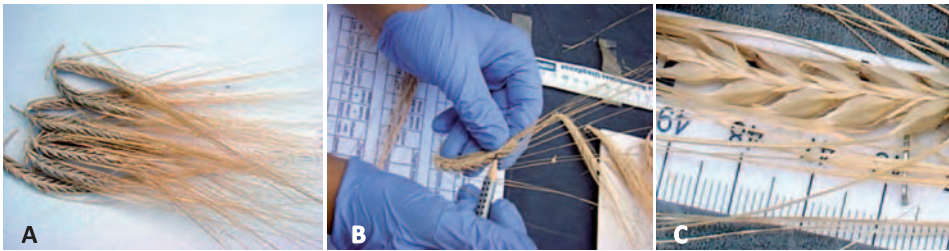


Fig. 6. Biometric analysis of spikes: A – main spikes collected from a pot; B – measurement of spikelets number per spike; and C – measurement of spike length

Genetics Polish Academy of Sciences experimental station at Cerekwica located 30 km north of Poznań (Western Poland, 52°53'N; 16°67'E) – populations of M<sub>1</sub>CamB and L<sub>1</sub>CamB in 2011-2013, and GH population in 2012-2014. Field trials were established on luvisol type of soil (according to the World Reference Base for Soil Resources 2006), and each year fertilization was applied according to soil-test recommendations for cultivation of fodder barley. Each population along with its parental and standard cultivars was examined in field experiments conducted in a completely randomized design with three replications, in each year. Seeds were sown in plots of 1 m<sup>2</sup> size with a sowing rate of 300 seeds m<sup>-2</sup>.

The soil moisture was recorded in each plot during the field experiments using FOM/mts metric (Fig. 7). Moreover, meteorological parameters were measured at Cerekwica.

The examined traits and methods of measurements are presented in Table 4.

Heading stage was noted during vegetation, whereas plant height, length of main spikes, grain number per spike, grain weight per spike, 1000-grain weight and grain yield per plot were observed in mature plants.



Fig. 7. FOM/mts – hand-held device designed for field measurements of soil moisture and temperature

**Table 4. Agronomic traits observed in the field experiments**

Trait (unit)	Method of measurements
Heading stage (days)	Number of days from sowing to the beginning of heading – approximately 50% of spikes in a plot (growth stage 51 according to the BBCH scale)
Length of main stem (cm)	Measured from soil surface to the tip of the spike (without awns) for 20 randomly selected plants
Length of main spike (cm)	Measured from the base of spike to the tip of the terminal spikelet (without awns) for 20 randomly selected plants
Number of grains per main spike	Counted on the basis of 20 randomly selected main spikes from the plot
Grain weight per main spike (g)	Average weight of hand-threshed grain from 20 randomly selected main spikes from the plot
1000-grain weight (g)	1000 × weight of one grain averaged for weight of grains from 20 main spikes
Grain yield (kg)	Weight of grain harvested from plot and converted to kilograms per 1 m <sup>2</sup>

## References

- Gamborg O.L., Miller R.A., Ojima K. 1968. Nutrient requirements of suspension cultures of soybean root cells. *Experimental Cell Research* 50: 151-158.
- Goulden C.H. 1939. Problems in plant selection. Proc. Seventh International Genetical Congress Edinburgh, Scotland, pp. 132-133.
- Górny A.G., Ratajczak D. 2008. Efficiency of nitrogen and phosphorus utilization in progenies of factorial crosses between European and exotic cultivars of spring barley. *J. Appl. Genet.* 49: 349-355.
- Grafius J.E. 1965. Short cuts in plant breeding. *Crop Sci.* 5: 377.
- Heun M., Kennedy A.E., Anderson J.A., Lapitan N.L.V., Sorrells M.E., Tanksley S.D. 1991. Construction of a restriction fragment length polymorphism map for barley (*Hordeum vulgare*). *Genome* 34: 437-447.
- Hori K., Kobayashi T., Shimizu A., Sato K., Takeda K., Kawasaki S. 2003. Efficient construction of high-density linkage map and its application to QTL analysis in barley. *Theor. Appl. Genet.* 107: 806-813.
- Krzemińska A., Górny A.G. 2003. Genotype-dependent variation in the transpiration efficiency of plants and photosynthetic activity of flag leaves in spring barley under varied nutrition. *J. Appl. Genet.* 44: 481-490.

- Kuczyńska A., Surma M., Kaczmarek Z., Adamski T. 2007. Relationship between phenotypic and genetic diversity of parental genotypes and the frequency of transgression effects in barley (*Hordeum vulgare* L.). *Plant Breed.* 126: 361-368.
- Mansour E., Casas A.M., Gracia M.P., Mollina-Cano J.L., Moralejo M., Cattiveili L., Thomas W.T.B., Igartua E. 2014. Quantitative trait loci for agronomic traits in an elite barley population for Mediterranean conditions. *Mol. Breed.* 33: 249-65.
- Ramsay L., Maccaulay M., Ivanissevich S., MacLean K., Cardle L., Fuller J. 2000. A simple sequence repeat-based linkage map of barley. *Genetics* 156:1997-2005.
- Riggs T.J., Snape J.W. 1977. Effects of linkage and interaction in a comparison of theoretical populations derived by diploidized haploid and single seed descent methods. *Theor. Appl. Genet.* 49: 111-115.
- Snape J.W. 1976. A theoretical comparison of diploidized haploid and single seed descent populations. *Heredity* 36: 275-277.
- Surma M., Adamski T., Kaczmarek Z. 2006. Phenotypic distribution of barley SSD lines and doubled haploids derived from F1 and F2 hybrids. *Euphytica* 149: 19-25.
- Zare M., Azizi M.H., Bazrafshan F. 2011. Effect of drought stress on some agronomic traits in ten barley (*Hordeum vulgare* L.) cultivars. *Tech. J. Engin. & App. Sci.* 1(3): 57-62.

## **A method for precision irrigation control in greenhouse experiment and its use to study drought stress effect on spring barley**

**Alicja Pecio<sup>1</sup>, Damian Wach<sup>1</sup>, Anna Koçoń<sup>1</sup>, Grzegorz Józefaciuk<sup>2</sup>**

<sup>1</sup> *Institute of Soil Science and Plant Cultivation – State Research Institute, Pulawy, Poland*

<sup>2</sup> *Institute of Agrophysics, Polish Academy of Sciences, Lublin, Poland*

### **Introduction**

#### *Water use by plants*

A plant requires water for photosynthesis, tissue rigidity (turgidity) and carbohydrate production (Jones 1992; Roberts 2005). The leaves drive up water from the soil, via the roots, through the plant's xylem. The driving force governing this process is transpiration: the loss of water from microscopic stomata openings in the leaves. The main purpose of stomatal opening is to exchange CO<sub>2</sub> and O<sub>2</sub> with the atmosphere; CO<sub>2</sub> is needed to build carbohydrates, allowing plants to grow, while O<sub>2</sub> is expelled during photosynthesis and taken up during respiration (during which CO<sub>2</sub> is disposed of), a process that serves to maintain existing tissue. The water obtained from the soil contains also vital mineral nutrients that plants require for biochemical processes.

Transpiration is, in many ways, an undesirable trade-off of canopy gas exchange; it entails a significant loss of water, much more than is needed to maintain turgidity and for photosynthesis. A plant therefore needs a continuous supply of water, with adequate nutrients dissolved within it, to maintain healthy functioning. In areas where the vegetation's water demand is frequently larger than the amount of water available in the soil, plants will suffer. This will result in reduced growth or even plant mortality. For natural vegetation, these periods of drought define the distinctive plant communities that have adapted to and can survive under these dry conditions.

High amount of water stored in the soil is used by a plant. At field capacity, when soil water content is near saturation and it is bound mainly by gravitational

forces, most water in the soil is readily available to the plant. Plants use little gravitational water since it drains quickly to a depth below the root zone. As the soil dries and the water content decreases, the remaining water is present as thin films around the soil particles. These films become increasingly thinner upon continued drying of the soil (Fig. 1), and the forces binding the remaining water become increasingly larger (pF value increases).

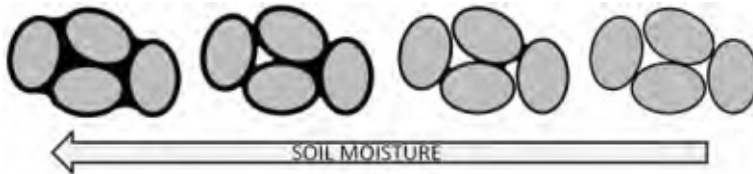


Fig. 1. Water films around soil particles

Consequently, the force that the plant has to exert to remove the remaining water increases as the soil dries. Eventually, a point is reached at which the force exerted by plants is not sufficient for sustaining growth. At this point, known as the wilting point, the plant starts to wilt. At wilting point, the soil moisture tension equals 15 bars (1500 kPa), which corresponds to pF of 4.2 (log 15,000 cm H<sub>2</sub>O). The unit Pa (Pascal) is the pressure unit in the SI system and 1 kPa=0.01 bar. The amount of water held between the field capacity and the wilting point is called available water.

Between the field capacity and the wilting point, water is available to the plant (Fig. 2).

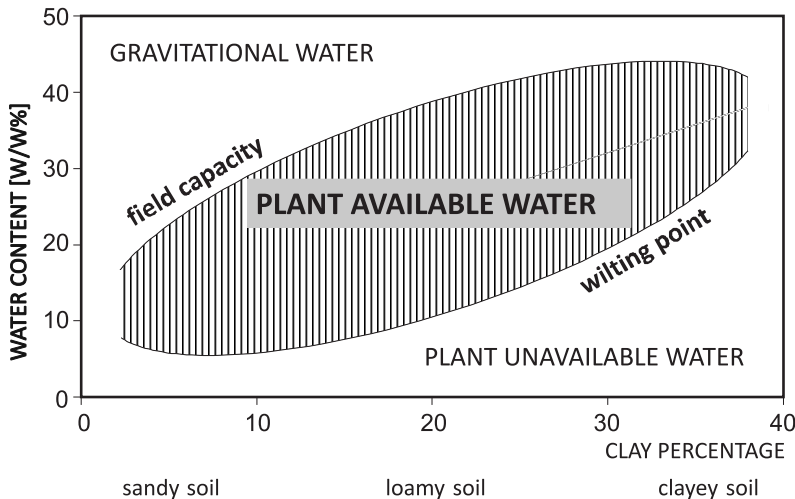


Fig. 2. Soil water between the field capacity and the wilting point is available to the plant

The amount of water available to plant varies with soil texture (and physical condition). A sandy soil, which has largest particles and lowest surface area, can store the smallest amount of water, and most of it would be available for plants. A clay soil, which has smallest particles and highest surface area, may hold more water, but because of the strong attraction of water to clay particles, only its small part may be available for plant. Soils with the greatest amount of available water are usually those with a loamy texture and good structure.

### *Drought*

Drought, from the point of view of plant stress, is the decreased water availability and decreased water potential. Even small changes in water supply from the soil can exacerbate diurnal patterns where plants are prone to dehydration during the day (when stomates are open and relative humidity is low); however, the plants rehydrate at night when stomates are closed. As a drought period persists and soil drying becomes severe, the plant will eventually become unable to maintain hydration even with the closed stomates. Thus, plants respond to drought both by rapid adjustment, particularly to stomatal aperture, throughout the course of a day and by longer-term adjustment to growth and dehydration-protective mechanisms (Henckel 1964; Raschke 1975; Farquhar and Sharkey 1982; Sexton and Roberts 1982; Jenks et al. 2002; Nambara and Marion-Poll 2005; Kerstiens 2006). Stress physiologists have traditionally described plant drought responses as escape, avoidance and tolerance mechanisms (Levitt 1972; Ludlow 1989).

Drought tolerance is the ability of the plant to cope with reduced water potential of the plant tissue (Jenks and Hasegawa 2014). This reduced water potential may be accompanied by either small or large changes in tissue water content, depending on the severity of the stress and the plant species involved. Drought tolerance mechanisms allow the plant to function, or at least survive, at reduced water potential. Drought tolerance can be difficult to quantify experimentally, as it requires that some steps be taken to ensure that different plants being tested are exposed to the same severity of stress (i.e., the same water potential).

Most often, we concentrate on drought tolerance differences between plant genotypes. Many of these differences are essentially differences in plant response to low water potential, often referred to as phenotypic plasticity. Other differences in tolerance are determined by constitutive differences in morphology, cellular structure or metabolism that are often referred to as drought adaptations. However, there is overlap between drought adaptation and phenotypic plasticity, as much of the variation between drought resistant versus less drought resistant plant varieties or species includes differences in the type or extent of phenotypic plasticity induced by drought.

In the case of barley (*Hordeum vulgare* L.), strains and cultivars differ considerably in their response and adaptation to drought stress (Zare et al. 2011).

These differences at phenotype level are manifested by compensation of one yield component by another one (Cossani et al. 2009). Therefore, comparative analysis of the yield components between plants superimposed to stress and unstressed may help in predicting their stress tolerance and selection of more tolerant genotypes.

### *Irrigation*

To meet field crop water requirements, supplementing water stored in soil via irrigation may be required. The irrigation can ideally provide the crop with enough water to grow successfully, with the aim to optimize water use efficiency (WUE), while avoiding waste or creation of excess water around the plant roots.

The irrigation system employed is a major determinant of on-farm irrigation performances and may be characterized by one of the three categories: surface irrigation, sprinkler irrigation, and micro or localized irrigation (Ayars et al. 1999; Pereira et al. 2002; Smith et al. 2005).

The choice of irrigation scheduling method depends, to a large extent, on the irrigator's objectives and the irrigation system available. When water supplies are limited, farmers place their emphasis on maximizing WUE. These scheduling principles clearly deviate from those aimed at maximizing yield by fully meeting crop water requirements. In this regard, deficit irrigation (DI) strategies have demonstrated that, under scarcity scenarios and with sufficient knowledge to manage DI optimally, the objective of maintaining or even increasing farmers' profit may be attainable while reducing irrigation water use (English 1990; English and Raja 1996; Fereres and Soriano 2007).

To reduce uncertainty and risk associated with the employment of irrigation strategies, computer models that stimulate crop performance can assist water managers in optimizing a limited supply of irrigation water. There are a few well-established models: two FAO crop models AquaCrop (Raes et al. 2009; Steduto et al. 2009) and CROPWAT 8.0, CropSyst (Stockle et al. 1997) and WOFOST (Diepen et al. 1989).

### *Automated irrigation scheduling*

The degree of automation of the irrigation systems, as well as their related advantages, is variable. An automated irrigation system saves time and effort for the irrigation manager and also allows higher flexibility in scheduling farm work. The irrigation control systems of these modern systems also offer the possibility to store information on control variables, which represent a valuable feedback to identify problems (e.g. water leakages, undesirable pH or electrical conductivity levels in the irrigation water, etc.).

There are three different ways to perform automated irrigation: time-based, volume-based or based on other (soil, plant or climate related) variables. In the

former two groups the irrigation scheduler plays a fundamental role by setting either the time and duration of irrigation (time-based) or the volume of water to be supplied to crops (volume-based). In the latter, however, the system is designed to work more autonomously.

In time-based automation, the irrigation interval is determined from the amount of water to be supplied, application rate of the emitters and number of emitters. Volume-based automation consists of measuring the water supplied during each irrigation event to automatically interrupt the water flow once the applied water volume has met the target volume. Both time-based and volume-based irrigation systems require an early estimate of crop evapotranspiration. An effective procedure to adjust estimated to real crop water needs is to monitor one or more of the available soil and plant water status indicators.

Irrigation automation based on measurements of one or more variables of the soil-plant-atmosphere continuum emerged from the need to increase precision in irrigation control to achieve specific objectives in crop management and to maximize irrigation efficiency. Effective operation of such systems requires a sensing system that determines irrigation need in real time; this prerequisite rules out large-scale manual monitoring programmes for such purposes and indicates a need for automated monitoring systems (Jones 2004). These systems set the irrigation calendar by assessing one or more control variables that are continuously recorded. Edaphic factors, such as soil moisture content, meteorological factors, such as atmospheric evaporative demand, relative humidity, air temperature or solar radiation, or plant physiology-based factors, such as leaf temperature, micromorphometric variations of some plant organs or sap flow have been proposed as indicators to develop self-controlled automatic irrigation systems. As indicated by Fernández and Cuevas (2010), the variable sensed by the indicator for irrigation scheduling must be closely related to production parameters of economic importance (e.g. crop yield and fruit quality).

Irrigation scheduling based on soil water determination has been widely reported. A soil water-based irrigation control system uses real-time information on the soil water status to bypass a time-based preprogrammed schedule or to maintain soil water content in the root zone within a specified moisture range that is optimal for plant growth (Muñoz-Carpena and Dukes 2005). Effectiveness of these soil sensor-based irrigation technologies has been successfully assessed on field crops (Meron et al. 2001; Wang et al. 2007; Muñoz-Carpena et al. 2008), on residential green areas (McCready et al. 2009) or on ornamental potted plants (Nemali and van Iersel 2006; Burnett and van Iersel 2008).

As pointed out by Greenwood et al. (2010), the use of sensor-based procedures for soil water management varies with the type of crop and environment. Accordingly, shallow-rooted crops (e.g. potted plants) could be managed with soil water sensors installed at one depth only, whereas deep-rooted agricultural

crops would require a vertical profile of sensors to allow irrigation according to the distribution of soil water down the profile. This ensures optimal use of the stored water in the soil profile and hence substantial saving of irrigation water.

When DI strategies are used, monitoring of the soil (or the plant) water status becomes even more critical for minimization of risks. These irrigation strategies normally exploit some plant physiological traits or sensitivity differences to water stress of specific phenological stages to enhance WUE (Feres and Soriano 2007). However, the fulfilment of the desired crop response under these strategies usually requires very precise irrigation water management, since the crop response may dramatically deviate from the expected response in a narrow range of soil moisture availabilities.

### Experimental method in Grabów Experimental Station

The system of irrigation control in the greenhouse experiment in Grabów Experimental Station (E 21° 39', N 51° 21') of the Institute of Soil Science and Plant Cultivation – State Research Institute in Puławy, Poland, was installed in year 2010 by Adviser company, [www.phu-adviser.pl](http://www.phu-adviser.pl). The system enabled automatic monitoring and regulation of soil moisture in pots of the experiment on “Studies of spring barley yield components under conditions of moisture deficit” in 2011-2014 years.

The purpose of the pot experiment was to determine the response of the population of 300 lines derived from parental forms of different climatic habits: Maresi (Germany), CAM/B1/CI08887//CI05761 and Harmal (Syria), Georgie (Great Britain) and 60 cultivars registered in Poland to temporal drought stress. The lines were tested against short-term drought stresses introduced at the tillering stage (BBCH 23, 31 days after sowings) for 11 days (S1) or at full flag leaf stage (BBCH 45-47, 50 days after sowings) for 14 days (S2). At the control treatment (C), soil moisture was maintained at the optimal level of 13%-15% w/w for the whole vegetation period, and in the treatments S1 and S2, at the level of 5%-6% w/w (see Table 1). After the drought stresses applications, barley plants showed visual symptoms of turgidity loss, but they were able to recover after re-watering.

**Table 1. Soil pF values and corresponding moisture content**

pF	3.2	3.4	3.6	3.8	4.2
Soil moisture (%w/w)	8.0	6.75	5.7	4.75	3.6

After harvest, grain yield and yield components – productive tillering (number of fertile tillers), number of grains per spike, weight of 1000 grains and harvest index – were measured.

### *Greenhouse*

The experiment was located in a greenhouse provided with mobile glass roof and walls, which enabled plants to grow under natural conditions and protect them against uncontrolled precipitation. The greenhouse is equipped with eight two-row tables designed for 1088 experimental containers (Fig. 3).

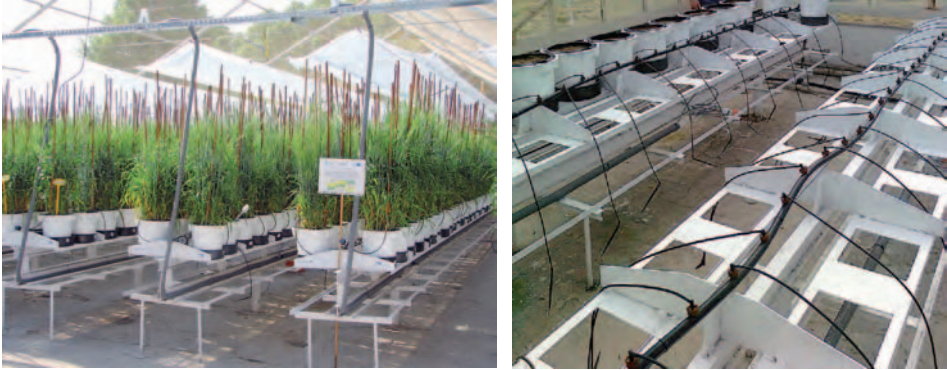


Fig. 3. Greenhouse with open roof and walls equipped with special tables

### *Air temperature and humidity control*

The air temperature and humidity inside the greenhouse was measured each second by the recorder AR 236 (Fig. 4). The mean air temperature at S1 stress equalled to 13.1°C and at S2 stress to 19.2°C. Air moisture varied at the mean level of 67% and 72%, respectively. Mean number of hours with sun per day varied from 8.2 during S1 stress to 8.5 at S2 stress.



Fig. 4. Air temperature and humidity recorder

### Procedure of soil preparation

Each experimental pot was filled with 9 kg of loamy soil taken from the field and mixed with sand in weight proportion 7 : 2. Before the mixture was used, its texture and chemical and physical properties were determined. It was characterized by very high phosphorus and potassium abundance, middle magnesium and low sulfur abundance. The content of available micronutrients necessary for plants stayed at the level of high Mo and Zn abundance (the fertilization was not applied), middle Fe, Cu, Mn abundance and low B abundance. On the base of chemical analysis, the soil mixture was sufficiently supplied with all nutrients. The nutrients in mineral medium were applied in the rates calculated per each pot (9 kg of the soil mixture) based on fertilization recommendations of the Institute of Soil Science and Plant Cultivation – State Research Institute (Fertilizer Recommendations, 1990; Jadczyzyn et al. 2008). Nitrogen rate, 2.4 g N in  $\text{NH}_4\text{NO}_3$ , was split into two doses, 1.2 g each applied just after sowings and on the end of tillering stage. The other macronutrients in the following rates: 0.9 g P in  $\text{KH}_2\text{PO}_4$ ; 1.62 g K in  $\text{KH}_2\text{PO}_4$  and  $\text{K}_2\text{SO}_4$ ; 0.6 g Mg in  $\text{MgSO}_4 \cdot 7\text{H}_2\text{O}$  and micronutrients: 5 mg  $\text{H}_3\text{BO}_3$ ; 2 mg  $\text{CuSO}_4$ ; 10 mg  $\text{MnSO}_4 \cdot 4\text{H}_2\text{O}$  and 50 mg  $\text{Fe}(\text{C}_6\text{H}_5\text{O}_7) \cdot 3\text{H}_2\text{O}$  were applied before sowings.

For irrigation purposes, its water properties were characterized by water retention curve pF (Fig. 5).

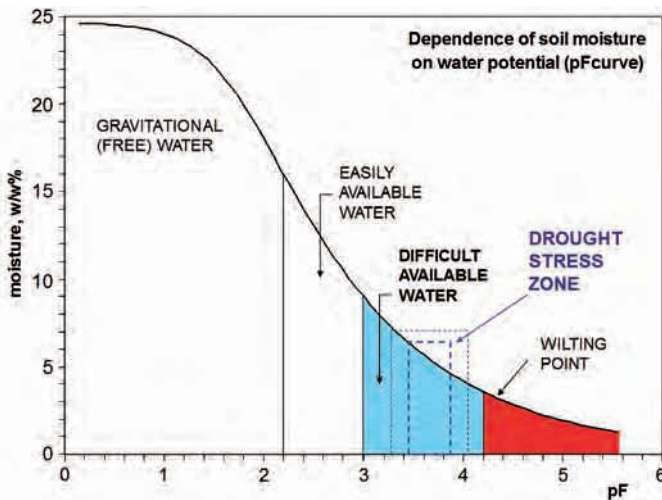


Fig. 5. Water retention curve

The pF value is defined as a logarithm of the pressure  $p$  (expressed in centimeters of water head) necessary for water removal from soil capillaries. The thinner the capillary, the higher the pressure and more difficult for plant to uptake water. Assuming that 1 cm of water column corresponds to 1 hPa, one has  $p[\text{hPa}] = 10^{\text{pF}}$ .

The areas of different soil water availability for plants are presented in Figure 6. So-called gravitational water flows out from soil profile due to gravitation, and practically it is not used by plants under field conditions. Plant available water is situated in the area between pF 2.2 (water field capacity) and pF 4.2 (permanent wilting point). Available water is divided into “easily” available or “difficult” available for plants.

The drought stress was conducted in the area of difficult water availability and always above permanent wilting point. The conditions for the drought stress were established by soil pF range from 3.4 to 3.6, that is, for soil moisture ranging from 6.7% to 5.7% (Fig. 5, Table 1). Practically, it was maintained between 8.0% and 4.75%.

### *Irrigation control strategy*

Drip irrigation of each pot individually was steered by GPI-SM300 computer system of soil moisture control and corrected using an intentionally constructed device with an electronic balance moved by a special trolley on wheels.

This irrigation control system is based on GPI data logger operating with DeltaLINK software installed on PC and SM300 soil moisture sensor supplied by Delta-T Devices Ltd (Fig. 6). It is particularly directed at container-grown plants.

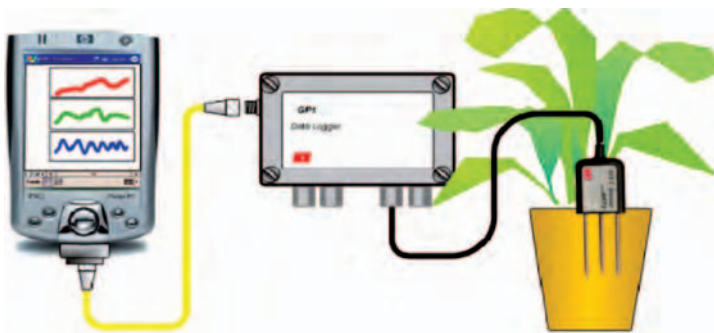


Fig. 6. Scheme of GPI-SM300 irrigation control system

The system in greenhouse of ES Grabów consists of eight GPI data loggers. Each of them cooperates with four SM300 soil moisture sensors installed at four containers on each table row.

### *GPI Data Logger*

The GPI data logger is a complete logging solution housed in an IP67 enclosure with battery power (Fig. 7). The internal memory can hold >600,000 readings – more than enough for 1 year’s operation. The optional GP-PBA-X50 Precision Bridge Adapter enables a GPI to log up to two bridge sensors such as



Fig. 7. GP1 loggers in greenhouse of Grabów experimental station

pressure transducers and strain gauges and allows for the logging of up to two water-filled tensiometers.

When connected to one or two SM300, the GP1 logger provides high-accuracy recording of moisture content. This compact data logger has two high-resolution differential analogue channels (0-2.5 V) that enable the ThetaProbe's outstanding accuracy to be achieved over its full operating range. With the optional GP-PBA-X50 Precision Bridge Adapter, a GP1 data logger can be used as a one- or two-channel tensiometer logger. The bridge adapter is optimized for use with Delta-T Devices SWT range of water-filled tensiometers but is compatible with many other bridge sensors.

### *Irrigation control*

The GP1 data logger, running DeltaLINK Software, controls irrigation directly on the basis of the soil moisture (Figs. 8 and 9). Start and stop control levels can be separately configured, and there is even an option for pulsing the output when it is desirable to match the water application rate to the soil's infiltration capacity.

**GP1 data loggers** monitor soil moisture and other key growing conditions, use data to optimize irrigation and directly control irrigation using on-board relay (Figs. 10 and 11). With the GP1 data logger, it is possible to optimize and control irrigation, with measurable water savings of up to 60% achievable without reductions in yield or decline in quality.

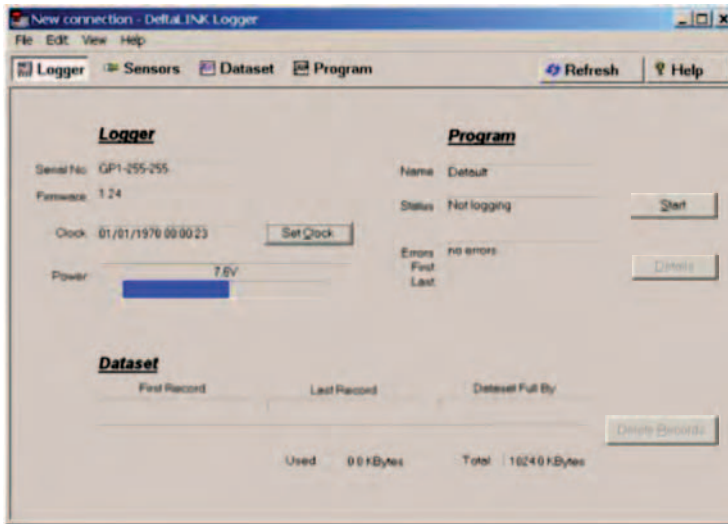


Fig. 8. Irrigation control and logger window

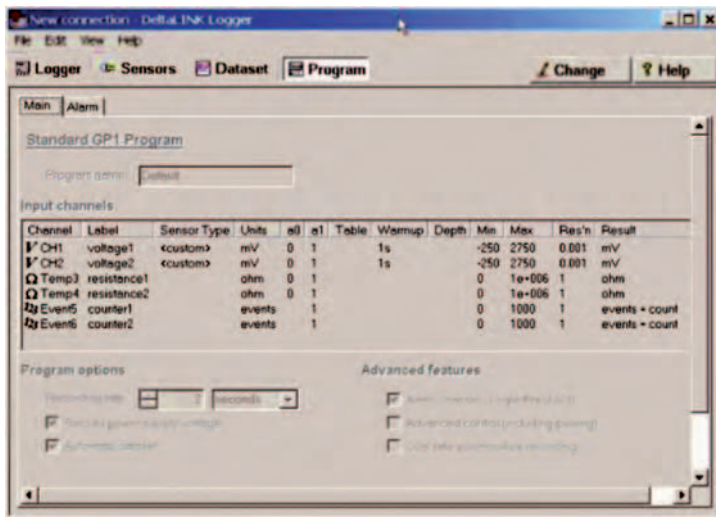


Fig. 9. Irrigation control algorithm

Dataset import wizard (Fig. 12) helps to seamlessly import data into MS Excel spreadsheets. Multiple dataset files may be imported and the data interleaved.

### *SM300 Soil moisture and temperature sensor*

The SM300 soil moisture sensor is a dual-purpose soil moisture probe – it can be used both with the HH2 meter for instant readings, or left in situ for continuous monitoring with a data logger (Fig. 13).

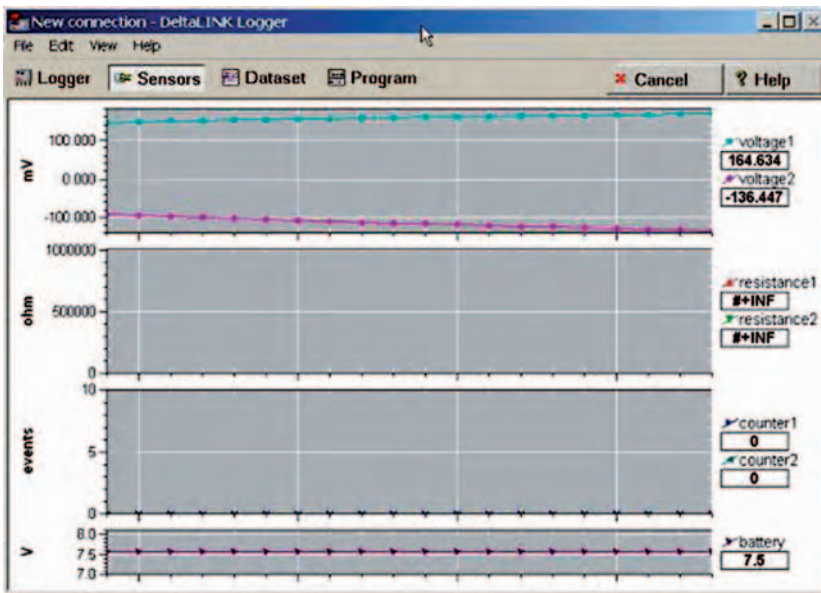


Fig. 10. Check sensor operation and start logging

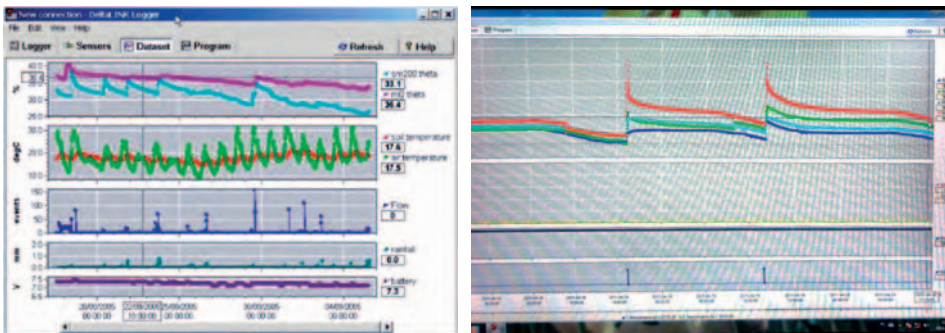


Fig. 11. Retrieve, view and save logged data

Engineered for reliability and high performance, the SM300 soil moisture sensor is well suited to both research and agricultural applications: research-grade performance, good temperature and salinity stability,  $\pm 2.5\%$  accuracy.

**Data logging.** The SM300 soil moisture sensor is compatible with all Delta-T devices loggers, and its 0–1 V DC output can be handled by most other types of logger. Temperature is measured by a 10 k precision thermistor mounted in the sensor body, which means that the SM300 should be fully buried to accurately measure soil temperature.



Fig. 12. Dataset import wizard

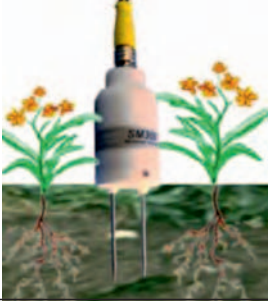
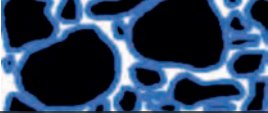
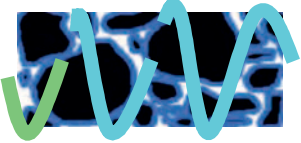


Fig. 13. SM300 Soil moisture and temperature sensor

**Easy installation.** The SM300 soil moisture sensor is buriable, and its cylindrical shape makes it easy to install in augered holes (45 mm diameter). The threaded base of the sensor can be connected to optional 50 and 100 cm extension tubes. The sharp twin pin design minimizes soil and substrate disturbance and allows for superior contact for more accurate measurements.

**Irrigation.** Accuracy and ease of use make SM300 soil moisture sensors well suited to irrigation applications. Readings can be used to optimize irrigation scheduling, or the SM300 can be installed as part of an automatic irrigation

Table 2. Operation principles of the SM300 sensor

	When power is applied to the <i>SM300</i> ...
	...it creates a 100 MHz waveform (similar to FM radio)
	The waveform is applied to a pair of stainless steel rods that transmit an electromagnetic field into the soil
	The water content of the soil surrounding the rods...
$\epsilon$	...dominates its <b>relative dielectric permittivity</b> $\epsilon$ being a measure of a material response to polarisation in an electromagnetic field. Water has high relative dielectric permittivity of 81, compared with soil (4) and air (1)
	The dielectric permittivity of the soil has a strong influence on the applied field...
$V_{out}$	...which is detected by the SM300, resulting in a stable voltage output that...
<b>Soil Moisture</b> 22 %	...acts as a simple, sensitive measure of <b>soil moisture content</b>

system. The sensor's compact size allows it to be installed in plant pots or grow bags.

### *Weighing control of soil moisture*

The two-level greenhouse tables are adapted for easy weighing, thus to control soil moisture in experimental pots. For that purpose, a special device was constructed (Fig. 14). The pots were placed on upper level of the tables supplied with large openings. Lower level served as a rail for a trolley with electronic balance.



Fig. 14. Weighing control of soil moisture status in pots

The trolley is equipped with a lever and a special ring, which enable moving up the pots through the openings, and taking the readings of the actual weight of the pot and to adjust soil moisture to required level.

The device was made in the framework of the consortium POLAPGEN-BD. It was granted a protection right no. 67015 for the design of “A device to

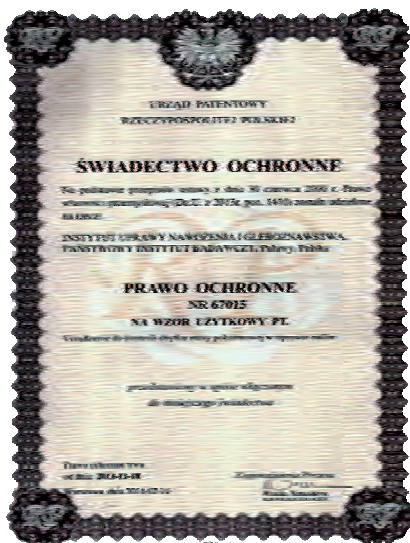


Fig. 15. Protection Certificate of the Polish Patent Office for the design of “A device to control nutritional weight loss in the cultivation of plants”

control nutritional weight loss in the cultivation of plants” by the Polish Patent Office. Certificate of Protection under the provisions of the Act of 30 June 2000. Industrial Property Right (Journal of Laws of 2013. Pos. 1410) was granted to the Institute of Soil Science and Plant Cultivation, State Research Institute, Pulawy, Poland (Fig. 15).

## Conclusions

The GPI-SM300 irrigation control system based on GPI data logger operating with DeltaLINK software installed on PC and SM300 soil moisture sensor supplied by Delta-T Devices Ltd was adjusted to a greenhouse soil moisture control system. The system enables to maintain soil water status at desirable level consistent through specific experimental treatments. It was used to investigate the effects of different soil water-deficit levels on spring barley growth and development.

## References

- Ayars J.E., Phene C.J., Hutmacher R.B., Davis K.R., Schoneman R.A., Vail S.S., Mead R.M. 1999. Subsurface drip irrigation of row crops: a review of 15 years of research at the Water Management Research Laboratory. *Agricultural Water Management* 42: 1-27.
- Burnett S.E., van Iersel M.W. 2008. Morphology and irrigation efficiency of Guara lindheimeri grown with capacitance sensor-controlled irrigation. *HortScience* 43: 1555-1560.
- Cossani C.M., Slafer G.A., Savin R. 2009. Yield and biomass in wheat and barley under a range of conditions in a Mediterranean site. *Field Crop Res.* 112: 205-213.
- Diepen C.A., Wolf J., Keulen H., Rappoldt C. 1989. WOFOST: a simulation model of crop production. *Soil Use and Management* 5: 16-24.
- English M. 1990. Deficit irrigation. I. Analytical framework. *Journal of Irrigation and Drainage Engineering* 116: 399-412.
- English M., Raja S.N. 1996. Perspectives on deficit irrigation. *Agricultural Water Management* 32: 1-14.
- Farquhar G.D., Sharkey T.D. 1982. Stomatal conductance and photosynthesis. *Annu. Rev. Plant Physiol.* 33: 317-345.
- Fereres E., Soriano M.A. 2007. Deficit irrigation for reducing agricultural water use. *Journal of Experimental Botany* 58: 147-159.
- Fernández J.E., Cuevas M.V. 2010. Irrigation scheduling from stem diameter variations: a review. *Agricultural and Forest Meteorology* 150: 135-151.

- Fertilization Recommendations. 1990. Limiting values for the soil macro- and micronutrients contents. IUNG-PIB Puławy, P(44): 26 pp.
- Greenwood D.J., Zhang K., Hilton H.W., Thompson A.J. 2010. Opportunities for improving irrigation efficiency with quantitative models, soil water sensors and wireless technology. *Journal of Agricultural Science* 148: 1-16.
- Henckel P.A. 1964. Physiology of plants under drought. *Annu. Rev. Plant Physiol.* 15: 363-386.
- Jadczyzyn T., Kowalczyk J., Lipiński W. 2008. Fertilization recommendations for field crops and permanent grassland. Dissemination Instruction IUNG-PIB 151: 24 pp.
- Jenks M.A., Eigenbrode S., Lemeix B. 2002. Cuticular waxes of Arabidopsis. In: C. Somerville, E. Meyerowitz, eds., *The Arabidopsis Book*. Rockville, M.D.: American Society of Plant Physiologists.
- Jenks M.A., Hasegawa P.M. 2014. Drought tolerance mechanisms and their molecular basis. *Plant Abiotic stress*. Wiley Blackwell: 15-46.
- Jones H.G. 1992. *Plants and Microclimate: A Quantative Approach to Environmental Plant Physiology* (ed H.G. Jones): p. 411. Cambridge University Press, Cambridge, UK.
- Kerstiens G. 2006. Water transport in plant cuticles: an update. *J. Exp. Bot.* 57: 2493-2499.
- Levitt J. 1972. *Responses of plants to environmental stresses*. New York: Academic Press.
- Ludlow M.M. 1989. Strategies of response to water stress. In: K.H. Kreeb, H. Richter, T.M. Hinckley, eds., *Structural and Functional Responses to Environmental Stresses*. The Hague: SPB Academic: 269-281.
- McCready M.S., Dukes M.D., Miller G.L. 2009. Water conservation potential of smart irrigation controllers on St. Augustinegrass. *Agricultural Water Management* 96: 1623-1632.
- Meron M., Hallel R., Peres M., Bravdo B., Wallach R., Gieling T. 2001. Tensiometer actuated automatic micro irrigation of apples. *Acta Horticulturae* 562: 63-69.
- Muñoz-Carpena R., Dukes M.D. 2005. Automatic irrigation based on soil moisture for vegetable crops. Fact Sheet ABE 356 of the Department of Agricultural and Biological Engineering. University of Florida. <http://edis.ifas.ufl.edu/ae354>. Accessed on January 2011.
- Muñoz-Carpena R., Dukes M.D., Li Y., Klassen W. 2008. Design and field evaluation of a new controller for soil-water based irrigation. *Applid Engineering in Agriculture* 24: 183-191.
- Nambara E., Marion-Poll A. 2005. Abscisic acid biosynthesis and catabolism. *Annu. Rev. Plant Physiol.* 56: 165-185.
- Nemali K.S., van Iersel M.W. 2006. An automated system for controlling drought stress and irrigation in potted plants. *Scientia Horticulturae* 110: 292-297.

- Pereira L.S., Oweis T., Zairi A. 2002. Irrigation management under water scarcity. *Agricultural Water Management* 57: 175-206.
- Raes D., Steduto P., Hsiao T.C., Fereres E. 2009. AquaCrop: the FAO crop model to simulate yield response to water: II. Main algorithms and software description. *Agronomy Journal* 101: 438-447.
- Raschke K. 1975. Stomatal action. *Annu. Rev. Plant. Physiol.* 26: 309-340.
- Roberts J. 2005. Transpiration. In: *Encyclopedia of Hydrological Sciences* (ed. M.G. Anderson), John Wiley & Sons, Ltd., Chichester, UK.
- Samarah N.H. 2005. Effects of drought stress on growth and yield of barley. *Agron. Sustain. Dev.* 25: 145-149.
- Sexton R., Roberts J.A. 1982. Cell biology of abscission. *Annu. Rev. Plant. Physiol.* 33: 133-162.
- Smith R.J., Raine S.R., Minkevich J. 2005. Irrigation application efficiency and deep drainage potential under surface irrigated cotton. *Agricultural Water Management* 71: 117-130.
- Steduto P., Hsiao T.C., Raes D., Fereres E. 2009. AquaCrop: The FAO crop model to simulate yield response to water: I. Concepts and underlying principles. *Agronomy Journal* 101: 426-437.
- Stockle C.O., Cabelguenne M., Debaeke P. 1997. Comparison of CropSyst performance for water management in southwestern France using submodels of different levels of complexity. *European Journal of Agronomy* 7: 89-98.
- Tan K.H. 2009. Liquid phase. *Environmental Soil Science*. CRC Press, Taylor&Francis Group: 189-250.
- Wang F.X., Kang Y., Liu S.P., Chen S.Y. 2007. Effects of soil matric potential on potato growth under drip irrigation in the North China Plain. *Agricultural Water Management* 88: 34-42.
- Zare M., Azizi M.H., Bazrafshan F. 2011. Effect of drought stress on some agronomic traits in ten barley (*Hordeum vulgare*) cultivars. *Tech. J. Engin. & App. Sci.* 1 (3): 57-62.

## **Construction of high quality ‘function’ maps for the identification of quantitative trait loci related to drought tolerance in barley**

**Justyna Guzy-Wrobelska, Kornelia Gudys**

*Department of Genetics, Faculty of Biology and Environmental Protection, University of Silesia, Katowice, Poland*

### **Introduction**

Drought is one of the most important environmental stresses in agriculture, which strongly decreases the production of main crops, including barley (*Hordeum vulgare* L.), in many growing areas (Barnabas et al. 2008). The improvement of the crop yield under drought conditions and the development of drought-tolerant cultivars is one of the major goals of breeding. However, drought tolerance is a very complex phenomenon associated with several biochemical, physiological, developmental and morphological adaptations. In order to produce cultivars that are better adapted to water deficit conditions, the mechanisms of plant tolerance to drought stress need to be unraveled, and numerous genes that control various phenotypic drought tolerance–related traits, mostly quantitative, need to be discovered (Cattivelli et al. 2011).

The dissection of complex traits may be more accessible with the use of so-called ‘function map’ approach (Tondelli et al. 2006). In this approach, medium- or high-density molecular maps are constructed and they are enriched with a set of candidate genes (CGs), chosen based on the information from literature or the result of transcriptome analysis experiments. These, so-called ‘function’ maps can be used then to precisely localize quantitative trait loci (QTL) for various complex phenotypic traits (e.g., drought tolerance–related traits) and to identify linkages between these QTLs and the genetic loci positioned on the map (markers, DNA sequences or CGs) in order to designate the most probable genes that control them. However, fine QTL mapping is the challenge, especially if the target is a gene of weak or moderate effect, and it requires large population sizes and the construction of dense, reliable maps. The quality of genetic maps can be

affected by a number of factors and several principles have to be applied at each stage of the mapping procedure to ensure the construction of high-quality maps (Semagn et al. 2006). In this paper, first, the issues involved in the construction of high-quality genetic linkage maps will be described; second, CGs approach will be presented; and third, an example of the CG selection and genotyping procedure will be showed.

### **Construction of high-quality genetic linkage maps**

A genetic linkage map is a graphical representation of chromosomes of a given species (e.g., barley). It is built using data on the allelic states of several polymorphic loci (markers or genes) in a set of individuals (called a mapping population), obtained from a cross between two different parent genotypes (Wu et al. 2008). The map shows the position and relative genetic distances between loci along chromosomes. Genetic mapping is based on the principle that genes/markers segregate through chromosome recombination during meiosis that allows their analysis in the progeny. During meiosis, chromosomes assort randomly into gametes. When two genes/markers are located on different chromosomes, the segregation of alleles of one gene/marker is independent of alleles of another gene/marker. When two genes/markers are nearby (tightly linked) on the same chromosome, their alleles are transmitted together from parent to progeny more frequently than those genes/markers located further apart. So, the mapping population represents a mixture of parental and recombinant genotypes in relation to each pair of genes/markers. The frequency of recombinant genotypes can be used to calculate recombination fractions, which may be used to define the genetic distance between two genes/markers. The distance between two linked genes/markers is measured in centimorgans (cM), and 1 cM is approximately equal to a 1% chance that these two genes/markers will be separated by recombination during meiosis (Collard et al. 2005; Semagn et al. 2006).

The construction of genetic maps involves several stages that should be performed properly in order to produce high-quality, reliable maps that are suitable for chromosomal locations of genes and QTL associated with various phenotypic traits of interest (Semagn et al. 2006). The crucial steps in the genetic linkage map construction are:

- 1) parental genotypes selection;
- 2) mapping population development;
- 3) molecular marker types selection;
- 4) screening of parents for marker polymorphism and genotyping of mapping population and
- 5) linkage analysis with the use of computer software.

### *Parent genotypes selection*

The construction of a linkage map requires a population of individuals segregating for one or more traits of interest, developed from controlled crosses. Therefore, the first crucial step in developing a mapping population is the selection of the appropriate parent genotypes for the cross. They should clearly differ for the traits to be studied. It is expected that the more the parental lines differ, the more genetic factors can be detected for the trait in the mapping population (Schneider 2005). A sufficient level of polymorphism between the parent lines at the nucleic acid level is also necessary for the construction of the comprehensive molecular map. From the other side, too high genetic distance between parent lines may cause sterility of the progenies and/or result in a very high level of segregation distortion during linkage analysis (Semagn et al. 2006). The other factor that should be taken into account is the possibility of the presence of heterogeneity in parent genotypes. Highly inbred lines may exhibit this variation at a limited level, whereas a much higher level of heterogeneity might be present within landraces or breeding lines. There are examples of the presence of within-cultivar variation in different species (Olufowote et al. 1997; Haun et al. 2011), including barley (Echart-Almeida and Cavalli-Molina 2000).

In barley (*Hordeum vulgare* L.), which is a diploid, self-pollinating species, mapping populations usually originate from the cross between parents that are highly homozygous (inbred), especially when modern barley cultivars are used. Several examples of barley mapping populations, developed from parents of genetically diverse pedigrees and successfully used in mapping, can be found in numerous reviews (Backs et al. 2006; Lehmensiek et al. 2009; Guzy-Wrobelska and Grzybkowska 2013). For studying genetic factors controlling complex, phenotypic traits like the drought tolerance or yield stability under drought conditions, barley landraces originating from water-limited environments with several adaptations to these unfavorable conditions can be used as one of the parent lines in crosses. However, landraces are not genetically uniform (Schneider 2005) and particular attention should be paid to the possibility of the heterogeneity in this type of parental lines that can cause the significant segregation distortion and/or the occurrence of non-parental alleles in a mapping population.

### *The development of mapping populations*

The second critical step in successful linkage mapping after the parent genotypes are crossed is the development of the appropriate mapping population regarding its type and size. Various types of populations have been used for genetic mapping, such as F<sub>2</sub> progenies, backcross (BC1), doubled haploid (DH) or recombinant inbred line (RIL) populations, etc. Several publications present detailed schemes of their development and specify their advantages and disadvantages (Collard et al. 2005; Schneider 2005; Semagn et al. 2006).

In barley, the most extensively used population type for the construction of linkage maps is DH population (Backes et al. 2006; Lehmensiek 2009; Guzy-Wrobelska and Grzybkowska 2013) as numerous, highly effective protocols for barley DH lines production through the crosses with *H. bulbosum* (bulbosum method) and anther/microspore culture have been developed (Cistue et al. 2003; Davies 2003; Devaux 2003; Szarejko 2003). However, there are also examples of the successful use of RIL and  $F_2$  populations in mapping (Backes et al. 2006; Lehmensiek et al. 2009; Guzy-Wrobelska and Grzybkowska 2013). The major advantage of the use in genetic analyses of DHs and RILs over  $F_2$  populations is their fixed nature. Both populations consist of fully (or nearly, in the case of RILs) homozygous lines and are genetically “immortal”. This allows DH and RIL populations to be reproduced without genetic change occurring, and to be widely distributed to be phenotyped in diverse environments, for many traits and/or in several years. They are therefore ideal for studying complex traits with a quantitative inheritance that requires replicated trials for several years and in different locations. The main drawbacks are the necessity of established protocols, high labor input and considerable resources for DH system, and the long time (six to eight generations) and high labor needed to produce RILs (Collard et al. 2005; Semagn et al. 2006; Lehmensiek et al. 2009).

Of course, DH and RIL populations differ genetically. DH populations are routinely produced by doubling the gametes of  $F_1$  plants (or rarely  $F_2$ ) and they represent a gametic level of the variation that should enable the selection of desirable recombinants within a population of smaller size (Snape 1989). RIL populations are derived by single-seed selections from individual  $F_2$  plants, through six to eight generations. In this process each line undergoes several rounds of meiosis before its homozygosity is achieved. Therefore, the degree of recombination of a RIL population is much higher compared to  $F_2$  population, and RIL populations of large size are suitable to create high-resolution maps and for mapping tightly linked markers (Schneider 2005).

Besides the type of a mapping population, the appropriate population size is required for the construction of reliable and accurate maps. The resolution of a map and the ability to determine the order of markers are largely dependent on the size of a mapping population. The simulation studies performed for the different population types of various sizes indicated that higher the size of the population, the higher the number of markers placed with high accuracy and the more precise the map. It was estimated that the samples of 200 individuals for all population types were required to construct reasonably accurate linkage maps. While the use of a population with smaller numbers of individuals resulted in several fragmented linkage groups and inaccurate ordering markers that were tightly linked (Ferreira et al. 2006). Moreover, much larger populations should be used for the construction of high-resolution maps or for the mapping of QTL

of minor effect (Young 2000). In practice, 66 barley DH populations, which were used for the construction of maps over the last 20 years, ranged from 46 to 301 individuals. In the case of 24 barley RIL populations, a range of 94–262 individuals was found (Guzy-Wrobelska and Grzybkowska 2013).

### *Selection of molecular marker types*

Over the past 20 years, several techniques of DNA markers have been used for genetic map construction in barley. Their advantages and disadvantages, and the various factors to be considered in selecting one or more of these marker systems have been well documented in numerous reviews (Nguyen and Wu 2005; Kahl et al. 2005; Agarwal et al. 2008). Among polymerase chain reaction (PCR)-based techniques, simple sequence repeats (SSR), which are co-dominant, highly reproducible, robust and quite easy for moderate screening automation, have become the favoured techniques for map building (Graner et al. 2011). In barley, SSR maps (Ramsay et al. 2000; Li et al. 2003) and integrated, consensus maps that joined SSRs with other marker techniques (Marcel et al. 2007; Varshney et al. 2007) have been constructed.

Currently, to construct comprehensive, high-density linkage maps, SSR markers are merged with recently developed gene sequence based and/or high throughput analysis techniques, such as expressed sequence tags (ESTs), diversity arrays technology( DArT) or single nucleotide polymorphisms (SNP) (Graner et al. 2011). SSR markers are used as a tool to align the gene-based maps with the old ones with various QTL mapped on them in order to position correctly these QTL on the new maps (Szűcs et al. 2009). Then, EST sequences are attractive as the source for marker development because they represent coding regions of the genome. In case of the tight linkage between an EST marker and a trait of interest, it is possible that the mapped gene, itself, is a factor that directly controls this trait (Semagn et al. 2006; Graner et al. 2011). They have been used also in barley for the development of EST-based markers of different types and the construction of the dense linkage maps (Stein et al. 2007). In turn, DArT is a whole genome profiling technique, which is based on DNA/DNA hybridization of the representation fragments from genomes. DArT is a polymorphic, reproducible and high-throughput method (Semagn et al. 2006; Graner et al. 2011). In barley, it has been used for high-density linkage maps construction integrating DArTs with other types of markers, including SSRs (Wenzl et al. 2006; Hearnden et al. 2007). Finally, the major breakthrough seems to be SNP markers. They are the most abundant, quite polymorphic and predominantly derived from gene sequences (EST-based SNPs). Moreover, different high throughput analysis techniques for SNP markers have been developed that enable the production of high-density maps for different species, including barley (Close et al. 2009; Druka et al. 2011). However, the use of SNP high throughput analysis techniques demands

high initial investment for a specialized equipment such as the GoldenGate BeadArray technology (Illumina Inc., San Diego, CA). Nevertheless, high-density consensus maps provide an excellent source of gene-based markers for very specific chromosomal regions, which might turn out tightly linked to QTL detected for various traits of interest. That is also why, proper curation of the large amounts of molecular data in mapping analyses, generated through SNP and DArT assays, is a very important issue.

#### *Screening of parents for marker polymorphism and genotyping of mapping populations*

The next crucial step in the construction of a dense linkage map is to identify a sufficient number of markers that discriminate between parent lines, and to perform correctly the genotyping of this set of markers in the mapping populations. With the advent of DNA markers the problem of unsatisfactory number of polymorphic markers has disappeared, as the variation at the DNA level is so vast that in any cross between two parent lines over thousand DNA markers may be segregating (Semagn et al. 2006). In barley, several dense maps, for individual populations or consensus, have been recently constructed with the use of 1328-6990 DNA markers (Agnoum et al. 2010; Li et al. 2010; Chutimanitsakun et al. 2011; Cistué et al. 2011; Muñoz-Amatriain et al. 2011).

Once a sufficient number of polymorphic markers between parents is available, they are screened across the entire mapping population. A genetic map is as good as the data collected during the genotyping, which are used to construct it. To facilitate the analysis and to minimize the risk of the errors, the parent lines (and  $F_1$  hybrid, if possible) should be included as references into the genotyping analysis of mapping populations. It is also essential to keep the identical order of the individuals over all loci in the data file. Moreover, the collected data must be carefully checked for different possible errors in recording: typing errors (e.g., introducing double recombinations), missing data, allele phase errors (reversal of parental genotype codes) and the order of genotypes along all loci (e.g., “frame shifts”). It has been found that even a low number of data-recording errors can have a serious impact on the order of markers and the length of a linkage map. Similarly, individuals with too much missing data may cause problems. If they are quite numerous, the essential information about the number and position of the true recombination events will be lost (Semagn et al. 2006; Lehmensiek et al. 2009).

#### *Linkage analysis with the use of computer software*

Large amounts of segregation data collected during marker analysis are processed by computer programs to construct a genetic map. Several computer packages have been developed over the last 20 years (Semagn et al. 2006). The

most widely used computer packages are freely available GMENDEL (Echt et al. 1992) or Map Manager QTX (Manly et al. 2001) and the commercial program JoinMap (Stam 1993).

The basic principles in map construction and the major steps in linkage analyses are similar for different statistical programs. Firstly, marker genotype data should be inspected once more (see the previous paragraph) to reveal progeny lines that have identical marker genotypes for all loci (unlikely for two random lines to be identical at a large number of loci) or which are identical to one of the parental genotypes (probably being a selfed parental line). If they are present, they have to be eliminated from the analysis (Lehmensiek et al. 2009).

Next, for each screened polymorphic marker, a chi-square analysis is performed to test for deviation from the expected segregation ratio for its alleles within the mapping population. In the case of DHs and RILs, the ratio of 1:1 is expected for each polymorphic marker. Segregation distortion is a problem often described in mapping studies. Especially, DH and RIL populations show higher segregation distortion compared to other types of populations (Semagn et al. 2006). It may occur due to real biological reasons or errors/biases during marker genotyping. When all markers from a particular region of the chromosome show segregation distortions it suggests various biological causes. Individual distorted markers in non-distorted regions may occur also due to scoring errors/biases and they need to be inspected (Xu et al. 1997; Semagn et al. 2006; Lehmensiek et al. 2009). Individual markers with strong segregation distortion caused by scoring errors or linked incorrectly with markers from the other group of linkages should be removed from the analysis. On the other hand, when the segregation distortion is a normal biological phenomenon it is better not to remove such loci from the map construction, as markers distorted towards the same direction are usually clustered in a small chromosome region. According to some researches, segregation distortion had very little effect on marker order and map length, but there are also contradictory results (Semagn et al. 2006).

The main part of multi-locus linkage analysis is a linkage map construction. The first step is to divide the markers genotyped in a mapping population into linkage groups. Markers are assigned to groups using the odds ratio, which is the ratio of the probability that two loci are linked with a given recombination value over a probability that the two are not linked. This ratio is called a logarithm of odds (LOD) value or LOD score. Pairs of markers with a recombination LOD score above a certain threshold value are considered to be linked whereas those with a LOD score below the threshold value are considered unlinked (Stam 1993). A LOD score value of 3 has been usually used as the minimum threshold value. However, data sets with very large numbers of markers show that even a LOD score of 6 may lead to false positive linkages. Higher LOD threshold values may result in a larger number of fragmented linkage groups, but it should

prevent markers from different chromosomes being incorrectly assigned to the same linkage group (Semagn et al. 2006). It is important to check the location of every marker in a linkage group before proceeding further. During this step, different analysis parameters are tested, and/or some markers/individuals are excluded in order to create good quality linkage groups. Ideally, the number of created linkage groups is the same as the haploid chromosome number of a given species. Sometimes, two or more linkage groups can be obtained for particular chromosomes, leading to a higher total number of linkage groups than the haploid chromosome number. Moreover, the established linkage groups can be assigned simultaneously to chromosomes based on the information for markers with known chromosomal location (Semagn et al. 2006; Lehmensiek et al. 2009).

The second step is ordering markers within linkage groups and simultaneously calculating distances among them. There is no perfect algorithm for ordering loci and different methods may provide slightly different orders, especially when a large number of markers should be located within a small distance (10 cM or less). At the beginning of this step, several parameters such as a recombination threshold value, minimum LOD value, jump threshold value and mapping function have to be specified. Ordering of loci is a multi-step, iterative process, based on adding loci one by one, starting from the most informative pair of the loci. A following marker is added to the map on the basis of its total linkage information with the markers that were ordered earlier on the map. For each added marker, the best position is searched and a goodness-of-fit measure is calculated. When the goodness-of-fit is too small, the marker is removed from ordering. This procedure is continued until all markers have been handled once. An initial ordering round usually is followed by repeated rounds of data verification and adjustment of locus order and distance. This procedure allows the identification of unstable regions of the map where more work is required to more accurately define an order of the markers. The final step in the construction of a map is verification of its quality, usually by comparisons to reference maps, including consensus maps (Semagn et al. 2006; Lehmensiek et al. 2009).

### **Candidate genes approach**

The recent accumulation of sequence data from model plant genomes has provided fundamental information for the design of the sequence-based research applications for accelerating molecular understanding of many biological processes (Mochida and Shinozaki 2010). One of them is the CG strategy, a promising tool to bridge the gap between quantitative and molecular genetic approaches. Dense, genetic maps enriched with various types of CGs, called 'function' maps, can be employed to identify genetic factors directly involved in the determination of very complex phenotypic traits, for example, tolerance to water

deficiency, especially in plants with large genomes such as barley (Tondelli et al. 2006; Sehgal and Yadav 2009). Identification and genetic mapping of numerous candidate genes for drought tolerance can be an excellent tool for discovering genes that determine various QTL related to the drought stress response, due to the fact that different alleles of a gene responsible for the phenotypic variation segregate in the chromosomal region corresponding to each QTL.

The typical candidate genes approach involves:

- 1) selection of a set of genes with reported involvement in a trait of interest (e.g., drought stress response) from available literature, public databases or transcriptome analysis experiments;
- 2) identification of genomic sequences of putative orthologs by prediction from sequence homology with known proteins across species;
- 3) designing specific PCR primers to amplify identified genes and
- 4) sequencing, uncovering polymorphisms between parents of a mapping population and developing procedure for genotyping.

Finally, genes that showed polymorphism between parental lines can be localized on a high-density genetic map to perform analysis of co-segregation with QTL regions. The above-mentioned steps are presented in detail as follows.

### *Selection of CGs*

There are two major resources of CGs to be positioned on high-density maps. Firstly, CGs may represent genes of known nucleotide sequence and biological function, involved in the development or physiology of a trait of interest that shows polymorphism at the DNA level (Vinod et al. 2006). There are examples of the use of function maps enriched with this type of candidate genes to explain the biotic and abiotic traits in different cereals (Ramalingam et al. 2003; Nguyen et al. 2004; Diab et al. 2008). For example Vinod et al. (2006) identified 21 putative candidate genes potentially involved in enhanced drought resistance in rice and two of them—*EXPI5* and *EXPI3*—were found to be associated with root number and silicon content in the stem, under both well-watered and low-moisture stress conditions. Diab et al. (2004) mapped several ESTs and CGs in the ‘Tadmor’ x ‘Er/Apm’ population of barley and 19 QTL for drought-related traits were associated with those genes.

The complexity of the mechanism of drought stress tolerance is caused by the highly multi-genic nature of this trait. Recent high-throughput technological advances also have provided tools for identification and functional analysis of many genes directly involved in different strategies of drought tolerance, especially in model plants, such as *Arabidopsis* or rice (*Oryza sativa*). Therefore, the large amount of sequence information, overexpression lines and knockout mutants for drought-related genes stored in public databases provide a second major resource for identifying putative CGs for map positioning (Segal and

Yadar 2010). Moreover, microarray technology has recently become a powerful and cost-effective tool for analyzing gene expression profiles of plants that are exposed to abiotic stresses. This strategy allows to identify a large number of novel genes with unknown molecular functions which are either up- or down-regulated in response to drought stress in different plant tissues (Shinozaki et al. 2003; Shanker et al. 2014). These genes also may be a promising basis of CGs to be positioned on high-density maps and used for QTL analysis.

#### *Identification of CG genomic sequences*

Efficiently collected sequence data from large-scale sequencing projects of model plants as well as cDNA (complementary DNA) and EST collections available for a number of species with unsequenced genomes provide essential genomic resources for effective identification of orthologous sequences of functionally annotated genes in agronomically important plants by sequence homology. The major nucleotide sequence-related databases possess GenBank (<http://www.ncbi.nlm.nih.gov/genbank/>) and EMBL-EBI European Nucleotide Archive (<http://www.ebi.ac.uk/ena/>). There are numerous sequence types freely available in these databases, which provide different biological information. Searching protein databases using translated coding sequence (CDS) as a query for BLAST (Basic Local Alignment Search Tool) program has been shown to be the most informative for the discovery of putative orthologs. Comparison of protein sequences reveals homology with greater sensitivity than comparison of the corresponding DNA sequences (Mochida and Shinozaki 2010). Identification of CGs in barley genome has been simplified due to the publication of barley physical map in 2012 (The International Barley Genome Sequencing Consortium 2012). Before that, the complicated and time-consuming procedure of cloning genes had to be performed. Currently, barley orthologs of functionally annotated drought-related genes can be straightforwardly identified on the basis of sequence homology of query against the assembly from Whole Genome Shotgun sequencing of barley cultivar 'Morex' and annotated genes being a combination of RNA-seq-derived and barley f1cDNAs-derived (full-length cDNA) predictions with the use of BLAST server at IPK Gatersleben (<http://webblast.ipk-gatersleben.de/barley/>).

#### *Designing of PCR primers*

PCR primers have to be designed to amplify genomic sequence of candidate genes in specific manner with a high yield of reaction. There are several criteria to be met in the design of primers. Optimal length should be approximately 18-25 bp (base pair) with melting temperature ( $T_m$ ) in the range of 57-63°C and the difference between the  $T_m$ s of forward and reverse primers not exceeding 1°C. The optimal GC content in primers is 50% with a single or double G or C at the 3' end of both primers (GC clamp) to promote specific binding. Self-

complementarity and complementarity between primers are unacceptable because of the possibility of the formation of hairpins or primer-dimers, which can lead to weak or no yield of the product. Primers designed for PCR amplification of a CG sequence must not amplify other genes in the genome; thus should be checked by BLAST for the specificity.

### *Sequencing, identification of polymorphism and developing procedure for genotyping*

PCR amplification of candidate genes has to be done for all parental genotypes of mapping populations. Afterwards, PCR amplicons are sequenced and aligned in order to reveal differences. Depending of the polymorphism type, different techniques have been developed for genotyping of CGs across entire mapping population. The most common types of polymorphism are SNP and INsertion/DELETions (INDEL). INDEL is a type of genetic variation in which a specific nucleotide sequence is present (insertion) or absent (deletion) in a product of amplification. PCR amplicons differing in size between parental genotypes can be separated on gels and CGs can be mapped as sequence tagged site (STS) markers with the same amplification conditions (Olson et al. 1989). If a single nucleotide change is found, fragments are inspected for the restriction enzyme cleavage sites to develop cleaved amplified polymorphic sequence (CAPS) markers. In this method, products are evaluated on the basis of differences in lengths of restriction fragments caused by SNP creating or eliminating restriction enzyme recognition sites in PCR amplicons (Konieczny and Ausubel 1993). In the case of lack of an enzyme for an SNP in CG sequence, the modification of the method, known as derived cleaved amplified polymorphic sequence (dCAPS), can be applied. The dCAPS technique introduces restriction enzyme recognition sites by using primers, containing one or more mismatches, for PCR amplification of the template DNA. The PCR product modified this way is then subjected to restriction enzyme digestion and the presence or absence of an SNP is determined by the resulting restriction pattern (Neff et al. 1998). A web-based program, dCAPS Finder 2.0, has been developed to facilitate the design of mismatched PCR primers and to select suitable restriction enzymes (Neff et al. 2002).

### **Identification and mapping of CG-encoding transcription factor *bZIP23* in barley genome – a case study**

*bZIP23* is a member of the basic leucine zipper (bZIP) transcription factor family in rice and its role in drought tolerance has been studied extensively. Expression of *Os bZIP23* is strongly induced by drought and salt stresses, abscisic acid (ABA) and polyethylene glycol treatments (PEG). Rice transgenic lines with overexpression of *Os bZIP23* showed significantly improved tolerance to drought

and high-salinity stresses and sensitivity to ABA, while the null mutant of this gene showed significantly decreased sensitivity to a high concentration of ABA and decreased tolerance to studied stresses. It has been proved that hundreds of genes encoding dehydrin proteins, LEA proteins, seed storage/lipid transfer proteins, amino acid metabolism proteins, protein kinases and phosphatases, are up- or down-regulated in rice plants overexpressing *OsZIP23* (Xiang et al. 2008).

*OsZIP23* gene is localized on chromosome 2 of rice. Its genomic sequence was found to consist of four exons and *OsZIP23* protein belongs to B\_zip1 superfamily. Complete coding sequence of *OsZIP23* was downloaded from NCBI (National Center for Biotechnology Information) database and used as a query for BLASTx analysis against the amino acid sequence database HC\_genes\_AA\_Seq at IPK Gatersleben server for the identification of the best putative ortholog in barley genome. HC\_genes\_AA\_Seq database includes barley gene annotations with high-confidence predictions based on homology of sequences derived from the Morex 55x WGS to other angiosperm proteins ([http://webblast.ipk-gatersleben.de/barley/docs/blast\\_databases.html](http://webblast.ipk-gatersleben.de/barley/docs/blast_databases.html)). A novel gene named MLOC\_53580 has been chosen as the best hit of sequence alignment that was strongly supported by the significant E-value and the highest amino acid sequence identity. Detailed information about a newly identified barley ortholog was found in Ensembl Plants database (<http://plants.ensembl.org/index.html>). MLOC\_53580 is located in the long arm of chromosome 6H and consists of four exons. This gene has five splice variants and encodes an uncharacterized protein containing leucine zipper domain, predicted by gene ontology (GO) to be involved in the regulation of transcription by sequence-specific DNA binding and transcription factor activity. The downloaded genomic sequence of this putative barley *bZIP23* gene was used to design primers, flanking mostly less conserved non-coding sequences of introns, with the use of Primer3 software (<http://bioinfo.ut.ee/primer3-0.4.0/>). PCR amplicons were sequenced and analyzed in CodonCode Aligner software to find polymorphisms. Four SNPs between parental genotypes of the studied mapping population were found. Then, the inspection of the restriction enzyme cleavage sites with the software NEBcutter V2.0 (<http://tools.neb.com/NEBcutter2/index.php>) revealed the polymorphic restriction site for *Hae*III enzyme. After experimental optimization of digestion conditions, products of restriction were separated on 2% agarose gels. This candidate gene was mapped as CAPS marker.

## References

- Agarwal M., Shrivastava N., Padh H. 2008. Advances in molecular marker techniques and their applications in plant sciences. *Plant Cell Rep.* 27: 617-631.

- Aghnoum R., Marcel T.C., Johrde A., Pecchioni N., Schweizer P., Niks R.E. 2010. Basal host resistance of barley to powdery mildew: connecting quantitative trait loci and candidate genes. *Mol. Plant-Microbe Interact.* 23: 91-102.
- Backes G., Orabi J., Fischbeck G., Jahoor A. 2006. Barley. In: Kole C. (ed) *Genome mapping and molecular breeding in plants. Volume 1. Cereals and millets.* Springer-Verlag, Berlin, Heidelberg, pp.155-210.
- Barnabas B., Jager K., Feher A. 2008. The effect of drought and heat stress on reproductive processes in cereals. *Plant Cell Environ.* 31: 11-38.
- Cattivelli L., Ceccarelli S., Romagosa I., Stanca M. 2011. Abiotic Stresses in Barley: Problems and Solutions. In: Ullrich S.E. (ed). *Barley: production, improvement, and uses.* Blackwell Publishing, pp.282-306.
- Chutimanitsakun Y., Nipper R.W., Cuesta-Marcos A., Cistue L., Corey A., Filichkina T., Johnson E.A., Hayes P.M. 2011. Construction and application for QTL analysis of a Restriction Site Associated DNA (RAD) linkage map in barley. *BMC Genomics* 12: 1-13.
- Cistué L., Cuesta-Marcos A., Chao S., Echáva rri B., Chutimanitsakun Y., Corey A., Filichkina T., Garcia-Mariño N., Romagosa I., Hayes P.M. 2011. Comparative mapping of the Oregon Wolfe Barley using doubled haploid lines derived from female and male gametes. *Theor. Appl. Genet.* 122: 1399-1410.
- Cistué L., Vallés M.P., Echávarri B., Sanz J.M., Castillo A. 2003. Barley anther culture. In: Maluszynski M., Kasha K.J., Forster B.P., Szarejko I. (eds). *Doubled haploid production in crop plants. A manual.* Kluwer, Dordrecht, pp.29-34.
- Close T.J., Bhat P.R., Lonardi S., Wu Y., Rostoks N., Ramsay L., Druka A., Stein N., Svensson J.T., Wanamaker S., Bozdag S., Roose M.L., Moscou M.J., Chao S., Varshney R., Szucs P., Sato K., PHayes.M., Matthews D.E., Kleinhofs A., Muehlbauer G.J., DeYoung J., Marshall D.F., Madishetty K., Fenton R.D., Condamine P., Graner A., Waugh R. 2009. Development and implementation of high-throughput SNP genotyping in barley. *BMC Genomics* 10: 582
- Collard B.C.Y., Jahufer M.Z.Z., Brouwer J.B., Pang E.C.K. 2005. An introduction to markers, quantitative trait loci (QTL) mapping and marker-assisted selection for crop improvement: The basic concepts. *Euphytica* 142: 169-196.
- Davies P.A. 2003. Barley isolated microspore culture (IMC) method In: Maluszynski M., Kasha K.J., Forster B.P., Szarejko I (eds). *Doubled haploid production in crop plants. A manual.* Kluwer, Dordrecht, pp.49-52.
- Devaux P. 2003. The *Hordeum bulbosum* (L.) method. In: Maluszynski M., Kasha K.J., Forster B.P., Szarejko I. (eds). *Doubled haploid production in crop plants. A manual.* Kluwer, Dordrecht, pp.15-19.
- Diab A.A., Teulat B., This D., Ozturk N.Z., Bensch D., Sorrells M.E. 2004. Identification of drought-inducible genes and differentially expressed sequence tags in barley. *Theor. Appl. Genet.* 109: 1417-1425.
- Diab A.A., Kantety R.V., Ozturk N.Z., Bensch D., Nachit M.M., Sorrells M.E. 2008. Drought-inducible genes and differentially expressed sequence tags associated with components of drought tolerance in durum wheat. *Sci. Res. Essays* 3: 9-26.

- Druka A., Sato K., Muehlbauer G.J. 2011. Genome Analysis: The State of Knowledge of Barley Genes. In: Ullrich S.E. (ed). Barley: Production, Improvement, and Uses. Oxford, Wiley-Blackwell, pp. 85-111.
- Echart-Almeida C., Cavalli-Molina S. 2000. Hordein variation in Brazilian barley varieties (*Hordeum vulgare* L.) and wild barley (*H. euclaston* Steud. and *H. stenostachys* Godr.). Genet. Mol. Biol. 23: 425-433.
- Echt C., Knapp S., Liu B.H. 1992. Genome mapping with non-inbred crosses using Gmndel 2.0. Maize Genet Coop Newslett 66: 27-29.
- Ferreira A., da Silva M.F., da Costa e Silva L., Cruz C.D. 2006. Estimating the effects of population size and type on the accuracy of genetic maps. Genet. Mol. Biol. 29: 182-192.
- Graner A., Kilian A., Kleinhofs A. 2011. Barley genome organization, mapping, and synteny. In: Ullrich S.E. (ed). Barley: Production, Improvement, and Uses. Oxford, Wiley-Blackwell, pp. 63-84.
- Guzy-Wrobelska J., Grzybkowska D. 2013. Dwadzieścia lat mapowania genów i QTL na mapach genetycznych jęczmienia. Postępy Biologii Komórki 40: 475-492.
- Haun W.J., Hyten D.L., Xu W.W., Gerhardt D.J., Albert T.J., Richmond T., Jeddloh J.A., Jia G., Springer N.M., Vance C.P., Stupar R.M. 2011. The composition and origins of genomic variation among individuals of the soybean reference cultivar Williams 82. Plant Physiology 155: 645-655.
- Hearnden P.R., Eckermann P.J., McMichael G.L., Hayden M.J., Eglinton J.K., Chalmers K.J. 2007. A genetic map of 1000 SSR and DArT markers in a wide barley cross. Theor Appl Genet 115: 383-391.
- Kahl G., Mast A., Tooke N., Shen R., van den Boom D. 2005. Single nucleotide polymorphisms: detection techniques and their potential for genotyping and genome mapping. In: Meksem and Kahl (eds) The handbook of plant genome mapping. WILEY-VCH Verlag GmbH & Co. KGaA, Weinheim, pp.75-107.
- Konieczny A., Ausubel F.M. 1993. A procedure for mapping Arabidopsis mutations using co-dominant ecotype-specific PCR-based markers. Plant Journal 4: 403-410.
- Lehmensiek A., Bovill W., Wenzl P., Langridge P., Appels R. 2009. Genetic mapping in the *Triticeae*. In: Muehlbauer G.J., Feuillet C. (eds). Genetics and genomics of the *Triticeae*. Springer US, pp. 201-235.
- Li H., Kilian A., Zhou M., Wenzl P., Huttner E., Mendham N., McIntyre L., Vaillancourt R.E. 2010. Construction of a high-density composite map and comparative mapping of segregation distortion regions in barley. Mol. Genet. Genomics 284: 319-331.
- Li J.Z., Sjakste T.G., Röder M.S., Ganai M.W. 2003. Development and genetic mapping of 127 new microsatellite markers in barley. Theor. Appl. Genet. 107: 1021-1027.
- Manly K.F., Cudmore Jr. R.H., Meer J.M. 2001. Map Manager QTX, crossplatform software for genetic mapping. Mamm. Genome 12: 930-932.
- Marcel T.C., Varshney R.K., Barbieri M., Jafary H., de Kock M.J.D., Graner A., Niks R.E. 2007. A high-density consensus map of barley to compare the distribution of QTLs for partial resistance to *Puccinia hordei* and of defense gene homologues. Theor. Appl. Genet. 114: 487-500.

- Mir R.R., Zaman-Allah M., Sreenivasulu N., Trethowan R., Varshney R.K. 2012. Integrated genomics, physiology and breeding approaches for improving drought tolerance in crops. *Theor. Appl. Genet.* 125: 625-645.
- Mochida K., Shinozaki K. 2010. Genomics and bioinformatics resources for crop improvement. *Plant Cell Physiol.* 51: 497-523.
- Muñoz-Amatriain M., Moscou M.J., Bhat P.R., Svensson J.T., Bartoš J., Suchánková P., Šimková H., Endo T.R., Fenton R.D., Lonardi S., Castillo A.M., Chao S., Cistué L., Cuesta -Marcos A., Forrest K.L., Hayden M.J., Hayes P.M., Horsley R.D., Makoto K., Moody D., Sato K., Vallés M.P., Wulff B.B.H., Muehlbauer G.J., Doležel J., Close T.J. 2011. An improved consensus linkage map of barley based on flow-sorted chromosomes and single nucleotide polymorphism markers. *Plant Genome* 4: 238-249.
- Neff M.M., Neff J.D., Chory J., Pepper A.E. 1998. dCAPS, a simple technique for the genetic analysis of single nucleotide polymorphisms: experimental applications in *Arabidopsis thaliana* genetics. *Plant J* 14:387-92.
- Neff M.M., Turk E., Kalishman M. 2002. Web-based primer design for single nucleotide polymorphism analysis. *Trends Genet.* 18: 613-615.
- Nguyen T.T., Klueva N., Chamareck V., Aarti A., Magpantay G., Millena A.C., Pathan M.S., Nguyen H.T. 2004. Saturation mapping of QTL regions and identification of putative candidate genes for drought tolerance in rice. *Mol. Genet. Genomics* 272: 35-46.
- Nguyen H.T., Wu X. 2005. Molecular marker systems for genetic mapping. In: Meksem and Kahl (eds) *The handbook of plant genome mapping*. WILEY-VCH Verlag GmbH & Co. KGaA, Weinheim, pp.23-74.
- Olson M., Hood L., Cantor C., Botstein D. 1989. A common language for physical mapping of the human genome. *Science* 245: 1434-1435.
- Olufowote J.O., Xu Y., Chen X., Park W.D., Beachell H.M., Dilday R.H., Goto M., McCouch S.R. 1997. Comparative evaluation of within-cultivar variation of rice (*Oryza sativa* L.) using microsatellite and RFLP markers. *Genome* 40: 370-378.
- Ramalingam J., Vera Cruz C.M, Kukreja K., Chittoor J.M., Wu J.L., Lee S.W., Baraoidan M., George M.L., Cohen M.B., Hulbert S.H., Leach J.E., Leung H. 2003. Candidate defense genes from rice, barley, and maize and their association with qualitative and quantitative resistance in rice. *Am. Phytopathol. Soc.* 16: 14-24.
- Ramsay L., Macaulay M., Ivanissevich S., MacLean K., Cardle L., Fuller J., Edwards K.J., Tuvevsson S., Morgante M., Massari A., Maestri E., Marmiroli N., Sjakste T., Ganai M., Powell W., Waugh R. 2000. A simple sequence repeat-based linkage map of barley. *Genetics* 156: 1997-2005.
- Schneider K. 2005. Mapping populations and principles of genetic mapping. In: Meksem and Kahl (eds) *The handbook of plant genome mapping*. WILEY-VCH Verlag GmbH & Co. KGaA, Weinheim, pp. 3-12.
- Sehgal D., Yadav R. 2009. Molecular markers based approaches for drought tolerance. In: *Molecular techniques in crop improvement*. Jain S.M., Brar D.S. (eds) Springer Netherlands pp. 207-230.
- Semagn K., Bjørnstad A., Ndjiondjop M.N. 2006. Principles, requirements and prospects of genetic mapping in plants. *Afr. J. Biotech* 5: 2569-2587.

- Shanker A.K., Maheswari M., Yadav S.K., Desai S., Bhanu D., Attal N.B., Venkateswarlu B. 2014. Drought stress responses in crops. *Funct. Integr. Genomics* 14:11-22.
- Shinozaki K., Yamaguchi-Shinozaki K., Seki M. 2003. Regulatory network of gene expression in the drought and cold stress responses. *Curr. Opin. Plant Bio.* 6: 410-417.
- Snape J.W. 1989. Doubled haploid breeding: theoretical basis and practical application. In: Review of Advances in Plant Biotechnology, 1985-1988. Proc. 2nd Int. Symp. on Genetic Manipulation in Crops, CIMMYT and IRRI, Mexico, Manila, pp. 19-30.
- Stam P. 1993. Construction of integrated genetic linkage maps by means of a new computer package: JoinMap. *Plant. J.* 3: 739-744.
- Szarejko I. 2003. Anther culture for double haploid production in barley (*Hordeum vulgare* L.). In: Maluszynski M., Kasha K.J., Forster B.P., Szarejko I. (eds). Doubled haploid production in crop plants: A manual. Kluwer, Dordrecht, pp. 35-42.
- Szűcs P., Blake V.C., Bhat P.R., Chao S., Close T.J., Cuesta -Marcos A., Muehlbauer G.J., Ramsay L., Waugh R., Hayes P.M. 2009. An integrated resource for barley linkage map and malting quality QTL alignment. *Plant Genome* 2: 134-140.
- The International Barley Genome Sequencing Consortium. 2012. A physical, genetic and functional sequence assembly of the barley genome. *Nature* 491: 711-717.
- Tondelli A., Francia E., Barabaschi D., Aprile A., Skinner J.S., Stockinger E.J., Stanca A.M., Pecchioni N. 2006. Mapping regulatory genes as candidates for cold and drought stress tolerance in barley. *Theor. Appl. Genet.* 112: 445-454.
- Varshney R.K., Marcel T.C., Ramsay L., Russell J., Roder M.S., Stein N., Waugh R., Langridge P., Nix R.E., Graner A. 2007. A high density barley microsatellite consensus map with 775 SSR loci. *Theor. Appl. Genet.* 114: 1091-1103.
- Vinod M.S., Sharma N., Manjunatha K., Kanbar A., Prakash N.B., Shashidhar H.E. 2006. Candidate genes for drought tolerance and improved productivity in rice (*Oryza sativa* L.). *J. Biosci.* 31: 69-74.
- Wenzl P., Li H., Carling J., Zhou M., Raman H., Paul E., Hearnden P., Maier C., Xia L., Caig V., Ovesna J., Cakir M., Poulsen D., Wang J., Raman R., Smith K.P., Muehlbauer G.J., Chalmers K.J., Kleinjans A., Huttner E., Kilian A. 2006. A high-density consensus map of barley linking DArT markers to SSR, RFLP and STS loci and agricultural traits. *BMC Genomics* 7: 206.
- Wu Y., Bhat P.R., Close T.J., Lonardi S. 2008. Efficient and accurate construction of genetic linkage maps from the minimum spanning tree of a graph. *PLoS Genet.* 4: e1000212.
- Xiang Y., Tang N., Du H., He X., Xiong L. 2008. Characterization of *OsbZIP23* as a key player of a basic leucine zipper transcription factor family for conferring abscisic acid sensitivity and salinity and drought tolerance in rice. *Plant Physiol.* 148: 1938-1952.
- Xu Y., Zhu L., Xiao J., Huang N., McCouch S.R. 1997. Chromosomal regions associated with segregation distortion of molecular markers in F<sub>2</sub> backcross, doubled haploid and recombinant inbred populations in rice (*Oryza sativa* L.). *Mol. Gen. Genet.* 253: 535-545.
- Young N.D. 2000. Constructing a plant genetic linkage map with DNA markers. In: Philips R.L., Vasil J.K. (eds). DNA-Based Markers in Plants. Kluwer Academic Publishers 3: 31-47.

## **Measuring anatomical variation in leaves of barley genotypes differing in drought tolerance**

**Tomasz P. Wyka, Agnieszka Bagniewska-Zadworna**

*Faculty of Biology, Institute of Experimental Biology, Department of General Botany, Adam Mickiewicz University, Poznań, Poland*

### **Introduction**

Drought, alone or in combination with other stressors, is the most important factor limiting plant productivity on a global scale. Plant adaptations to the survival of drought involve modifications at all levels of organization, including organ structure. Some plant species exhibit specialized structural traits clearly enhancing their performance under drought (e.g., water storage tissues, pronounced indumenta); however, most drought-related traits are subtle modifications of structures that otherwise commonly occur in a given taxonomic group (Fahn and Cutler 1992; Dickinson 2000). Such traits may be constitutive features of species or infra-specific taxa (e.g., cultivars), or may arise in response to drought signals through plastic modification of organ development.

Leaves are principal photosynthetic organs. Therefore, their functioning under particular environmental conditions influences plant biomass productivity as well as the economic yield. The environment for photosynthesis is to some extent controlled by the anatomical structure of the leaf. In addition to accommodating chloroplasts, internal organization of the leaf must allow adequate illumination of photosynthetic cells, provide access and internal distribution of CO<sub>2</sub>, ensure replacement of transpired water and export of reduced carbon compounds. The leaf must also secure its own survival in the face of various abiotic and biotic stresses. Leaf structure therefore reflects a compromise between the requirements of photosynthesis and those of stress tolerance.

The importance of leaf anatomy with respect to preservation of leaf functionality under water shortage has been recognized by comparing leaves of plants adapted

to habitats differing in water availability (e.g., Hacke and Sperry 2001; Taylor et al. 2011) or adapted to drought through the breeding process (Ristic and Cass 1991; Bresta et al. 2011). The syndrome of traits associated with tolerance to drought is known as xeromorphism (Fahn and Cutler 1992). Xeromorphic leaves tend to have reduced surface area and are thicker than mesomorphic leaves; they are also constructed of smaller, more densely packed cells, have thicker outer walls of epidermal cells and often have thicker cuticles, denser trichomes and smaller stomatal apertures (Fahn and Cutler 1992; Dickinson 2000).

Xeromorphic leaf adaptations have been documented in species from different taxonomic groups, including the economically important family Poaceae (Fahn and Cutler 1992; Taylor et al. 2011). Much insight into functional consequences of particular anatomical traits for drought tolerance can be obtained through studies of ecotypes or cultivars differing in their vulnerability to drought (Ridley and Todd 1966; Ristic and Cass 1991). For example, drought-adapted ecotypes of *Phragmites* had larger leaf bundle sheath and greater vessel pit-field frequencies compared to wetland ecotypes, and exhibited chemical modifications of walls that could potentially influence water transfer pathways in the leaf (Chen et al. 2006). Such studies, however, have been based on comparisons of pairs or small numbers of genotypes while there are few data sets combining ecophysiological and agronomic responses to drought with anatomical characteristics for large numbers of diverse genotypes [e.g., see the study by Khaliq et al. (1999) covering 22 genotypes of wheat].

Much valuable information has been obtained by studying leaf modifications under experimentally induced drought. Plant responses have included the production of leaves with increased stomatal frequencies in *Triticum aestivum* (Khaliq et al. 1999) and *Leymus chinensis* (Xu and Zhou 2008), reduced cell sizes in *Festuca arundinacea* (Durand et al. 1995), *Zea mays* (Ristic and Cass 1991) and *Cynodon dactylon* (Utrillas and Alegre 1997), thicker mesophyll cell walls in *Cynodon dactylon* (Utrillas and Alegre 1997), greater vein density in *Triticum turgidum* var. *durum* (Bresta et al. 2011), and smaller vessel diameters in *Paspalum dilatatum* (Vasellati et al. 2001) and *Triticum turgidum* var. *durum* (Bresta et al. 2011). In addition to deepening our understanding of functional anatomy, data of this kind may be useful as documentation of infraspecific variability but may also allow identification of marker traits for drought tolerance and, possibly, indicate target traits for selection (Monneveux et al. 2012; Varshney et al. 2012). This is especially true in studies of recombinant inbred lines where parental trait associations are broken down.

Breeding of cereal species has benefited from exploration of natural variability in a variety of functional traits, although plant organ anatomy appears to have been neglected as a source of useful variation (Monneveux et al. 2012). Additionally, the potential of phenotypic plasticity of structural traits in improving

the tolerance to drought has not been sufficiently exploited. This is in part caused by the still insufficient understanding of the connection between anatomy and leaf functioning but also by the laborious procedures required to accumulate sufficient amounts of anatomical data in a wide sample of plant material. Here, we describe the complete protocol used in a large-scale study of recombinant inbred lines of barley (*Hordeum vulgare* L.) to generate an extensive data set on genetic and plastic variability of leaf anatomical traits at the level of scanning electron and standard light microscopy.

### **Development of protocol**

Plants used for the preliminary study of fixation methods originated from a growth chamber where they were grown under fluorescent light at photosynthetic photon flux density of  $180 \mu\text{mol quanta m}^{-2} \text{ s}^{-1}$  with 16h/8h light/dark cycle at 21°C and 60% relative humidity. Leaf samples were collected at the tillering stage, saved individually in plastic bags and taken immediately to the laboratory for processing.

Leaves used for observation and analysis of traits were harvested from a greenhouse experiment where single seed–descent barley lines were cultivated in pots under well-watered or drought-and-rewatering treatments. Details of the plant material and the experiment have been described elsewhere in this volume (Ogrodowicz et al. 2014). To ensure that leaves used for analyses have developed under the influence of drought, on the first day of the drought treatment we randomly selected six plants in each treatments and marked the youngest leaves ( $L_0$ ) whose tips were barely protruding through the sheath of the previous leaf, using a permanent marker and a colour thread. After rewatering, when all  $L_0$  leaves were expanded (determined by repeated measurement of lamina length) and consecutive leaves ( $L_1$ ) were produced and at least matched the length of  $L_0$ , we harvested the  $L_0$  leaves. At harvest, leaves were placed in plastic bags containing moist paper towels and kept in a portable cooler chilled with an ice pack until arrival in laboratory.

In the laboratory, the length of leaf laminae and their width in the broadest point (typically middle of the linear sector of the lamina) were measured. Samples for light microscopy were excised from this sector of the lamina by cutting approximately  $2 \text{ mm} \times 5 \text{ mm}$  segments perpendicular to the lamina axis, including part of the midrib. For scanning electron microscopy (SEM), additional  $5 \text{ mm} \times 5 \text{ mm}$  segments were taken from an adjacent lamina area. To offset any protoplast shrinking caused by leaf dehydration during handling, excised samples were placed on moist filter paper in Petri dishes and kept in a refrigerator at 4°C overnight. The next morning, leaf segments were fixed.

*Embedding and slide preparation for light microscopy*

Since our objective was to devise a routine protocol for efficient handling of large numbers of leaf samples, we ran preliminary trials of sample fixation methods. To select the appropriate fixation method, we tested eight combinations of fixative formulation/exposure times (Table 1). Leaf segments were placed in the fixative and exposed to  $-0.3$  atm vacuum for 2 h and then left for the remainder of the fixation time at  $4^{\circ}\text{C}$ . Subsequently samples were washed 3 times in the respective buffer and dehydrated in a series of 5%, 10%, 15%, 20%, 30%, 50% and 70% ethanol for 10 min at each concentration. Results of fixation protocols were evaluated in sections prepared using the paraffin method.

For evaluation of fixation methods, samples were embedded in paraffin according to the standard technique (Sass 1958) with modifications. Samples stored in 70% ethanol were further dehydrated in 80%, 90%, 96% and 100% ethanol for 30 min at each concentration followed by 3:1, 1:1 and 1:3 mixtures of ethanol/butanol for 30 min in each and two changes of 100% butanol (30 min and overnight). Butanol was replaced by two changes (2 h and overnight) of melted Paraplast Plus (melting point =  $57^{\circ}\text{C}$ ; Sigma Aldrich, Saint Louis, MO, USA). Blocks of embedded material were cast by pouring Paraplast containing leaf

**Table 1. Fixation and embedding methods evaluated for barley leaf samples**

No.	Fixative	Buffer	Exposure time (h)	Embedding material
1a	2% glutaraldehyde and 2% formaldehyde	0.1 M sodium cacodylate pH 7.2	4	Paraplast Plus
1b	2% glutaraldehyde and 2% formaldehyde	0.1 M sodium cacodylate pH 7.2	16	Paraplast Plus
2a	2% glutaraldehyde and 2% formaldehyde	0.1 M PBS <sup>1</sup> pH 7.4	4	Paraplast Plus
2b	2% glutaraldehyde and 2% formaldehyde	0.1 M PBS <sup>1</sup> pH 7.4	16	Paraplast Plus
3a	3% glutaraldehyde and 1% formaldehyde	0.1 M phosphate pH 7.2	4	Paraplast Plus
3b	3% glutaraldehyde and 1% formaldehyde	0.1 M phosphate pH 7.2	16	Paraplast Plus
4a	3% glutaraldehyde	0.1 M phosphate pH 7.2	4	Paraplast Plus
4b	3% glutaraldehyde	0.1 M phosphate pH 7.2	16	Paraplast Plus
5	2% glutaraldehyde and 2% formaldehyde	0.1 M sodium cacodylate pH 7.2	16	Technovit

<sup>1</sup>phosphate buffer saline

samples into wax-paper molds at room temperature. Blocks were trimmed and then sectioned on a HM 340E rotary microtome (Microm, Walldorf, Germany) to 12  $\mu\text{m}$  thickness. Sections were spread out on water, placed on Haupt adhesive coated slides and dried at 43°C followed by incubation at 36°C for 24 h. Paraffin was removed with 100% xylene. For staining, slides were passed through 100% xylene/100% ethanol (1:1 v/v), then 100%, 96%, 80% and 70% ethanol, and dipped in 1% solution of safranin O in 70% ethanol. Slides were washed in 96% ethanol, dipped in 0.1% solution of fast green in 96% ethanol, washed with isopropanol, followed by xylene and closed using Entellan (Merck, Darmstadt, Germany). They were then kept at 36°C for at least 48 h. For evaluation of fixation methods, slides were code-numbered and three slides from each method were evaluated by two experienced microscopists who ranked methods according to preservation of cell integrity, shape and overall quality of preparations.

In an attempt to achieve finer image resolution, we used commercially available acrylic resin Technovit 7100 (Heraeus Kulzer GmbH, Wahrheim, Germany) as an embedding medium. Samples stored in 70% ethanol were dehydrated in 80%, 90 and 96% ethanol for 30 min at each concentration followed by pre-infiltration in 1:10, 1:3, 1:1 v/v mixtures of 100% ethanol and Technovit 7100 lasting for 2 h, 24 h and 24 h respectively. Samples were finally immersed in pure Technovit 7100 for 24 h and then infiltrated in a solution of 1.25 g hardener I in 100 ml<sup>-1</sup> Technovit 7100 for 48 h. Infiltration was performed at 4°C. Resin was prepared by mixing the above infiltration solution with Hardener II liquid at 15:1 v/v ratio. Leaf segments were cleaned of excess infiltration solution using blotting paper, placed individually in wells of Histoform S mould (Heraeus Kulzer GmbH, Wahrheim, Germany) and quickly covered with resin. Cured blocks were mounted in plastic holders using Technovit 3040 resin as described in manufacturer's instructions. Leaf sections were cut using the RM2265 microtome (Leica, Vienna, Austria), with optimal thickness found to be 4  $\mu\text{m}$ . Sections were placed on a thin layer of water on de-greased slides and warmed at 37 °C until water evaporated and adhesion occurred. Sections were stained with 0.05% solution of toluidine blue in 1% sodium tetraborate.

Sections were examined under the AxioScopeA1 microscope and photographed with an attached AxioCam MRc5 digital camera (Carl Zeiss GmbH, Jena, Germany).

### *Scanning electron microscopy*

Samples stored in 70% ethanol were further dehydrated in 80% and 90% ethanol (20 min in each) and transferred into acetone via a series of 3:1, 1:1, 1:3 v/v mixtures of 90% ethanol and 90% acetone followed by two changes of each 90% and 96% acetone and three changes of 100% acetone (20 min in each solution). Samples were CO<sub>2</sub> critical-point dried (CPD drier, Balzers, Balzers,

Lichtenstein), mounted on metal stubs and sputter-coated with gold particles using and SCD 050 apparatus (Balzers). Samples were examined with an Evo 40 Scanning Electron Microscope (Carl Zeiss, Jena, Germany) at an accelerating voltage of 12 kV and digital images were recorded.

### *Image processing*

Micrometric measurements of leaf sections were taken with an AxioVision 4.7 software (Carl Zeiss, 2009) and measurements of scanning microscope images with ImageJ (National Institutes of Health, USA).

## **Evaluation of the protocol**

The purpose of this report is to present a protocol suitable for quantitative anatomical analysis of leaves of barley genotypes differing in susceptibility to water stress subjected to experimental drought. We developed a sample collection and processing protocol as well as devised a standardized set of morpho-anatomical trait measurements.

### *Sample collection and treatment*

Drought stress affects leaf growth, development and, finally, structural features, not only through a direct restriction of cell expansion rates due to low-tissue water potential but also through a feed-forward acclimatory mechanism, whereby drought stress signals are perceived by growing tissues and cause developmental modifications (Chaves and Oliveira 2004). Determination of the leaf phenotype takes place during its expansion. Therefore, after reaching its final size, the leaf can undergo only very limited structural changes mostly involving cell wall modifications and accumulation of secondary deposits. Shoot development in barley, as in other Poaceae, is telescopic, that is, leaf primordia as well as the terminal spike primordium are formed very early, and initially remain covered by sheaths of older leaves. Leaf expansion proceeds mostly due to activity of intercalary meristems at the bases of both the sheath and the lamina. These zones are sensitive to water deficit and stop growing very rapidly in response to osmotic stress (Rayan and Matsuda 1988). Leaves sampled for the study of drought-induced modifications should complete their lamina expansion after drought treatment has been implemented. To recognize this stage, it was necessary to tag a random sample of leaves and monitor the timing of cessation of their growth. Since following individual leaf fates in a large-scale study was impractical, we thus determined the moment when sufficient time has elapsed for the target leaves to emerge and finish expansion.

Plant development and leaf production during drought period were inhibited while they continued in well-watered control. Although leaves collected from

the droughted plants were of the same age as those of controls, they inevitably represented morphologically different (more basipetal) position on the stem (Dannenhoffer et al. 1990). This sampling approach was preferable over collecting leaves inserted at the same morphological position because, given the developmental delay of droughted plants, it avoided sampling leaves developed at different times, that is, under non-uniform atmospheric and thermal conditions. To account for the possible anatomical variability associated with leaf position (and therefore size), we determined leaf lamina dimensions (length and width) for every leaf and used them as co-variates in any subsequent analyses of leaf trait responses to drought.

Leaf tissues are composed of diverse cell types and their structure exhibits variability among different leaf regions. This is especially true in the case of linear leaves whose growth is predominantly unidirectional and maturation of tissues is basipetal, as is the case in grasses (Martre et al. 2000). Moreover, barley genotypes exhibit various degrees of lamina tapering. Since for comparative work it is desirable to standardize the anatomical “region of interest” among leaves of different genotypes, we always sampled tissues from the widest part of leaf lamina (usually near the middle of the lamina) and always included the midrib.

The accuracy of micrometric measurements is dependent on the preservation of tissue shape. Factors, such as cell turgidity, fixation method and embedding technique are therefore critical, especially in soft organs, such as leaves of greenhouse-cultivated barley. A non-routine step introduced in our fixation protocol involving an overnight rehydration of live samples on moist tissue paper at 4°C prior to fixation considerably reduced the incidence of plasmolyzed cells. A side advantage of this step was that it allowed quick harvesting of large numbers of leaf segments before proceeding with fixation.

Cell shrinking and distortion are frequent when strongly hyperosmotic fixatives are used; however, the use of too diluted fixatives may result in slow killing of cells leading to their deterioration. Even though all fixative solutions tested by us (Table 1) are considered to have low osmotic strength, they differed considerably in the quality of tissue preservation. Least evidence of plasmolysis and cell distortion in examined slides was found when a mixture of 2% glutaraldehyde and 2% formaldehyde in 0.1 M cacodylate or phosphate buffer saline was applied for 16 h (methods 1b and 2b, Table 1). Moreover, fixation for 16 h gave better effects than for 4 h in case of all fixative solutions. Based on prior experience, we also emphasize the importance of very gradual dehydration through a series of increasing ethanol concentrations.

Basic paraffin embedding was considered unsatisfactory because of frequent mechanical distortions and tearing of the delicate leaf tissue due to inadequate support provided by this medium. Only vascular bundles were properly preserved

and did not undergo distortions (Fig. 1A). Leaf samples fixed via protocol 1b or 2b were therefore embedded in Technovit 7100, a commercially available acrylic resin, which is, however, infrequently used in plant anatomy. Based on previous experience, we introduced several modifications to the infiltration protocol recommended by the manufacturer extending the infiltration time from

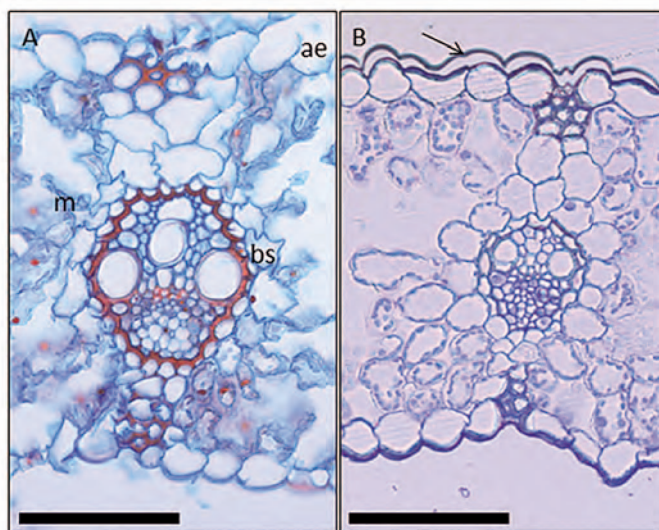


Fig. 1. Cross-sections of barley leaves embedded in Paraplast Plus (A) and Technovit (B). In both cases, samples were fixed in a mixture of 2% glutaraldehyde and 2% formaldehyde in 0.1M cacodylate buffer for 16 h (Method 1b). Notice torn adaxial epidermis (ae) and severely distorted mesophyll (m) and bundle sheath (bs) cells in (A). The arrow in (B) indicates separation of Technovit film from the epidermis. Bars = 100  $\mu$ m

maximum 14 h stated in the manufacturer's instructions to as long as 5 days with a step-wise increase of resin concentration in the pre-infiltrating solution. We found that longer infiltration times were also possible. Compared to paraffin, Technovit provided better support to cells and ensured good preservation of tissue structure. From Technovit-embedded materials it was also possible to cut thinner sections and therefore obtain better definition of cell shapes (Fig. 1B).

Technovit-embedded materials were used for the study of leaf cross-section, whereas leaf surface images from scanning electron microscope were used to examine the surface details. Importantly, both types of sections were taken from adjacent regions of the same leaf.

#### *Choice of anatomical traits: Leaf surface*

The choice of anatomical traits for characterization of leaf responses to drought was dictated on the one hand by the ease of measurement and possibility

of locating corresponding structures in different leaves and on the other by the understanding of relationships between traits and functional requirements placed on the leaf structure, that is, growth, photosynthesis, water supply and mechanical strength. When genotypes or experimental treatments are compared it is important to draw comparisons between structures that are directly homologous, that is, are measured at corresponding locations within the leaves. Given the regular parallel arrangement of veins in the linear barley leaves, it was possible to make measurements of traits on exactly homologous vein orders and measure vein and adjacent tissue dimensions at exactly defined locations.

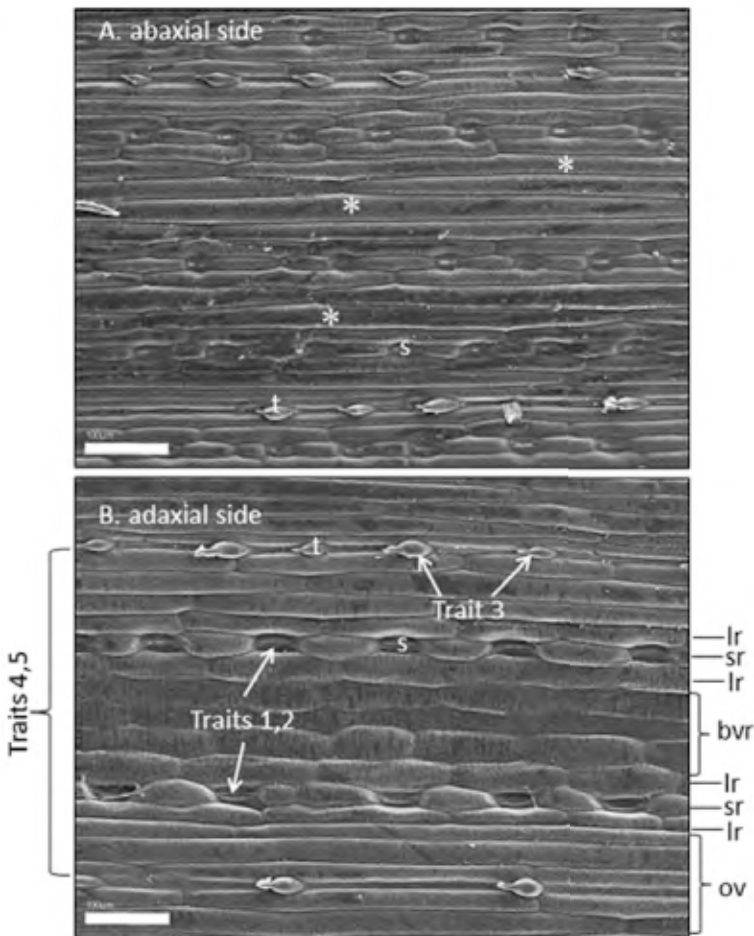


Fig. 2. SEM micrographs of abaxial (A) and adaxial (B) sides of barley leaves. Principal cell-row types are labelled in accordance with Wenzel et al. (1997): sr – stomatal row, lr – lateral row, bvr – rows between veins and ov – rows over the vein. Letter s indicates stomata, t indicates trichomes and asterisks in (A) mark elongated cells between veins. Micrograph B shows features used in determination of traits 1–5 (see Table 2). Bars = 100  $\mu$ m

Epidermal cells of the Poaceae are very diverse, but at the same time they show a regular organization into files arranged in relation to the underlying veins (Wenzel et al. 1997). Parenchymatic and sclerenchymatic extensions of the vascular bundles are merged with the single-layered epidermis. Epidermal files overlying the vascular bundles are easily identified in SEM images by the long sclerenchymatic-type cells and the presence of trichomes (Fig. 2). Stomata are arranged in rows located between those bundle-associated cells on both abaxial (lower) and adaxial (upper) surfaces of the leaf. Each stomatal row is flanked on each side by a single lateral row. The remaining rows located between the veins are composed of elongated pavement cells (Fig. 2; Wenzel et al. 1997). Since, as shown by SEM views of abaxial and adaxial epidermis (Fig. 2A vs. B), the adaxial side presented a more consistent cell-file pattern and lower variability of epidermal cell length especially in between-vein files, we chose to take measurements from the adaxial side.

Epidermal traits selected for measurements are listed in Table 2a and indicated in Figure 2B and Figure 3. We studied the sizes of selected types of epidermal pavement cells (traits 6 and 7, Table 2a) as indicators of leaf growth restriction since epidermis is considered to control leaf expansion (Quarrie and Jones 1977; van Volkenburgh 1999). We also determined stomatal density (traits 1 and 2), one of the most frequently recorded anatomical traits that is often correlated with leaf stomatal conductance (Xu and Zhou 2008; Tanaka et al. 2013). In water-stressed plants, stomatal density usually increases (Mc Cree and Davis 1974; Zhang et al. 2006; Bresta et al. 2011), largely because stomatal differentiation is inhibited by drought to a lower extent than leaf area expansion. However, the response of stomatal density to drought may in fact be non-linear with progressive water stress leading to a reduction in stomatal density (Xu and Zhou 2008). Stomatal dimensions (traits 8 and 9) are also known to be reduced under drought (Quarrie and Jones 1977; Xu and Zhou 2008). This response may result from the same growth-inhibiting mechanism that causes the reduction of epidermal cell size,

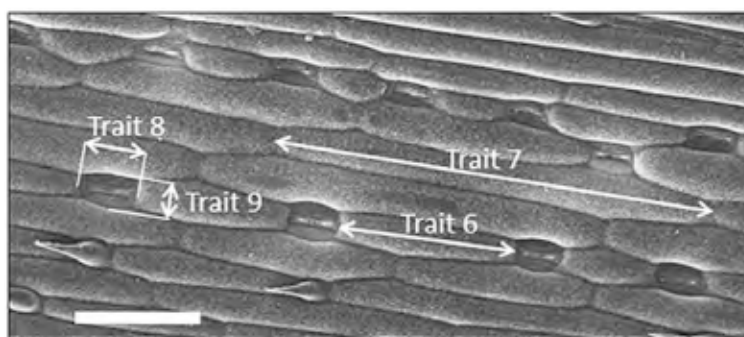


Fig. 3. SEM micrograph of a fragment of adaxial leaf surface. Arrows show dimensions used in calculation of traits 6-9. Bar = 100  $\mu\text{m}$

Table 2. List of traits selected for measurements in *Hordeum* leaves. For illustration of traits, see Figures 2, 3 and 4

Trait number	Trait name	Unit	Remarks
<i>(a) Adaxial lamina surface</i>			
1.	density of stomatal rows	mm <sup>-1</sup>	calculated as the number of rows per mm of lamina width
2.	density of stomata per leaf area unit	mm <sup>-2</sup>	
3.	density of trichomes	mm <sup>-1</sup>	calculated as the number of trichomes per mm of cell file
4.	number of cell files between veins		
5.	density of cell files between veins	mm <sup>-1</sup>	calculated by dividing trait (4) by distance between veins
6.	length of the longest inter-stomatal cell	µm	mean length of three longest cells in this category
7.	length of the longest epidermal cell in a between-stomata row	µm	mean length of three longest cells in this category
8.	stomatal length	µm	mean length of guard cells of three adjacent stomata
9.	stomatal width	µm	mean width of guard cells of three adjacent stomata
<i>(b) Lamina cross-section</i>			
10.	Midrib thickness	µm	
11.	Distance between midrib and first vein	µm	
12.	Distance between first and second veins	µm	
13.	Lamina thickness	µm	Measured mid-way between bundles
14.	Mesophyll thickness	µm	Measured mid-way between bundles
15.	Mesophyll volume fraction	%	Fraction of lamina cross-section occupied by mesophyll tissue
16.	Adaxial epidermis thickness	µm	Measured mid-way between bundles
17.	Adaxial epidermis volume fraction	%	Fraction of lamina cross-section occupied by adaxial epidermal cells
18.	Abaxial epidermis thickness	µm	Measured mid-way between bundles
19.	Abaxial epidermis volume fraction	%	Fraction of lamina cross-section occupied by abaxial epidermal cells
20.	Area of adaxial sclerenchyma	µm <sup>2</sup>	
21.	Area of abaxial sclerenchyma	µm <sup>2</sup>	
22.	Midrib vascular bundle area	µm <sup>2</sup>	
23.	Midrib xylem area	µm <sup>2</sup>	
24.	Midrib metaxylem vessel diameter	µm	Mean of two perpendicular measurements of vessel lumen width

but it may also have an adaptive function because smaller stomata are able to undergo faster closing and opening movements than large stomata (Raven 2014). In addition, we determined the density of foliar trichomes (trait 3). Trichomes in this species probably do not play a role in leaf water relations because of their small size (Fig. 3) but their density may be correlated with other, more direct aspects of drought resistance (Sletvold and Ågren 2012).

#### *Choice of anatomical traits: Leaf cross-section*

In the lamina cross-section, in addition to studying general size modifications (traits 10–12) we focused on traits related to leaf gas exchange potential, water relations and mechanical durability (Table 2b). Lamina thickness and, especially, mesophyll thickness determine the space available for packaging of chlorenchyma cells, thus influencing area-based photosynthetic potential. Drought adaptation and acclimation in grasses are often associated with lamina thickening (Fu and Huang 2003; Chen and Wang 2009). We measured lamina and mesophyll thickness (trait 13 and 14) in the flat part of the lamina, midway between the large (major) vascular bundle and the next, usually a small bundle located in the direction of the midrib (Fig. 4A; bundle nomenclature follows Dannenhoffer et al. 1990).

Adaxial epidermis in many species of Poaceae is modified to contain so-called bulliform cells, designed to undergo drastic volume changes in response to alterations in leaf water status and to cause leaf rolling (Kadioglu and Terzi 2007). These cells may be extremely well developed in some xerophytic grasses (Fahn and Cutler 1992). The thickness of adaxial epidermis (trait 16) measures the degree of development of bulliform cells (Fig 4B). Measurements of abaxial epidermis thickness (trait 18) allow to evaluate the degree of specialization between both epiderms. The calculation of volume fractions of both epiderms and the mesophyll (equal to the surface area of each tissue divided by the width of the section; traits 15, 17, 19; Fig. 4B) helps to examine possible trade-offs involved in the allocation of space among the particular tissues.

Grass leaves contain sclerenchyma fibre strands located parallel to the veins and extending from the epidermis to various depths. Increased leaf sclerification is a repeated pattern in xerophytic leaves (Fahn and Cutler 1992; Dickinson 2000). Therefore, we determined the cross-sectional area of sclerenchyma associated with vascular bundles on the adaxial (trait 20) and abaxial (trait 21) lamina sides (Fig. 4C).

Finally, we measured traits related to water transport capacity and hydraulic safety of the leaves. Evidence indicates that xylem hydraulic capacity, by limiting leaf transpiration potential, may restrict stomatal opening and photosynthetic capacity (Brodribb et al. 2010). Xylem structure in xeromorphic leaves features traits that reduce the probability of disturbance of hydraulic conductance caused

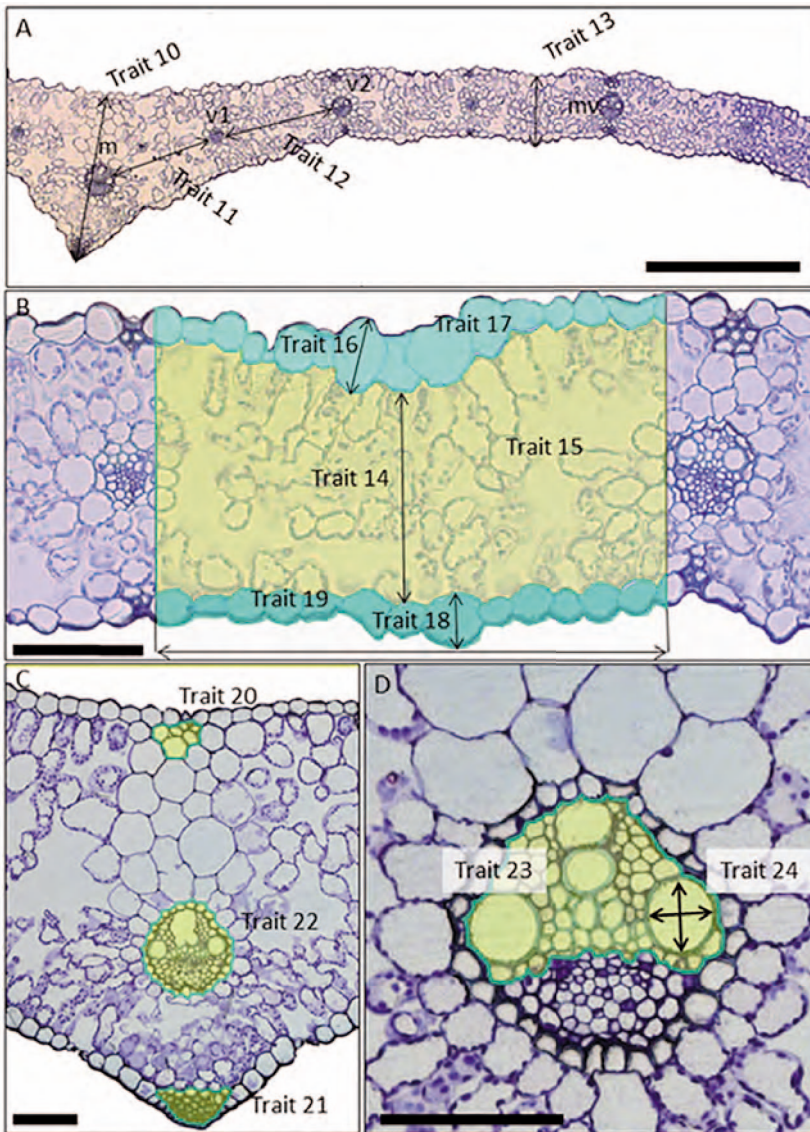


Fig. 4. Cross-sections of Technovit-embedded barley leaves. (A) part of lamina including the midvein (m), two nearest veins (v1 and v2) and the nearest large vein (lv); (B) lamina segment in the proximity of the large vein (lv) nearest to the midrib used for determination of tissue dimensions and volume fractions; (C) midrib region; (D) midvein. Traits selected for measurements are marked by arrows or, in case of areas, shaded in light green, green and yellow. Horizontal arrow under the shaded section in (C) indicates section width used for calculation of tissue volume fractions. Bars = 500 μm (A); 100 μm (B, C); 50 μm (D).

by air bubbles blocking the tracheal elements or by conduit wall collapse (Cochard et al. 2004; Nardini et al. 2012). These traits are usually not consistent with high hydraulic capacity. The cross-sectional area of vascular bundle in the midrib (trait 22; Fig. 4C) and the xylem itself (trait 23; Fig. 4D) should reflect overall transport capacity with much variability resulting from different cellular compositions of both phloem and xylem tissues (Dannanoffer et al. 1990). Given that leaf hydraulic capacity is much dependent on the diameter of largest vessels (Tyree and Zimmermann 2002) and that reducing vessel diameter appears to improve vessel resistance to xylem tension–caused dysfunction by increasing the ratio of cell wall thickness to cell lumen diameter (Blackman et al. 2010), we determined lumen dimensions of large metaxylem vessels in the midrib (trait 24; Fig. 4D).

In summary, by collecting leaves that have experienced drought early in their development, sampling a pre-defined leaf region, using fixation protocol 2b, using leaf samples embedded in Technovit resin for studying cross-sections and SEM images for adaxial epidermal traits, we have assembled a dataset that will provide information on genetic and plastic variability of leaf anatomy of barley genotypes with respect to drought-relevant traits.

#### Acknowledgement

We thank Ms. Ewa Raj for assistance in the laboratory.

#### References

- Blackman C.J., Brodribb T.J., Jordan G.J. 2010. Leaf hydraulic vulnerability is related to conduit dimensions and drought resistance across a diverse range of woody angiosperms. *New Phytol.* 188: 1113-1123.
- Bresta P., Nikopoulos D., Economou G., Vahamidis P., Lyra D., Karamanos A., Karabourniotis G. 2011. Modification of water entry (xylem vessels) and water exit (stomata) orchestrates long term drought acclimation of wheat leaves. *Plant Soil* 347: 179-193.
- Brodribb T.J., Feild T.S., Sack L. 2010. Viewing leaf structure and evolution from a hydraulic prospective. *Funct. Plant Biol.* 37: 488-498.
- Chaves M.M., Oliveira M.M. 2004. Mechanisms underlying plant resilience to water deficits: prospects for water saving agriculture. *J. Exp. Bot.* 55: 2365-2384.
- Chen K.M., Wang F., Wang Y.-H., Chen T., Hu Y.-X., Lin J.-X. 2006. Anatomical and chemical characteristics of foliar vascular bundles in four reed ecotypes adapted to different habitats. *Flora* 201: 555-569.
- Chen L., Wang R. 2009. Anatomical and physiological divergences and compensatory effects in two *Leymus chinensis* (Poaceae) ecotypes in Northeast China. *Agr. Ecosyst. Environ.* 134: 46-52.

- Cochard H., Froux F., Mayr S., Coutand C. 2004. Xylem wall collapse in water-stressed pine needles. *Plant Physiol* 134: 401-408.
- Dannenhoffer J.M., Ebert W. Jr., Evert R.F. 1990. Leaf vasculature in barley, *Hordeum vulgare* (Poaceae). *Am. J. Bot.* 77: 636-652.
- Dickinson W.C. 2000. Integrative plant anatomy. Harcourt Academic Press, San Diego, 534 p.
- Durand J.L., Onillon B., Schnyder H., Rademacher I. 1995. Drought effects on cellular and spatial parameters of leaf growth in tall fescue. *J. Exp. Bot.* 46: 1147-1155.
- Fahn A, Cutler D.F. 1992. Xerophytes. *Encyclopedia of plant anatomy XIII*, 3. Gebrüder Borntraeger, Berlin, 178 p.
- Fu J., Huang B. 2003. Leaf characteristics associated with drought resistance in tall fescue cultivars. *Acta Hort. (ISHS)* 661: 233-239.
- Hacke U., Sperry J. 2001. Functional and ecological xylem anatomy. *Perspect. Plant Ecol. Evol.* 4: 97-115
- Kadioglu A., Terzi R. 2007. A dehydration avoidance mechanism: leaf rolling. *Bot. Rev.* 73: 290-302.
- Khaliq I., Shah S.A.H., Ahsan M. 1999. Evaluation of spring wheat (*Triticum aestivum* L.) for drought field conditions: A morpho-physiological study. *Pak. J. Biol. Sci.* 2: 1006-1009
- Martre P., Durand J.L., Cochard H. 2000. Changes in axial hydraulic conductivity along elongating leaf blades in relation to xylem maturation in tall fescue. *New Phytol.* 146: 235-247.
- McCree K.J., Davis S.D. 1974. Effect of water stress and temperature on leaf size and on the size and number of epidermal cells in grain sorghum. *Crop Sci.* 14: 751-755.
- Monneveux P., Jing R., Misra S.C. 2012. Phenotyping for drought adaptation in wheat using physiological traits. *Frontiers in Physiology* 3, art. 429.
- Nardini A., Pedá G., La Rocca N. 2012. Trade-offs between leaf hydraulic capacity and drought vulnerability: morpho-anatomical bases, carbon costs and ecological consequences. *New Phytol.* 196: 788-798.
- Ogrodowicz P., Mikołajczak P., Kuczyńska A., Krystkowiak K., Surma M., Adamski T. 2014. Plant materials and analysed traits in the greenhouse and field experiments. In this volume: 19-28.
- Quarrie S.A., Jones H.G. 1977. Effects of abscisic acid and water stress on development and morphology of wheat. *J. Exp. Bot.* 28: 192-203.
- Raven J. 2014. Speedy small stomata? *J. Exp. Bot.* 65: 1415-1424.
- Rayan A., Matsuda K. 1988. The relation of anatomy to water movement and cellular response in young barley leaves. *Plant Physiol.* 87: 853-858.
- Ridley E.J., Todd G.W. 1966. Anatomical variations in the wheat leaf following internal water stress. *Bot. Gaz.* 127: 235-238.

- Ristic Z., Cass D.D. 1991. Leaf anatomy of *Zea mays* L. in response to water shortage and high temperature: a comparison of drought-resistant and drought-susceptible lines. *Bot. Gaz.* 152: 173-185.
- Sass J.E. 1958. *Botanical microtechnique*. The Iowa State College Press, Ames, 228 p.
- Sletvold N., Ågren J. 2012. Variation in tolerance to drought among Scandinavian populations of *Arabidopsis lyrata*. *Evol. Ecol.* 26: 559-577.
- Tanaka Y., Shigeno S.S., Shimada T., Hara-Nishimura I. 2013. Enhancement of leaf photosynthetic capacity through increased stomatal density in *Arabidopsis*. *New Phytol.* 198: 757-764.
- Taylor S.H., Franks P.J., Hulme S.P., Spriggs E., Christin P.A., Edwards E.J., Woodward F.I., Osborne C.P. 2011. Photosynthetic pathway and ecological adaptation explain stomatal trait diversity amongst grasses. *New Phytol* 193: 387-396.
- Tyree M.T., Zimmermann M.H. 2002. *Xylem structure and the ascent of sap*. Springer, Berlin, 283 p.
- Utrillas M.J., Alegre L. 1997. Impact of water stress on leaf anatomy and ultrastructure in *Cynodon dactylon* (L.) Pers. under natural conditions. *Int. J. Plant Sci.* 158:313-324.
- van Volkenburgh E. 1999. Leaf expansion – an integrating plant behaviour. *Plant Cell Environ.* 22: 1463-1473.
- Varshney R.K., Paulo M.J., Grando S., van Eeuwijk F.A., Keizer L.C.P., Guo P., Ceccarelli S., Kilian A., Baum M., Graner A. 2012. Genome wide association analyses for drought tolerance related traits in barley (*Hordeum vulgare* L.). *Field Crop. Res.* 126: 171-180.
- Vasellati V., Oesterheld M., Medan D., Loreti J. 2001. Effects of flooding and drought on the anatomy of *Paspalum dilatatum*. *Ann. Bot.* 88:355-360.
- Wenzel C.L., Chandler P.M., Cunningham R.B., Passioura J.B. 1997. Characterization of the leaf epidermis of barley (*Hordeum vulgare* L. 'Himalaya'). *Ann. Bot.* 79: 41-46.
- Xu Z., Zhou G. 2008. Responses of leaf stomatal density to water status and its relationship with photosynthesis in a grass. *J Exp. Bot.* 59: 3317-3325.
- Zhang Y.P., Wang Z.M., Wu Y.C., Zhang X. 2006. Stomatal characteristics of different green organs in wheat under different irrigation regimes. *Acta Agronomica Sinica* 32: 70-75.

## **Contact angle and surface free energy of plant leaves and their changes under drought conditions**

**Malgorzata Łukowska, Henryk Czachor**

*Institute of Agrophysics, Polish Academy of Sciences, Lublin, Poland*

### **Introduction**

Most leaves are non-wettable on their upper surface and wettable underneath (Juniper and Jeffree 1983). Water contact angles can range from 29° on the *Vicia faba* leaf to 170° on surfaces of *Eucalyptus globus* (Wosten et al. 1995). For barley leaves the contact angles vary between 139° and 158° (Wiśniewska et al. 2003). Holloway (1969) stated that the differences in leaf wettability result from the chemical heterogeneity of plant wax surfaces, leaf architectures and surface roughness. The hydrophobicity of plant surface waxes depends upon their chemical constitution and almost certainly upon the orientation of molecules of their constituents. Epicular wax plays a very important role in plant's resistance to a variety of abiotic stresses like freezing, warm temperatures, salinity and drought (Jenks and Ashworth 1999). Some previous studies revealed that drought stress can induce changes (increase) in the amount of wax deposited on leaf surface in many plants, including common and durum wheat (Johnson et al. 1983; Uddin and Marshall 1988), velvet leaf (Levene and Owen 1995), thyme (Letchamo and Gosselin 1996), cotton (Bondada et al. 1996), rose (Jenks et al. 2001), pea (Sánchez et al. 2001), peanut (Samdur et al. 2003) and sesame (Kim et al. 2007). Moreover, some reports show that the increase in wax production is associated with better drought tolerance in oat (Bengstone et al. 1978) and transgenic alfalfa (Zhang et al. 2005). Increase in the amount of wax on the leaf surface causes its hydrophobization. Contact angle and surface free energy measurement can be the tools for rapid assessment of leaf hydrophobization progress under drought, which also allow for quantitative characterization of wettability parameters. There is only a few literature reports concerning surface free energy (SFE) of plant leaves (Khayet and Fernandez 2012; Zhu et al. 2014) despite it being a very sensitive parameter on changes in surface structure and chemical composition. Even very small changes in the nature of the surface can be reflected by SFE

(Zhu et al. 2014). To determine the SFE, the contact angle measurements of two or three liquids exhibiting different interactions with the solid substrate should be done. In this paper, we perform preliminary tests to show the applicability of SFE as an indicator of plant response to drought stress.

## Theory

### *Plant surface*

The upper parts of the plant are covered by the epicuticular waxes, which contribute to making the leaves' surface waterproof. The leaf and stem possess a multilayered structure. The top layer, cuticle, represents the interface between the plant and the environment (Bartel et al. 2003). Cuticles consist of the insoluble polymers cutin (a polyester matrix) and, in some species, cutan. In addition, it contains polysaccharides such as cellulose and various soluble lipids – a complex mixture of long-chain alkanes, branched chain alkanes, alkenes, esters of fatty acids and primary alcohols (monoesters, diesters, polyesters, estolides and glycerides), free fatty acids and alcohols, aldehydes, ketons (diketons, substituted  $\beta$ -diketones), terpenoids and phenolic substances (Jetter et al. 2000). These lipids are often called 'waxes'. The two major functions of the cuticle are to protect plants from an uncontrolled loss of water and to reduce the leaching of organic and inorganic substances from the leaf interior (Warth 1960; Hamilton 1995). Waxes have been shown to be responsible for these barrier properties (Martin and Juniper 1970). Moreover, the plant waxes enhance reflectance which results in the decrease of absorption of visible and infrared radiation, and thus the leaf temperature and transpiration loss are reduced.

The cuticle thickness of different species is generally less than 1  $\mu\text{m}$  but for some species it can vary from 0.1 to 20  $\mu\text{m}$  (Barthlott et al. 1998; Wagner et al. 2003). However, fossil plants with cuticles as thick as 50-500  $\mu\text{m}$  are known (Barthlott et al. 1998). The upper part of the cuticle is a wax layer in the form of an unspecified thin film, a smooth thin layer or characteristic crystals (Davis and Rideal 1966). Cuticular waxes cover only the outer part of the stem and leaves, while the internal part of the stem consists only of the remaining cells of parenchyma. On a molecular level, the cuticular waxes are arranged in three-dimensional crystals creating hydrophobic, macrostructured surface of



Fig. 1. Cross section of barley leaf

low wettability (Lavi and Marmur 2004). There are 18 distinguishable forms of plant wax coverages which can be divided into two main groups: layers and crystalloids (Barthlott et al. 1998). The first group consists of thin films, smooth layers (less than 1  $\mu\text{m}$  thickness), crusts (more than 1  $\mu\text{m}$  thickness) and fissured layers. The crystalloids group is represented by granules, irregular platelets, plates, rodlets, tubules and transitional crystalloid forms. It is well known that the surface structures and chemistry influence the surface wettability.

### *Wettability*

The water droplet can more or less spread over the solid surface (e.g. leaf surface). If the water molecules cover the surface as a thin layer, it is called wetting. When the water molecules are not attracted to solid phase and water is in a drop shape, the liquid does not moist the surface. Wetting of a solid by a liquid is a surface phenomenon in which the surface of the solid is covered by the liquid placed over it. Spreading is a physical process through which a liquid wets the surface. Different wetting states of a drop of liquid placed on a solid substrate are shown in Fig. 2.

Wettability can be defined as a tendency of a liquid to spread on a solid substrate. It describes the extent of intimate contact between a liquid and a solid. There are two important parameters to characterize the wettability of a liquid on a solid:

- degree or extent of wetting – contact angle,
- rate of wetting.

The degree of wetting is indicated by a contact angle formed at the interface between the solid and liquid. It is dependent on the surface and interfacial energies at the solid/liquid interface. The rate of wetting indicates how fast the liquid wets the surface and spreads over. It is guided by a number of factors such as thermal conditions of a system, capillary forces, viscosity of a liquid and chemical reactions occurring at the interface.

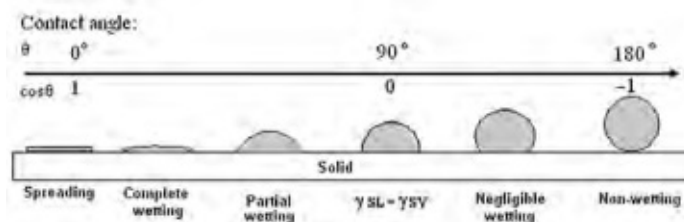


**Fig. 2.** Liquid drop on solid surface. The condition  $\theta < 90^\circ$  indicates that the solid is wettable by the liquid and  $\theta > 90^\circ$  indicates non-wetting. The limits  $\theta = 0$  and  $\theta = 180^\circ$  define complete wetting and complete non-wetting, respectively

When a drop of a liquid is placed on a solid surface, any of the following phenomena may take place either alone or in combination depending on the properties of the solid and the spreading liquid as well as on the system/environmental conditions:

- The drop of liquid may spread continuously to cover the whole solid surface forming a film on the solid surface. It is known as complete wetting.
- The liquid drop may spread partially to some extent and come to equilibrium within a short period of time – a case referred as partial or incomplete spreading.
- The liquid may spread a little or may not spread at all. For highly lyophobic (superhydrophobic) surfaces, such behavior is called ‘lotus leaf effect’.

These phenomena clearly indicate the complexity of the wetting processes and related forces responsible for their occurrence. In the simplest case of spreading of a non-reactive liquid on smooth and inert solid, only surface tension and viscous forces act upon and determine the equilibrium state. However, the real situation is more complex as already pointed out and a great number of factors affect the process, and in most cases they do not allow the equilibrium to be reached.

The process of wetting of a solid by a liquid has a great technical importance. A large number of general/biological/industrial/manufacturing/fabrication processes essentially involve wetting phenomena (Lavi and Marmur 2004). Some applications require a good wetting between liquid and substrate surface whereas some others demand poor wetting or repellency. For example, superhydrophobic surfaces are very useful in soldering and brazing. Similarly, evaporation of the spreading liquid found application in quenching operations involved in industrial heat treatment (Chandra et al. 1996; Sefiane et al. 2003; Bhushan and Jung 2011).

### *Contact angle*

To investigate the wetting process, the measurements of contact angles are used (Fig. 3). Contact angle is the angle, conventionally measured through the liquid phase at the point where a liquid/vapor interface meets a solid surface.

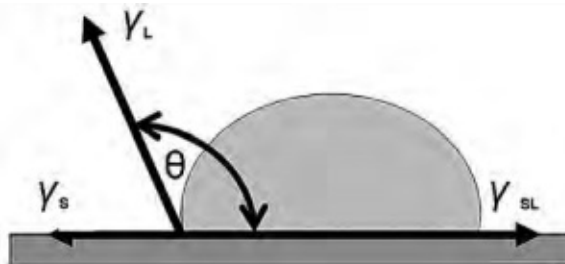


Fig. 3. Scheme of liquid droplet in contact with solid surface

The surface forces balance between the solid and liquid phases are described by Young's equation (Young 1805):

$$\gamma_s - \gamma_{SL} = \gamma_L \cos \theta_c, \quad (1)$$

where  $\gamma_{SL}$  is solid/liquid interfacial free energy,  $\gamma_L$  the SFE of liquid,  $\gamma_s$  the SFE of solid and  $\theta_c$  the contact angle of the liquid on a solid.

Dupre defined the work of adhesion between solid and liquid as follows (Dupre 1869):

$$W_{SL} = \gamma_s + \gamma_L - \gamma_{SL}. \quad (2)$$

Combining Eqs. 1 and 2, the Young–Dupre equation is obtained:

$$W_{SL} = \gamma_L (1 + \cos \theta). \quad (3)$$

The contact angle of a given liquid increases as the adhesion between the liquid and the solid decreases. An angle of  $180^\circ$  indicates no adhesion between the liquid and surface, and therefore represents a total non-wetting condition. For the hydrophobic surfaces, the contact angle is higher than  $90^\circ$  and for a hydrophilic surface it is lower than this value. In such cases, the liquid drops tend to move easily on the substrate surface and do not have any tendency to enter into pores or holes by capillary action. It is generally accepted that the smaller the contact angle, the better the wettability. Good wettability can be expected when  $\gamma_L$  is small and  $\gamma_s$  is high.

#### *Contact angle measurements*

Contact angle is measured either directly or by fitting a mathematical expression to the shape of the liquid drop and then calculating the slope of the tangent to the liquid drop at the liquid/solid/vapor interface line. There are two possibilities of contact angle measurement using a drop-shape analyser: sessile drop (Fig. 3) and captive bubble (Fig. 4). Sessile drop is a drop sitting on a surface, and captive bubble is a bubble floating up in fluid and touching the sample bottom thus shifting the positions of liquid and vapor.



Fig. 4. Captive bubble

Sessile drop contact angle measurements on barley leaves are technically difficult. The leaf should be placed on a glass plate using double-side tape so that it does not move during taking measurements. The drop volume should be adjusted to leaf size. The temperature of the ambient environment must be on the same level during the whole time of measurement. Some authors (Wiśniewska et al. 2003) distinguish contact angles along the veins and perpendicular to veins present on leaf surface.

*Contact angle hysteresis*

If the volume of a drop of liquid settled on a solid surface increases (say, by the addition of a liquid from a pipette, Fig. 5A), the measured ‘advancing’ contact angle increases, and the opposite is also true: if the drop volume decreases, the ‘receding’ contact angle is smaller. This phenomenon is called ‘contact angle hysteresis’.

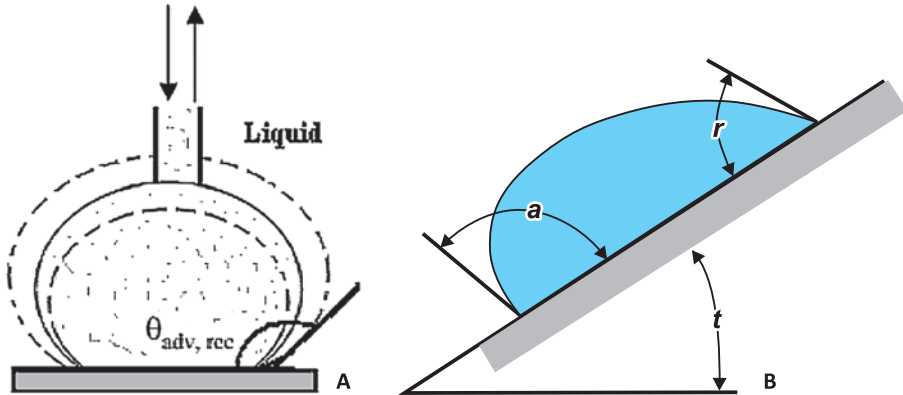


Fig. 5. (A) Contact angle hysteresis phenomenon,  $\theta_{adv}$  – advancing contact angle,  $\theta_{rec}$  – receding contact angle; (B) advancing ( $a$ ) and receding ( $r$ ) contact angles during liquid drop movement

In real systems, the macroscopic contact angles depend on solid surface heterogeneity, surface roughness and equilibrium time. According to Wenzel (1936), the surface roughness  $r$  has an effect on the equilibrium contact angle:

$$\cos\theta_w = r \cos\theta, \tag{4}$$

where  $\theta$  is the equilibrium contact angle,  $\theta_w$  the apparent contact angle on a rough surface,  $r$  the roughness factor which is equal to the ratio of surface area  $A_S$  to its flat projected area  $A_F$ :

$$r = \frac{A_S}{A_F} \tag{5}$$

and  $r$  is always greater than 1.

When the contact angle is less than  $90^\circ$ , apparent contact angle decreases with increase in roughness, whereas it tends to increase with increasing roughness for contact angles greater than  $90^\circ$ . Lyophilicity and lyophobicity are reinforced by roughness (Nosonovsky and Bhushan 2005).

When a surface is composed of two fractions, one of the fractional area  $f_1$  and the contact angle  $\theta_1$ , and second of  $f_2$  and  $\theta_2$ , ( $f_1 + f_2 = 1$ ), the contact angle for the heterogeneous interface is given by the Cassie (1948) equation:

$$\cos\theta = f_1 \cos\theta_1 + f_2 \cos\theta_2. \quad (6)$$

When the composite interface is a mixture of a solid ( $f_1 = f_{SL}$ ,  $\theta_1 = \theta_0$ ) and a non-wettable liquid ( $f_2 = f_{LA} = 1 - f_{SL}$ ,  $\cos\theta_2 = -1$ ), the contact angle for this interface is given by Cassie–Baxter equation (Cassie and Baxter 1945):

$$\cos\theta = r \cos\theta_0 - f_{LA}(r \cos\theta_0 + 1). \quad (7)$$

In the third option, when the  $\cos\theta_2 = 1$  ( $\theta_2 = 0^\circ$  corresponds to the liquid-on-liquid contact), the contact angle for this interface is given by Cassie equation (Cassie 1948):

$$\cos\theta = 1 + f_{SL}(\cos\theta_0 - 1). \quad (8)$$

Equation 8 is often used for the homogeneous interface instead of Eq. 4 if the surface is covered by holes filled with water (Bhushan and Jung 2011). Schematics of different interfaces considering homogeneous and heterogeneous friction are given in Fig. 6.

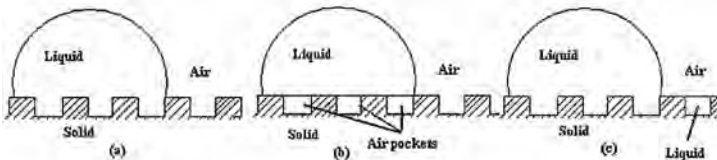


Fig. 6. Schematics of different interfaces according to: (a) Wenzel equation, (b) Cassie–Baxter equation and (c) Cassie equation

### Surface free energy

The SFE ( $\gamma$ ) depends on the type of forces on the surface of a condensed phase (solid or liquid): always existing dispersive forces (London's type) and the forces of polar nature (electrostatic between ions, permanent dipoles, induced dipoles, hydrogen bonds, bridges and acceptor–donor interactions). The value of  $\gamma$  of the liquid ( $\gamma_L$ ) can be determined by direct methods, whereas for estimation of  $\gamma_S$  of solids many indirect methods such as Fowkes, Owen–Wendt, Wu, Zisman, Neuman and van Oss–Chaudhury–Good have been designated.

According to Owen–Wendt method, the SFE ( $\gamma$ ) is the sum of two components: a polar  $\gamma^P$  (consisting of the sum of all polar interactions) and dispersion  $\gamma^D$  (Owens and Wendt 1969):

$$\gamma = \gamma^D + \gamma^P. \quad (9)$$

Regarding the thermodynamic equilibrium at the surface (Young’s equation, Eq. 1), interfacial SFE is described by the following formula (Owens and Wendt 1969):

$$\gamma_{SL} = \gamma_S + \gamma_L - 2(\gamma_S^D \gamma_L^D)^{0.5} - 2(\gamma_S^P \gamma_L^P)^{0.5}, \quad (10)$$

where  $\gamma_S$ ,  $\gamma_S^D$ ,  $\gamma_S^P$  – SFE of the solid and its dispersion and polar components;  $\gamma_L$ ,  $\gamma_L^D$ ,  $\gamma_L^P$  – SFE of the liquid and its dispersion and polar components,  $\gamma_{SL}$  – interfacial SFE.

Calculation of the SFE and its components for the solid surface is based on contact angle measurements of two different liquids (diiodomethane and water). Dispersion and polar components are given by Park et al. (2000) and Żenkiewicz (2005):

$$(\gamma_S^D)^{0.5} = \frac{\gamma_d(\cos \theta_d + 1) - \sqrt{\frac{\gamma_d^P}{\gamma_w^P}} \gamma_w(\cos \theta_w + 1)}{2 \left[ \sqrt{\gamma_d^D} - \sqrt{\gamma_d^P \frac{\gamma_w^D}{\gamma_w^P}} \right]}, \quad (11)$$

$$(\gamma_S^P)^{0.5} = \frac{\gamma_w(\cos \theta_w + 1) - 2\sqrt{\gamma_S^D \gamma_w^D}}{2\sqrt{\gamma_w^P}}, \quad (12)$$

where subscripts ‘ $d$ ’ and ‘ $w$ ’ hold for diiodomethane and water, respectively.

The most recent concept of SFE is the van Oss–ChaudhuryGood’s approach (van Oss et al. 1988). According to it, the SFE ( $\gamma_{SL}$ ) is the sum of two components: Lifshitz van der Waals component  $\gamma^{LW}$  (consisting the input of long-distance interactions such as London, Keesom and Debye forces) and acid–base component  $\gamma^{AB}$  (consisting the input of short distance interactions such as acid–base ones). The SFE is given by

$$\gamma_{SL} = \left[ (\gamma_S^{LW})^{0.5} - (\gamma_L^{LW})^{0.5} \right]^2 + 2 \left[ (\gamma_S^+)^{0.5} - (\gamma_L^+)^{0.5} \right] \left[ (\gamma_S^-)^{0.5} - (\gamma_L^-)^{0.5} \right] \quad (13)$$

$$\gamma_S = \gamma_S^{LW} + \gamma_S^{AB} = \gamma_S^{LW} + 2(\gamma_S^+ \gamma_S^-)^{0.5}, \quad (14)$$

where the  $\gamma^+$  and  $\gamma^-$  are (solid  $S$  or liquid  $L$ ) acid and base components, respectively.

In combination with the Young equation (Eq. 1), van Oss method gives

$$\left(\gamma_S^{LW} \gamma_{Li}^{LW}\right)^{0.5} + \left(\gamma_S^+ \gamma_{Li}^-\right)^{0.5} + \left(\gamma_S^- \gamma_{Li}^+\right)^{0.5} = \gamma_{Li} (1 + \cos \theta_i) / 2, \quad (15)$$

where  $i = 1, 2, 3$  and refers to the given liquid. There are three unknowns in the Eq. 15:  $\gamma_S^{LW}$ ,  $\gamma_S^+$  and  $\gamma_S^-$ . To determine SFE, a system of those three equations with three unknowns must be solved. In place of  $L_i$  the appropriate values for the three measuring liquids such as water, diiodomethane and formamide must be substituted.

One of the latest methods of determining SFE of a solid is based on contact angle hysteresis (Chibowski et al. 2002; Chibowski 2003). It involves measurements of advancing  $\theta_a$  and receiving  $\theta_r$  contact angle of the same liquid  $\gamma_L$ . Value of SFE of a solid is determined by the equation:

$$\gamma_S = \gamma_L (\cos \theta_r + \cos \theta_a) \left\{ (1 + \cos \theta_a)^2 / [(1 + \cos \theta_r)^2 - (1 + \cos \theta_a)^2] \right\}. \quad (16)$$

## Example

Five cultivars of spring barley (*Hordeum vulgare* L.): Cam/B1/CI08887//CI05761 (here after referred as CamB1), Maresi, Georgie, Sebastian and Stratus were tested under optimal (control) and water stress conditions. Plants were grown in cylinders placed in a growing chamber. The soil water potential was stabilized at pF around 2.2 (10% w/w moisture). After the plants developed three leaves (about 3 weeks of germination), the addition of water to cylinders with the stressed plants was stopped until the soil reached pF around 3.5 (6-8% w/w moisture). The stress was continued for 10 days. Then three samples from each fresh leaf were taken and fixed on a glass plate using a double-sided adhesive tape. The contact angle of water, formamide and diiodomethane droplets (5  $\mu$ l) was determined on the upper leaf surfaces using a microscope (DSA100, KRÜSS) equipped with a goniometer and CCD camera. The measurements were done with nine replicates. Similar experiment was performed for air-dry leaves.

Exemplary photos of various liquid drops placed on barley leaf surface measured using Drop shape analyser DSA 100 KRÜSS 2010 (Figs. 7 and 8) are shown in Tables 1 and 2.

The water contact angle is the most reliable to characterize surface wettability. Typically, the surface of most plant leaves is hydrophobic due to the epicuticular waxes. The contact angle value depends on the composition of the wax and the spatial position of wax crystals on the leaf surface. Water contact angle for barley cultivars grown under control condition varied from 134.9° to 143.5°, and under drought from 139.6° to 155.1°. The increase in the value of the contact angle during stress shows plant defence to drought stress.

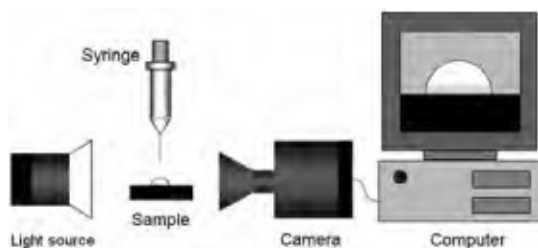


Fig. 7. Scheme of experimental set-up



Fig. 8. KRÜSS drop shape analyser

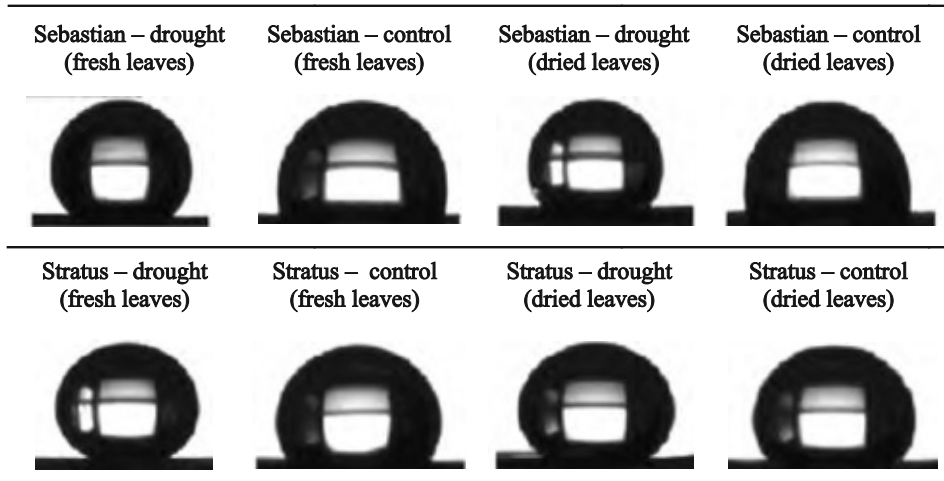
Table 1. Photographs of contact angles on fresh barley leaves

Cultivar/treatment	Water contact angle	Diiodomethane contact angle	Formamide contact angle
CamB1 control			
CamB1 drought			
Maresi control			
Maresi drought			

The water contact angle of dried leaves was smaller than that of fresh ones.

Some results of SFE and contact angle of barley leaves grown under control conditions (C) and under drought stress conditions (D) are summarized in Tables 3 to 6. SFE is a very sensitive parameter due to changes in the nature of the interactions on the surface. It may be noticed that  $\gamma_s$  of barley leaves is higher for plants grown under control conditions than under drought conditions. Leaf surface becomes more hydrophobic hence the SFE decreases. The dominating component in the  $\gamma_s$  is the dispersive one  $\gamma_s^D$  or  $\gamma_s^{LW}$  which refers to long-range

**Table 2. Water contact angle of two varieties of barley leaves (fresh and dried) from plants grown under drought and control conditions**



interactions, such as those present in hydrocarbons which are components of the epicuticular wax. Other components  $\gamma_s^P$  or  $\gamma_s^{AB}$  contribute less to the  $\gamma_s$  and refer to the polar groups interactions, such as -OH, -COOH, -COH, =O, occurring as components of wax esters of fatty acids and primary alcohols, long-chain alcohols, aldehydes, ketones, etc. Drought in general leads to an increase in the input of  $\gamma_s^D$  or  $\gamma_s^{LW}$  components to SFE, whereas the input of  $\gamma_s^P$  and/or  $\gamma_s^{AB}$  generally decreases.

It seems that the intensity in change of the value of SFE due to water stress condition may be related to plant's resistance to drought. The closer the ratio of  $\gamma_s^{stress}/\gamma_s^{contr}$  to 1, the lower the response of plants to drought stress. Analysis revealed that Sebastian responded to drought more rapidly than the CamB1 variety.

**Table 3. The values of contact angles  $\theta$  (deg), surface free energy  $\gamma_s$  ( $mJ m^{-2}$ ) and its components ( $\gamma_s^P$ ,  $\gamma_s^D$ ) determined for fresh leaves of barley plants grown under drought (D) and control (C) conditions using Owens–Wendt method**

Cultivar	$\theta_{water}$	$\theta_{diiodomethane}$	$\gamma_s$	$\gamma_s^D$	$\gamma_s^P$
Sebastian C	136.5	121.0	14.7	12.6	2.1
Sebastian D	148.2	123.6	9.7	8.5	1.2
CamB1 C	146.2	131.3	11.9	10.4	1.5
CamB1 D	150.0	130.7	10.9	9.6	1.3

**Table 4. The values of contact angles  $\theta$  (deg), surface free energy  $\gamma_s$  ( $\text{mJ m}^{-2}$ ) and its components ( $\gamma_s^{\text{LW}}$ ,  $\gamma_s^{\text{AB}}$ ) determined for fresh leaves of barley plants grown under drought and control conditions using van Oss–Chaudhury–Good methods**

Cultivar	$\theta_{\text{water}}$	$\theta_{\text{diiodomethane}}$	$\theta_{\text{formamide}}$	$\gamma_s$	$\gamma_s^{\text{LW}}$	$\gamma_s^{\text{AB}}$
Sebastian C	136.5	121.0	128.5	7.0	5.2	1.8
Sebastian D	148.2	123.6	134.4	3.8	2.4	1.4
CamB1 C	146.2	131.3	129.0	8.1	5.6	2.5
CamB1 D	150.0	130.7	134.0	7.8	5.6	2.2

**Table 5. The ratio of the surface free energy  $\gamma_s$  and its components  $\gamma_s^{\text{P}}$  and  $\gamma_s^{\text{D}}$  of stressed plants to control plants determined using Owen–Wendt method**

Cultivar	$\gamma_s^{\text{stress}}/\gamma_s^{\text{contr}}$	$\gamma_s^{\text{D stress}}/\gamma_s^{\text{D contr}}$	$\gamma_s^{\text{P stress}}/\gamma_s^{\text{P contr}}$
Sebastian	0.66	0.67	0.57
CamB1	0.92	0.92	0.87

**Table 6. The ratio of the surface free energy  $\gamma_s$  and its components  $\gamma_s^{\text{LW}}$  and  $\gamma_s^{\text{AB}}$  of stressed plants to control plants determined using van Oss–Chaudhury–Good methods**

Cultivar	$\gamma_s^{\text{stress}}/\gamma_s^{\text{contr}}$	$\gamma_s^{\text{LW stress}}/\gamma_s^{\text{LW contr}}$	$\gamma_s^{\text{AB stress}}/\gamma_s^{\text{AB contr}}$
Sebastian	0.54	0.46	0.78
CamB1	0.96	1.00	0.88

In our opinion, the sessile drop method is a useful tool to study wettability and SFE of plant leaves under various growing conditions. However, more studies should be performed to evaluate the influence of drought on the properties of leaves that should be complemented by other methods allowing estimating the surface build-up and properties of surface waxes.

## References

- Bartel H., Barthlott W., Koch K., Schreiber L., Neinhuis C. 2003. Plant cuticles: multifunctional interfaces between plant and environment. In: Hemsley, A.R., Poole, I (eds.) *Evolution of Plant Physiology*, Academic Press, London: 171-194.

- Barthlott W., Neinhuis C., Cutler D., Ditsch F., Meusel I., Theisen I., Wilhelm H. 1998. Classification and terminology of plant epicuticular waxes. *Botanical Journal of the Linnean Society* 126: 237-260.
- Bengston C., Larsson S., Liljenberg C. 1978. Effect of water stress on cuticular transpiration rate and amount and composition of epicuticular wax in seedlings of six oat varieties. *Physiologia Plantarum* 44: 319-324.
- Bernardin D., Mudawar I., Walsh C.B., Franses I. 1997. Contact angle temperature dependence for water droplets on practical aluminum surfaces. *International Journal of Heat and Mass Transfer* 40: 1017-1033.
- Bhushan B., Jung Y.C. 2011. Natural and biomimetic artificial surfaces for superhydrophobicity, self-cleaning, low adhesion, and drag reduction. *Progress in Materials Science* 56: 1-108.
- Bondada B.R., Oosterhuis D.M., Murphy J.B., Kim K.S. 1996. Effect of water stress on the epicuticular wax composition and ultrastructure of cotton (*Gossypium hirsutum* L.) leaf, bract, and boll. *Environmental and Experimental Botany* 36: 61-69.
- Cassie A.B.D. 1948. Contact angles. *Discussions of the Faraday Society* 3: 11-16.
- Cassie A.B.D., Baxter S. 1945. Large contact angles of plant and animal surfaces. *Nature* 155: 21-22.
- Chandra S., di Marzo M., Qiao Y.M., Tartarini P. 1996. Effect of liquid-solid contact angle on droplet evaporation. *Fire Safety Journal* 27: 141-158.
- Chibowski E. 2003. Surface free energy of a solid from contact angle hysteresis. *Advances in Colloid and Interface Science* 103: 149-172.
- Chibowski E., Ontiveros-Ortega A., Perea-Carpio R. 2002. On the interpretation of contact angle hysteresis. *Journal of Adhesion Science and Technology* 16: 1367-1404.
- Davis J.T., Rideal E.K. 1966. *Interfacial phenomena* (2nd edn.). Academic Press, New York: 1-52.
- Dupre A. 1869. *Theorie Mecanique de La Chaleur*. Gauthier-Villan, Paris.
- Hamilton R.J. 1995. *Waxes: Chemistry, Molecular Biology and Function*. The Oily Press. Dundee: 131-155.
- He B., Lee J., Patankar N.A. 2004. Contact angle hysteresis on rough hydrophobic surfaces. *Colloids and Surfaces A: Physicochemical and Engineering Aspects* 248: 101-104.
- Holloway P.J. 1969. The effects of superficial wax on leaf wettability. *Annals of Applied Biology* 63: 145-153.
- Hołysz L. 2000. Investigation of the effect of substrata on the surface free energy components of silica gel determined by thin layer wicking method. *Journal of Materials Science* 35: 6081-6091.
- Jańczuk B., Białopiotrowicz T., Zdziennicka A. 1999. Some remarks on the components of the liquid surface free energy. *Journal of Colloid And Interface Science* 211: 96-103.

- Jenks M.A., Andersen L. Teusink R.S., Williams M.H. 2001. Leaf cuticular waxes of potted rose cultivars as affected by plant development, drought and paclobutrazol treatment. *Physiologia Plantarum* 112: 62-70.
- Jenks M.A., Ashworth E.N. 1999. Plant epicuticular waxes: function, production, and genetics. *Horticultural Reviews* 23: 1-68.
- Jetter R., Schaffer S., Riederer. 2000. Leaf cuticular waxes are arranged in chemically and mechanically distinct layers: evidence from *Prunus laurocerasus* L. *Plant Cell and Environment* 23: 619-628.
- Johnson D.A., Richards R.A., Turner N.C. 1983. Cuticular conductance, water use efficiency and drought tolerance of durum wheat isolines of differing glaucousness. *Crop Science* 23: 318-325.
- Juniper B.E. 1959. The effect of pre-emergent treatment of peas the ascorbic acid system in plant tissues. *New Physiologist* 58: 1-4.
- Juniper B.E., Jeffree C.E. 1983. *Plant Surfaces*. Edward Arnold, London: 93.
- Khayet M., Fernandez V. 2012. Estimation of the solubility parameters of model plant surfaces and agrochemicals: a valuable tool for understanding plant surface interactions. *Theoretical Biology and Medical Modelling* 9: 45-67.
- Kim K.S., Park S.H., Jenks M.A. 2007. Changes in leaf cuticular waxes of sesame (*Sesamum indicum* L.) plants exposed to water deficit. *Journal of Plant Physiology* 164: 1134-1143.
- Kolattukudy P.E. 1980. Biopolyester Membranes of Plants: Cutin and Suberin. *Science* 208: 990-1000.
- Lavi B., Marmur A. 2004. The exponential power law: partial wetting kinetics and dynamic contact angles. *Colloids and Surfaces A: Physicochemical and Engineering Aspects* 250: 409-414.
- Letchamo W., Gosselin A. 1996. Transpiration, essential oil glands, epicuticular wax and morphology of *Thymus vulgaris* are influenced by light intensity and water supply. *The Journal of Horticultural Science and Biotechnology* 71: 123-134.
- Levene B.C., Owen M.D.K. 1995. Effect of moisture stress and leaf age on bentazon absorption in common cocklebur (*Xanthium strumarium*) and velvetleaf (*Abutilon theophrasti*). *Weed Science* 43: 7-12.
- Linskens H.F. 1950. Quantitative Bestimmung der Benetzbarkeit von Blattoberflächen. *Planta* 38: 591-600.
- Martin J.T., Juniper B.E. 1970. *The Cuticles of Plants*. St. Martin's Press. New York: 54-61.
- Nosonovsky M., Bhushan B. 2005. Roughness optimization for biomimetic superhydrophobic surfaces. *Microsystem Technologies* 11: 535-549.
- Nosonovsky M., Bhushan B. 2008. Patterned nonadhesive surfaces: Superhydrophobicity and wetting regime transitions. *Langmuir* 24: 1525-1533.
- Owens D.K., Wendt R.C. 1969. Estimation of the surface free energy of polymers. *Journal of Applied Polymer Science* 13: 1741-1747.

- Park S.J., Cho S.M., Lee J.R. 2000. Studies on the surface free energy of carbon-carbon composites: Effect of filler addition on the ILSS of composites. *Journal of Colloid and Interface Science* 226: 60-64.
- Samdur M.Y., Manivel P., Jain V.K., Chikani B.M., Gor H.K., Desai S., Misra J.B. 2003. Genotypic differences and water-deficit induced enhancement in epicuticular wax load in peanut. *Crop Science* 43: 1294-1299.
- Sánchez F.J., Manzanares M., de Andrés E.F., Tenorio J.L., Ayerbe L. 2001. Residual transpiration rate, epicuticular wax load and leaf colour of pea plants in drought conditions. Influence on harvest index and canopy temperature. *European Journal of Agronomy* 15: 57-70.
- Sefiane K., Tadrist L., Douglas M. 2003. Experimental study of evaporating water-ethanol mixture sessile drop: influence of concentration. *International Journal of Heat and Mass Transfer* 46: 4527-4534.
- Uddin M.N., Marshall D.R. 1988. Variation in epicuticular wax content in wheat. *Euphytica* 38: 3-9.
- Van Oss C., Chaudhury M.K., Good R.J. 1988. Interfacial Lifshitz-van der Waals and polar interactions in macroscopic systems. 88: 927-941.
- Wagner P., Furstner R., Barthlott W., Neinhuis C. 2003. Quantitative assessment to the structural basis of water repellency in natural and technical surfaces. *Journal of Experimental Botany* 54: 1295-1303.
- Warth A.H. 1960. *The Chemistry and technology of waxes*. Reinhold, New York: 122-124.
- Wenzel R.N. 1936. Resistance of solid surfaces to wetting by water. *Industrial and Engineering Chemistry* 28: 988-994.
- Wiśniewska S.K., Nalasowski J., Witka-Jeżewska E., Hupka J., Miller J.D. 2003. Surface properties of barley straw. *Colloids and Surfaces B: Biointerfaces* 29: 131-142.
- Wosten H.A.B., Ruardy T.G., van der Mei H.C., Busscher H.J., Wessels J.G.H. 1995. Interfacial self-assembly of a *Schizophyllum commune* hydrophobin into an insoluble amphipathic protein membrane depends on surface hydrophobicity. *Colloids and Surfaces B: Biointerfaces* 5: 189-195.
- Young T. 1805. An Essay on the Cohesion of Fluids. *Philosophical Transactions of the Royal Society of London*. 95: 65-87.
- Żenkiewicz M. 2005. Wettability and surface free energy of radiation modified polyethylene film. *Polimery* 50: 365-370.
- Zhang J.Y., Broeckling C.D., Blancaflor E.B., Sledge M.K., Sumner L.W., Wang Z.Y. 2005. Overexpression of *WXPI*, a putative *Medicago truncatula* AP2 domain-containing transcription factor gene, increases cuticular wax accumulation and enhances drought tolerance in transgenic alfalfa (*Medicago sativa*). *The Plant Journal* 42: 689-707.
- Zhu Y., Yu C., Li Y., Zhu Q., Zhou L. Cao C., Yu T., Du F. 2014. Research on the changes in wettability of rice (*Oryza sativa*) leaf surface at different development stages using the OWRK method. *Pest Management Science* 70: 462-469.



## **Determination of proline, carbohydrates and ethylene content and their role in drought stress in plant**

**Maria Filek, Jolanta Biesaga-Kościelniak, Michał Dziurka**

*The Franciszek Górski Institute of Plant Physiology, Polish Academy of Sciences, Kraków, Poland*

### **Introduction**

The mechanism of action of stress factors, as well as the role of specific substances synthesized under stress conditions, is not fully recognized. An important element in the research conducted in many laboratories in the world is to show which of these substances may be indicative of tolerance of plants to stress. Synthesis of osmoprotectants, including proline and carbohydrates, is regarded as one of the stages of the mechanism of plant cell protection under conditions of water stress associated with drought. In addition, ethylene – easily transferring gas hormone – can be included into the mechanism of ‘intercellular signalling’ under action of stress factors.

The paper presents the methodology for the determination of these substances, which are used in the study of drought stress in barley, preceded by the information on their importance in the mechanism of plant resistance. Furthermore, the technique of electron spin resonance applied for the identification of the sugar radicals is described.

### **Proline**

The significance of proline (endogenous  $\alpha$ -amino acid) as an osmoprotectant was first proposed by Csonka et al. (1989) on the basis of research conducted on the bacteria *Escherichia coli*. Subsequent papers by these authors confirmed this assumption and also expanded the osmoprotective role of proline under stress to include plant cells (Csonka and Hanson 1991; Grzesiak et al. 2013). Further studies showed that the proline concentration under stress conditions often rises to values several times higher than those observed in the control sample.

Sharma et al. (2011) argue that in addition to the osmoprotective properties, proline also acts as a buffer controlling the pH of the cytosol and promotes the maintenance of redox balance in cells. Furthermore, proline is considered to be a reserve source of carbon and nitrogen, capable of maintaining the metabolic activity of tissues when subjected to stress factors (Sharma et al. 2011). Proline is also attributed to the antioxidant activity and participation in the deactivation of the hydroxyl radical ( $\bullet$ OH) and singlet oxygen ( $^1\text{O}_2$ ) formed under conditions of oxidative stress (Alia et al. 2001; Matysik et al. 2002).

Proline is synthesized in the cytosol (Szabados and Savoure 2010). During usual functioning of the cells, proline biosynthesis may occur involving two precursors. One of them is glutamate, which is reduced in reactions catalysed by synthase of nitric pyrroline-5-carboxylate (P5CS, EC 2.7.2.11) and pyrroline-5-carboxylate reductase (P5CR, EC 1.5.1.2) (Savouré et al. 1995). An alternative proline precursor is ornithine, which is converted to  $\Delta^1$ -pyrroline-5-carboxylate (P5C) with the participation of the enzyme of orn- $\delta$ -aminotransferase (OAT, EC 2.6.1.13) (Xue et al. 2009), whereas the enzymes proline dehydrogenase (PDH; 1.5.99.8) and pyrroline-5-carboxylate dehydrogenase (P5CDH; EC 1.5.1.12) take part in proline degradation (Szabados and Savouré 2010).

Proline biosynthesis under osmotic stress occurs mainly through glutamic acid, but Roosens et al. (1998), while examining *Arabidopsis thaliana*, suggested that it is synthesized directly from ornithine. In view of the importance of proline for plants treated with stressors, Seki et al. (2007) and Tatar and Gevrek (2008) postulated that the modifications of the genes involved in proline biosynthesis may contribute to increased plant tolerance to stress.

#### *Determination of the proline content*

First, 0.4 g of fresh plant material was homogenized in 1.5 ml of distilled water and then incubated in water bath at 100°C for 30 min. Then, the samples were cooled to room temperature (22°C) and centrifuged (MPW Med. Instruments, 351RH, Poland) for 10 min at 14 000 g. Next, 1 ml of a 1% solution of ninhydrin (Sigma-Aldrich, St Louis, USA) in 60% acetic acid was added to 0.5 ml of the supernatant and incubated at 100°C for 20 min. After cooling to 22°C, 3 ml of toluene was added and the samples were shaken and left in the dark for 24 h for phase separation. 1 ml of proline extract was introduced to a cuvette and the absorbance was measured at a wavelength of  $\lambda = 520$  nm (UV/Vis spectrophotometer UV-1800, Rayleigh, Beijing, China). Proline concentration was determined based on the standard curve (Filek et al. 2014).

#### *The activity of the enzymes of the proline synthesis pathway*

Before determining the activity of enzymes of the proline synthesis pathway, 1 g of fresh mass of plant material was homogenized in 7 ml of

100 mM potassium phosphate buffer KP (a mixture of  $\text{KH}_2\text{PO}_4$  and  $\text{K}_2\text{HPO}_4$ , pH 7.4) containing 1 mM disodium versenate (EDTA), 10 mM  $\beta$ -mercaptoethanol, 1% (w/v) polyvinylpyrrolidone (PVPP), 5 mM magnesium chloride and 0.6 M potassium chloride. All reagents were from Sigma-Aldrich (St Louis, USA). The homogenate was then centrifuged (MPW Med. Instruments, 351RH, Poland) for 15 min at 13,000 g at 4°C. The resulting supernatant was used for the determination of the activity of all enzymes of proline biosynthesis (Lutts et al. 1999; Filek et al. 2014).

#### *Pyrroline-5-carboxylate synthase (P5CS)*

Amount of 1.5 ml of a reaction mixture having the composition 75 mM L-glutamate, 20 mM  $\text{MgCl}_2$ , 100 mM Tris-HCl, 5 mM adenosine triphosphate (ATP) and 0.4 mM nicotinamide adenine dinucleotide phosphate (NADPH) was added to 0.4 ml of the supernatant (Stines et al. 1999). Thus, the prepared samples were incubated for 20 min in a water bath (temperature 37°C) and then cooled to room temperature. To determine the activity of P5CS, absorbance of 1 ml of the solution (in a quartz cuvette) was measured after 1 min at a wavelength of  $\lambda = 340$  nm using a UV/Vis spectrophotometer (UV-1800, Rayleigh, Beijing, China).

#### *Pyrroline-5-carboxylate reductase (P5CR)*

Amount of 1.5 ml of a reaction mixture having the composition 120 mM potassium phosphate buffer KP containing 0.06 mM nicotinamide adenine dinucleotide (NADH), 0.15 mM of pyrroline-5-carboxylic acid and 2 mM dithiothreitol was added to 0.5 ml of the supernatant (Madan et al. 1995). P5CR activity was measured after 1 min of reaction in quartz cuvettes as a decrease in absorbance (spectrophotometer UV/VIS, UV-1800, Rayleigh, Beijing, China) at a wavelength of  $\lambda = 340$  nm.

#### *Ornithine- $\delta$ -aminotransferase (OAT)*

Amount of 0.2 ml of the supernatant was mixed with 0.8 ml of a solution having the composition 100 mM phosphate buffer KP, pH 8.0 containing 50 mM L-ornithine, 20 mM  $\alpha$ -ketoglutarate and 5 mM phosphate 1 – pyridoxal. This mixture was incubated in a water bath at 37°C for 30 min (Vogel and Kopac 1960). Then, 0.5 ml of 10% trichloroacetic acid (TCA) and 0.5% ethanolic solution of o-aminobenzaldehyde were added and re-incubated (25°C, 1 h). Next, the samples were centrifuged (MPW Med. Instruments, 351RH, Poland) for 10 min at 10,000 g (at 4°C). The supernatant, after being heated to room temperature, was introduced into the measuring cuvette. OAT activity was measured spectrophotometrically after 1 min at a wavelength of  $\lambda = 440$  nm.

### *Proline dehydrogenase (PDH)*

Amount of 1.5 ml of 0.15 mM Na<sub>2</sub>CO<sub>3</sub>-HCl buffer (pH 10.3) containing 13 mM L-proline, and 1.5 mM NADH was added to 0.5 ml of the supernatant (Lutts et al. 1999). Samples were incubated for 5 min in a water bath at a temperature of 25°C. Then, PDH activity was measured spectrophotometrically at a wavelength of  $\lambda = 340$  nm.

All reagents used for the determination of the activity of the enzymes were from Sigma-Aldrich (St Louis, USA).

## **Carbohydrates**

Participation of carbohydrates in the maintenance of the osmotic equilibrium of cells was postulated based on the observed increased accumulation of predominantly mono-sugars (glucose and fructose) as well as disaccharides (sucrose and maltose) (Kerepesi and Galiba 2000). Furthermore, Qayyum et al. (2011) demonstrated that under drought stress conditions, resistant varieties have a higher content of monosaccharides and sucrose as compared to susceptible varieties. Under stress-free conditions, the photosynthesis process is responsible for the synthesis of soluble sugars. However, under stress-inducing conditions, an increase in their accumulation is mainly attributed to the degradation of starch (Bartels and Sunkar 2005). These assumptions were confirmed in the studies conducted by Mohammadkhani and Heidari (2008), who showed a decrease in starch accumulation while increasing the concentration of soluble sugars (glucose and fructose) in maize plants subjected to drought stress.

It is postulated that an increase in the accumulation of soluble sugars ensures that cell osmotic balance is maintained, which helps maintain turgor and stomatal conductivity in the leaves. Furthermore, it is suggested that both simple and complex (starch) sugars may participate in the protection of cells against the destructive effects of reactive oxygen species (ROS) (Couée et al. 2006). Their protective action in the presence of ROS involves trapping electrons from the oxygen radicals to the more 'stable' (in terms of reactivity) carbon radicals of carbohydrate molecules (Łabanowska et al. 2011). Studies by Xu et al. (2009) indicate that the antioxidant function of carbohydrates may also be due to the possible effect of these compounds on the activity of antioxidant enzymes (through specific regulation of the expression of genes responsible for their synthesis). In addition, saccharides, after relief from the stress, can be a source of carbon, used for reconstruction of biomolecules that were destroyed during the action of stress (Smeekens et al. 2010).

### *Carbohydrate analysis*

The plant material was lyophilized and then ground for 3 min in a ball mill (Retsch MM 400) at a frequency of 30 Hz. Then about 10 mg of ground leaves

were weighed into capped 2 ml microtubes. After adding 1 ml of deionized water, the samples were shaken for 60 min on a shaker (250 rev/min, JW-Electronics, RL-2002), and centrifuged for 5 min at 2 000 g (Hettich, Universal 32R). To precipitate the proteins, 0.5 ml of the clear supernatant was diluted with acetonitrile at a volume ratio of 1:1 (in a capped 1.5 ml microtube). The samples were mixed and kept overnight in a refrigerator (4°C). The next day the samples were centrifuged (15 min, 2,000 g), the supernatant was filtered through a 0.22 µm membrane (Costar Spin-X) and injected onto the chromatographic column. Sugars (glucose, fructose, sucrose, maltose, raffinose) were analysed using a liquid chromatograph with an amperometric detector (Janeczko et al. 2010). Measurements were made using a high performance liquid chromatography consisting of the following modules: a gradient pump (Agilent 1200), autosampler (Agilent 1200), the thermostat STH 585 (Dionex), ESA detector Coulochem II Analytical Cell 5040 with a gold working electrode and a palladium reference electrode, an analog/digital converter (Agilent), program control and data collector software ChemStation Rev.B.04.01 (Agilent).

The sugars were separated on a Hamilton RCX-10 250×4.1 mm column at a mobile phase flow rate of 1.5 ml/min. Isocratic elution with an aqueous solution of 75 mM NaOH was used. Amperometric detection was performed using the pulse technique at analytical potential of 200 mV, oxidation potential of 800 mV and a reduction potential of -900 mV (relative to palladium reference electrode). The injected volume was 10 µl and the column temperature was 35°C.

Identification of individual sugars was based on the retention parameters of appropriate standards injected under identical conditions as the analysed samples (Fig. 1). The quantitative analysis was based on five- or six-point calibration curves.

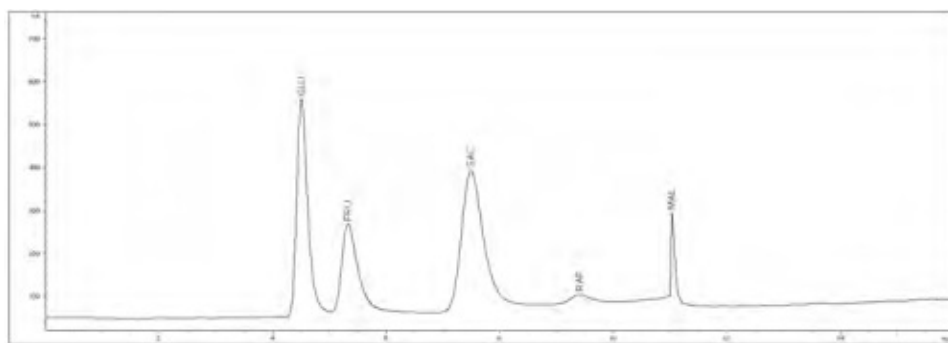


Fig 1. An example of a chromatogram of a mixture of standards of glucose (GLU), fructose (FRU), sucrose (SAC), raffinose (RAF) and maltose (MAL)

## **Radicals in biological systems**

ROS are characterized by a short half-life (up to several seconds). This fact and their high reactivity make their analysis by standard biochemical methods difficult. One of the methods allowing the analysis of these radicals is the electron paramagnetic resonance (EPR) technique, using molecules known as spin traps (chemical compounds forming with radicals stable forms) (Reinke 2002). In biological systems, the presence of long-lived radicals was demonstrated, in addition to ROS. These radicals are characterized by a relatively long half-life (days, months) and lower activity (Łabanowska et al. 2011). They may be located on the carbon atoms of carbohydrate molecules (such as glucose, fructose, starch, amylose and amylopectin), semiquinones (quinone and hydroquinone) and proteins (amino acids and transition metal ion cofactors). They are relatively easy to register by the standard EPR technique.

### **The phenomenon of electron paramagnetic resonance (EPR)**

Electron paramagnetic resonance (EPR) spectroscopy, also called electron spin resonance (ESR) spectroscopy, is a type of absorption spectroscopy working in the range of microwave radiation (Tabata et al. 1991). The EPR technique is based on the Zeeman effect which involves splitting energy levels of paramagnetic species such as atoms, ions or molecules having unpaired electrons in the magnetic field. It consists in measuring the magnetic field intensity at which resonance absorption of electromagnetic radiation by the sample occurs. An EPR signal has a specific shape dependent on the interaction of the paramagnetic centre with adjacent centres.

Samples for testing in the EPR spectrometers may be liquid or solid. The sample volume should be about 0.001 l To prevent the line broadening due to spin-spin interactions, the concentration of radicals in the solution should be less than  $10^{-4}$ M. When such interactions occur, the samples must be diluted with diamagnetic substances. In contrast, when the concentration of paramagnetic centres is low and when the recorded signals have a low intensity, spectra accumulation is required in order to enhance their intensity. The proposed mechanism of formation of long-lived hydrocarbon radicals suggests that these radicals are generated by the removal of hydrogen from a carbon atom by oxygen radicals generated on the oxygen atoms of the OH groups of the glucose molecules (Madden and Bernhard 1982), or due to breaking of the glycosidic bond (Kuzuy et al. 1999). Dehydration of carbohydrates that occurs under the influence of supplied thermal energy may lead to the formation of subsequent radical structures of slightly different EPR characteristics, for example by disconnecting the water molecules, resulting from the removal of a hydrogen atom (H) and a hydroxyl group (OH) from C-2 and C-3

of glucose units, respectively (Łabanowska et al. 2011). The mechanism of radical formation depends on the type of polysaccharide as well as on the stressor. It has been shown that the amount of radicals generated increases in proportion to the intensity of the action of this factor. The quantitative relation between the content of starch and the amount of free radicals has also been shown in studies carried out on the plant material (leaves) (Łabanowska et al. 2011).

## **Ethylene**

The plant hormone ethylene is a potential modulator of many aspects of the plant cycle (Wang et al. 2002). An increase in ethylene production by a number of biotic and abiotic stresses, including osmotic stress, was also reported (Grzesiak et al. 2013). Synthesis pathways of this gas hormone are the basis of S-adenosylmethionine and 1-aminocyclopropane-1-carboxylic acid (ACC), as the precursors of ethylene. Under stress conditions, ethylene production is connected with ROS generations which directly or indirectly stimulate the expression of ACC synthase.

### *Ethylene determination*

Amount of 500 mg samples of fresh plant material were closed in 3 ml vials for 30 min. After the time had elapsed, 100 ml of air was taken through the septa and introduced to other vials with a rubber stopper and shaken for 5 min with 4  $\mu$ M ACC (internal standard), 1  $\mu$ M mercuric perchlorate and a mixture of 5% perchloric acid and saturated NaOH (2:1, v/v) according to Mól et al. (2004). For ethylene analysis, 1.5 ml gas samples were taken from the vials. The measurements were performed in a gas chromatography (Hewlett-Packard 5890 Series II) with RTX-5 Q-PLOT column (30 m length  $\times$  0.53 mm inner diameter, RESREC Corp. USA). The column temperature was 60°C and the injector and detector (flame ionization) temperatures were 80 and 120°C, respectively; the carrier gas flow rate, N<sub>2</sub> at 50 ml min<sup>-1</sup>. Ethylene was quantified in triplicate for each sample and the conversion factor determined by comparison with the production of ethylene from the internal standard. A calibration curve with commercial ethylene was performed at the beginning.

## **Conclusions**

Applied analytical methods allowed the demonstration of the similarities and differences in the accumulation of proline, soluble sugars and ethylene under drought stress in parental cultivars of barley (sensitive to drought stress - CAM/B1 and resistant – Maresi) and 99 recombinant inbred lines obtained from them. It has been found that the synthesis of proline in the tested varieties

proceeds via the activation of enzymes pyrroline-5-carboxylate synthase (P5CS) and ornithine- $\delta$ -aminotransferase (OAT). In addition, increased concentrations of proline correlated with the synthesis of ethylene. Under drought conditions, mainly glucose and/or sucrose level was increased. It is suggested that sugar particles can function as ‘traps’, stabilizing electrons coming from reactive oxygen species (ROS) generated under stress conditions.

## References

- Alia A., Mohanty P., Matysik J. 2001. Effect of proline on the production of singlet oxygen. *Amino Acids* 21: 195-200.
- Bartels D., Sunkar R. 2005. Drought and salt tolerance in plants. *Crit. Rev. Plant Sci.* 24: 23-58.
- Csonka L.N. 1989. Physiological and genetic response of bacteria to osmotic stress. *Microbiol. Rev.* 53: 121–147.
- Csonka L.N., Hanson A.D. 1991. Prokaryotic osmoregulation: genetics and physiology. *Annu. Rev. Microbiol.* 45: 569-606.
- Couée I., Sulmon C., Gouesbet G., El Amrani A. 2006. Involvement of soluble sugars in reactive oxygen species balance and responses to oxidative stress in plants. *J. Exp. Bot.* 57: 449-459.
- Filek M., Łabanowska M., Kościelniak J., Biesaga-Kościelniak J., Kurdziel M., Szarejko I., Hartikainen H. 2014. Characterization of barley leaf tolerance to drought stress by chlorophyll fluorescence and electron paramagnetic resonance studies. *J. Agro. Crop Sci.* doi.10.1111/ajc.12063.
- Grzesiak M., Filek M., Barbasz A., Kreczmer B., Hartikainen H. 2013. Relationships between polyamines, ethylene, osmoprotectants and antioxidant enzymes activities in wheat seedlings after short-term PEG- and NaCl-induced stresses. *Plant Growth Regul.* 69: 177-189.
- Janecko A., Biesaga-Kościelniak J., Oklestkova J., Filek M., Dziurka M., Szarek-Łukaszewska G., Kościelniak J. 2010. 24-Epibrassinolide in wheat production: physiological activity and uptake. *J. Agro. Crop Sci.* 196: 311-321.
- Kerepesi I., Galiba G. 2000. Osmotic and salt stress-induced alteration in soluble carbohydrate content in wheat seedlings. *Crop Sci.* 40: 482-487.
- Kuzuy M., Yamauchi Y., Kondo S. 1999. Mechanolysis of glucose-based polysaccharides as studied by electron spin resonance. *J. Phys. Chem.* 103: 8051- 8059.
- Lutts S., Majerus V., Kinet J.M. 1999. NaCl effects on proline metabolism in rice (*Oryza sativa*) seedlings. *Physiol. Plant.* 105: 450-458.
- Łabanowska M., Bidzińska E., Pietrzyk S., Juszczak L., Fortuna T., Błoniarczyk K. 2011. Influence of copper catalyst on the mechanism of carbohydrate radicals generation in oxidized potato starch. *Carbohydr. Polym.* 85: 775-85.

- Madan S., Nainawatee H.S., Jain R.K., Chowdhury J.B. 1995. Proline and proline metabolising enzymes in *in-vitro* selected NaCl-tolerant *Brassica juncea* L. under salt stress. *Ann. Bot.* 76: 51-57.
- Madden K.P., Bernhard W.A. 1982. Thermally induced free-radical reactions in  $\alpha$ -D-glucopyranose single crystals. An electron spin resonance-electron nuclear double resonance study. *J. Phys. Chem.* 86: 4033-4036.
- Matysik J., Ali Bhalu B., Mohanty P. 2002. Molecular mechanism of quenching of reactive oxygen species by proline under water stress in plants. *Curr. Sci.* 82: 525-532.
- Mohammadkhani N., Heidari R. 2008. Drought-induced accumulation of soluble sugars and proline in two maize varieties. *World Appl. Sci. J.* 3: 448-453.
- Mól R., Filek M., Macháčková I., Matthys-Rochon E. 2004. Ethylene synthesis and auxin augmentation in pistil tissues are important for egg cell differentiation after pollination in maize. *Plant Cell Physiol.* 45: 1396-1405.
- Qayyum A., Razaq A., Ahmad M., Jenks M.A. 2011. Water stress causes differential effects on germination indices, total soluble sugar and proline content in wheat (*Triticum aestivum* L.) genotypes. *Afr. J. Biotechnol.* 10: 14038-14045.
- Reinke L.A. 2002. Spin trapping evidence for alcohol-associated oxidative stress. *Free Rad. Biol. Med.* 32: 953-957.
- Roosens N.H., Thu T.T., Iskandar H.M., Jacobs M. 1998. Isolation of the ornithine- $\delta$ -aminotransferase cDNA and effect of salt stress on its expression in *Arabidopsis thaliana*. *Plant Physiol.* 117: 263-271.
- Savouré A., Jaoura S., Hua X.J., Ardiles W., Montagu M., Verbruggen N. 1995. Isolation, characterization, and chromosomal location of a gene encoding the  $\Delta$ 1-pyrroline-5-carboxylate synthetase in *Arabidopsis thaliana*. *FEBS Lett.* 372: 13-19.
- Seki M., Umezawa T., Urano K., Shinozaki K. 2007. Regulatory metabolic network in drought stress responses. *Curr. Opin. Plant Biol.* 10: 296-302.
- Sharma S., Villamon J.G., Verslues P.E. 2011. Essential role of tissue-specific proline synthesis and catabolism in growth and redox balance at low water potential. *Plant Physiol.* 157: 292-304.
- Smekens S., Ma J., Hanson J., Rolland F. 2010. Sugar signals and molecular networks controlling plant growth. *Curr. Opin. Plant Biol.* 13: 273-278.
- Stines A.P., Naylor D.J., Hoj P.B., Heeswijck R.V. 1999. Proline accumulation in developing grapevine fruit occurs independently of changes in the level of pyrroline-5-carboxylate synthetase mRNA or protein. *Plant Physiol.* 120: 923-931.
- Szabados L., Savouré A. 2010. Proline: a multifunctional amino acid. *Trends Plant Sci.* 15: 89-97.
- Tabata Y., Ito Y., Tagawa S. 1991. *CRC Handbook of Radiation Chemistry*. CRC Press, Boca Raton, FL.
- Tatar O., Gevrek M.N. 2008. Influence of water stress on proline accumulation, lipid peroxidation and water content of wheat. *Asian J. Plant Sci.* 7: 409-412.

- Vogel R.H., Kopac M.J. 1960. Some properties of ornithine-ctransaminase from neurospora. *Biochem. Biophys. Acta* 37: 539-540.
- Wang K.L.-C, Li H., Ecker J.R. 2002. Ethylene biosynthesis and signaling networks. *Plant Cell*. V 14 S1: 131-151.
- Xue X., Liu A., Hua X. 2009. Proline accumulation and transcriptional regulation of proline biothesynthesis and degradation in *Brassica napus*. *BMB Rep.* 42: 28-34.
- Xu W., Zhang F., Luo Y., Ma L., Kou X., Huang K. 2009. Antioxidant activity of a water soluble polysaccharide purified from *Pteridium aquilinum*. *Carbohydr. Res.* 344: 217-222.

## **Analysis of antioxidant system under abiotic stress**

**Jolanta Biesaga-Kościelniak<sup>1</sup>, Maria Filek<sup>1</sup>, Michał Dziurka<sup>1</sup>,  
Agnieszka Ostrowska<sup>1</sup>, Anna Maksymowicz<sup>1</sup>, Apolonia Sieprawska<sup>2</sup>**

<sup>1</sup> *The Franciszek Górski Institute of Plant Physiology, Polish Academy of Sciences,  
Kraków, Poland*

<sup>2</sup> *Institute of Biology, Pedagogical University, Kraków, Poland*

### **Introduction**

In recent years, many of the natural sciences devote considerable attention to topics related to the formation, characteristics and effects of free radicals on the living body, in particular to active forms of oxygen, often referred to as ROS (reactive oxygen species). ROS is wider term describing chemically reactive molecules containing oxygen (e.g. oxides and peroxides) The term free radical should be understood as an atom or a molecule having an unpaired electron in the valence orbital. This property results in high reactivity of free radicals and ability to ‘attack’ the various components of living cells (Quan et al. 2008). External factors causing oxidative stress (ROS formation) include: ionizing radiation, UV radiation, ultrasound and others. The so-called oxygen burst is often observed in plant tissues as a result of environmental stressors, such as water stress (drought or flooding), salt stress, low temperature stress (cold weather conditions or frost), light, the effect of heavy metals, mechanical damage, application of pesticides, invasion of pathogens as well as other factors (Elstner 1987; Casano et al. 1994; Badiani et al. 1996; Mittler 2002; Ferreira et al. 2002; Bhattacharjee 2005; Halliwell 2006; Razinger 2008; Gill and Tutej 2010). The level of free radicals in cells is a consequence of both normal metabolism and adverse conditions caused by the environment, and is largely determined by the capacity and the activity of antioxidant system (Foyer and Noctor 2005; Navrot et al. 2007). Living organisms have developed various defence mechanisms to ensure the proper functioning of the cells in the presence of ROS and their derivatives (Apel and Hirt 2004; Halliwell 2006). The elements of antioxidant barrier include antioxidant enzymes and small molecule antioxidants, e.g., glutathione, vitamin

C and E, and others (Alscher et al. 2002). A special role in the antioxidant barrier is played by enzymes, such as superoxide dismutase (SOD), catalase (CAT) and GSH-dependent enzymes, i.e., glutathione peroxidase (GSHPx), glutathione transferase (GST) and glutathione reductase (GSHR) (Melchiorre et al. 2009). The enzyme superoxide dismutase, present in the cytoplasm, mitochondria and chloroplasts, converts superoxide anion in the disproportionation reaction into hydrogen peroxide molecule:



In turn, a molecule of hydrogen peroxide, a member of ROS, is decomposed by catalase, an enzyme characteristic for the peroxisome:



or peroxidase system (ascorbate peroxidase, glutathione peroxidase) present in the soluble fraction as well as associated with the membrane and cell wall structures:



where A is antioxidant molecule.

These enzymes, often called ‘enzymatic triad’, are the main cell protection system against active forms of oxygen (Lee et al. 2007). Small molecule antioxidants react directly with the reactive oxygen species, or with intermediate metabolites of redox reactions, preventing the formation of ROS. These compounds are less specific than enzymes, and thus they are classified as ‘universal defenders’, active both in the hydrophilic (ascorbic acid) as well as hydrophobic phases (tocopherols, carotenoids). The primary hydrophobic antioxidant is vitamin E, which is a mixture of four tocopherols and four tocotrienols. These compounds are primarily involved in the ‘scavenging’ reactions of organic free radicals, thereby inhibiting lipid peroxidation (Smirnov 2005). Alpha-tocopherol also plays regulatory functions in the chain of photosynthetic electron transport and exhibits antioxidant properties (Strzałka et al. 2009). Carotenoids (hydrophobic antioxidants) have the ability to bind free radicals due to the presence of conjugated double bonds. They also react with singlet oxygen and organic radicals, formed as a result of lipid peroxidation (Smirnov 2005).

### Measuring the activity of antioxidant enzymes

The plant material was homogenized at 4°C in 0.05 mmol dm<sup>-3</sup> KP buffer containing K<sub>2</sub>HPO<sub>4</sub> + KH<sub>2</sub>PO<sub>4</sub> and 0.1 mmol dm<sup>-3</sup> EDTA (pH 7). The clear supernatant was divided into subsamples after centrifugation for 15 min at 10,000 × g at 4°C and sequentially activity assays for SOD, catalase, peroxidase, and protein concentration were performed.

### **The activity of superoxide dismutase (SOD)**

SOD activity was determined spectrophotometrically using cytochrome method (McCord and Fridovich 1969). The reaction mixture contained phosphate buffer at a concentration of  $0.05 \text{ mol dm}^{-3}$  (pH 7.8), EDTA,  $0.1 \text{ mmol dm}^{-3}$ , and cytochrome c and xanthine ( $1 \text{ mmol dm}^{-3}$ ). The oxidized cytochrome was reduced with the superoxide, generated by xanthine oxidase-xanthine system (activity 50 U, Grade I, Sigma). The kinetics of the reaction was measured spectrophotometrically for 3 min at  $\lambda = 550 \text{ nm}$ . The reaction rate ( $\Delta A$ ) was a reference to the measurements performed on the plant material. To  $50 \times 10^{-3} \text{ cm}^3$  volume of the supernatant obtained after homogenization of the plant fragments,  $2 \text{ cm}^3$  of the reaction mixture and  $8\text{-}10 \times 10^{-3} \text{ cm}^3$  of xanthine oxidase were added, and the reaction kinetics was measured for 3 min. SOD present in plants caused the inhibition of cytochrome c reduction, giving lower  $\Delta A$  values than control. The amount of enzyme resulting in 50% inhibition of the reduction of cytochrome c at  $25^\circ\text{C}$  was adopted as a unit of activity (1 Unit, cytochrome unit). The activity of SOD was calculated per 1 mg of protein.

### **Measurements of the catalase (CAT) activity**

Catalase activity was measured spectrophotometrically according to the procedure described by Aebi (1984). Phosphate buffer at the concentration of  $0.05 \text{ mol dm}^{-3}$  and pH 7.0 was used for analysis and  $0.03 \text{ mol dm}^{-3}$  of  $\text{H}_2\text{O}_2$  solution in the same buffer. The spectrophotometer was reset with the pure buffer, followed by the addition of  $0.5 \text{ cm}^3$  of  $\text{H}_2\text{O}_2$  solution and the two components were mixed. Then  $50 \times 10^{-3} \text{ cm}^3$  of the supernatant (tissue extract) was added, and after mixing, a decrease in absorbance was measured for 2 min at  $\lambda = 240 \text{ nm}$  and  $20^\circ\text{C}$ . The difference in absorbance equal to 0.015 units within 60 s was adopted as a unit of enzyme activity. The activity of each sample was normalized to the amount of protein present in the sample.

### **Measurements of the peroxidase (POD) activity**

POD activity was measured by using a modified Lücke's method (1962). The measurement was carried out using spectrophotometry at  $\lambda = 485 \text{ nm}$  to determine the amount of oxidation products of p-phenylenediamine in the presence of  $\text{H}_2\text{O}_2$ . The incubation mixture contained  $3 \text{ cm}^3$  of the plant supernatant and  $2 \text{ cm}^3$  of 1% p-phenylenediamine in  $0.05 \text{ mol dm}^{-3}$  of KP buffer. The reaction was initiated by the addition of  $0.05 \text{ cm}^3$  of  $0.03 \text{ mol dm}^{-3}$   $\text{H}_2\text{O}_2$  followed by the measurement of absorbance increment. The incubation time was selected so that the absorbance increase did not exceed 0.4 units.

## Determination of soluble proteins

Determination of soluble proteins was performed using the method of Bradford (1976).  $8-15 \times 10^{-3} \text{ cm}^3$  of the supernatant was collected for the analysis and mixed with  $930 \times 10^{-3} \text{ cm}^3$  of Bradford solution in the measuring cuvette and filled up with water to a total volume of  $1000 \times 10^{-3} \text{ cm}^3$ . Absorbance reading was performed using a Bio-Lambda spectrometer (Perkin-Elmer, USA) at a wavelength of 595 nm after 20 min incubation. BSA bovine serum albumin (Sigma-Aldrich, Poland) at a concentration of  $0.5-1 \text{ mg cm}^{-3}$  diluted in distilled water was used for preparation of the calibration curve.

## Determination of tocopherols and beta-carotene

Determination of beta-carotene, tocopherols and tocotrienols was performed by a modified method described by Janeczko et al. (2010, 2013). Samples of lyophilized leaves in an amount of approximately 100 mg were extracted with 5 ml mixture of ethanol/acetone/methanol/isopropanol (16/6/3/2) for 15 min in a shaking water bath (JW-Electronics, JWE 357) at  $75^\circ\text{C}$ . Then 250  $\mu\text{l}$  of 80% KOH was added and heating and shaking were continued for 30 min. After this incubation, the samples were cooled down, 5 ml of water was added and samples were centrifuged. The resulting supernatant was purified on a 45 ml

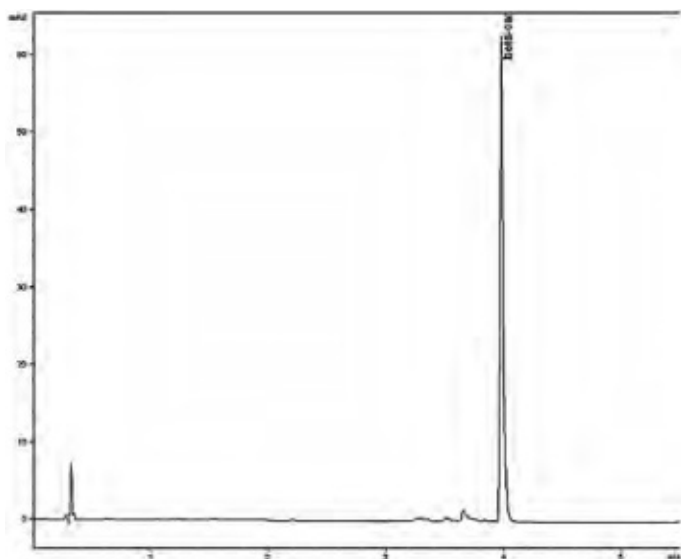


Fig. 1. The chromatogram of beta-carotene (beta-car) standard

Chromabond XTR cartridge. Sample were loaded on the cartridge and allowed to stand for 15 min to completely adsorb water phase. After this time, the lipid fraction containing compounds of interest was eluted with 50 ml of n-hexane. The hexane fraction was evaporated on a rotary evaporator (Buchi Rotavapor R-215), the residue was dissolved in 1.5 ml of methanol/methyl chloride (3/1 v/v) and after filtration through a 0.22  $\mu\text{m}$  membrane, the sample was injected on to a chromatography column.

Carotenoids were analysed by HPLC with spectrophotometric detection at a wavelength of 450 nm. Agilent 1100 liquid chromatograph with DAD detector and Spherisorb ODS2, 3  $\mu\text{m}$ , 150  $\times$  4.1 mm analytical column (Waters) were used. The following mobile phase was used: (A) acetonitrile/water (250/33 v/v), (B) ethyl acetate, in a gradient (from 0 min to 6.5 min 40% A, then to 8 min 20% A and to 12 min 20% A). Beta-carotene was used as a standard. Figure 1 shows the chromatogram of a beta-carotene standard, while Figure 2 presents the analysis performed for the plant sample.

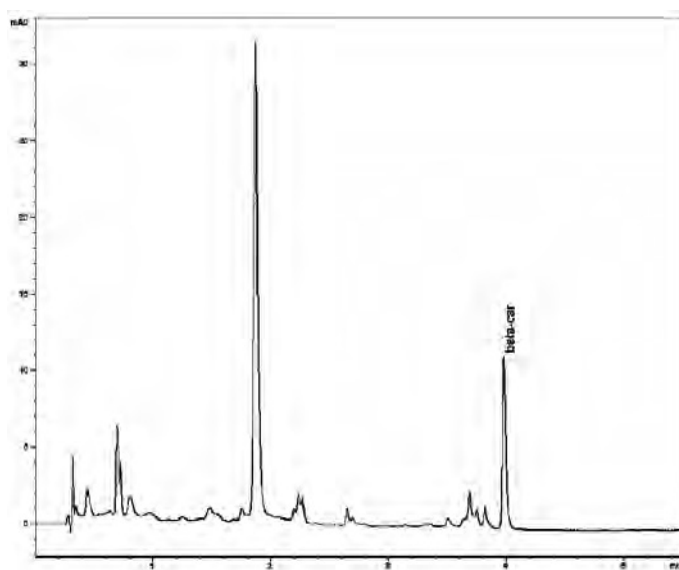


Fig. 2. The chromatogram of the plant sample containing beta-carotene ( $\beta$ -car)

Determination of tocochromanols was carried out spectrofluorimetrically using an Agilent 1200 chromatograph with spectrofluorimetric detector. The measurements were performed at an excitation wavelength of 295 nm, and emission wavelength of 330 nm. Excitation and emission parameters were selected on the basis of the absorption and emission spectra performed online for pure standards of the tested compounds. Separation was performed on a Zorbax

Eclipse XBD 5  $\mu\text{m}$ , 150  $\times$  4.1 mm analytical column (Agilent). The following mobile phase was used: (A) methanol/acetonitrile/water (250/250/33 v/v), (B) acetonitrile/methylene chloride (50/50 v/v), in a gradient (from 0 min 95% A, to 15 min 30% A). Alpha-tocotrienol, gamma-tocotrienol, delta-tocotrienol, alpha-tocopherol, gamma-tocopherol, delta-tocopherol were used as standards. Figure 3 shows a chromatogram of the standards, while Figure 4 demonstrates a chromatogram of the plant sample containing tocotrienols and tocopherols.

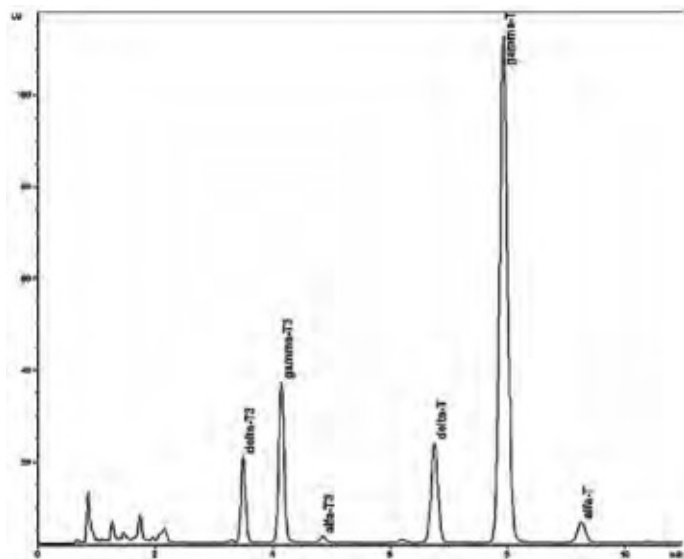


Fig. 3. The chromatogram of a mixture of tocochromanol standards tested. Delta-tocotrienol (delta-T3), gamma-tocotrienol (gamma-T3), alpha-tocotrienol (alpha-T3), delta-tocopherol (delta-T), gamma-tocopherol (gamma-T), alpha-tocopherol (alpha-T)

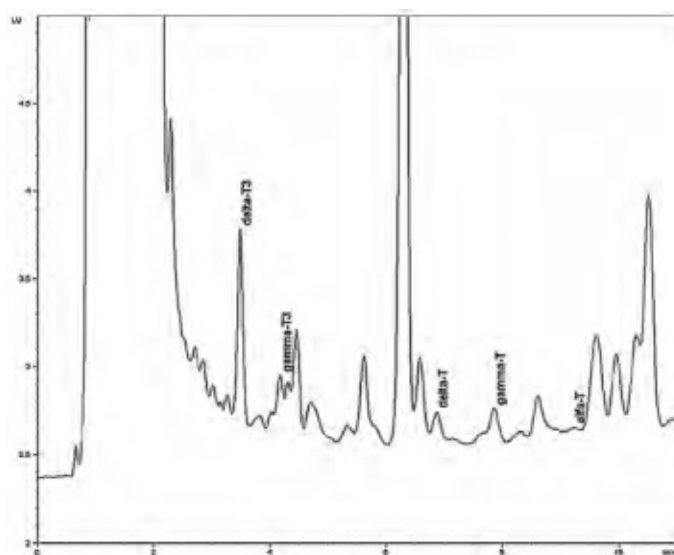


Fig. 4. The chromatogram of the plant sample containing tocochromanols. Delta-tocotrienol (delta-T3), gamma-tocotrienol (gamma-T3), delta-tocopherol (delta-T), gamma-tocopherol (gamma-T), alpha-tocopherol (alfa-T)

Presented methods of antioxidative enzyme activity and small lipophilic antioxidant content (tocochromanols and beta-carotene) measurements were applied in the research on drought sensitivity of parental lines and recombinant inbred lines (RIL) of barley (*Hordeum vulgare* L.). They enabled to distinguish between drought susceptible and tolerant lines. Information they brought is crucial for estimation of antioxidative system performance in environmental stress conditions. That could be considered as a toll for selection of desired genotypes.

## References

- Aebi H. 1984. Catalase in vitro. *Meth. Enzymol.* 105: 121-126.
- Alscher R.G., Erturk N., Heath L.S. 2002. Role of superoxide dismutases (SODs) in controlling oxidative stress in plants. *J. Exp. Bot.* 53: 1331-1341.
- Apel K., Hirt H. 2004. Reactive oxygen species: metabolism, oxidative stress, and signal transduction. *Annu. Rev. Plant Biol.* 55: 373-399.
- Badiani M., Paolacci A.R., Miglietta F., Kimball B.A., Pinter P.L. Jr, Garcia R.L., Hunsaker D.L., La Morte R.L., Wall G.W. 1996. Seasonal variations of antioxidants in wheat (*Triticum aestivum*) leaves grown under field conditions. *Aust. J. Plant Physiol.* 23: 687-698.

- Bhattacharjee S. 2005. Reactive oxygen species and oxidative burst: roles in stress, senescence and signal transduction in plant. *Curr. Sci.* 89: 1113-1121.
- Bradford M.M. 1976. A rapid and sensitive method for the quantification of microgram quantities of protein utilizing the principle of protein-dye binding. *Anal. Biochem.* 72: 248-254.
- Casano L.M., Martin M., Sabater B. 1994. Sensitivity of superoxide dismutase transcript levels and activities to oxidative stress is lower in mature-senescent than in young barley leaves. *Plant Physiol.* 106: 1033-1039.
- Eltner E.F. 1987. Metabolism of activated oxygen species. In: D.D. Davies (ed.), *Biochemistry of Plants*. Academic Press, London: 253-315.
- Ferreira R.R., Fornazier R.F., Vitoria A.P., Lea P.J., Azevedo R.A. 2002. Changes in antioxidant enzyme activities in soybean under cadmium stress. *J. Plant Nutr.* 25: 327-342.
- Foyer C.H., Noctor G. 2005. Redox homeostatic and antioxidant signaling: a metabolic interface between stress perception and physiological responses. *Plant Cell* 17: 1866-1875.
- Gill S.S., Tutej N. 2010. Reactive oxygen species and antioxidant machinery in abiotic stress tolerance in crop plants. *Plant Physiol. Biochem.* 48: 909-930.
- Halliwell B. 2006. Reactive species and antioxidants redox biology is a fundamental theme of aerobic life. *Plant Physiol.* 141: 312-322.
- Janecko A., Oklešťková J., Siwek A., Dziurka M., Pocięcha E., Kocurek M., Novák O. 2013. Endogenous progesterone and its specific binding sites in wheat exposed to drought stress. *J. Steroid Biochem. Mol. Biol.* 138: 384-394.
- Janecko A., Biesaga-Kościelniak J., Oklešťková J., Filek M., Dziurka M., Szarek-Lukaszewska G., Kościelniak J. 2010. 24-Epibrassinolide in wheat production: physiological activity and uptake. *J. Agron. Crop Sci.* 196: 311-321.
- McCord J.M., Fridovich I. 1969. Superoxide dismutase an enzymic function for erythrocyte hemocuprein (hemocuprein). *J. Biol. Chem.* 244: 6049-6055.
- Melchiorre M., Robert G., Trippi V., Racca R., Lascano H.R. 2009. Superoxide dismutase and glutathione reductase overexpression in wheat protoplast: photooxidative stress tolerance and changes in cellular redox state. *Plant Growth Regul.* 57: 57-68.
- Mittler R. 2002. Oxidative stress, antioxidants and stress tolerance. *Trends Plant Sci.* 7: 405-410.
- Navrot N., Rouhier N., Gelhaye E., Jaquot J.P. 2007. Reactive oxygen species generation and antioxidant systems in plant mitochondria. *Physiol. Plant.* 129: 185-195.
- Lee S.H., Ahsan N., Lee K.W., Kim D.H., Lee D.G., Kwak S.S., Kwon S.Y., Kim T.H., Lee B.H. 2007. Simultaneous overexpression of both CuZn superoxide dismutase and ascorbate peroxidase in transgenic tall fescue plants confers increased tolerance to a wide range of abiotic stresses. *J. Plant Physiol.* 164: 1626-1638.
- Lück 1962. *Methoden der enzymatischen Analyse*. Verlag Chemie, GmbH Weinheim: 895-897.

- Quan L.J., Zhang B.W., Shi H., Li Y. 2008. Hydrogen peroxide in plants: a versatile molecule of the reactive oxygen species network. *J. Integrat. Plant Biol.* 50: 2-18.
- Razinger J., Dermastia M., Koce J.D., Zrimec A. 2008. Oxidative stress in duckweed (*Lemna minor* L.) caused by short-term cadmium exposure. *Environ. Poll.* 153: 687-694.
- Smirnoff N. 2005. Ascorbate, tocopherol and carotenoids: metabolism, pathway engineering and functions. In: N. Smirnoff (ed.), *Antioxidants and Reactive Oxygen Species in Plants*. Blackwell Publishing Ltd., Oxford, UK: 53-86.
- Strzałka K., Szymańska R., Świeżewska E., Skorupińska-Tudek K., Suwalsky M. 2009. Tocochromanols, plastoquinone and polyphenols in selected plant species from Chilean patagonia. *Acta Biologica Cracoviensia Series Botanica* 51/1: 39-44.



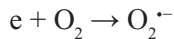
## **The assay of oxygen free radicals and the enzyme decomposing them in barley leaves subjected to drought**

**Renata Bączek-Kwinta**

*Department of Plant Physiology, University of Agriculture, Kraków, Poland*

### **Introduction**

The shortage of water in plant leads to numerous adverse metabolic changes. One of them is the excessive formation of so-called reactive oxygen species (ROS). There are mainly superoxide anion radical  $O_2^{\cdot-}$ , singlet oxygen  $^1O_2$ , hydrogen peroxide  $H_2O_2$  and hydroxyl radical  $\cdot OH$ . Superoxide radical is relatively easily formed from diatomic oxygen when a one-electron reduction of oxygen occurs, and this happens usually when the electrons 'leak' from various biochemical reactions:



The formation of anion radical occurs in every second, in each cell of any aerobic organism. For example, in the chloroplasts, about 10% of the pool of electrons of the light phase of photosynthesis is transferred to oxygen in the so-called Mehler reaction (Foyer and Noctor 2000). In mitochondria, 1-2% of oxygen used in respiration can be transformed into superoxide radical, mainly at the I and III complexes of the respiratory chain (Puntarulo et al. 1988; Møller 2001). However, the intensity of such reaction during the stress conditions (e.g. lack of water) increases even by half (Biehler and Fock 1996). This does not mean, however, that the cells are completely vulnerable to excess free radicals – these ions are transformed by the enzyme superoxide dismutase (SOD):



The above transformation is a redox reaction in which two molecules (in this case, two ions) are subjected to disproportionation (dismutation), hence the name of the enzyme. The protons are derived from a variety of biochemical reactions.

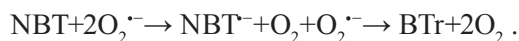
As can be seen, this reaction generates another reactive form of oxygen, hydrogen peroxide. One can make a question whether such formation of another ROS makes any biological sense, since it has been established by evolution? The

answer is yes, for several reasons. The molecule of hydrogen peroxide is uncharged, so it can be moved through the cell membrane water channels (aquaporins), and its stability (measured as a half-life) is high (Vranová et al. 2002). In a cell-scale, it means the ability to move through a certain path, which allows the use of this compound as a signal carrying information between cells. The excessive amount of  $H_2O_2$  is removed by the enzymes belonging to peroxidase class, to which belong catalase peroxidases dependent on their specific electron donor (ascorbate or glutathione peroxidase), and non-specific peroxidases. If, however, the synthesis of these enzymes is depleted or there is a lack of such co-factors, signalling role of ROS is disrupted, and the oxidizing nature of these compounds leads to oxidative damage and transformation of important biomolecules (mainly proteins and lipids), resulting in disorder within biological structures (e.g. membranes) and the cellular processes (e.g. light phase of photosynthesis).

Thus, in the chain of oxygen alterations, superoxide anion is formed as the first ROS, whereas SOD is the first enzyme initiating redox reaction cascade. For this reason, during the design of the POLAPGEN project, we paid attention to the possibility of the synthesis of superoxide anion and its neutralization ('*scavenging*'). We assumed that the viable plants despite the lack of water can synthesize more  $O_2^{\cdot-}$  than those whose life processes are weakened, and that will be accompanied by adequate SOD activity.

### **Determination of superoxide anion in leaves of barley plants subjected to drought**

Detection of oxygen free radicals is possible using different methods (Lin et al. 2009). We used the one which we have tested in our previous studies (Bączek-Kwinta and Kościelniak 2003; Bączek-Kwinta 2010), utilizing a colour reaction of blue nitro tetrazolium (NBT). In oxidized state, this compound is yellow, but in a redox reaction it creates formazan (BTr) of navy blue colour (Abugo and Rifkind 1994):



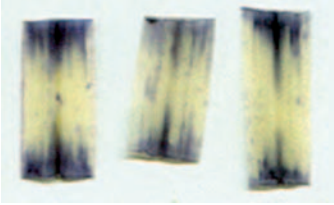
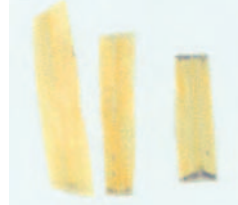
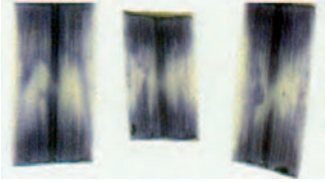
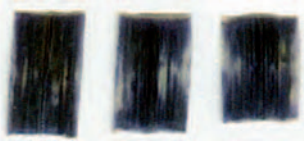
The test should be performed only on freshly collected leaves. The time from the cut to the beginning of the analysis should be as short as possible, because the cut causes rapid influx of oxygen to the cells, which affects the result of the assay. Thus, to do the research on plants from a field experiment, one should take the entire specimen with its root system, whereas the leaves should be taken immediately before the assay. Leaf selection is also important. If we study the plants that are in a particular physiological stage, we need to ensure that the same leaf is taken from each of them. On the basis of the research conducted within the

project POLAPGEN, we can conclude that in the case of seedlings, the third or fourth leaf is a proper material, and in the case of plants in the phase before the heading – the first leaf below the flag leaf. This is due to the fact that the seedling being in the stage of third or fourth leaf is relatively well developed, but sensitive to water deficit, and the third leaf performs its metabolism independently of the substance stored in the kernel, in contrast to the first or second leaf.

On the other hand, in the case of grown-up plants, which initiate their generative stage, flag leaf is important for the development of the spike and reflects the plant's ability to produce yield. However, the results obtained in the biochemical analyses reflect other processes also, including ageing of the leaf (Bączek-Kwinta et al. 2006). For this reason, a better object of the study is a leaf under the flag one. Moreover, in any case it should be ensured that the samples are taken at the same time of day, because various cellular processes, including redox reactions, occur in a circadian clock (Wu and Reddy 2014). During all manipulations one must ensure that the tissue is not damaged in any way (broken, crushed), because the site of injury will produce a large amount of superoxide anion.

The leaf has to be carefully cut at its base, then cut off the part closer to the petiole and from the top, leaving a middle part of 2-3 cm length. It is important that all parameters of the procedure used (time, pressure, power, etc.) are uniform. The assays can be performed at room temperature, and in the course of the experiment, the temperature should not vary significantly during the subsequent testing of samples. Laboratory gloves are necessary. As the chloral hydrate is toxic, the operations must be conducted when the fume hood is on. Moreover, when working with a vacuum pump, the laboratory goggle has to be put on.

Table 1. Examples of the results of leaf staining against  $O_2^-$  in barley genotypes sensitive and resistant to drought

Genotype	Control	Drought
MCam drought-sensitive		
MCam drought-resistant		

### Equipment

- Vacuum pump and vacuum flask wrapped up with dark or aluminium foil;
- Water bath or magnetic stirrer with heating;
- Fluorescent lamp emitting white light (40-100 W) and non-emitting heat;
- Laboratory gloves (NBT dyes the skin) and safety eyewear;
- Containers for liquid chemical waste.

### Chemicals

- NBT, 0.5%. (w/v) in a phosphate-potassium buffer (10 mM, pH 7.0; with 0.005% (w/v));
- Triton X-100 to diminish surface tension and enable tissue infiltration;
- Chloral hydrate, saturated;
- Ethanol, 90%.

### Procedure

1. Cut the leaves into transverse segments of approximately the same size, place in a vacuum flask wrapped in the aluminium foil, pour a NBT solution so that leaves are immersed and switch on the pump. Establish the pressure of -0.8 MPa and infiltrate for 15 min.
2. Reduce the pressure to zero and turn off the pump. Pour the sample (the leaves and the liquid) into Petri dishes. If a section of the leaf had remained in the flask, gently grab the marginal part with tweezers or pincette. Set an open dish under a lamp (white light, the power of 40-100 W), for 15 min.
3. Remove NBT solution\* with a Pasteur pipette, and stop the reaction with chloral hydrate (15 mL, 15 min incubation), which partially removes chlorophyll and preserves the tissue.
4. Remove the chloral hydrate\*, and immerse the leaves in a small amount of ethanol of a temperature of approximately 45°C to wash out the residue of photosynthetic pigments and make the NBT-dyed areas visible. Keep at this temperature for 15 min, then remove the ethanol, and immerse the sample in a new portion.

In few days, after removing the photosynthetic pigments and preserving tissue, the places of the intense synthesis of formazan can be seen as dark blue dots and irregular spots, whose number can be determined qualitatively. In case of large number of samples and small differences, one should scan the objects and subject them to digital image analysis.

---

\* Pour the chemical wastes into labelled waste containers

## Determination of the activity of superoxide dismutase (SOD)

In contrast to the determination of the intensity of superoxide anion generation, the assay of SOD activity is possible in samples preserved by quick freezing (preferably in liquid nitrogen) and stored at low temperature (ca.  $-80^{\circ}\text{C}$  is the best). Such preservation, widely used in the biochemical preparations, allows to maintain the structure of the enzyme. Similarly to the determinations of superoxide anion levels, the samples should also be taken at the last possible moment and at the same time of the day. The assay is carried out using a spectrophotometer. It is also a common method in enzymology that allows to estimate the loss of enzyme substrate or the increase of its product. In this case, the rate of increase of the reaction product is analysed.

After adding leaf supernatant containing SOD to the reaction mixture, the reaction is inhibited and the degree of such enhancement reflects the enzyme activity (the greater the inhibition, the higher the activity). The extract must be properly prepared, stored on ice and protected from light (see the procedure below).

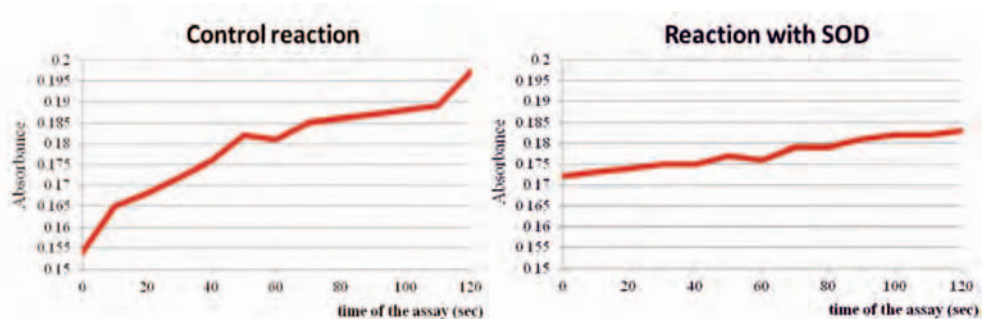


Fig. 1. The example of the curves obtained during the spectrophotometric assay of SOD with cytochrome *c* method

The steps of the assay proceed as follows:

- Oxidize the cytochrome solution through intensive aeration by ca. 2-3 hours on a magnetic stirrer, in a dark glass container, in the dark, at room temperature ( $20-25^{\circ}\text{C}$ );
- Reduce the oxidized cytochrome with superoxide generated by xanthine/xanthine oxidase couple;
- By adding the leaf extract, SOD inhibits the reaction;
- Repeat the procedure except that using phosphate buffer instead of the leaf extract (control reaction).

The monitoring process occurs at a wavelength of 550 nm (green light), since this is the maximum absorbance of the reduced cytochrome *c* (of red-pink colour).

The reaction can be performed at room temperature, but because the thermal SOD activity maximum is 25°C, a thermostated spectrophotometer, or the conditioned laboratory room is a big advantage.

### Equipment

- Spectrophotometer;
- Laboratory pipettes with tips;
- Magnetic stirrer with mixing magnets;
- Spectrophotometric cuvettes, polystyrene;
- Laboratory gloves;
- Laboratory spoons and weighing dishes;
- Measuring cylinder, beakers.

### Reagents

- Phosphate buffer, 50 mM, pH 7.8 (WARNING! Do not use HCl while adjusting pH) + 0.1 mM EDTA. The buffer is the basis for the other solutions used in the assay;
- PVPP – polyvinyl polypyrrolidone to extract impurities;
- Xanthine, 1 mM, dissolved in a small amount of NaOH (1 mM), then in the buffer of a room temperature. The solution should be protected from light;
- Cytochrome c, 1 mM in a buffer (WARNING! The lyophilized cytochrome has to be kept at -20°C; before weighing the vial with the chemical should be wrapped in a filter paper to get rid of the moisture; then perform weighing in the presence of a desiccant such as silica gel);
- Xanthine oxidase from buttermilk – dissolve 10 µl of pure enzyme (50 U in 0.5 cm<sup>-3</sup> of prechilled buffer (4°C). Protect from the light and store on ice; prepare a new solution every 2-3 hours.

### Procedure

1. Turn the spectrophotometer on, set  $\lambda = 550$  nm;
2. Prepare the sample: homogenize in a prechilled buffer with 0.1% PVPP (1:10, e.g. 1 g of leaf per 10 mL of buffer). WARNING! PVPP does not dissolve, stir the buffer before use. Keep the sample on ice;
3. Prepare the reaction mixture: buffer (room temperature) + buffered cytochrome c + buffered xanthine, 100:1.5:11 ratio (v/v/v);
4. Aerate the reaction mixture on a stirrer (in darkness), for 2-3 hours, so the cytochrome is maximally oxidized;
5. Blank the spectrophotometer on a cuvette filled with oxidized cytochrome;
6. In another cuvette, add 0.8 mL of oxidized cytochrome c, 25-50 µL of plant homogenate/prechilled buffer (control), gently stir with the tip of the pipette, add 8–10 µL of xanthine oxidase, stir gently again, and measure for 2-3 min. The absorbance should gradually increase, and the curve should be as linear as possible;

7. Read or calculate the slope of the curve. The reaction rate ( $\text{tg } \alpha$ ,  $\alpha$ = the angle of the slope) should be 0.2-0.25 in case of the control. If the values are too small, increase the amount of xanthine oxidase and *vice versa*. In case of the sample containing plant extract, SOD inhibits cytochrome c reduction, giving a less value than for the control.
8. Calculate the enzyme activity assuming that one unit of cytochrome (cytochrome unit) is the amount of enzyme that gives 50% inhibition of cytochrome c reduction.

Enzymatic activity is often related to protein content. However, drastic alterations in the protein amount is often noticed and this greatly affects the so-called 'specific activity'. One must remember that SOD protein is only a part of the total soluble protein pool, hence its activity should be analysed in various ways, not only as related to protein (Bączek-Kwinta and Zaczyński 2009; Bączek-Kwinta and Kościelniak 2009).

### **Application of the methods**

So far, both methods were applied in the research on drought sensitivity of parental lines and recombinant inbred lines (RIL) of barley (*Hordeum vulgare* L.) as well. The process of breeding the lines via single seed descent (SSD) technology provides the benefits of using 5-6 rounds of crossing-over (Surma et al. 2003). The aim of the POLAPGEN project is to supply breeding companies with some tools that are useful in the generation of new cultivars of barley resistant to water scarcity, new methods for assessing plants' resilience, and to develop plant ideotype for drought resistance. One of the elements of such resistance is the activity of an antioxidant system.

It was established that high metabolic activity is strongly linked with redox processes, hence drought-tolerant plants can produce more ROS and/or have higher SOD activity than drought-susceptible ones (Bączek-Kwinta et al. 2012). Preliminary results indicate that the methods are more useful during the seedling stage than in the heading stage (Bączek-Kwinta et al. 2013, 2014). The comparison of the results with those obtained in the other tasks of the project may improve the phenotyping of barley lines tested for antioxidant efficiency and signalling processes. As it has been already mentioned and established in other studies (Bączek-Kwinta et al. 2012, 2013, 2014), while calculating SOD activity, one must remember that the protein content should not be the only basis for enzymatic activity of living leaf tissue.

## References

- Abugo O. O., Rifkind J. M. 1994. Oxidation of hemoglobin and the enhancement produced by nitroblue tetrazolium. *J. Biol. Chem.* 269: 24845-24853.
- Bączek-Kwinta R., Borek M., Żmuda K., Kościelniak J. 2014. Is free radical phenotyping of barley possible? Conference “Genetic Resources for Food and Agriculture in a Changing Climate”, 27-29 January 2014, Lillehammer, Norway. Book of Abstracts: 55-56.
- Bączek-Kwinta R., Borek M., Kościelniak J., Żmuda K. 2013. Different patterns of SOD generation and scavenging in barley SSD lines during drought. V Congress of Polish Biotechnology and V EUROBIOTECH 2013, 8-11.10.2013, Cracow, Poland. Abstracts: 91.
- Bączek-Kwinta R., Borek M. 2012. Estimation of redox processes in leaves of barley subjected to drought – a tool for further breeding? 9th International Conference “Plant functioning under environmental stress”, 12-15.09.2012, Cracow, Poland. Book of Abstracts: 35.
- Bączek-Kwinta R. 2010. Produkcja rodników tlenowych i potencjał antyoksydacyjny młodych oraz starzejących się liści pomidora (Generation of oxygen radicals and antioxidant potential in young and senescing leaves of tomato). *Zesz. Probl. Post. Nauk Roln.* 545: 313-323.
- Bączek-Kwinta R., Zaczyński M. 2009. Antioxidant aspect of thermal hardening of maize seedlings. *Oxidation Commun.* 32: 685-696.
- Bączek-Kwinta R., Kościelniak J. 2009. The mitigating role of environmental factors in seedling injury and chill-dependent depression of catalase activity in maize leaves. *Biol. Plantarum* 53: 278-284.
- Bączek-Kwinta R., Filek W., Grzesiak S., Hura T. 2006. The effect of soil drought and rehydration on growth and antioxidative activity in flag leaves of triticale. *Biol. Plantarum* 50: 55-60.
- Bączek-Kwinta R., Kościelniak J. 2003. Anti-oxidative effect of elevated CO<sub>2</sub> concentration in the air on maize hybrids subjected to severe chill. *Photosynthetica* 41(2): 161-165.
- Biehler K., Fock H. 1996. Evidence for the contribution of the Mehler peroxidase reaction in dissipating excess electrons in drought-stressed wheat. *Plant Physiol.* 112: 265-272.
- Doke N., Ohashi Y. 1988. Involvement of an O<sub>2</sub>•<sup>-</sup> generating system in the induction of necrotic lesions on tobacco leaves infected with tobacco mosaic virus. *Physiol. Molec. Plant Pathol.* 32: 165-175.
- Mc Cord I.M., Fridovich I. 1969. Superoxide dismutase: an enzymic function for erythrocuprein (hemocuprein). *J. Biol. Chem.* 244: 6049-6055.
- Foyer Ch.H., Noctor G. 2000. Oxygen processing in photosynthesis: regulation and signalling. *New Phytologist* 146: 359-388.

- Lin Z-F., Liu N., Lin G-Z., Peng Ch-L. 2009. In situ localisation of superoxide generated in leaves of *Alocasia macrorrhiza* (L.) shoot under various stresses. *J. Plant Biol.* 52: 340-347.
- Møller I.M. 2001. Plant mitochondria and oxidative stress: electron transport, NADPH turnover, and metabolism of reactive oxygen species. *Annu Rev. Plant Physiol. Plant Mol. Biol.* 52: 561-591.
- Puntarulo S., Galleano M., Boveris A. 1988. Hydrogen peroxide metabolism in soybean embryonic axes at the onset of germination. *Plant Physiol.* 86: 626-630.
- Vranová E., Inzé D., Van Breusegem F. 2002. Signal transduction during oxidative stress. *J. Exp. Bot.* 53: 1227-1236.
- Surma M., Adamski T., Kaczmarek Z., Czajka S. 2003. Zmienność cech ilościowych w populacjach linii DH i SSD jęczmienia. *Biuletyn IHAR* 226/227/1: 277-283.
- Wu L., Reddy A.B. 2014. Rethinking the clockwork: redox cycles and non-transcriptional control of circadian rhythms. *Biochem. Soc. Trans.* 42: 1-10.



## **Physiological indicators of drought tolerance in barley**

**Katarzyna Hura<sup>1</sup>, Barbara Jurczyk<sup>1</sup>, Agnieszka Ostrowska<sup>2</sup>, Marcin Rapacz<sup>1</sup>, Katarzyna Śniegowska-Świerk<sup>1</sup>, Magdalena Wójcik-Jagła<sup>1</sup>, Katarzyna Żmuda<sup>1</sup>, Jolanta Biesaga-Kościelniak<sup>2</sup>, Janusz Kościelniak<sup>1</sup>**

<sup>1</sup> *Department of Plant Physiology, Agricultural University, Kraków, Poland*

<sup>2</sup> *The Franciszek Górski Institute of Plant Physiology, Polish Academy of Sciences, Kraków, Poland*

### **Introduction**

A number of physiological traits are proposed as selection criteria for drought tolerance. Physiological traits affected by drought can be correlated with the CO<sub>2</sub> assimilation rate (Lal et al. 1996; Escalona et al. 1999; Lawlor and Cornic 2002; Guo et al. 2008; Robredo et al. 2010), PSII photochemical activity (Araus et al. 1998; Lu and Zhang 1999; Kocheva et al. 2005; Oukarroum et al. 2007; Kalaji et al. 2011; Jedmowski et al. 2013), leaf water conservation (stomatal conductance, transpiration rate, relative water content – RWC) (Chen et al. 2004; Bencze et al. 2011; Jedmowski et al. 2013) or plasma membrane integrity (Babu et al. 2004). The reliability of physiological and biochemical traits in the discrimination of drought susceptibility depends on species, genotypes (Kumar 2005; Praba et al. 2009) and developmental stage (Szira et al. 2008).

This paper presents a method to perform the above measurements.

### **Preparation of plant material**

Seeds of barley lines and cultivars were sown in pots with a capacity of 9 dm<sup>3</sup> and filled with a mixture of soil and sand (3.5 : 1, v/v) at a 16-h photoperiod, an irradiance of 650 μmol (photon) m<sup>-2</sup> s<sup>-1</sup> (provided by high pressure sodium lamps, 400 W; Philips SON-T AGRO, Brussels, Belgium), at 50% air humidity. Initially, 20 seedlings were placed in pots and after germination the number of plants was reduced to 10. During germination (4 days), a constant temperature of 25°C was

maintained. After emergence during the next 10 days, the temperature was kept at 5°C (day/night) and later, the temperature was set to 25/16°C. Seedlings were watered and fertilized with a half-strength Hoagland nutrient solution (Hoagland and Arnon 1938). The soil water content was determined by monitoring the weight (based on the water retention curve, Fig. 1) and was stabilized at 11% water content of the dry weight of the soil (i.e. 3.2 pF). Soil drought (5.7%, i.e., 4.0 pF) was used 16 days after the emergence of the fourth leaf and was continued for 10 days. Plants grown in pots with 11% water content were used as controls.

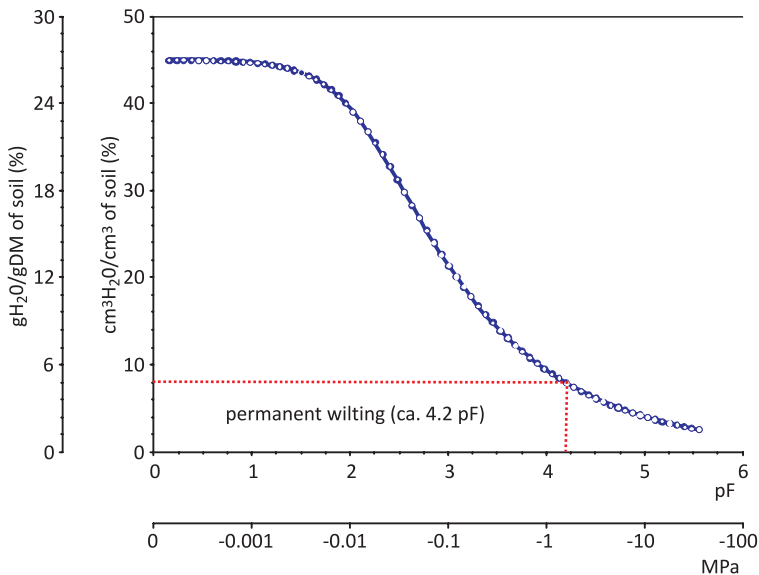


Fig. 1. Soil retention curve (courtesy of Prof. A. Pecio)

## Measurements

The measurements were performed on the third leaf of the plants after 10 days of drought. The experiments concerned: (a) water relations of seedlings and integrity of cell membranes, (b) a fast chlorophyll *a* fluorescence kinetics – the OJIP test, (c) gas exchange and (d) photochemical activity of PSII under high light intensity conditions.

### *Water relations of seedlings and the integrity of the cell membranes*

Water relations were determined by the measurements of RWC and water content in the leaves. RWC was determined according to Barrs (1968):  $RWC = (FW - DW) \times (TW - DW)^{-1} \times 100\%$ ; where FW indicates fresh weight, DW the dry weight and TW the turgid weight. To measure TW, leaf sections were placed in darkness for 24 h in vials containing water (7°C), thus permitting

complete rehydration. Water content was calculated as  $(DW/FW) \times 100\%$ . All these measurements were performed in five replications, both during drought and control conditions.

Plasma membrane's integrity was determined by means of an electrolyte leakage (EL) test (Dexter et al. 1932; Bajji et al. 2001). For each genotype, 1-cm-long five segments were cut from the leaf. Samples were washed and immersed in 10 cm<sup>3</sup> of deionized water. After 24 h ( $t_1$ ) of shaking at room temperature, samples were placed in a boiling-water bath for 20 min, and then cooled to 24°C and shaken again (24 h,  $t_2$ ). EL was calculated as follows:  $EL = (EL_1/EL_2) \times 100\%$ , where  $EL_1$  and  $EL_2$  represent the specific electrical conductance ( $\mu\text{S cm}^{-1}$ ) at time  $t_1$  and  $t_2$ , respectively. Measurements of electrical conductance were performed using a microcomputer conductivity meter CC-317 (Elmetron, Warsaw, Poland) with a platinum electrode at a frequency of 3 kHz. The total measurements during drought were carried out in 12 replications.

#### *Fast kinetics of chlorophyll a fluorescence – the OJIP test*

The development of microelectronics facilitated the construction of instruments which enable the registration of the intensity of chlorophyll fluorescence *in vivo* and *in situ* with a frequency of 100,100 Hz. The theory of energy flow in biomembranes has become a basis for application of fast fluorescence kinetics (the JIP test) to estimate the specific (in relation to reaction centres – RC) and phenomenological (on an excited leaf segment – CS) energy flows in PSII, the ratios of those energy flows and the indicators of photosystem vitality. The JIP test enables the following:

- Analyse the response to chemical and physical changes in the environment (inhibitors, gases: CO<sub>2</sub>, O<sub>2</sub>, O<sub>3</sub> and the quality and intensity of illumination and temperature)
- Study various aspects of plant parts, whole plant and ecosystem physiology, such as vitality, productivity, sensitivity and tolerance to stress; transgenic plants; and ecodynamic studies (grasses, agrocenoses, and forests)
- Establish the productivity of agrocenoses dependent on chemicals regulators (herbicides, pesticides and hormones) and plant selection
- Estimate the influence of greenhouse conditions on plants (temperature, humidity and illumination)
- Establish the influence of pollutants on plants
- Study the response of agrocenoses on global scale to global warming, the increase in UV intensity and so on.

Fast chlorophyll *a* fluorescence kinetics was measured using a plant efficiency analyser (Hansatech Ltd., Kings Lynn, UK). Before measurements, the LED-light source of the fluorimeter was calibrated using an SQS light meter (Hansatech Ltd, Kings Lynn, UK). The excitation irradiance had an intensity

Table 1. Definitions and explanation of selected parameters of the OJIP test

<i>Fast kinetics of chlorophyll a fluorescence – the OJIP test</i>	
<i>Density of RCs and energy flux per excited leaf cross section at t=max (CSm)</i>	
ABS/CSm	Light energy absorption, in this study the proportion of ABS/CSm $\approx$ Fm was used
DIo/CSm	The amount of energy dissipated from PSII, ABS/CSm-TRo/CSm
ETo/CSm	Amount of energy used for electron transport, further than Q <sub>A</sub> , $ET_o/CSm = \phi_{P_o} \times \psi_o \times (ABS/CSm)$
RC/ABS	Density of reaction centres per PSII antenna chlorophyll
RC/CSm	Number of active reaction centres, $RC/CSm = ABS/CSm \times \phi_{P_o} \times (V_j/Mo)$
TRo/CSm	Amount of excitation energy trapped in PSII, $TR_o/CSm = \phi_{P_o} \times (ABS/CSm)$
<i>Quantum efficiency/flux ratios</i>	
$\phi_{P_o}$	Maximal quantum yield for primary photochemistry shows the probability that an absorbed photon leads to a reduction of Q <sub>A</sub> , $\phi_{P_o} (F_v/F_m) = 1 - (F_o/F_m)$ , maximum quantum efficiency to reduce Q <sub>A</sub> to Q <sub>A</sub> <sup>-</sup>
$\psi_o$	Efficiency with which a trapped exciton can move an electron into the electron transport chain further than Q <sub>A</sub> , $\psi_o = (1 - V_j)$
$\phi_{E_o}$	Electron transport quantum yield, expresses the probability that an absorbed photon leads to an electron transport further than Q <sub>A</sub> , $\phi_{E_o} = [1 - (F_o/F_m)] \times (1 - V_j)$
$\phi_{P_o}/(1 - \phi_{P_o})$	A 'conformation' term for primary photochemistry
$\psi_o/(1 - \psi_o)$	A 'conformation' term for non-light-dependent reactions
<i>Vitality indexes</i>	
(1-B) <sub>av</sub>	The average fraction of open RC during the time needed to complete the closure of all the RCs, $(1 - B)_{av} = Sm/t_{F_{max}}$ , Sm: area under the curve of fluorescence, $t_{F_{max}}$ : time to reach Fm
DF <sub>abs</sub>	Total driving force for photosynthesis, $DF_{abs} = \log(PI_{abs})$
OEC	Fraction of O <sub>2</sub> evolving centres in comparison with the control sample, $OEC = [1 - V_K/V_j]_{treated} / [1 - V_K/V_j]_{control}$
PI <sub>abs</sub>	Performance index (on absorption basis), $(RC/ABS) \times [\phi_{P_o}/(1 - \phi_{P_o})] \times (\psi_o/(1 - \psi_o))$
<i>Another abbreviations</i>	
F <sub>2ms</sub>	Fluorescence intensity at 2 ms
F <sub>m</sub>	Maximum fluorescence intensity
F <sub>o</sub>	Fluorescence intensity at 50 $\mu$ s when all RCs are open, all Q <sub>A</sub> molecules are in the oxidized state
Mo	$Mo = 4 \times (F_{300\mu s} - F_o) / (F_m - F_o)$ , F <sub>300<math>\mu</math>s</sub> is the fluorescence intensity at 300 $\mu$ s
PSII	Photosystem II
Q <sub>A</sub>	Primary quinone acceptor of PSII
Q <sub>B</sub>	Secondary quinone acceptor of PSII
V <sub>j</sub>	V <sub>j</sub> is used to characterize the efficiency of the electron transfer between Q <sub>A</sub> and Q <sub>B</sub> , $V_j = (F_{2ms} - F_o) / (F_m - F_o)$
V <sub>K</sub>	Variable fluorescence at 300 $\mu$ s, $V_K = (F_{300\mu s} - F_o) / (F_m - F_o)$

of  $3,000 \mu\text{mol}(\text{quanta}) \text{m}^{-2}\text{s}^{-1}$  (peak at 650 nm). Measurements were taken after 30 min of leaves' adaptation to darkness. Fluorescence intensity was measured with a PIN-photodiode after being passed through a long-pass filter. Changes in fluorescence were registered during irradiation between 10  $\mu\text{s}$  and 1 s of starting the irradiation. During the initial 2 ms, data were collected every 10  $\mu\text{s}$  with a 12-bit resolution. After this period, the frequency of measurements was reduced automatically. The measurements during drought were performed in 22-25 replicates. Transient curves upon chlorophyll fluorescence induction were analysed and additional parameters were calculated using the JIP test (Strasser et al. 2000; Strasser and Tsimilli-Michael 2001; Oukarroum et al. 2007) (Table 1). The  $\text{O}_2$ -evolving complex (OEC) can also be calculated by the OJIP test (Srivastava and Strasser 1997; Strasser 1997; Lazar et al. 1999).

### *Gas exchange*

Net photosynthetic (Pn) and transpiration (E) rates as well as stomatal conductance (gs) were measured using an infrared gas analyser (Ciras-1, PP Systems, Hitchin, UK), with a Parkinson leaf chamber (PLC6; PP Systems, Hitchin, UK), which automatically controlled the measurement conditions. The irradiation system was equipped with halogen lamps. The flow rate of air with constant  $\text{CO}_2$  concentration [ $400 \mu\text{mol}(\text{CO}_2) \text{mol}^{-1}(\text{air})$ ] through the assimilation chamber was  $350\text{-}400 \text{cm}^3 \text{min}^{-1}$ . The measurements were taken in the middle part of the second leaf at  $25^\circ\text{C}$  (the leaf temperature), where irradiance was equal to  $700 \mu\text{mol}(\text{quanta}) \text{m}^{-2}\text{s}^{-1}$  and RH was 30%. The measurements were performed in seven replicates in the middle part of the leaf, both during drought and under control conditions.

### *Photochemical activity of PSII under high light intensity*

Fluorescence parameters of PSII efficiency were measured with a FMS2 pulse modulation fluorometer (Hansatech Ltd, Kings Lynn). The first step of measurements was an adaptation of plants to the dark for 30 min.  $F_o$  was measured at an irradiance of  $0.65 \mu\text{mol}(\text{quanta}) \text{m}^{-2}\text{s}^{-1}$ .  $F_m$  was measured with a saturation pulse of  $5,800 \mu\text{mol}(\text{quanta}) \text{m}^{-2}\text{s}^{-1}$  for 800 ms. After 20 s, the plants were exposed to actinic light ( $1,000 \mu\text{mol}(\text{quanta}) \text{m}^{-2}\text{s}^{-1}$ ) for 60 min. At the end of the actinic light period, the photochemical quantum yield of PSII ( $\Phi_{\text{PSII}}$ ), the photochemical quenching (qP), the efficiency of excitation energy capture by PSII reaction centres ( $F_v'/F_m'$ ) and non-photochemical quenching of variable chlorophyll fluorescence (qN) were measured,  $qN=1-(F_m'-F_o')/(F_m-F_o)$  (Horton and Hague 1988, Genty et. al 1989; Quick and Stitt 1989). The saturating pulse ( $F_m'$ ) had an intensity of about  $5,800 \mu\text{mol}(\text{quanta}) \text{m}^{-2}\text{s}^{-1}$  and lasted 800 ms.  $F_o'$  was measured after turning off the actinic light, by immediately irradiating the

leaf for 3 s with a far-red-emitting diode of about 15 Wm<sup>-2</sup>. The measurements were performed in five replicates.

Summarizing, the use of conventional measurement of physiological processes of plants allowed for identification of barley line tolerant to drought stress.

## References

- Araus J.L., Amaro T., Voltas J., Nakkoul H., Nachit M.M. 1998. Chlorophyll fluorescence as a selection criterion for grain yield in durum wheat under Mediterranean conditions. *Field Crop Res.* 55: 209-223.
- Babu R.C., Zhang J., Blum A., Ho T.-H., Wu R., Nguyen H.T. 2004. *HVA1*, a LEA gene from barley confers dehydration tolerance in transgenic rice (*Oryza sativa* L.) via cell membrane protection. *Plant Sci.* 166: 855-862.
- Bajji M., Kinet J.-M., Lutts S. 2001. The use of the electrolyte leakage method for assessing cell membrane stability as a water stress tolerance test in durum wheat. *Plant Growth Regul.* 00: 1-10.
- Barrs H. D. 1968. Determination of water deficits in plant tissues. In: T. T. Kozlowski (ed.), *Water Deficits and Plant Growth*, Vol. I, pp. 235-368. Academic Press, New York.
- Bencze S., Bamberger Z., Janda T., Balla K., Bedő Z., Veisz O. 2011. Drought tolerance in cereals in terms of water retention, photosynthesis and antioxidant enzyme activities. *Cent. Eur. J. Biol.* 6(3): 376-387.
- Chen G., Sagi M., Weining S., Krugman T., Fahima T., Korol A. B., Nevo E. 2004. Wild barley *eib1* mutation identifies a gene essential for leaf water conservation. *Planta* 219: 684-693.
- Dexter S.T., Tottingham W.E., Garber L.F. 1932. Investigations of the hardiness of plants by measurements of electrical conductivity. *Plant Physiol.* 7: 63-78.
- Escalona J.M., Flexas J., Medrano H. 1999. Stomatal and nonstomatal limitations of photosynthesis under water stress in field-grown grapevines. *Aust. J. Plant Physiol.* 26: 421-433.
- Genty B., Briantais J.-M., Baker N.R. 1989. The relationship between the quantum yield of photosynthetic electron transport and quenching of chlorophyll fluorescence. *Biochem. Biophys. Acta* 990: 87-92.
- Guo P., Baum M., Varshney R.K., Graner A., Grando S., Ceccarelli S. 2008. QTLs for chlorophyll and chlorophyll fluorescence parameters in barley under post-flowering drought. *Euphytica* 163: 203-214.
- Hoagland D. R., Arnon D. I. 1938. The water-culture method for plants without soil. *Univ. Calif. Agr. Exp. Stn. Cir.* 347: 29-32.
- Horton P., Hague A. 1988. Studies on the induction of chlorophyll fluorescence in isolated barley protoplasts. 4. Resolution of non-photochemical quenching. *Biochim. Biophys. Acta* 932: 107-115.

- Jedrowski C., Ashoub A., Brüggemann W. 2013. Reactions of Egyptian landraces of *Hordeum vulgare* and *Sorghum bicolor* to drought stress, evaluated by the OJIP fluorescence transient analysis. *Acta Physiol. Plant.* 35: 345-354.
- Kalaji H., Govindjee M., Bosa K., Kościelniak J., Žuk-Golaszewska K. 2011. Effects of salt stress on photosystem II efficiency and CO<sub>2</sub> assimilation of two Syrian barley landraces. *Environ. Exp. Bot.* 73: 64-72.
- Kocheva K.V., Busheva M.C., Georgiev G.I., Lambrev P. H., Goldsev V.N. 2005. Influence of short-term osmotic stress on the photosynthetic activity of barley seedlings. *Biol. Plant.* 49: 145-148.
- Kumar D. 2005. Breeding for drought resistance. In: M. Ashraf, and P. J. C. Harris (eds.), *Abiotic Stresses. Plant Resistance Through Breeding and Molecular Approaches*, pp. 145-176. Haworth Press, New York.
- Lal A., Ku M.S.B., Edwards G.E. 1996. Analysis of inhibition of photosynthesis due to water stress in the C<sub>3</sub> species *Hordeum vulgare* and *Vicia faba*: electron transport, CO<sub>2</sub> fixation and carboxylation capacity. *Photosynth. Res.* 49: 57-69.
- Lawlor D.W., Cornic G. 2002. Photosynthetic carbon assimilation and associated metabolism in relation to water deficits in higher plants. *Plant Cell Environ.* 25: 275-294.
- Lazar D., Pospisil P., Naus J. 1999. Decrease of fluorescence induction is suppressed by electron acceptors and donors to photosystem 2. *Photosynthetica* 37: 255-265.
- Lu C., Zhang J. 1999. Effects of water stress on photosystem II photochemistry and its thermostability in wheat plants. *J. Exp. Bot.* 50(336): 1199-1206.
- Oukarroum A., El Madidi S., Schansker G., Strasser R.J. 2007. Probing the responses of barley cultivars (*Hordeum vulgare* L.) by chlorophyll a fluorescence OLKJIP under drought stress and re-watering. *Environ. Exp. Bot.* 60: 438-446.
- Praba M. L., Cairns J.E., Babu R. C., Lafitte H.R. 2009. Identification of physiological traits underlying cultivar differences in drought tolerance in rice and wheat. *J. Agron. Crop Sci.* 195: 30-46.
- Quick W.P., Stitt M. 1989. An examination of factors contributing to non-photochemical quenching of chlorophyll fluorescence in barley leaves. *Biochim. Biophys. Acta* 977: 287-296.
- Robredo A., Pérez-López U., Lacuesta M., Mena-Petite A., Muñoz-Rueda A. 2010. Influence of water stress on photosynthetic characteristics in barley plants under ambient and elevated CO<sub>2</sub> concentrations. *Biol. Plantarum* 54 (2): 285-292.
- Srivastava A., Strasser R.J. 1997. Constructive and destructive actions of light on the photosynthetic apparatus. *J. Sci. Ind. Res.* 56: 133-148.
- Strasser R.J. 1997. Donor side capacity of photosystem II probed by chlorophyll *a* fluorescence transients. *Photosynth. Res.* 52: 147-155.
- Strasser R.J., Sivastava A., Tsimilli-Michael M. 2000. The fluorescence transient as a tool to characterize and screen photosynthetic samples. In: P. Mohanty, U. Yunus, M. Pathre (eds.), *Probing Photosynthesis: Mechanism, Regulation and Adaptation*, pp. 443-480, Taylor and Francis, London.

- Strasser R. J., Tsimilli-Michael M. 2001. Stress in plants, from daily rhythm to global changes, detected and quantified by the JIP-test. *Chem. Nouv.* 75: 3321-3326.
- Szira F., Bálint A. F., Börner A., Galiba G. 2008. Evaluation of drought-related traits and screening methods at different developmental stages in spring barley. *J. Agron. Crop Sci.* 194: 334-342.

## **Methods for the measurement of drought-induced changes in the expression of selected barley genes**

**Katarzyna Śniegowska-Świerk, Barbara Jurczyk, Marcin Rapacz**

*Department of Plant Physiology, Faculty of Agriculture and Economics, University of Agriculture, Kraków, Poland*

### **Introduction**

While searching for drought-resistant genotypes, one should analyse different levels of plant response, for example molecular or physiological. Since there are many possible approaches, the best solution would be combining different methods; however, it will require more time and resources. For example, molecular methods would be easy to use, and less time-consuming than the physiological ones. The evaluation of the expression level of selected genes is also a commonly used approach. A few criteria need to be met for this technology to be considered an effective tool in assessing the plant response to drought. The first obligatory criterion is sampling. Each sample should be collected at the same time of day, in exactly the same conditions. They should be immediately frozen in liquid nitrogen to avoid RNA degradation and/or unspecific induction of gene expression. Another important requirement is a selection of corresponding genes, endogenous control gene and a correct indication of the transcript level. An effective method can be developed only if all these requirements are properly met.

Real-time PCR has gained wide acceptance due to the fact that it is rapid, sensitive and reliable. In addition, the risk of contamination is highly reduced (Radonic et al. 2004). The sensitivity of this technique allowed for a significant reduction of an initial amount of analysed cDNA as compared to, for example, the Northern blot method (Bubner and Baldwin 2004). The most common method for the product detection is a TaqMan double-labelled hydrolysis probe (Bubner and Baldwin 2004). Furthermore, to get the right results, it is necessary to apply the appropriate reference gene (housekeeping gene), which should be constitutively expressed and characterized with stable expression level. That gene should be

tested and verified for each experiment, for the specific objects and conditions used. By using appropriate and commonly available algorithms, the selection of the best reference gene from the pool of candidate reference genes is possible. The choice of measurement method, probe type and reference gene are preparatory and essential steps to obtain a reliable result. The next step, compulsory to achieve the results, is a proper data analysis. It ensures the accuracy of the technology used for determination of gene expression level.

Barley *HVA1* gene is a member of group 3 late embryogenesis abundant (LEA) protein gene. LEA proteins comprise up to 4% of total cellular protein (Wise and Tunnacliffe 2004) and have been categorized into six groups (Battaglia et al. 2008; Khurana et al. 2008). These proteins are accumulated in seeds and in drought stressed tissues and confer to desiccation tolerance (Lal et al. 2008). Variable protective responses speculated for LEA proteins include ion sequestration, stabilization of macromolecules and membranes and affecting the redox balance as antioxidants (Kovacs et al. 2008). A group 3 LEA protein, *HVA1*, was isolated and characterized from barley aleurone layers and was found to be stress induced (Hong et al. 1992). The role of *HVA1* in maintaining cellular membrane stability plays an equally important part in keeping the photosynthetic machinery intact.

The functional roles of LEAs remain speculative, although many studies have shown that barley *HVA1* confers stress tolerance to many important crops. Transformation of rice and wheat with *HVA1* gene caused an increase in drought resistance in the transgenic lines (Xu et al. 1996; Sivamani et al. 2000; Xiao et al. 2007). Also the transgenic mulberry with barley *HVA1* gene increased its drought and salinity tolerance compared to wild type (Lal et al. 2008).

The barley stress-responsive gene *SRG6* is a hypothetical transcription factor comprising 11 exons and encoding 379 amino acids and it is highly conserved in plants and present in other organisms, including yeast and mammals. *SRG6* gene was mapped between ABC455 and salfp76 markers (Tong et al. 2007) located in the region of the short arm of barley chromosome 7H that also contains one of the QTLs that controls osmotic adjustment potential (Teulat et al. 1998), and which is considered to be one of the most important mechanisms for drought tolerance. Also, Malatrasi et al. (2002) reported that *SRG6* gene expression was elevated under drought stress as well as upon exposure to ABA. *SRG6* protein is hydrophobic with a helix-loop-helix region (HLH) characteristic for DNA-binding domain in many transcription factors. HLH is a superfamily binding as dimers to specific DNA target sites and plays a role in the regulation of multiple transcriptional programs. An *Arabidopsis* transformation using wheat *TaSRG6* caused an increase in drought tolerance and also resulted in lower relative water loss and higher membrane stability (Tong et al. 2007). Genetic map location and the factors stimulating this gene make it a candidate for a broadly conserved determinant of drought tolerance (Malatrasi et al. 2002).

The aim of the study was to develop a method for measurements of drought-induced changes in the expression of *HVA1* and *SRG6* genes in two developmental stages of barley. The work consists of the validation of candidate reference gene and measurements of expression of selected genes using real-time PCR (RT-PCR).

### **Measurements of drought-induced changes in the expression of *HVA1* and *SRG6***

Drought treatment and sample collection have been performed as described by Rapacz et al. (2012). All primers and probes used in the experiments were designed in Primer Express Software v. 2.0 (Applied Biosystems, Foster City, CA, USA). The sequences of primers and probes and sequences origins are given in the works of Rapacz et al. (2010, 2012). The expression stability of ten candidate reference genes was examined during leaf growth and increasing drought level. RNeasy Plant Mini Kit (Qiagen, Hilden, Germany) was used for RNA extraction. The first strand cDNA synthesis combined with genomic DNA elimination was performed using QuantiTect Reverse Transcription Kit (Qiagen, Hilden, Germany). PCR reactions were run in 96-well plates using a 7500 Real-Time PCR System (Applied Biosystem, Foster City, CA, USA) with the cycling parameters: 10 min at 90°C, 40 cycles of 15 s at 95°C and 1 min at 60°C. The reactions were 25 µl in volume and contained 12.5 µl of Power SYBR Green PCR Master Mix (Applied Biosystems by Life Technologies, Carlsbad, CA, USA), 2.5 µl of each primer (the concentration 900 nM), 2.5 µl of cDNA (about 10 ng of template) and 5 µl of nuclease-free water (other details are described by Rapacz et al., 2012). The selection of genes with stable expression was performed using qBase<sup>PLUS</sup> (Hellemans et al. 2007), NormFinder (Andersen et al. 2004) and BestKeeper (Pfaffl 2004) algorithms. QBase<sup>PLUS</sup> gene stability measure is defined as the average pairwise variation of a particular gene with all other candidates (Hellemans et al. 2007). NormFinder selects the genes with minimal inter- and intra-group variation and adds these two sources of variation (Andersen et al. 2004) and the BestKeeper calculates the standard deviations between samples (Pfaffl 2004). The protocols are based on different statistical approaches and often yield different rankings. It is recommended to prepare a consensus ranking, taking into account all protocols (Andersen et al. 2004; Schmidt and Delaney 2010). Throughout all rankings, *ADP* gene has been selected for comparisons between both stages (Rapacz et al. 2012).

Real-time PCR analysis of *HVA1* and *SRG6* genes was performed with the protocol as described in details by Rapacz et al. (2010) with modifications. In the work of Rapacz et al. (2010), *actin* gene was used for normalization, but after the validation experiment, *ADP* was shown to be more stably expressed than

*actin* in the examined conditions. RNA extraction, cDNA synthesis and PCR reactions were run as described by Rapacz et al. (2010). Briefly, PCR reactions were run in 96-well plates, each reaction was 25  $\mu$ l in volume and contained 250 nM of TaqMan MGB, 900 nM Sequence Detection Primers, 12.5  $\mu$ l of TaqMan Universal PCR Master Mix and 2.5  $\mu$ l of cDNA (corresponding to about 38 ng). The thermal profile reaction was the same as in the validation experiment, as described above. The results obtained by Rapacz et al. (2010) were calculated using the comparative Ct method as described by Livak and Schmittgen (2001). The amplification efficiency of target genes was proved to be the same as the amplification efficiency of endogenous control. The data obtained in this study was analysed with the Pfaffl (2001) mathematical model with *ADP* as endogenous control gene. The relative quantification of a target gene in comparison to a reference gene is calculated from the PCR efficiencies (*E*) and the CP (crossing point) deviation of an unknown sample compared to a control, and expressed in comparison to a reference gene according to the equation:

$$\text{relative expression} = \frac{E_{\text{target}} \Delta CP_{\text{target}}^{\text{(control-sample)}}}{E_{\text{ref}} \Delta CP_{\text{ref}}^{\text{(control-sample)}}},$$

where *E* is PCR amplification efficiency and CP is defined as the point at which fluorescence starts rise above the background fluorescence. The efficiencies of PCR reactions of target genes and endogenous control gene have to be estimated, but they need not to be equal for both genes as in the comparative Ct method.

## Preliminary results

The results of *HVA1* gene expression level at the third leaf stage (phase 1) and at the heading stage (phase 2) of selected barley genotypes grown under the drought treatment are presented in Fig. 1. The accumulation of the investigated transcript was detected only for the plants exposed to drought stress. The fact that in the control plants a transcript of this gene was not detected is a signal that this gene is associated with drought response. These results coincide with previous reports, where the steady-state level of *HVA1* transcripts increased dramatically after a treatment with ABA, drought and cold (Hong et al. 1992; Straub et al. 1994). In others plants like oat (Maqbool et al. 2002; Oraby et al. 2005) and bent grass (Fu et al. 2007), a correlation between *HVA1* overexpression and stress tolerance has also been established.

The level of *SRG6* transcript accumulation varied for the selected lines, but was higher for Syrian variety CAM/B1/CI than for Maresi. The same relationships were reported by Rapacz et al. (2010), where *SRG6* gene was reported as having a higher expression level in barley genotypes more tolerant to drought. Also,

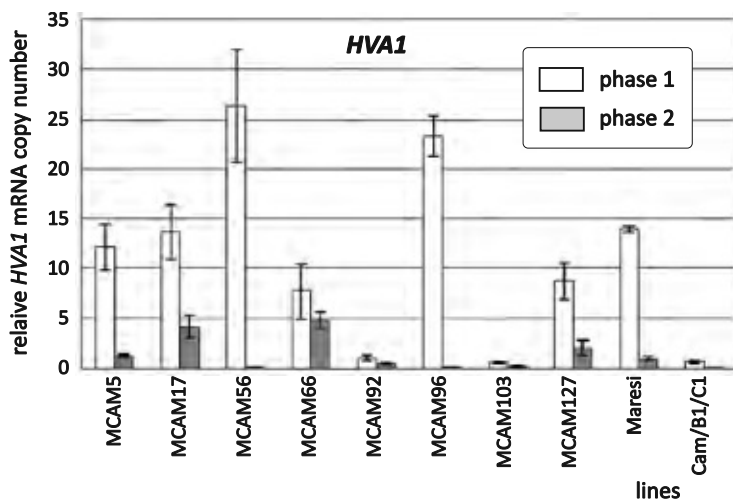


Fig. 1. Accumulation of *HVA1* transcript (relative to cv. Maresi plants drought-treated in phase 1) with *ADP* as a reference gene during drying of the leaves of selected lines at the third leaf stage (phase 1) and at the heading stage (phase 2) (mean  $\pm$  SE)

Wójcik-Jagła et al. (2012) revealed increased *SRG6* expression during drought. Interestingly, *SRG6* gene transcript accumulation, in contrast to the previously described *HVA1*, was measurable in the control plants, which means that *SRG6* is expressed constitutively in plant leaves. This suggests a completely different mechanism of action and stimulation of the described genes (Fig. 2).

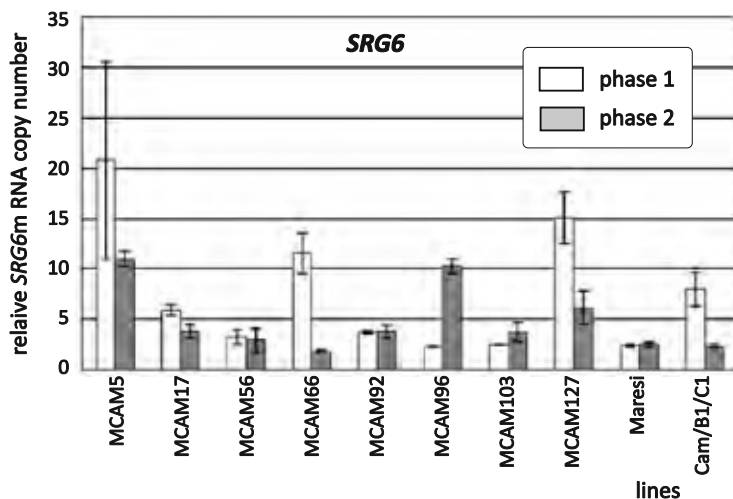


Fig. 2. Relative to the well-watered control accumulation of *SRG6* transcript with *ADP* as a reference gene during drying of the leaves of selected lines at the third leaf stage (phase 1) and at the heading stage (phase 2) (mean  $\pm$  SE)

Real-time PCR technique is easy to perform, reliable and has high sensitivity. However, the accurate quantification of gene expression requires the normalization of the obtained results. The stability of the *ADP* expression has been proved for the experimental conditions applied in this study. The results of gene expression are obtained using the Pfaffl (2001) mathematical model using that gene as a reference. They indicate that in genotypes with different drought tolerance, both genes show different expression in response to drought.

## References

- Andersen C.L., Jensen J.L., Ørntoft T.F. 2004. Normalization of real-time quantitative reverse transcription-PCR data: a model-based variance estimation approach to identify genes suited for normalization, applied to bladder and colon cancer data sets. *Cancer Res.* 64: 5245-5250.
- Battaglia M., Olvera-Carrillo Y., Garcíarrubio A., Campos F., Covarrubias A.A. 2008. The enigmatic LEA proteins and other hydrophilins. *Plant Physiol.* 148: 6-24.
- Bubner B., Baldwin I.T. 2004. Use of real-time PCR for determining copy number and zygosity in transgenic plants. *Plant Cell Rep.* 23: 263-271.
- Fu D., Huang B., Xiao Y., Muthukrishnan S., Liang G.H. 2007. Overexpression of barley *HVA1* gene in creeping bentgrass for improving drought tolerance. *Plant Cell Rep.* 26: 467-477.
- Hellemans J., Mortier G., Paeppe A.D., Speleman F., Vandesompele J. 2007. qBase relative quantification framework and software for management and automated analysis of real-time PCR data. *Gen. Biol.* 8: R19.
- Hong B., Barg R., Ho T.H.D. 1992. Developmental and organ- specific expression of an ABA- and stress-induced protein in barley. *Plant Mol. Biol.* 18: 663-674.
- Khurana P., Vishnudasana D., Chhibbar A.K. 2008. Genetic approaches towards overcoming water deficit in plants- special emphasis on LEAs. *Physiol. Mol. Biol. Plants* 14: 277-298.
- Kovacs D., Agoston B., Tompa P. 2008. Disordered plant LEA proteins as molecular chaperones. *Plant Signal. Behav.* 3: 710-713.
- Lal S., Gulyani V., Khurana P. 2008. Overexpression of *HVA1* gene from barley generates tolerance to salinity and water stress in transgenic mulberry (*Morus indica*). *Transgenic Res.* 17: 651-663.
- Livak K.J., Schmittgen Y.D. 2001. Analysis of relative gene expression data using Real-Time Quantitative PCR and the  $\Delta\Delta C_t$  method. *Methods* 25: 402-408.
- Malatrasi M., Close T.J., Marmioli N. 2002. Identification and mapping of a putative stress response regulator gene in barley. *Plant Mol. Biol.* 50: 143-152.
- Maqbool B., Zhong H., El-Maghraby Y., Ahmad A., Chai B., Wang W., Sabzikar R., Sticklen B. 2002. Competence of oat (*Avena sativa* L.) shoot apical meristems for

- integrative transformation, inherited expression, and osmotic tolerance of transgenic lines containing *hval*. *Theor. Appl. Genet.* 105: 201-208.
- Oraby H.F., Ransom C.B., Kravchenko A.N., Sticklen M.B. 2005. Barley *HVAL* gene confers salt tolerance in R3 transgenic oat. *Crop Sci.* 45: 2218-2227.
- Pfaffl M.W. 2001. A new mathematical model for relative quantification in real-time RT-PCR. *Nucleic Acid Res.* 29: 2002-2007.
- Pfaffl M.W. 2004. Quantification strategies in real-time PCR. In: Busin SA (ed) A-Z of quantitative PCR. International University Line (IUL), La Jolla, pp. 87-112.
- Radonic A., Thulke S., Mackay I.M., Landt O., Siebert W., Nitsche A. 2004. Guideline to reference gene selection for quantitative real-time PCR. *Biochem. Biophys. Res. Comm.* 313 4: 856-862.
- Rapacz M., Kościelniak J., Jurczyk B., Adamska A., Wójcik M. 2010. Different patterns of physiological and molecular response to drought in seedlings of malt- and feedtype barleys (*Hordeum vulgare*). *J. Agron. Crop Sci.* 196: 9-19.
- Rapacz M., Stępień A., Skorupa K. 2012. Internal standards for quantitative RT-PCR studies of gene expression under drought treatment in barley (*Hordeum vulgare* L.): the effects of developmental stage and leaf age. *Acta Physiol. Plant.* 34: 1723-1733.
- Sivamani E., Bahieldin A., Wraith J.M., Al-Niemi T., Dyer W.E., Ho T.D., Qu R. 2000. Improved biomass productivity and water use efficiency under water deficit conditions in transgenic wheat constitutively expressing the barley *HVAL* gene. *Plant Sci.* 155: 1-9.
- Schmidt G.W., Delaney S.K. 2010. Stable internal reference genes for normalization of real-time RT-PCR in tobacco (*Nicotiana tabacum*) during development and abiotic stress. *Mol. Genet. Genomics* 283: 233-241.
- Straub P.F., Shen Q., Ho T.H.D. 1994. Structure and promoter analysis of an ABA- and stress-regulated barley gene, *HVAL*. *Plant Mol. Biol.* 26: 617-630.
- Teulat B., This D., Khairallah M., Borries C., Ragot C., Sourdille P., Leroy P., Monneveux P., Charrier A. 1998. Several QTLs involved in osmotic-adjustment trait variation in barley (*Hordeum vulgare* L.). *Theor. Appl. Genet.* 96: 688-698.
- Tong S., Ni Z., Peng H., Dong G., Sun Q. 2007. Ectopic overexpression of wheat *TaSrg6* gene confers water stress tolerance in Arabidopsis. *Plant Sci.* 172: 1079-.
- Wise M.J., Tunnacliffe A. 2004. POPP the question: what do LEA proteins do? *Trends Plant Sci.* 9: 13-17.
- Wójcik-Jagła M., Rapacz M., Barcik W., Janowiak F. 2012. Differential regulation of barley (*Hordeum distichon*) *HVAL* and *SRG6* transcript accumulation during the induction of soil and leaf water deficit. *Acta Physiol. Plant.* 34: 2069-2078.
- Xiao B., Huang Y., Tang N., Xiong L. 2007. Over-expression of a LEA gene in rice improves drought resistance under the field conditions. *Theor. Appl. Genet.* 115: 35-46.
- Xu D., Duan X., Wang B., Hong B., Ho T.-H.D., Wu R. 1996. Expression of a late Embryogenesis Abundant Protein Gene, *HVAL*, from Barley Confers Tolerance to Water Deficit and Salt Stress in Transgenic Rice. *Plant Physiol.* 110: 249-257.



## **The application of functional genomics to identify genes associated with adaptation of barley plants to water deficit**

**Tadeusz Rorat, Anna Turska-Taraska, Agnieszka Kielbowicz-Matuk, Mateusz de Mezer**

*Institute of Plant Genetics, Polish Academy of Sciences, Poznań, Poland*

### **Introduction**

Plants are often subjected to periods of soil and atmospheric water deficit during their life cycle that impairs their morphological, physiological, biochemical and molecular processes resulting in growth inhibition. Fluctuations in rainfall affect the cultivation of most crop plants leading to yield instability. To maintain yield stability under unpredicted water availability, improvement of drought tolerance in crop plants and better adaptation to drought-prone environments are needed. Application of methods of classical and molecular genetics for the identification of drought-tolerance markers to select genotypes displaying better adaptive performance did not bring expected results. Though genetic analysis based on molecular markers led to the identification of many QTLs for drought tolerance and adaptation to water-deficit conditions in many crop plants, the genes representing QTLs are rather not available and they cannot be applied for the selection of the genotypes displaying better performance to drought tolerance. A solution is to isolate the genes that confer adaptation to water deficit. Many drought-inducible genes with various functions have been identified by molecular and genomic analyses in *Arabidopsis*, rice and other plant species and contributions of some of them to drought tolerance have been demonstrated (Bartels and Sunkar 2005). Genes encoding signal transduction and transcriptional regulatory components are of great importance in plant response to water deficit. They trigger the expression of appropriate target genes, the protein products of which lead to the development of protective and adaptive mechanisms. The SnRK2 kinases, PP2C phosphatases and CDPK and MAPK kinases are the main signal transduction components of plant response to water deficit (Boudsocq et al. 2004), and members of the DREB/CBF,

MYB, basic leucine zipper (bZIP) and zinc-finger families of transcription factors (TFs) have been shown to be the main transcription regulators in drought response, and their roles in the regulation of plant stress responses are well-characterized (Bartels and Sunkar 2005; Yamaguchi-Shinozaki and Shinozaki 2006; Nakashima and Yamaguchi-Shinozaki 2006; Umezawa et al. 2006; Shinozaki and Yamaguchi-Shinozaki 2007; Hu et al. 2010; Morran et al. 2011). In barley, genes encoding DREB1 transcription factor (Xu et al. 2009) and members of bZIP transcription factors (Casaretto and Ho 2003; Matsumoto et al. 2011) have been isolated and the molecular structure of some of them, e.g. HvABI5, characterized.

In this review, we provide methodology for isolation and expression characterization of members of DREB1 and bZIP1 transcription factor families from barley seedlings, the expression of which is associated with adaptation to water deficit. The isolated *HvDREB1* and *HvbZIP1* genes can be used as expression markers for the selection of barley genotypes with higher adaptive ability to water deficit.

### **Selection of transcription factors as potential transcription regulators in response to water deficit**

Transcription factors belonging to DREB/CBF, MYB, bZIP and zinc-finger families have been widely demonstrated to be associated with response to water deficit and other environmental stressors leading to cellular dehydration in many plant species. However, the factors belonging to the DREB/CBF families were shown to be the key players in plant adaptation to low temperature and water deficit. These factors induce expression of majority of genes encoding functional proteins upon stress conditions. In Arabidopsis, there are two DREB/CBF transcript families, DREB1 that mainly functions in response to low temperature and DREB2 that is functional in response to water deficit. In addition, MYC, MYB and NAC families of transcription factors identified in response to stress play a complementary role in transcription regulation under the stress conditions. Unfortunately, most of the data on the signal transduction and transcription regulation in response to stress factors (water deficit, low temperature and salinity) was obtained using model plants such as Arabidopsis. Current knowledge regarding signal transduction and transcription regulation in response to stress is very limited in barley. However, a gene encoding *Hordeum vulgare* dehydration-responsive element binding protein 1 (*HvDREB1*), homologous to the DREB1 transcription factor subfamily, was isolated from barley seedlings (mRNA acc. DQ01294), (Xu et al. 2009). Analysis of *HvDREB1* protein sequence revealed that the *HvDREB1* protein contains an AP2/ERF DNA-binding domain (typical of DREB transcription factors) located at the N-terminal end that binds to the characteristic 6-bp dehydration-responsive element (A/GCCGAC) in the promoter regions of the target genes in a sequence-specific manner (Sakuma

et al. 2002). As shown (Xu et al. 2009), the *HvDREB1* gene was induced in leaves by salt, drought, low temperature and exogenous ABA. On the other hand, it was reported that transgenic barley and wheat plants overexpressing *DREB1* gene exhibited increased tolerance to stress (Morran et al. 2011).

The basic leucine zipper (bZIP) transcription factor family is one of the largest and most diverse families. The bZIP transcription factors are characterized by a 40- to 80-amino-acid-long conserved domain (bZIP domain) that comprises two motifs: a basic region responsible for specific binding of the transcription factor to its target DNA and a leucine zipper required for transcription factor dimerization. Although many bZIP transcription factors have been identified in Arabidopsis (75 bZIPs) (Jakoby et al. 2002), rice (89 bZIPs) (Nijhawan et al. 2008), maize (125 bZIPs) (Wei et al. 2012) and soybean (131 bZIPs) (Liao et al. 2008), only a few of the identified *bZIP* genes have been functionally validated in plants. Genetic, molecular and biochemical analyses indicate that bZIP transcription regulators are involved in important processes such as organ and tissue differentiation, cell elongation, nitrogen/carbon balance control, pathogen defence, energy metabolism, unfolded protein response, hormone and sugar signalling, light response, osmotic control and seed storage protein gene regulation. These bZIP transcription factors have been classified into different orthologous groups based on the distribution of the main and additional domains. Plant bZIP proteins exhibit a relaxed binding specificity for DNA sequence motifs containing an ACGT core, and preferentially bind to the G-box (CACGTG), C-box (GACGTC) and A-box (TACGTA). During DNA binding, the N-terminal part of the basic region locates into the major groove of dsDNA and the C-terminal part of the Leu zipper is involved in the dimerization to create a superimposed coiled-coil structure (Landschulz et al. 1988).

Plant hormone abscisic acid (ABA) plays an important role under abiotic stresses. When plants encounter the adverse environment conditions, ABA levels increase and the released ABA signalling pathway induces expression of numerous genes that improve adaptive ability to stress conditions. We are looking for the bZIP transcription factors that are involved in ABA signalling of plant response to drought treatment. In barley, two bZIP transcription factors – *HvABI5* and *bZIP1* (Casaretto and Ho 2003) – were identified in aleurone cells that are responsible for ABA-dependent gene regulation during seed development. These transcription factors belong to separate bZIP families. Similar to *HvABI5*, members of the *bZIP1* family share great similarity in the basic region and contain only four Leu residues forming the Leu zipper. In addition, there are four other conserved regions of the *bZIP1* protein, including putative phosphorylation sites. The gene encoding *bZIP1* transcription factor shows homology to *OsZIP1a*, *CPRF4* and *EmBPI*, and is only one representative of a very unique group characterized by a Pro-rich region near N-terminus. Both *HvABI5* and *HvZIP1* can recognize ABRC1 and ABRC3 of ABRC site *in vitro* and have a preference for the ACGT boxes. ABF1 is the

other basic leucine zipper transcription factor involved in ABA-dependent signal transduction pathway under drought and high salinity (Johnson et al. 2008).

In ABA-dependent regulatory systems governing drought-inducible gene expression in response to drought, transcription factors MYB, MYC and NAC are also involved. These classes of transcription factors are synthesized in the tissues following accumulation of endogenous ABA, and they need ABA-mediated phosphorylation for activation. A member from these groups, an NAC transcription factor, was isolated by a yeast one-hybrid system using *cis*-elements present in *Hordeum spontaneum* rehydration response gene (*Hsdr4*) promoter region.

### **Identification and isolation of drought-specific genes encoding transcription factors**

For the isolation of a cDNA encoding DREB1 and ZIP1 transcription factors, we have searched the GenBank database (<http://www.ncbi.nlm.nih.gov/>) and barley database (<http://www.harvest-web.org/>) for homology sequences using barley DREB1 mRNA, accession DQ01294 (Xu et al. 2009) and ZIP mRNA, acc. AY150677 (Matsumoto et al. 2011), as queries. Amino acid sequences of identified homologous sequences were aligned using the ClustalW program, version 1.81 (Thompson et al. 1994). Fragments with the highest specificity for each of the analysed gene were identified and used as probes for semi-quantitative RT-PCR to analyse expression profiles of *DREB1* and *bZIP1* genes in the nine barley genotypes subjected to a progressive increase in water deficit (de Mezer et al. 2014). To ensure that the expression profiles refers only to the genes of interest and not to the paralog genes, the location of the *DREB1* and *bZIP1* sequences in the barley genome was analysed using the Plants Ensembl sequences databases web site (Plants.ensembl.org/). The barley genome sequence in Plants Ensembl is version 030312v2, a gene-space assembly of *Hordeum vulgare* cv. Morex generated by the International Barley Genome Sequencing Consortium (IBGSC). The DREB1 sequence (acc. DQ01294) was shown to have the highest homology (99% identity) to the single gene localized to chromosome 3, location 39,855,748–39,872,379 in the barley genome. There is also a copy of the *bZIP1* gene (accession: AK373997) localized to chromosome 5, location: 28,689,902–28,699,249. The analysis of *ABI5* and *ABF1* genes encoding bZIP transcription factors was performed similarly.

### **Semi-quantitative RT-PCR analysis of expression profiles of *DREB1*, *bZIP1*, *ABI5* and *ABF1* genes**

Primers matching the specific regions of *DREB1*, *bZIP1*, *ABI5* and *ABF1* cDNAs from barley were designed using Primer-BLAST web site (<http://www.ncbi.nlm.nih.gov/tools/primer-blast/index.cgi>), subjected to  $T_m = 60 \pm 3^\circ\text{C}$  and used for semi-

quantitative RT-PCR analysis of expression of the *HvDREB1*, *HvZIP1*, *HvABI5* and *HvABF1* genes. Sequences of the primers matching the *HvDREB1* cDNA generated a fragment of 584 bp DNA, and sequences of the primers matching the *HvZIP1*, *HvABI5* and *HvABF1* cDNAs generated fragments of 298 bp, 225 bp and 131 bp, respectively. A gene encoding  $\alpha$ -tubulin (*HvTubA*) from barley was used as an endogenous control gene, the expression of which remained nearly constant when the SWC declined from 65% to 10% (de Mezer et al. 2014).

The RT-PCR analysis revealed that the increase in the expression level of the *HvZIP1* gene in response to water deficit paralleled the higher adaptive ability of the genotypes upon stress, indicating the association of the *HvZIP1* expression with the adaptation of the genotypes to water deficit. Lower correlation between the increase in the transcript level and the ability of the genotypes to adapt to drought was observed for *HvDREB1* gene. The changes in the expression levels of the *HvABI5* and *HvABF1* genes were not significant and did not differentiate the barley genotypes.

### **Isolation of full-length *HvDREB1* and *HvZIP1* cDNA**

Full-length cDNA sequence of *HvDREB1* and *HvZIP1* genes were prepared to verify the expression profiles of the corresponding genes under water deficit obtained using the fragments of these genes (de Mezer et al. 2014), and to prepare the antibodies against the proteins encoded by *HvDREB1* and *HvZIP1* genes.

Full-length cDNA sequences of *HvDREB1* and *HvZIP1* were generated from the cellular RNA prepared from seedlings of cv. Saida using the RACE method. The RACE method generates cDNA by using PCR to amplify copies of the region between a single point in the transcript and the 5' and 3' ends. From this region (i.e. from the internal fragments of the *HvDREB1* and *HvZIP1* cDNAs), primers oriented towards the 3' and 5' ends were chosen that produced overlapping cDNA fragments when fully extended. Extension of the cDNA from the ends of the mRNA for *HvDREB1* and *HvZIP1* to the specific primer sequences was accomplished by using primers that are anneal to the natural 3'-end (poly(A) tail and synthetic 5'end (adaptor). Finally, the overlapping 3'- and 5'-end RACE products of *HvDREB1* and *HvZIP1* were combined to produce an intact full-length cDNA. The RACE method was used as described in the manufacturer's instruction manual (Invitrogen, Carlsbad, CA), using the primer sets matching the internal region of the specific fragments of *HvDREB1* and *HvZIP1* genes mentioned earlier.

### **Analysis of *HvDREB1* and *HvZIP1* protein abundance upon water deficit**

A 837-bp fragment of the coding sequence of *HvDREB1* cDNA encoding a 278-residue protein and a 1143-bp fragment of the coding sequence of *HvZIP1* cDNA encoding a 380-residue protein were cloned into the pQE30 expression

vector (Qiagen) to produce recombinant proteins fused to a 6xHis-tag in the M15[pRep4] *Escherichia coli* strain. The recombinant proteins were purified on Ni-NTA resin (Qiagen) and used to raise antibodies in rabbits. The antibodies have been produced in Eurogentec (Belgium), and used for Western blot analysis as described by Kielbowicz-Matuk et al. (2008). The antibody concentration was determined using an indirect ELISA technique. Bound antibodies were detected by subsequent incubation using biotinylated goat antirabbit secondary antibodies conjugated with Qdot 625-streptavidin (Invitrogen). Visualization of the proteins was performed by exposing membranes to standard UV light. Band intensity (relative) was analysed using densitometry, ImageMaster (Amersham Pharmacia) and Gel-Pro Analyzer 3.1 (Media Cybernetics, MD, USA) software. Western blot experiments were carried out using plant protein extracts originating from two independent stress experiments and were replicated at least once for each experiment and each barley cultivars.

If Western blot analysis confirms association of *HvDREB1* and *HvZIP1* genes with adaptation of barley to water deficit, these genes could serve as expression markers of adaptive ability to water deficit and their expression characteristics become subjects of the patents.

## **Isolation of MYC/NAC transcription factors using yeast one-hybrid system**

### *Isolation of nuclear DNA and a gene promoter region*

Genomic DNA from cv. Saida was isolated using a DNeasy Plant Mini Kit (Qiagen). The upstream region of *Hsdr4* gene (another gene, the expression of which is associated with adaptation to water deficit; de Mezer et al. 2014) was amplified according to the manual protocol of Genome Walker Universal Kit (Clontech, Palo Alto, CA, USA). The first step of the isolation of the promoter was to prepare pools of uncloned, adaptor-ligated genomic DNA fragments (GenomeWalker “libraries”). Genomic DNA was digested with eight restriction enzymes forming blunt ends. Each batch of the genomic DNA digests was ligated to the GenomeWalker Adaptor and subjected to two nested PCR amplifications. The primary PCR uses the outer adaptor primer (AP1) and an inner gene-specific primer (GSP1). The primary PCR product was used as a template for a secondary or “nested” PCR with the nested adaptor primer (AP2) and a nested gene-specific primer (GSP2). The final PCR product was recovered from the gel, ligated into the linear vector and sequenced. The promoter regions from four barley genotypes (cv. Saida, Georgie, Express and a breeding line M. Dingo) and from *H. spontaneum* were isolated.

### *Yeast one-hybrid system*

*In silico* analysis of the promoter region of the *Hsdr4* gene using the PlantCare and the Place programs allowed identification of several putative *cis*-regulatory elements, including many *cis*-elements for the MYB and MYC transcription factor families and an element for the NAC transcription factor. Interestingly, in the promoter regions of cv. Express and Georgie that exhibit the lowest adaptive ability to water deficit, there were no *cis*-element ‘CATGTG’ for NAC-type transcription factor. It suggested that the low expression of the *Hsdr4* gene in Express and Georgie in response to water deficit is result of a lack of induction by the NAC transcription regulator. We tried to isolate the gene encoding the NAC transcription factor using yeast one-hybrid system. In the Matchmaker Gold Yeast One-Hybrid System (Clontech), a selected threefold repeated *cis*-regulatory ‘CATGTG’ sequence (bait) was introduced into the pAbAi vector, and the pAbAi vector was then transfected into the genome of Y1H Gold yeast strain *via* homologous recombination. This strain serves as the host for library screening. The template for construction of cDNA library was cellular RNA isolated from cv. Saida seedlings subjected to drought treatments. Screening a cDNA library in the direction of the protein–DNA interaction was a result of co-transformation and *in vivo* homologous recombination between the linear form of the pGADT7-Rec yeast vector and a reporter strain containing a selected *cis*-regulatory ‘CATGTG’ sequence. Selection of yeast colonies after transformation was performed on a selection medium supplemented with Aureobasidin A (Aba). *Aba* resistance gene activation occurs only when the protein (transcription factor) from the library binds to a *cis*-regulatory sequence. After three series of reducing unspecific clones, no gene encoding NAC transcription factor was screened.

### **Isolation of MYC/NAC transcription factors using electrophoretic mobility shift assay (EMSA)**

Electrophoretic mobility shift assay (EMSA) is another way for identification of transcription factors that bind to defined *cis*-elements in the promoter region responsible for response to a stress factor. This is an extraordinarily sensitive system for performing electrophoretic mobility shift assays (EMSA) to identify and characterize protein–DNA binding interactions. This technique is based on the fact that DNA–protein complexes migrate slower than non-bound DNA in a native polyacrylamide or agarose gel, resulting in a ‘shift’ in migration of the labelled DNA band. Biotin end-labelled DNA containing the binding site of interest is incubated with a purified recombinant protein or nuclear protein extract. After incubation, the reaction mix is subjected to gel electrophoresis on a non-denaturated polyacrylamide gel and then transferred to a nylon membrane using

a semi-dry blotting apparatus. Transferred DNA is then crosslinked for 15 minutes on a trans-illuminator with 312 bulbs. The biotin end-labelled DNA is detected using the Streptavidin-Horseradish Peroxidase Conjugate and a Chemiluminescent Substrate. Autoradiography was performed by exposing nylon membrane to an X-ray film.

## References

- Bartels D., Sunkar R. 2005. Drought and salt tolerance in plants. *Crit. Rev. Plant Sci.* 24: 23-58.
- Boudsocq M., Barbier-Brygoo H., Lauriere C. 2004. Identification of nine sucrose nonfermenting 1-related protein kinases 2 activated by hyperosmotic and saline stresses in *Arabidopsis thaliana*. *J. Biol. Chem.* 279: 41758-41766.
- Casaretto J., Ho T.H. 2003. The transcription factors HvABI5 and HvVP1 are required for the abscisic acid induction of gene expression in barley aleurone cells. *Plant Cell* 15: 271-284.
- de Mezer M., Turska-Taraska A., Kaczmarek Z., Glowacka K., Swarczewicz B., Rorat T. 2014. Differential physiological and molecular response of barley genotypes to water deficit. *Plant Physiol. Biochem.* 80: 234-248.
- Hu L., Wang Z., Huang B. 2010. Diffusion limitations and metabolic factors associated with inhibition and recovery of photosynthesis from drought stress in a C perennial grass species. *Physiol. Plant.* 139: 93-106.
- Jakoby M., Weisshaar B., Droge-Laser W. et al. 2002. bZIP transcription factors in *Arabidopsis*. *Trends Plant Sci.* 7: 106-111.
- Johnson R.R., Shin M., Shen J.Q. 2008. The wheat PKABA1-interacting factor TaABF1 mediates both abscisic acid-suppressed and abscisic acid-induced gene expression in bombarded aleurone cells. *Plant Mol. Biol.* 68: 93-103.
- Kielbowicz-Matuk A., Rey P., Rorat T. 2008. The organ-dependent abundance of a *Solanum* lipid transfer protein is up-regulated upon osmotic constraints and associated with cold acclimation ability. *J. Exp. Bot.* 59: 2191-2203.
- Landschulz W.H., Johnson P.F, McKnight S.L. 1988. The leucine zipper: a hypothetical structure common to a new class of DNA binding proteins. *Science* 240: 1759-1764.
- Liao Y., Zou H-F., Wei W., Hao Y-J., Tian A-G., Huang J., Liu Y-F., Zhang J-S., Chen S-Y. 2008. Soybean GmbZIP44, GmbZIP62 and GmbZIP78 genes function as negative regulator of ABA signaling and confer salt and freezing tolerance in transgenic *Arabidopsis*. *Planta* 228: 225-240.
- Matsumoto T., Tanaka T., Saka H., Amano N., Kanamori H., Kurita K., Kikuta A., Kamiya K., Yamamoto M., Ikawa H., Fujii N., Hori K., Itoh T., Sato K. 2011. Comprehensive sequence analysis of 24,783 barley full-length cDNAs derived from 12 clone libraries. *Plant Physiol.* 156: 20-28.

- Morran S., Ein O., Pyvovarenko T., Parent B., Singh R., Ismagul A., Eliby S., Shirley N., Langridge P., Lopato S. 2011. Improvement of stress tolerance of wheat and barley by modulation of expression of DREB/CBF factors. *Plant Biotechnol. J.* 9: 230-249.
- Nakashima K., Yamaguchi-Shinozaki K. 2006. Regulons involved in osmotic stress-responsive and cold stress-responsive gene expression in plants. *Physiol. Plant.* 126: 62-71.
- Nijhawan A., Jain M., Tyagi A.K., Khurana J.P. 2008. Genomic survey and gene expression analysis of the basic leucine zipper transcription factor family in rice. *Plant Physiol.* 146: 333-350.
- Sakuma Y., Liu Q., Dubouzet J.G., Abe H., Shinozaki K., Yamaguchi-Shinozaki K. 2002. DNA-binding specificity of the ERF/AP2 domain of Arabidopsis DREBs, transcription factors involved in dehydration- and cold-inducible gene expression. *Biochem. Biophys. Res. Commun.* 290: 998-1009.
- Shinozaki K., Yamaguchi-Shinozaki K. 2007. Gene networks involved in drought stress response and tolerance. *J. Exp. Bot.* 58: 221-227.
- Thompson J.D., Higgins D.G., Gibson T.J. 1994. CLUSTAL W: improving the sensitivity of progressive multiple sequence alignment through sequence weighting, position-specific gap penalties and weight matrix choice. *NAR* 22: 4673-4680.
- Umezawa T., Fujita M., Fujita Y., Yamaguchi-Shinozaki K., Shinozaki K. 2006. Engineering drought tolerance in plants: discovering and tailoring genes to unlock the future. *Curr. Opin. Biotechnol.* 17: 113-122.
- Wei K., Chen J., Wang Y., Chen Y., Chen S., Lin Y., Pan S., Zhong X., Xie D. 2012. Genome-wide analysis of bZIP-encoding genes in maize. *DNA Res.* 19: 463-476.
- Yamaguchi-Shinozaki K., Shinozaki K. 2006. Transcriptional regulatory networks in cellular responses and tolerance to dehydration and cold stresses. *Annu. Rev. Plant Biol.* 57: 781-803.
- Xu Z-S., Ni Z-Y., Li Z-Y., Li L-C., Chen M., Gao D-Y., Yu X-D., Liu P., Ma Y-Z. 2009. Isolation and functional characterization of HvDREB1-a gene encoding a dehydration-responsive element binding protein in *Hordeum vulgare*. *J. Plant Res.* 122: 121-130.



## **Tools for defining barley microtranscriptome expression at the level of primary microRNAs and mature microRNAs**

**Aleksandra Świda-Barteczka<sup>1\*</sup>, Katarzyna Kruszka<sup>1\*</sup>, Andrzej Pacak<sup>1\*</sup>,  
Wojciech Karłowski<sup>2</sup>, Artur Jarmolowski<sup>1</sup> and Zofia Szweykowska-  
Kulińska<sup>1,2</sup>**

<sup>1</sup> *Department of Gene Expression, Institute of Molecular Biology and Biotechnology, Faculty of Biology, Adam Mickiewicz University in Poznan, Poznań, Poland*

<sup>2</sup> *Bioinformatics Laboratory, Institute of Molecular Biology and Biotechnology, Faculty of Biology, Adam Mickiewicz University in Poznan, Poznań, Poland*

### **Introduction**

MicroRNAs (miRNAs) are key regulators of gene expression in *Eukaryota*. Plant miRNAs are short, usually of 21 nucleotides long, single-stranded RNA molecules with sequence almost perfectly complementary to mRNAs of controlled genes (Llave et al. 2002; Reinhart et al. 2002; Jones-Rhoades et al. 2004; Nozawa et al. 2012). They act post-transcriptionally, predominantly by targeting mRNAs for cleavage, but also by translation suppression (Tang et al. 2003; Brodersen et al. 2008).

MiRNA genes (*MIR*) are hundreds or thousands nucleotides long, and many of them contain one or more introns (Szarzynska et al. 2009; Szarzynska et al. 2011; Kruszka et al. 2013). *MIR* are located predominantly in inter-genic loci but there is an increasing number of data describing their intragenic localization in introns of protein-coding genes (Brown et al. 2008). The *MIR* encode transcripts called primary miRNAs (pri-miRNAs). Pri-miRNAs are transcribed by RNA polymerase-II hence they are 5' capped and 3' polyadenylated (Xie et al. 2005). The pri-miRNAs contain a sequence forming hairpin structure (pre-miRNA) where miRNA is located. The miRNA together with a near-perfectly complementary partner, microRNA\*, occupy the stem of the hairpin. The effective processing

---

\*These authors equally contributed to this work; author for correspondence: Zofia Szweykowska-Kulinska, zofszwey@amu.edu.pl

of the pre-miRNA stem-loop structure and accurate dicing out the miRNA/miRNA\* duplex is triggered by a microprocessing complex formed mainly by DICER-LIKE 1 (DCL1), SERRATE and HYPONASTIC LEAVES 1 (Yang et al. 2006; Kurihara et al. 2006, Dong et al. 2008).

The miRNAs research confirmed their existence in all plant species studied. They not only regulate plant response to various environmental stresses and pathogen invasions, but also act in development, signal transduction and protein degradation (Kruszka et al. 2012). Moreover, miRNAs regulate their own biogenesis by targeting DCL1 mRNA degradation (Rajagopalan et al. 2006).

*Hordeum vulgare* (L.) is a monocotyledonous crop plant of great economic importance. To understand the barley gene expression regulation, it is crucial to establish information regarding its microtranscriptome. We have combined various molecular biology approaches to gain data concerning pre-miRNA structures, *MIR* characteristics, pri-miRNA expression profiles and mature miRNA levels. Here, we present methods which were used for defining microtranscriptome expression at the level of pri-miRNAs and mature miRNAs. To observe dynamic changes in microtranscriptome in various environments, water deficiency stressed barley plants and controls were used in this study. In nature, drought stress often correlates with heat, so we also applied heat stress with optimal watering to better understand the mechanisms of gene expression regulation process leading to drought stress adaptation (Bita and Gerats 2013).

In this study, we used Illumina deep sequencing technique to analyse the miRNAs expression level in barley plants treated with severe drought (20% soil water content, SWC) and 6 h after re-watering (70% 6 h SWC). We also determined the pri-miRNAs expression by a quantitative real-time PCR (qPCR) analysis in barley treated with minor drought (30% SWC), severe drought (20% SWC) and 6 h after re-watering (70% 6 h SWC). We chose four examples from the miRNA sequence data sets – miRNA156g, miRNA166n, miRNA171e and miRNA397b-3p – which were differently expressed in drought stress conditions. These miRNAs are presented for better describing our strategy of microtranscriptome analysis. The deep sequencing and qPCR methods were optimized by us for barley and are described in details in this study. We also provide information on growing plant material and revealing stress conditions with the use of stress markers. Moreover, two RNA isolation methods improved by us for deep sequencing or quantitative real-time PCR are also presented.

## Results and discussion

To determine the level of expression of microtranscriptome in barley, the miRNAs and their pri-miRNAs expression profiles were analysed. The expression profiles of pri-miRNAs and mature miRNAs were described in two-row spring

barley, cultivar Rolap. Plants, treated with water deficiency stress or heat stress, were grown in a Conviron growth chamber with 16-h day/8-h night photoperiod and 800  $\mu\text{m}$  light conditions. Seeds, obtained from the Institute of Plant Genetics of the Polish Academy of Sciences (Poznań, Poland), were soaked in water for 24 h before sowing. Plants were grown in a medium composed of 7 parts of field soil and 2 parts of sand and supplemented with standard fertilizer (see Pecio et al. 2014 in this volume). Barley plants were collected in three biological replicates, aerial parts of four plants were pooled together and treated as one biological replicate. For drought stress treatment, six plants were grown in 5 litre pots, optimal watering conditions (70% SWC) were maintained until the plants had developed flag leaf, code 39 of the Zadoks decimal code, when plants ceased to be watered (Zadoks et al. 1974). Plants were collected when SWC dropped to 30% (24 h after the beginning of stress treatment), to 20% (48 h after the beginning of stress treatment), to 10% (60 h after the beginning of stress treatment) and 6 h and 24 h after rehydration (70% SWC) (Fig. 1).

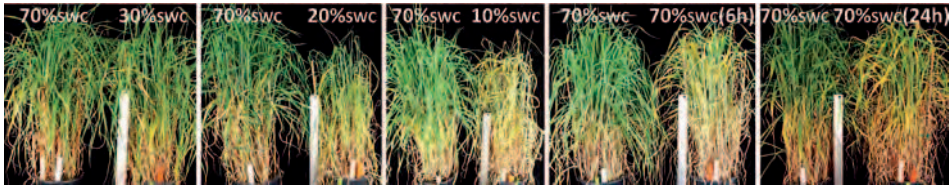


Fig. 1. Control and drought stress–treated barley plants collected for microtranscriptome expression analysis

As drought is very often accompanied by heat stress, we were also interested in finding the miRNAs-induced response common for and distinguishing between these two stresses. For heat stress treatment two plants were grown in 0.3 litre pots. Heat stress of 35.5°C was applied when the third leaf developed, code 13 of the Zadoks system (2-week-old plants). Plants were collected after 1, 3, 4, 5, 6, 7, 8, 12, 24 and 48 h of stress duration (Fig. 2). SWC of 70% was carefully maintained during the experiment. For one biological replicate, not only shoots but also roots were collected.

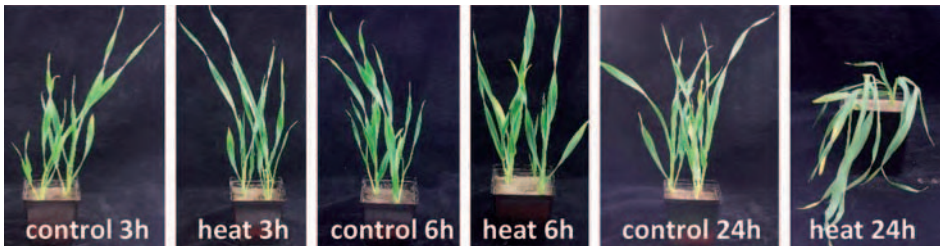


Fig. 2. Control and heat stress–treated barley plants collected for microtranscriptome expression analysis

The plant response to drought and heat stress was defined by testing the level of the molecular stress markers expression with semi-quantitative RT-PCR method. The RNA extraction is described in “Determining the expression level of pri-miRNAs with quantitative real-time PCR” section. The total RNA isolation was followed by the detection of stress genetic markers with semi-quantitative RT-PCR. One microgram (drought) or 3 µg (heat) of DNA-free total RNA was reverse-transcribed with Invitrogen SuperScript III Reverse Transcriptase (Life Technologies) and oligo(dT)<sub>15</sub> (Novazym, Poland) primer. cDNAs were diluted 10 times and 2 µl were used as a RT-PCR template. The lack of gDNA in total RNA samples was controlled by PCR of 977 bp of promoter fragment of barley phosphate transporter 1 (HvPht1-1, GenBank: AF543197.1) (Schuman et al. 2004). RT-PCR of ubiquitin (GenBank: X04133.1) fragment was used as a positive control reaction and to estimate the effectiveness of reverse-transcription. The genetic stress markers’ amplifications and control RT-PCRs and PCRs were performed with Taq DNA polymerase (Thermo Scientific, Lithuania) and two gene-specific oligonucleotides (500 nM each). The following thermal profile was used – 1 cycle: denaturation at 94°C/1 min, annealing at 65°C/30 s, elongation at 72°C/2 min; 29 cycles: denaturation at 94°C/30 s, annealing at 63°C/30 s ( $\Delta$  - 0.5°C/cycle), elongation 72°C/2 min; 10 cycles: denaturation at 94°C/30 s, annealing at 53°C/30 s, elongation 72°C/2 min. The cycles’ number was adjusted according to particular gene expression level. Genomic DNA template was used as a positive PCR control and water was used as chemicals purity control. Reaction products were separated on 1.2% agarose gel and stained with ethidium bromide. The products length was estimated with GeneRuler 100 bp Plus or 1 kb Plus DNA Ladders (Thermo Scientific, Lithuania) separated on the same gel. Dehydrins (DHN) accumulation is induced during embryogenesis or after several abiotic stress treatment like: drought, salinity or low temperatures (Kosova et al. 2014). Heat shock proteins (HSP) act as chaperons preserving proteins from misfolding during high temperature exposure (Baniwal et al. 2004). *DHN1* and *DHN9* in plants subjected to drought, as well as *HSP17* and *DHN9* expression in heat stress–treated plants were tested as a control of suitable stress treatment (Fig. 3). Barley shoots showed expression of *DHN1* only under severe drought conditions (20% and 10% SWC). The *DHN1* expression increases with the progress of water limitation and decreases after re-watering of the barley plants. The *DHN1* expression is not detectable 24 h after rehydration. While the *DHN1* marker expresses only under severe drought, the *DHN9* is detectable under control and in all tested drought conditions. When compared to control plants, the *DHN9* expression in barley shoots is elevated in minor (30% SWC) to severe (20% and 10% SWC) drought stress conditions. The re-watered plants show *DHN9* expression levels similar to controls. During the heat stress in barley shoots, we observed an increased expression of heat-inducible gene *HSP17* as

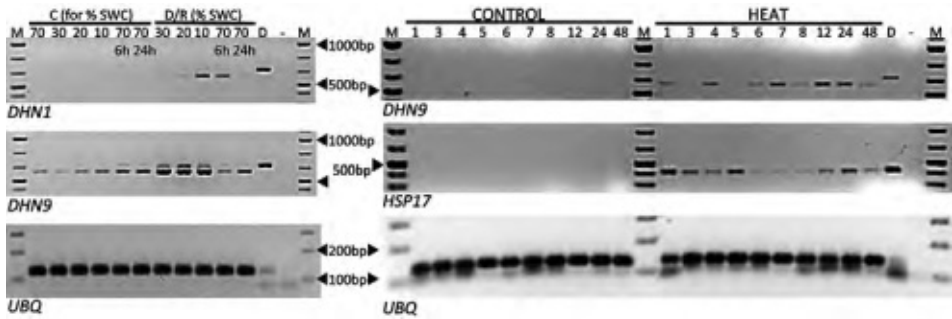


Fig. 3. The expression of drought stress markers: *DHN1*, *DHN9*, and heat shock marker: *HSP17* in aerial parts of drought stress- (left panel) and heat stress-treated barley (right panel). Abbreviations: C – control, D – drought, R – rehydration

well as drought stress responsive gene *DHN9*. Both control and heat stressed plants are grown with optimal watering (70% SWC). Such observation suggests that heat can either directly induce *DHN9* gene expression or can cause osmotic stress which upregulates *DHN9* expression. An influence of 12 h heat stress on water and osmotic potentials as well as relative water content was shown in sugarcane leaves (Wahid and Close 2007). Moreover, our unpublished data show that *HSP17* expression is induced by heat, whereas drought treatment of barley does not induce the *HSP17* gene expression.

### Determining the expression level of pri-miRNAs with quantitative real-time PCR

The first step was to isolate total RNA. Total RNA extraction method was optimized for barley which allowed to achieve high quality and integrity of RNA, suitable for RT-PCR and quantitative real-time PCR. Barley tissue was powdered in liquid nitrogen with a mortar and pestle. 100 mg of powder was transferred to 2 ml tubes. RNA was extracted with two portions of TRIZOL Mix (1.5 ml of TRIZOL, 75  $\mu$ l of 10% sodium sarcosyl, 15  $\mu$ l of EDTA, pH 8.0) mixed into the sample with vigorous vortexing. 100  $\mu$ l of Ambion Plant RNA Isolation Aid (Life Technologies, Carlsbad, CA, USA) was added and mixed with sample by gentle vortexing. After 5 min incubation with gentle mixing at room temperature (RT), the sample was centrifuged at  $14,000 \times g$  for 5 min, RT. The supernatant was transferred to a fresh tube and 300  $\mu$ l of chloroform was added and mixed by shaking the tube for 20 s. Next, the sample was centrifuged at  $12,000 \times g$  for 15 min at  $4^{\circ}\text{C}$  and the resulting aqueous phase was transferred to a fresh 2 ml tube. RNA was precipitated with 1 volume of isopropanol and 1 volume of 0.8 M sodium citrate in a 1.2 M sodium chloride solution for 60 min at  $-20^{\circ}\text{C}$ . The

pellet was collected by centrifugation at  $18,600 \times g$  for 30 min at  $4^{\circ}\text{C}$ . After the supernatant was removed, the pellet was washed with 75% ice-cold ethanol and centrifuged at  $18,600 \times g$  for 10 min at  $4^{\circ}\text{C}$ . RNA was air-dried and dissolved in DEPC-treated milliQ water (Fig. 4). The excess of salt was removed from RNA samples with an additional desalting procedure. 2 M solution of ammonium acetate was added to the final concentration of 0.5 M. RNA was recovered with

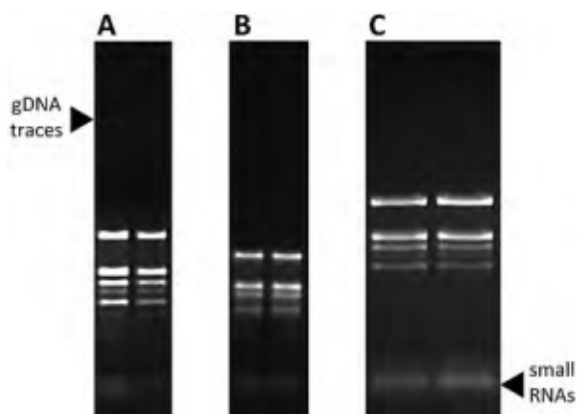


Fig. 4. RNA samples separated on 1% agarose gel. A – total RNA isolated from aerial parts of barley before DNase treatment, genomic DNA traces are visible; B – total RNA isolated from aerial parts of barley after DNase treatment; C – total RNA increased in small RNA fraction isolated from aerial parts of barley

1 volume of isopropanol in the presence of glycogen at  $-20^{\circ}\text{C}$  for 15 min. The pellet was spun down at  $18,600 \times g$  for 15 min at  $4^{\circ}\text{C}$  and washed two times with 70% ethanol, air-dried and dissolved as previously described. RNA quality and quantity were measured with a NanoDrop ND-1000 spectrophotometer and its integrity estimated on 1% agarose gel. RNA samples were stored in  $-80^{\circ}\text{C}$  for further use. DNA contaminants from the total RNA samples were removed with Ambion TURBO DNase (Life Technologies) according to the manufacturer protocol.

The relative changes in expression profile of barley pri-miRNAs were described in plants treated with drought stress, after rehydration and in control ones. We have designed a set of unique oligonucleotide primer pairs for 150 barley pre-miRNAs identified by us. All primers have the same annealing temperature, which allowed us to set them together on a platform for analysis of the pri-miRNAs expression dynamics in barley grown under conditions studied. The analysis was performed with qPCR method optimized by us for barley. To obtain first strand of cDNA, 3  $\mu\text{g}$  of DNA-free total RNA was reverse-transcribed with Invitrogen SuperScript III Reverse Transcriptase (Life Technologies) and oligo(dT)<sub>15</sub> (Novazym, Poland) according to the Invitrogen protocol. cDNA samples were diluted four times and

1  $\mu$ l was used as a template. Applied Biosystems Power SYBR® Green PCR Master Mix (Life Technologies) and two pri-miRNA-specific oligonucleotides (final concentration 200 nM each) were used for executing qPCR on 7900HT Fast Real-Time PCR System (Applied Biosystems) in 384 well plates in 10  $\mu$ l final reaction volumes. The following thermal profile was used: 10 min at 90°C, 40 cycles: denaturation at 95°C/15 s, annealing/elongation at 60°C/1 min. The reaction was ended by additional dissociation stage: 95°C/15 s, 60°C/15 s and 95°C/15 s. Each qPCR was performed independently in three biological replicates and two technical ones. LinRegPCR software was used to calculate  $R^2$  values ( $\geq 0.997$ ) of the data analysed (Ramakers et al. 2003). The levels of pri-miRNAs expression were calculated with relative quantification method ( $2^{-\Delta Ct}$ ) and fold change values were presented in a form of  $\log_{10} 2^{-\Delta Ct}$ . The expression level of barley ADP-ribosylation factor 1-like [GenBank: AJ508228.2] 61 nt long gene fragment was detected as an internal reference (Rapacz et al. 2012). The expression level of the reference gene is higher than the pri-miRNAs. To demonstrate the expression profiles of pri-miRNAs in a positive data range, we have shifted the zero value of the graph's y-axis to the basal expression level of the whole experiment. The expression levels of the pri-miRNAs in drought

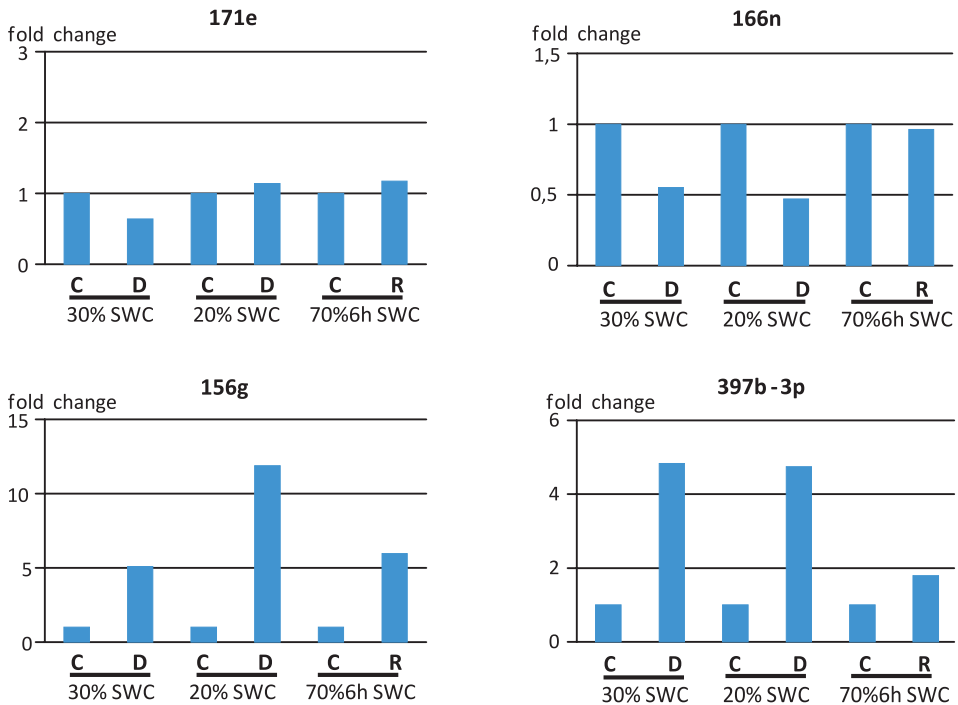


Fig. 5. Relative expression of four selected pri-miRNAs. Abbreviations: C – control, D – drought, R – rehydration

stress-treated plants were compared to their expression in control plants. The relative expression of the pri-miRNAs defined by us can be grouped into three categories: (i) expression unchanged, (ii) expression downregulated and (iii) expression upregulated (Fig. 5).

The expression of pri-miRNA171e illustrates slight decrease during minor drought and constant levels under severe drought and rehydration conditions, whereas pri-miRNA166n expression is downregulated under minor and severe drought conditions. Re-watering of the barley plants restores the pri-miRNA166n level within 6 h. Pri-miRNA156g and pri-miRNA397b-3p are upregulated under drought stress treatment. Moreover, the pri-miRNA156g expression is increasing while the water becomes less available for plants, while pri-miRNA397b-3p level remains invariably raised up. For both, pri-miRNA156g and pri-miRNA397b-3p expression is dropping after re-watering plants.

### Deep sequencing of small RNAs

The first step of microtranscriptome analysis with Illumina deep sequencing is the construction of libraries. The preparation of small RNA libraries requires some critical steps which are necessary for successful deep sequencing analysis. TruSeq small RNA sample preparation kit by Illumina was used for the construction of small RNA libraries in barley. The additional tools which we used together with TruSeq Small RNA kit are described here. RNA enriched in small RNAs was obtained according to the procedure described by Kruszka et al. (2013), modified from Pant et al. (2009).

Total RNA isolation method was modified to improve the quantity of small RNAs fraction and to remove genomic DNA contaminants. The RNA samples obtained with this protocol were used to prepare libraries for small RNAs deep sequencing. The plant tissue was powdered in liquid nitrogen and 100 mg of the tissue powder was transferred to a 2 ml tube. 750  $\mu$ l of TRIZOL Mix was added two times and the sample was mixed with pipette after each addition of TRIZOL Mix. 100  $\mu$ l of Ambion Plant RNA Isolation Aid (Life Technologies, Carlsbad, CA, USA) was added and mixed with sample by gentle vortexing. After 5-min incubation with gentle mixing, the sample was centrifuged at  $14,000 \times g$  for 5 min, RT. The supernatant was transferred to a fresh tube and 300  $\mu$ l of chloroform was mixed with vigorous shaking of the tube for 15 s. After 3 min incubation at room temperature, the sample was centrifuged at  $12,000 \times g$  for 10 min at  $4^{\circ}\text{C}$ . The aqueous phase was transferred to a new tube and 100  $\mu$ l of phenol (Roti Aqua Phenol, Roth, Karlsruhe, Germany) saturated with 0.1 M sodium acetate was mixed with the sample by vortexing. Next 300  $\mu$ l of chloroform was added and mixed by vortexing for 20 s. The sample was centrifuged at  $12,000 \times g$  for 3 min at  $4^{\circ}\text{C}$ . The phenol/chloroform extraction step was repeated

two more times and followed by two extractions with 400  $\mu\text{l}$  of chloroform solely. RNA was precipitated from 750  $\mu\text{l}$  of water phase in the presence of 0.5  $\mu\text{l}$  of glycogen (Thermo Scientific, 20 mg/ml) with 1.25 volume of ethanol and 0.5 volume of 0.8 M sodium citrate in a 1.2 M sodium chloride solution. After 30 min of incubation at room temperature, the pellet was collected by centrifugation at  $12,000 \times g$  for 30 min at  $4^\circ\text{C}$  and remaining salt solution was removed by additional centrifugation at  $12,000 \times g$  for 3 min at  $4^\circ\text{C}$ . The RNA pellet was washed three times with 80% ethanol and centrifuged at  $12,000 \times g$  for 3 min at  $4^\circ\text{C}$ . The air-dried RNA pellet was resuspended in DEPC-treated milliQ water. The RNA solution was desalted as described in total RNA extraction procedure, except for washing step, where 80% ethanol was used (Fig. 4). The RNA samples were stored at  $-80^\circ\text{C}$  for further use. Since Illumina requires high-quality RNAs used for the construction of small RNA libraries (RNA Integrity Number = RIN greater than 8), we analysed our RNAs using Agilent 2100 Bioanalyzer and RNA Nano kit (Agilent Technologies). It is important to dilute RNA to a range of 5 to 500 ng/ $\mu\text{l}$  of total RNA before measurements. An example of electropherogram of barley RNA sample having a RIN value of 9.40 (assay class – Plant RNA Nano) is showed in Fig. 6.

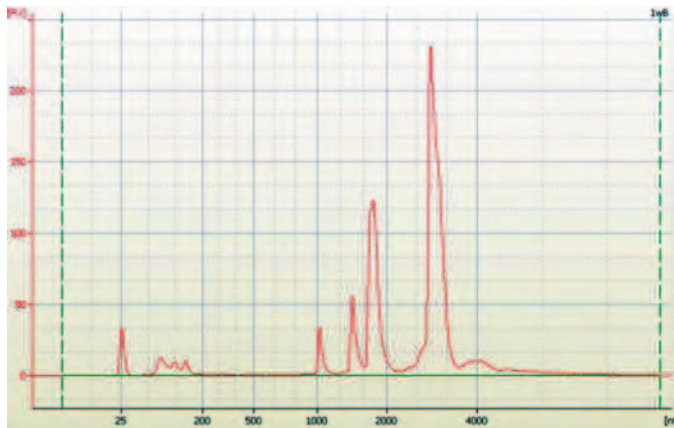


Fig. 6. Electropherogram of the barley RNA

Ten micrograms of high-quality total RNA enriched in small RNAs fraction was separated on 15% 8 M urea polyacrylamide gel. First, the samples were mixed with Gel Loading Buffer II (Ambion), or equivalent, and denatured for 2 min in  $90^\circ\text{C}$  and directly loaded on the gel, without ice-cooling the sample. After electrophoresis, gel was stained with SYBR Gold nucleic acid gel stain (Molecular Probe) in  $0.5 \times \text{TBE}$  buffer by 20 min with gentle shaking and light protection. Then RNA bands of 15-30 nucleotides long were excised from the gel, purified and dissolved in 5  $\mu\text{l}$  DEPC-treated water (Fig. 7.A, B). The whole

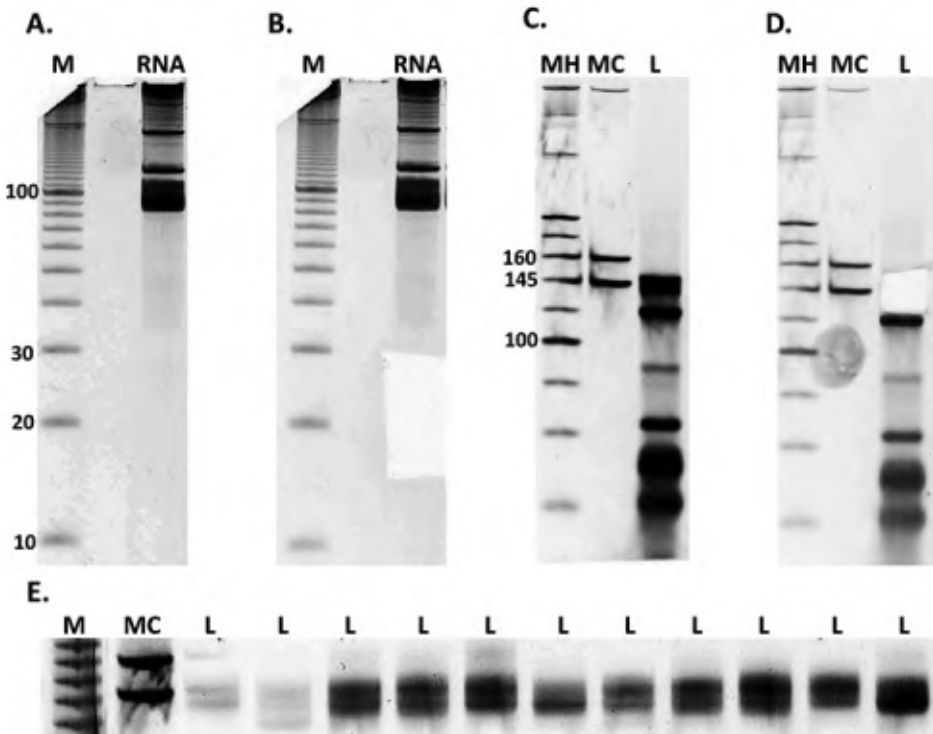


Fig. 7. Construction of small RNAs libraries in barley. A – total RNA separated on denaturing PAA gel; B – small RNAs fraction excised from the gel; C – non-denaturing PAA electrophoresis of amplified DNA libraries; D – DNA fragment excised from the gel; E – purified and precipitated DNA libraries separated in non-denaturing gel. Abbreviations: M – 10 bp DNA ladder (Invitrogen); MH – high resolution ladder; MC – custom ladder, both from Illumina; L – library

5  $\mu$ l volume of purified small RNAs fraction of 15-30 nucleotides long was then used in a 3' adaptor ligation and further reaction steps are described in TruSeq small RNA sample preparation Guide (Illumina). Finally, small RNA libraries were amplified using PCR (Illumina recommended use of no more than 15 cycles in PCR reaction). PCR products of 140-160 bp in size were excised from the 6% non-denaturing PAA, with 1% glycerol gel and then purified (Fig. 7.C, D, E). The example PCR product of 147 bp in size consists of 5' and 3' adaptor sequences and 22 nucleotides small RNA. One of the most critical steps during library preparation is the library concentration measurement. Quality of the measurement has a big impact on cluster yield and deep sequencing quality. Illumina raw cluster density recommendation for Flow Cell v3 (TruSeq SR Cluster Kit v3-cBot-HS) is 750 000-850 000/mm<sup>2</sup>. We used Quant-iT PicoGreen dsDNA assay according to the Invitrogen manual. Measurements were done

using Infinite 200 Pro plate reader together with NanoQuant plate (Tecan). First standard curve is created based on  $\lambda$ DNA and equation which describes relations between concentration (ng/ $\mu$ l) and fluorescence (Fig. 8). After the measurement (we used  $20 \times$  diluted samples in  $1 \times$  TE for the measurement), the particular samples concentration is calculated based on the equation shown in

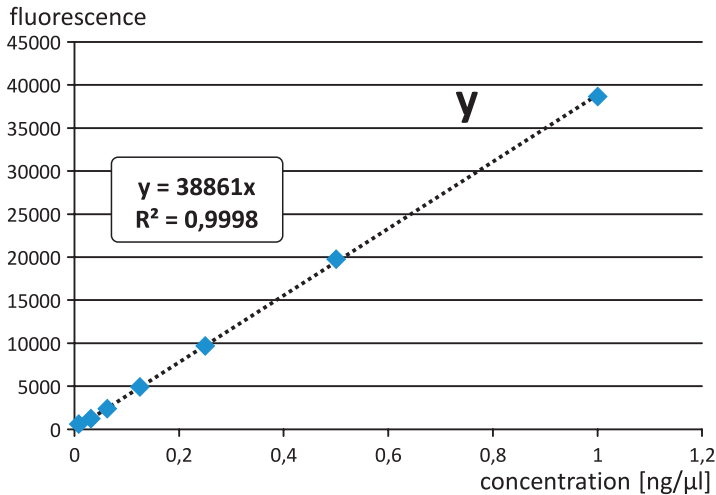


Fig. 8. Chart representing standard curve calculated with PicoGreen dye measurements

the chart. Then, ng/ $\mu$ l concentration was converted to nM concentration using Illumina Library Dilution Calculator. A sample containing 1 nM library in 10 mM Tris pH 8.5 was then prepared and so 15 pM library was used in one deep sequencing reaction. The next step after obtaining a set of deep sequencing reads is bioinformatical analysis. After rejecting sequences without adaptors, the analysis included 5' and 3' adapter sequences trimming. Next, we carried out a length distribution analysis of the obtained 3-28-nucleotide long sequences. A correctly carried out deep sequencing reveals some discrepancies within the RNA molecule abundances. The most abundant molecules are 24, 21-22 and 16 nucleotides long. RNA fragments with identical sequence were treated as one RNA molecule with given number of reads. The RNAs shorter than 18 or longer than 24 nucleotides were rejected from further analysis as not being an object of the study. The final step in the bioinformatical analysis was mapping the small RNAs to known small RNA sequences deposited in various databases, such as miRBase. We have compared our resulted sequences to the miRNA sequences of following monocotyledonous plants: common wheat (*Triticum aestivum*), durum wheat (*Triticum turgidum*), maize (*Zea mays*), purple false brome (*Brachypodium distachyon*), rice (*Oryza sativa*), sugarcane (*Saccharum officinarum*), sorghum (*Sorghum bicolor*), tall fescue (*Festuca arundinacea*), and to dicotyledonous

*Arabidopsis thaliana* miRNAs. This allowed us to identify conserved barley miRNA sequences which we used for searching of hairpin structure forming sequences in miRBase (<http://www.mirbase.org/>) and the International Barley Genome Sequencing Consortium (<http://webblast.ipk-gatersleben.de/barley/>) databases (Kozomara et al. 2011; International Barley Genome Sequencing Consortium et al. 2012).

The examples of mature miRNA expression levels described with deep sequencing method are presented in Fig. 9. Deep sequencing was performed for three biological replicas and mean value of the number of reads obtained for particular miRNAs is shown in the graphs. For miRNA166a/b/c/n we were not able to distinguish between mature molecules originating from different precursors because of the same sequences. The expression level of the mature miRNA171e after drought treatment and in re-watered plants varies only slightly when compared to the control ones. This is in agreement with pri-miRNA171e expression, which is constant after the severe drought/rehydration plant treatment. For miRNA166a/b/c/n the mature molecule level decreases under severe drought and reverts after rehydration, the same phenomenon is observed for pri-miRNA expression detected with qPCR. However, while pri-miRNA156g and pri-miRNA397b-3p are strongly upregulated under stress treatment, the number of miRNAs originating from these particular precursors decreases for both drought

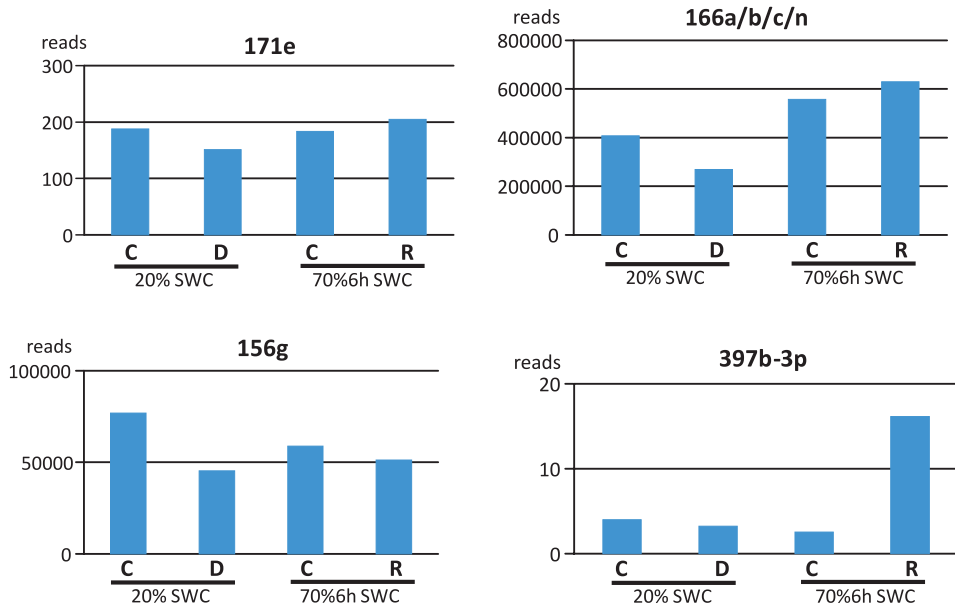


Fig. 9. Examples of mature miRNAs expression described with deep sequencing method. Deep sequencing was performed for control (C), severe drought treated (D) and 6 h after re-watering (R) plants

and re-watering in case of miRNA156g, while remains unchanged during drought and dramatically increases after re-watering for miRNA397b-3p. The differences between levels of miRNAs and their pri-miRNAs can be explained by post-transcriptional expression regulation at the level of pri-miRNA or pre-miRNA processing. This has to be further studied by northern hybridization of pre-miRNAs that will show putative accumulation of the dissected structures.

To sum up, we provide new tools for defining changes in the expression profiles of the miRNAs and pri-miRNAs in barley. We have described changes in barley microtranscriptome at the level of pri-miRNAs and miRNAs, in control and minor to severe drought conditions, as well as after rehydration. Additionally, we have subjected barley to heat stress with optimal watering, which allowed us to distinguish between plant response to drought and heat. We conclude that during drought stress miRNAs expression is regulated not only at the level of primary transcripts, but also at the level of partially processed precursors. Having the nucleotide sequences of the mature miRNAs and their pre-miRNAs, we are able to investigate the primary transcripts and the gene structures of the selected miRNAs. The accession to mature miRNA sequences allows us to look for target mRNAs of the microRNAs.

### Acknowledgements

This work was supported by POLAPGEN-BD project no. UDA.POIG.01.03.01-00-101/08 “Biotechnological tools for breeding cereals with increased resistance to drought”, subject 20: “The role of microRNA in regulation of mechanisms leading to drought adaptation in plants”, executed within Innovative Economy Programme 2007-2013, subject “Biological progress in agriculture and environment protection”.

Small RNA sequencing was performed in Genome Analysis Laboratory funded by National Multidisciplinary Laboratory of Functional Nanomaterials NanoFun nr POIG.02.02.00-00-025/09 (Innovative Economy Operational Programme, Priority Axis 2: R&D Infrastructure, Action 2.2: Support of Formation of Common Research Infrastructure of Scientific Units).

Oligonucleotide sequences for RT-PCR measurements of DHN1 and DHN9 expression were kindly provided by prof. Tadeusz Rorat (Institute of Plant Genetics of the Polish Academy of Sciences, Poznań, Poland).

### References

- Baniwal S.K., Bharti K., Chan K.Y., Fauth M., Ganguli A., Kotak S., Mishra S.K., Nover L., Port M., Scharf K-D., Tripp J., Weber C., Zielinski D., von Koskull-Döring P. 2004. Heat stress response in plants: a complex game with chaperones and more than twenty heat stress transcription factors. *J. Biosci.* 29(4): 471-487.
- Bitá C.E., Gerats T. 2013. Plant tolerance to high temperature in a changing environment: scientific fundamentals and production of heat stress-tolerant crops. *Front. Plant. Sci.* 4: 273.

- Brodersen P., Sakvarelidze-Achard L., Bruun-Rasmussen M., Dunoyer P., Yamamoto Y.Y., Sieburth L., Voinnet O. 2008. Widespread translational inhibition by plant miRNAs and siRNAs. *Science* 320: 1185-1190.
- Brown J.W.S., Marshall D.F., Echeverria M. 2008. Intronic noncoding RNAs and splicing. *Trends Plant Sci.* 13: 335-342.
- Dong Z., Han M-H., Fedoroff N. 2008. The RNA-binding proteins HYL1 and SE promote accurate in vitro processing of pri-miRNA by DCL1. *Proc. Natl. Acad. Sci. USA.* 105: 9970-9975.
- International Barley Genome Sequencing Consortium, Mayer K.F., Waugh R., Brown J.W., Schulman A., Langridge P., Platzer M., Fincher G.B., Muehlbauer G.J., Sato K., Close T.J., Wise R.P., Stein N. 2012. A physical, genetic and functional sequence assembly of the barley genome. *Nature* 491(7426): 711-6.
- Jones-Rhoades M.W., Bartel D.P. 2004. Computational identification of plant microRNAs and their targets, including a stress-induced miRNA. *Mol Cell.* 14: 787-799.
- Kosova K., Vitamvas P., Prasil I.T. 2014. Wheat and barley dehydrins under cold, drought, and salinity – what can LEA-II proteins tell us about plant stress response? *Front. Plant Sci.* 5: 343.
- Kozomara A., Griffiths-Jones S. 2011. miRBase: integrating microRNA annotation and deep-sequencing data. *Nucleic Acids Res.* 39(Database Issue): D152-D157.
- Kruszka K., Pieczynski M., Windels D., Bielewicz D., Jarmolowski A., Szweykowska-Kulinska Z., Vazquez F. 2012. Role of microRNAs and other sRNAs of plants in their changing environments. *J. Plant Physiol.* 169: 1664-1672.
- Kruszka K., Pacak A., Swida-Barteczka A., Stefaniak A.K., Kaja E., Sierocka I., Karlowski W., Jarmolowski A., Szweykowska-Kulinska Z. 2013. Developmentally regulated expression and complex processing of barley pri-microRNAs. *BMC Genomics* 14: 34.
- Kurihara Y., Takashi Y., Watanabe Y. 2006. The interaction between DCL1 and HYL1 is important for efficient and precise processing of pri-miRNA in plant microRNA biogenesis. *RNA* 12: 206-212.
- Llave C., Kasschau K.D., Rector M.A., Carrington J.C. 2002. Endogenous and silencing-associated small RNAs in plants. *Plant Cell.* 14: 1605-1619.
- Nozawa M., Miura S., Nei M. Origins and evolution of microRNA genes in plant species. 2012. *Genome Biol. Evol.* 4: 230-239.
- Pant B.D., Musialak-Lange M., Nuc P., May P., Buhtz A., Kehr J., Walther D., Scheible W.R. 2009. Identification of nutrient-responsive Arabidopsis and rapeseed microRNAs by comprehensive real-time polymerase chain reaction profiling and small RNA sequencing. *Plant Physiol.* 150: 1541-1555.
- Rajagopalan R., Vaucheret H., Trejo J., Bartel D.P. 2006. A diverse and evolutionarily fluid set of microRNAs in *Arabidopsis thaliana*. *Genes Dev.* 20: 3407-3425.
- Ramakers C., Ruijter J.M., Lekanne Deprez R.H., Moorman A.F.M. 2003. Assumption-

- free analysis of quantitative real-time polymerase chain reaction (PCR) data. *Neurosci. Lett.* 339: 62-66.
- Rapacz M., Stepień A., Skorupa K. 2012. Internal standards for quantitative RT-PCR studies of gene expression under drought treatment in barley (*Hordeum vulgare* L.): the effects of developmental stage and leaf age. *Acta Physiol. Plant.* 34: 1723-1733.
- Reinhart B.J., Weinstein E.G., Rhoades M.W., Bartel B., Bartel D.P. 2002. MicroRNAs in plants. *Genes Dev.* 16: 1616-1626.
- Schumann P.H.D., Richardson A.E., Smith F.W., Delhaize E. 2004. Characterization of promoter expression patterns derived from Pht1 transporter genes of barley (*Hordeum vulgare* L.). *J. Exp. Bot.* 55: 855-865.
- Szarzynska B., Sobkowiak L., Pant B.D., Balazadeh S., Scheible W.R., Mueller-Roeber B., Jarmolowski A., Szweykowska-Kulinska Z. 2009. Gene structures and processing of *Arabidopsis thaliana* HYL1-dependent pri-miRNAs. *Nucleic Acids Res.* 37: 3083-3093.
- Szarzynska B., Sobkowiak L., Jarmolowski A., Szweykowska-Kulinska Z. 2011. Gene structures and processing of plant pri-miRNAs. *Res. Adv. in Nucleic Acids Res.* 1: 1-12.
- Tang G., Reinhart B.J., Bartel D.P., Zamore P.D. 2003. A biochemical framework for RNA silencing in plants. *Genes Dev.* 17: 49-63.
- Wahid A., Close T.J. 2007. Expression of dehydrins under heat stress and their relationship with water relations of sugarcane leaves. *Biologia Plantarum* 51(1):104-109.
- Xie Z., Allen E., Fahlgren N., Calamar A., Givan S.A., Carrington J.C. 2005. Expression of *Arabidopsis* MIRNA genes. *Plant Physiol.* 138: 2145-2154.
- Yang L., Liu Z., Lu F., Dong A., Huang H. 2006. SERRATE is a novel nuclear regulator in primary microRNA processing in *Arabidopsis*. *Plant J.* 47: 41-850.
- Zadoks J.C., Chang T.T., Konzak C.F. 1974. A decimal code for the growth stages of cereals. *Weed Res.* 14: 415-421.



## **POLAPGEN-BD data collection, retrieval and processing infrastructure: a solution for systems biology research in plants**

**Wojciech Frohberg<sup>1,2</sup>, Aneta Sawikowska<sup>1</sup>, Hanna Ćwiek<sup>1</sup>, Zygmunt Kaczmarek<sup>1</sup>, Paweł Krajewski<sup>1</sup>**

<sup>1</sup> *Institute of Plant Genetics, Polish Academy of Sciences, Poznań, Poland*

<sup>2</sup> *Laboratory of Algorithm Design and Programming Systems, Institute of Computing Sciences, Poznań University of Technology, Poznań, Poland*

### **Introduction**

Data management of a large project consisting of several research tasks dispersed among a number of research centres is a big challenge, comprising data collection, integration, storage and sharing. Data integration is a laborious work which includes data cleansing, validation, unification, annotation, etc. Biological data is often affected by several errors, which mainly include human, device and format errors. This article explains solutions and assumptions on the database system adopted in POLAPGEN-BD project, facilitating data integration and further comprehensive analysis.

### **Data organisation**

Results of experiments stored as raw data are the most valuable material from the viewpoint of information retrieval. Abstraction systems called databases are used to gather and store these results. Database unifies the access and interaction models. In the context of scientific experiments, a database can be perceived as a communication protocol between the project centres and their global data repository. As every protocol needs to be strict and transparent, several important architectural decisions have to be made before the first data can appear in a database.

The nature of the field and greenhouse experiments in POLAPGEN-BD imposes harsh restrictions on database schemas. The experiments are designed to discover the connections between phenotypes and genotypes rather than only collect one

type of information. In its early stage, the data management task of POLAPGEN-BD project focused on the system architecture. An existing solution was adapted instead of starting a new one from scratch. There were only few databases allowing integration of phenotypic with genotypic information available at that time. The database structure that could meet our needs was GERMINATE 2.0 [1]. Owing to the collaboration with the James Hutton Institute (JHI), Dundee, we adjusted GERMINATE 2.0 to the POLAPGEN-BD dataflow. The model of the database schema is shown in Figure 1.

### *Database structure*

This section describes the most important tables of GERMINATE 2.0 structure as well as comments on the changes made to it to store POLAPGEN-BD data. The most important table called *phenotypedata* collects experiment results; the observed values are kept in the field *phenotype\_value*. We allowed any character string into the *phenotype\_value* field, bearing in mind that although most of the traits will be numeric, there can be a need to store qualitative information as well. Our intention was to hold both the data observed directly in greenhouse/field studies and the one already transformed in the process of statistical aggregation as long as it is not redundant. The table *phenotypedata* does not contain complete information regarding the meaning of the values. To find out details of the traits of particular values, we need to go along the reference to the *phenotype* table and in its field called *name* we can find the trait name. Most of the values also need the unit reference for proper interpretation. That is the reason why *phenotypedata* is also connected with the table *units*. Additional experimental factors characterising the data, e.g. specific drought treatment, or the task the data comes from are grouped in the table *datasets*. Each dataset also identifies a file from which the data was taken.

An equivalent of *phenotypedata* for genotypic information is the table *genotypes*. In this table, we store marker data of two types – SNP and SSR. The former uses fields *allele1* and *allele2* to store single nucleotide polymorphism and thus consumes only one character, while the latter fills, in an extreme case, the entire four-character string of these fields with the simple-sequence repeat length. Description of the markers is stored in the table *markers*. Both *phenotypedata* and *genotypes* have references to varieties for which the data was collected and whose names are stored in the table *germinatebase*.

### *Changes to GERMINATE 2.0*

To access the database and process the data, we initially planned to use ready-made tools distributed with GERMINATE. To ensure their full compatibility, we decided to install the most up-to-date version of the MySQL server application 5.5.23. Soon, we realised that the tools provided by JHI are specialised for the purposes of their experiments and we would not be able to utilise them easily in



our project. We were also compelled to create our own mechanisms of inserting the data into the database, provide an interface to access it, establish the way of data search, etc. To achieve full compatibility of our tools and GERMINATE, some changes in the original database schema were necessary. Some other changes were required because of the data characteristics of POLAPGEN-BD.

The first and most significant change is at the same time the most transparent from the point of view of a database user as it does not affect data organisation logic. The change consists in the selection of the alternative database engine. Database engine called MyISAM, the default in MySQL until version 5.5.4, is not transactional and does not support MVCC and ACID standards, yet it was used in GERMINATE 2.0 as it supports full-text indexing in contrast to InnoDB ( $\leq$ MySQL 5.6.4) [2]. As one of the tools that we had planned to use required ACID features while full-text indexing was not crucial, we decided to migrate the entire database to InnoDB. This process actually led to further changes in the database. We were able to create foreign keys and connect the tables with previously artificial reference (the fields with the suffix ‘\_id’) to one another to enable intuitive table joining. Additionally, at this stage we performed database efficiency tests on the queries which we supposed were the most frequent and which revealed performance problems while joining some tables. We overcame these issues by creating additional indices.

Apart from the above-mentioned changes in database mechanisms, we had introduced several auxiliary tables and fields to GERMINATE 2.0 database structure. The following were the two main reasons for these changes:

- 1) to enable natural data access – to simplify access through web interface, and
- 2) to store additional data – so as to better identify, update and withdraw data, if needed.

As pointed out, a lot of additional information concerning experiments is connected to the data through datasets. This information is organized in entity-attribute-value (EAV) model. This is done using a single table called groups connected to datasets by the many-to-many relationship. This kind of relationship allowed to define multiple predefined tags to a single dataset. Tags can be divided into five categories:

- 1) Task
- 2) Drought treatment
- 3) Time point
- 4) Organ
- 5) Replication

To categorise the groups, our schema holds a *grouptypes* table. The EAV model proved efficient in terms of storage space, yet was problematic to some auxiliary

tools that we had planned to use. A Biomart service (described in the following text) combined with the topology of GERMINATE 2.0 provided no easy method to filter data automatically on the specific tag category. To overcome this problem we created five additional tables connected to the table *datasets*, one for each tag category. Every table was being filled in and updated by mysql triggers, whenever data in *groups* changes. This prevents redundant data manipulation from the programmatic side and keeps the data always up-to-date.

The last essential change made to adjust GERMINATE 2.0 to our needs was the addition of several tables, namely, *dfile*, *dfiledataset*, *dfileentry*, *mfile*, *mfiledataset* and *mfileentry*, which help organize the data into logical structures and assign them to the files from which they were loaded. It was important to keep records of the files, so as to be able to reload or withdraw certain datasets in cases of unplanned data updates and human errors. The link from each data value to the filename gives a natural method that allows data management.

Finally, we added a few columns in the table *phenotypes* to better describe and annotate the observed phenotypic traits and link them to ontological terms.

## **POLAPGEN-BD dataflow**

To manage the dataflow in POLAPGEN-BD, several tools have been used. Each of them is targeted to different user group. This section highlights the most important tools, formats and approaches that we have adopted or created. The following subsections describe them one by one. The first subsection focuses on the data curation, adopted naming schema and specific file format established to facilitate collecting data and enabling fast and easy data exchange between experimental tasks. Further, we discuss a tool, implemented by our team from scratch, which serves as the data importer. We also introduce the file format for importing data. Next subsection is about the Biomart service available in our server. Then we focus on the advanced data search engine of Solr that we embedded in POLAPGEN-BD's Biomart. Finally, we discuss briefly about the data analysis.

### *Data acquisition*

Collecting data from multiple partners is a big challenge owing to plurality of data types and files formats. For the unification of the data files among research centres and project tasks, we decided to create a template spreadsheet to be used by the partners. The file is a universal form to be filled in by the data providers. It comprises a few mechanisms that simplify data insertion, maintain consistent naming, keep users from passing mistaken values, and also makes it faster to complete the form by providing suggestions and autocompletion mechanisms. The file was created using Microsoft Excel and can be filled in (to the best of our knowledge) using any of its versions.

The file consists of two worksheets. The first one contains metadata, i.e. general information about an experiment, such as the names and descriptions of drought treatments, varieties, time points and phenotypic traits. The second sheet contains a matrix where the user can enter the actual observations for each sample described by combinations of factors imported from the first sheet. The imported terms appear as a menu choice, so as to minimise the number of typing errors and to standardise terminology.

After the form is completed by a task data provider and sent to integration, and before the insertion of data into the database, the content has to be curated, standardised, pre-processed and reformatted.

Both metadata and data undergo biocuration. The vocabulary used in metadata description is mapped to the terms already present in the database and standardised accordingly. Presumable equivalent terms are unified and misspellings are removed to align with the existing names, while the new terms are verified and added. Phenotype (trait) names are also annotated with ontology terms, wherever possible. Phenotypic trait names are mapped to corresponding terms from Trait Ontology (TO), Plant Ontology (PO), Chemical Entities of Biological Interest (ChEBI) and other public trait dictionaries. Standardisation of metadata helps ensure clarity and consistency of concepts throughout the project.

The data provided by the partners are statistically examined and pre-processed, depending on its type. Traditional phenotypes undergo typical analysis: for technical replications a mean of the values is calculated and used, whereas biological replications stay untouched. Outliers are removed based on scatter-plot matrix and box-and-whisker diagrams produced in GenStat software [3]. After proper formatting for Genstat scripts, the data is ready for import into the database.

As mentioned in the beginning, not all POLAPGEN-BD data can be collected in the prepared Excel files, and some need extensive pre-processing before it can be imported into the database. In POLAPGEN-BD there are several types of such high-throughput data, for instance, those coming from untargeted proteomic and metabolomic analysis, or gene expression data. Raw data generated by specific devices are deposited directly in specialised databases (MetaboLights, ArrayExpress) and, in parallel, processed locally by various methods and programs (own scripts in R and GensStat, among others, see Fig. 2) depending on their nature. The results — processed, standardised and ready for further integrative analysis — are stored in POLAPGEN-BD database.

### *Data import*

Data import is done using a Java-based application. Each table from the database is mapped one-to-one into a class in the application. In this way, the place for any potential change in the program can be easily localised and quickly committed. The application is user-friendly and has ergonomic interface. The main window

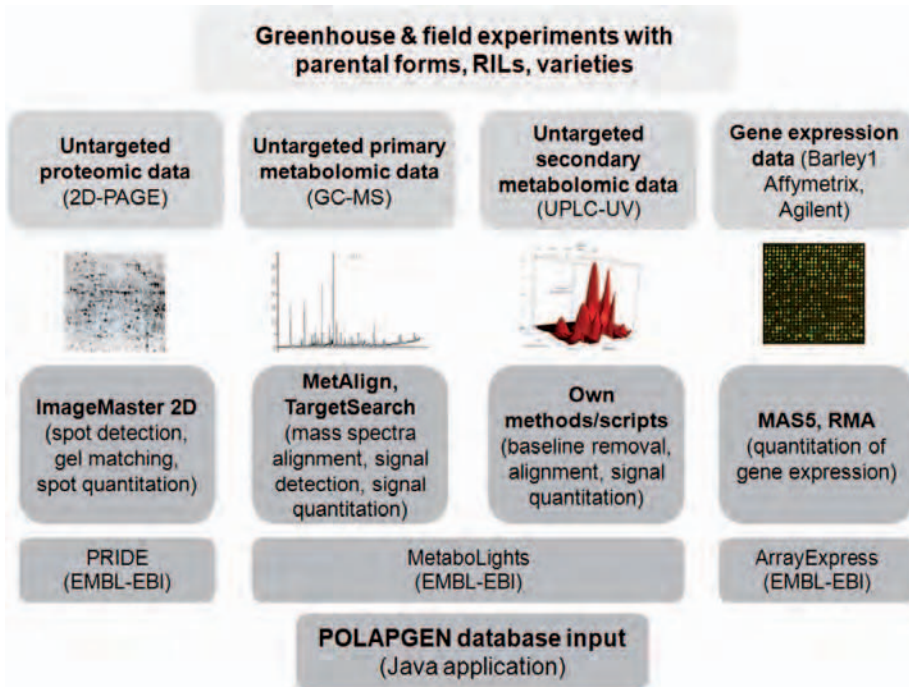


Fig. 2. Processing of high-throughput data and storage in databases

of the application is shown in Figure 3. The combo box placed at the top of the window allows the user to choose what should be imported to the database. The choice of import is as follows:

- 1) Phenotypes
- 2) Markers (SNP)
- 3) Markers (SSR)

Right next to the combo box there are two buttons. The first of them — with the label ‘Administration’ — allows removal of data files previously inserted into the database as well as access basic data file statistics. The button with the label ‘Options’ opens a window with database connection preferences and credentials. Below the combo box is(are) the load file(s) button(s). Depending on the type of the data (the combo-box option chosen above) there can be one or two files needed here. For instance, the import of phenotype data requires trait information provided in a separate file. Finally, the ‘Load’ button starts loading the data into the database.

The application accepts comma separated files (CSV) of specific formats, depending on the import data type. We present the formats (text within triangle brackets should be replaced with values, wherein NUM should be replaced with numeric value and UPxxx should be replaced with a text of up to xxx characters) in the following.

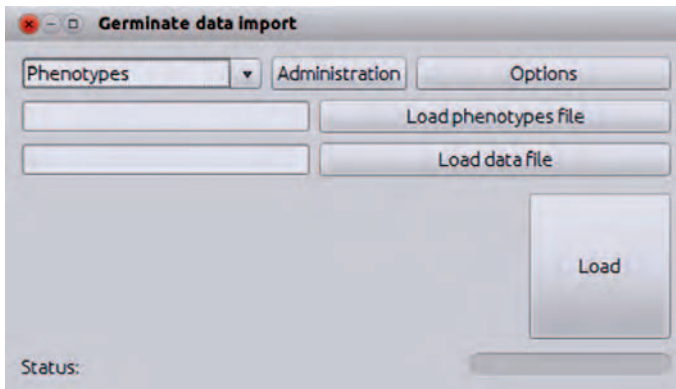


Fig. 3. Main window of the database data importer

### 1) Phenotypes

– trait file

```
PhenotypeNo, Name, ShortName, Units, Description
<NUM>, <UP255>, <UP15>, <UP255>, <UNLIMITED_TEXT>
<NUM>, <UP255>, <UP15>, <UP255>, <UNLIMITED_TEXT>
...
```

– data file

```
Lp, Experiment, Task, Organ, Drought_treatment, Time_point, Germinatebase_name, Replicate, <TRAIT_NAMES>, ...
<NUM>, <UP255>, <UP255>, <UP255>, <UP255>, <UP255>, <UP255>, <UP255>, <UP255>, ...
<NUM>, <UP255>, <UP255>, <UP255>, <UP255>, <UP255>, <UP255>, <UP255>, <UP255>, ...
...
```

where Germinatebase\_name means variety

### 2) Markers (SNP)

```
Lp, Experiment, Task, Markertype, Marker_name, Mapped, Reference, <PLANT_SPECIES>, ...
<NUM>, <UP255>, <UP255>, <UP255>, <UP45>, <NUM>, <UP45>, <UP1>, ...
<NUM>, <UP255>, <UP255>, <UP255>, <UP45>, <NUM>, <UP45>, <UP1>, ...
...
```

### 3) Markers (SSR)

```
Lp, Experiment, Task, Markertype, Marker_name, Mapped, Reference, Chr, <PLANT_SPECIES>, ...
<NUM>, <UP255>, <UP255>, <UP255>, <UP45>, <NUM>, <UP45>, <UP3>, <UP4>, ...
<NUM>, <UP255>, <UP255>, <UP255>, <UP45>, <NUM>, <UP45>, <UP3>, <UP4>, ...
...
```

where Chr column values should be formatted as ‘??H’ and ?? should be replaced with chromosome number, e.g. for chromosome 1, ‘1H’.

Because the loading modules for phenotypes and markers are separate, they have different requirements for the input files. Marker data loader is more liberal about the column order, and it even allows to exclude some columns from the file. Phenotypic data loader, on the other hand, does not require that the header row have the column names identical with the model, as it assumes that column order is fixed and the content is determined by its index.

### Data accessing

To share the data we used generic and scalable Biomart approach [4]. Figure 4 shows the screenshot from the public POLAPGEN-BD database accessed by Biomart. Biomart is an out-of-the-box system that allows instant access to the data with an option of simple data filtering. Data can be filtered by exact values that we want in the retrieved rows on specific columns. If we do not know the exact values that interest us, we can choose them from the presented lists. The data are accessible immediately after import; however, the filters are updated every half an hour.

After applying the filters and choosing the columns to be displayed, by clicking 'Go >>' button we are redirected to preview the data page. If the data we have chosen is the one that really interests us, we can click the 'Download data' button to finalize our query. The download file will be obtained in the Space Separated Values (SSV) format.

The full-user manual (in Polish) for the POLAPGEN-BD Biomart is accessible on our webpage [5].

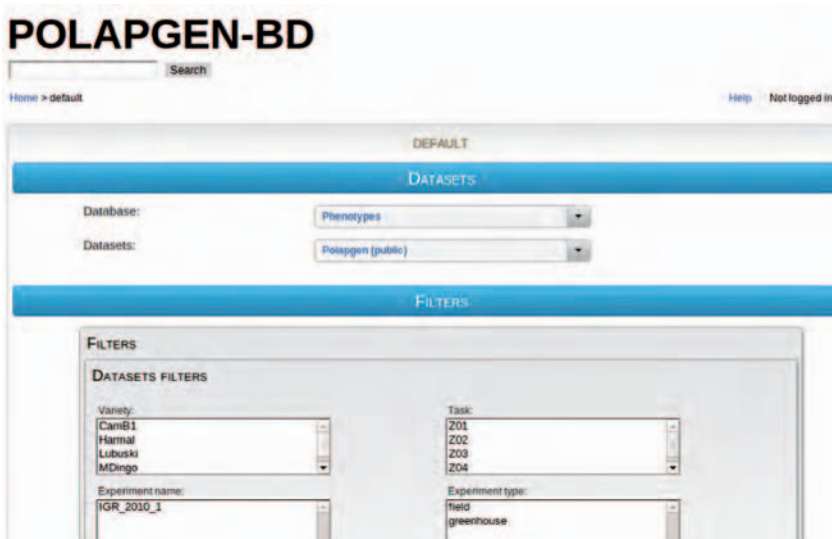


Fig. 4. Accessing POLAPGEN-BD database using Biomart

### *Metadata search*

To facilitate usage of Biomart interface for POLAPGEN-BD database, we provided a metadata search tool. We installed and configured Apache Solr tool [6] – a full-text search engine, based on information retrieval library Lucene.

Solr performs indexing of all metadata from our database (i.e. names and descriptions of objects, factors, observed phenotypic traits and markers), and when queried, finds the characteristics corresponding to the keywords entered by the user. The tool is integrated within Biomart interface and is available any time as a tiny search widget at the top of the screen (Fig. 4). A query entered by the user results in a display of a list of matching entities, grouped within type, i.e. phenotypes, markers, experiments and varieties. By pointing to the metadata described by the given terms, the tool simplifies choosing and filtering attributes in Biomart to access the relevant data.

Temporarily, two POLAPGEN-BD databases exist – one public and the other for internal use – and each has a separate Solr core with an index and a search mechanism that point to the data currently available to a particular user. Whenever the state of metadata in the database is modified, the indices are updated via a direct connection with POLAPGEN-BD's RDBMS using a data import handler provided by Solr (currently v4.5.1).

### *Data analysis*

When necessary, the data is extracted from the database using Biomart interface and submitted to statistical analysis. The adopted structure allows for easy integration of all data into one table for chosen lines, traits or experimental conditions. Such tables serve as input to scripts in Genstat or R that perform data post-processing, model fitting and parameter estimation and allow for visualisation of results:

- genotype data (SNP, SSR) is processed to provide files appropriate for linkage map construction,
- field and greenhouse phenotype data is processed by multi-way analysis of variance and submitted to multivariate analysis procedures (e.g. visualisation by biplots),
- metabolomic profiling and proteomic profiling data is submitted to signal detection and quantitation procedures, and then to ANOVA-based inference,
- gene expression data is submitted to normalization procedures followed by ANOVA.

In all statistical procedures, comparisons of values and parameters obtained in control conditions with those obtained for water-deficit plants (plots, samples) play an important role. Multivariate methods and correlation network analysis play a prominent role in the integration of data obtained by different project teams.

Figure 5. Search widget integrated in Biomart; search result window

Details of the methodologies used for each particular experiment and data type will be described in the separate publications dealing with the biological interpretation and integration of the project's results.

## System environment configuration

To achieve increased control over data access and to prevent resource overloading, we have distributed the system among three servers. The first server can be considered a gateway that is accessible from the Internet, the second can be perceived as the data storage and the third is to maintain the backup.

POLAPGEN-BD database access is partially restricted, and it contains data that should not have been available publically. To separate the data that can be freely downloaded from that with limited admission, we provide two databases on the storage server. Both the databases are easily browsable from the local network. The gateway server, however, restricts the private database service only for logged-in users.

As databases are constantly updated and they store more and more data, and – on the other hand – no one can be entirely sure of the reliability of the hardware, creating a backup is strictly advised. We systematically perform the backup every five minutes. The backup state is maintained in the distributed version control system GIT [7].

## Concluding remarks

The data collection and processing infrastructure created for POLAPGEN-BD project by members of the Department of Biometry and Bioinformatics IPG PAS is based on software tools that were kindly provided to the project by the owners, were publically available or were specially created by the team. The infrastructure is sufficiently flexible to be used in other similar research projects. Work on this infrastructure and on the data collected by the POLAPGEN-BD project created several collaborations with other teams interested in similar work. For example, the phenotypic traits observed in the project were submitted as a basis for creation of an ontology of barley traits to the Crop Ontology Project ([www.croponontology.org](http://www.croponontology.org)). The publicly accessible part of the database was used as an exemplary data source for the standardization and search engine creation tasks in the FP7 project transPLANT coordinated by the European Bioinformatics Institute and is indexed in its search facility (available at [www.transplantdb.eu](http://www.transplantdb.eu)).

## Acknowledgements

We are grateful to the members of the Information and Computational Sciences Group, James Hutton Institute, Dundee, for providing the GERMINATE database schema and help in its implementation. Some elements of data processing infrastructure use the facilities provided by the Poznań Supercomputing and Networking Center. The work of WF and HĆ was partially supported by the EU FP7 project transPLANT ‘Trans-national infrastructure for plant genomic science’ (contract number 283496) within its WP2 ‘Interaction with national and trans-national genomics and informatics activities’.

## References

- [1] Lee J.M., Davenport G.F., Marshall D., Ellis T.H.N., Ambrose M.J., Dicks J., van Hintum T.J.L., Flavell A.J. (2005). GERMINATE. A Generic Database for Integrating Genotypic and Phenotypic Information for Plant Genetic Resource Collections. *Plant Physiology* 139: 619-631.
- [2] *InnoDB official manual pages* <http://dev.mysql.com/doc/refman/5.5/en/innodb-storage-engine.html>
- [3] VSN International (2011). GenStat for Windows 14th Edition. VSN International, Hemel Hempstead, UK. Web page: [GenStat.co.uk](http://GenStat.co.uk)

- [4] Smedley D., Haider S., Ballester B., Holland R., London D., Thorisson G. and Kasprzyk A. (2009). BioMart – biological queries made easy. BMC Genomics 10: 22.
- [5] <http://cropnet.pl/login/pomoc.pdf>
- [6] <http://lucene.apache.org/solr/>
- [7] <http://git-scm.com/documentation>



## Technological deliverables of POLAPGEN-BD project

Prace opublikowane w tym tomie stanowią sprawozdania wykonawców projektu WND-PO-IG.01.03.01-00-101/08 POLPAGEN-BD z osiągnięcia rezultatów pod wspólną nazwą „Opracowanie nowych rozwiązań technologicznych” określonych w zał. 14 do Umowy o Wykonanie Projektu

Lp.	Opracowane rozwiązanie	Rozdział
1	Sieć monitoringu wilgotności gleby w stacjach hodowli roślin (zad. 1)	<b>Andrzej Kędziora, Janusz Jankowiak, Damian Józefczyk, Grzegorz Karg, Joanna Andrusiak</b> <i>Methodology for assessing of water conditions in Poland in terms of cultivation of spring barley</i>
2	System automatycznej regulacji i monitoringu wilgotności (zad. 3)	<b>Alicja Pecio, Damian Wach, Anna Kocoń, Grzegorz Józefaciuk</b> <i>A method for precision irrigation control in greenhouse experiment and its use to study drought stress effect on spring barley</i>
3	Molekularne markery odporności roślin na stres suszy (zad. 2, 4)	<b>Piotr Ogrodowicz, Krzysztof Mikołajczak, Anetta Kuczyńska, Karolina Krystkowiak, Maria Surma, Tadeusz Adamski</b> <i>Plant materials and analysed traits in the greenhouse and field experiments</i> <b>Justyna Guzy-Wrobelska, Kornelia Gudys</b> <i>Construction of high quality 'function' maps for the identification of quantitative trait loci related to drought tolerance in barley</i>
4	System analizy cech anatomicznych roślin poprzez analizę obrazu (zad. 5)	<b>Tomasz P. Wyka, Agnieszka Bagniewska-Zadworna</b> <i>Measuring anatomical variation in leaves of barley genotypes differing in drought tolerance</i>
5	Technologia pomiarów szybkiej kinetyki fluorescencji chlorofilu (zad. 9)	<b>Katarzyna Hura, Barbara Jurczyk, Agnieszka Ostrowska, Marcin Rapacz, Katarzyna Śniegowska-Świerk, Magdalena Wójcik-Jagła, Katarzyna Żmuda, Jolanta Biesaga-Kościelniak, Janusz Kościelniak</b> <i>Physiological indicators of drought tolerance in barley</i>
6	Technologia oznaczania aktywności SOD i akumulacji anionorodnika ponadtlenkowego (zad. 11)	<b>Renata Bączek-Kwinta</b> <i>The assay of oxygen free radicals and the enzyme decomposing them in barley leaves subjected to drought</i>
7	Technologia pomiarów wymiany gazowej i niemotocchemicznego tłumienia energii wzbudzeń u roślin (zad. 12)	<b>Katarzyna Hura, Barbara Jurczyk, Agnieszka Ostrowska, Marcin Rapacz, Katarzyna Śniegowska-Świerk, Magdalena Wójcik-Jagła, Katarzyna Żmuda, Jolanta Biesaga-Kościelniak, Janusz Kościelniak</b> <i>Physiological indicators of drought tolerance in barley</i>
8	Technologia oznaczania poziomu ekspresji wybranych genów jęczmienia (zad. 18)	<b>Katarzyna Śniegowska-Świerk, Barbara Jurczyk, Marcin Rapacz</b> <i>Methods for the measurement of drought-induced changes in the expression of selected barley genes</i>
9	Platforma analizy mikroRNA jęczmienia (zad. 20)	<b>Aleksandra Świda-Barteczka, Katarzyna Kruska, Andrzej Pacak, Wojciech Karłowski, Artur Jarmolowski, Zofia Szweykowska-Kulińska</b> <i>Tools for defining barley microtranscriptome expression at the level of primary microRNAs and mature microRNAs</i>
10	Sondy molekularne do oceny zdolności roślin do adaptacji do warunków suszy (zad. 21)	<b>Tadeusz Rorat, Anna Turska-Taraska, Agnieszka Kielbowicz-Matuk, Mateusz de Mezer</b> <i>The application of functional genomics to identify genes associated with adaptation of barley plants to water deficit</i>